

# **TOXICITY OF METAL DEBRIS FROM HIP IMPLANTS**

**Ilona Świątkowska**

This thesis is submitted in accordance with the requirements for  
the degree of Doctor of Philosophy (PhD)

University College London

Faculty of Medical Sciences

Division of Surgery and Interventional Science

November 2019



## **Declaration**

I, Ilona Świątkowska, confirm that the work presented in this thesis is my own. Where information has been derived from other sources, I confirm that this has been indicated in the thesis.

Signature

---

Date

---





## Abstract

Hip implants are commonly made of cobalt-chromium and titanium alloys. Once inside the body, implants wear and corrode, releasing metal particles and ions into the local tissue and blood. Metal debris can cause local adverse effects, such as bone loss and tissue necrosis, ultimately leading to implant failure. More recently, systemic cobalt toxicity has gained publicity as reports of neurotoxicity, cardiomyopathy and hypothyroidism increased among recipients of metal hip implants. Widespread dissemination of metal debris, and its accumulation in organ tissue, is of a particular concern.

The aim of this thesis is to better understand how metallic implant debris affects the body, and how blood metal levels relate to any toxicity symptoms.

Prevalence of neurotoxicity and cognitive decline among patients with a history of highly elevated blood cobalt was assessed, using a set of validated questionnaires. Although a number of statistically significant differences were detected between the high cobalt group and controls, clinically relevant neuro-cognitive adverse effects were not observed.

Distribution and chemical speciation of cobalt, chromium and titanium deposits were investigated in cadaveric samples of organs from hip replacement patients. Though synchrotron analysis identified the presence of highly oxidised chromium, further work is needed to assess if the results can be extrapolated to the *in vivo* situation.

Genetic factors that might predispose some patients to the adverse effects of cobalt were explored *in vitro*, using CRISPR/Cas9 gene editing technology. Results of the feasibility study identified several candidate genes for further investigation.

Blood titanium was measured in a large group of patients with titanium-based implants, using high resolution ICP-MS. This allowed a reliable laboratory reference range to be defined for use in future patient monitoring.

Results from this thesis inform on potential consequences of implant degradation, and demonstrate the clinical utility of blood metal measurements to monitor implant performance.



## Impact statement

The number of people undergoing hip arthroplasty (HA) is on the rise due to the ageing of the population. Additionally, indications for the surgery are now being offered to younger patients (<60 years old), with the mean length of exposure to metal debris hereby increasing. Hip implant recipients enjoy improved quality of life, lower rates of comorbidities and all-cause mortality than the general population. However, high cobalt and chromium release from metal-on-metal (MoM) hip implants has been linked to adverse local tissue reactions, leading to multiple medical device alerts and recalls over the past decade. In a small number of patients, systemic effects, such as neurotoxicity and cardiomyopathy, were also reported. While MoM constructs are no longer widely used, over 5 million patients worldwide have hip implants with cobalt-chromium components, and could be at risk of toxicity.

Findings from the present thesis revealed no clinically significant self-reported neuro-cognitive sequelae in MoM implant recipients with a history of highly elevated blood cobalt. These results do not support the need for systemic health check-ups in asymptomatic patients, which, aside from providing much-needed reassurance, could influence healthcare regulators and impact the economy.

It is possible that some people are genetically predisposed to cobalt toxicity. The effect of differential gene inactivation on cell viability was investigated *in vitro*, and several potential cobalt susceptible genes pinpointed. While our findings are only preliminary, they are an important first step in the exploration of genetic vulnerabilities in the setting of HA. Ultimately, this work could help predict which patients are more likely to react to their implant, influence implant type recommendations, and affect management guidelines in the predisposed patients.

Toxicity of chromium depends on its valence- the trivalent state ( $\text{Cr}^{\text{III}}$ ) is fairly benign, while the hexavalent form ( $\text{Cr}^{\text{VI}}$ ) is a known human carcinogen. The release of  $\text{Cr}^{\text{VI}}$  from implants, and *in vivo* oxidation of implant-derived  $\text{Cr}^{\text{III}}$ , are highly debated, and a causal link between metal implants and increased risk of cancer has not been reported. Synchrotron analysis of cadaveric organ tissue from HA recipients detected highly oxidised chromium species, which could mean that these forms of chromium

might arise in vital organs of TJA patients. Further studies are needed to evaluate the clinical implications of these findings.

The growing popularity of uncemented hip implants has led to an increased use of titanium in implant manufacture. An updated threshold value for normal blood and plasma titanium was defined in patients with well-functioning titanium-based implants, in order to overcome the analytical limitations of previous studies. The reference range could be used as an adjunct to imaging, to monitor implant wear and help ensure a timely revision operation of poorly functioning prostheses.

In conclusion, results from this thesis will help surgeons monitor implant performance and facilitate patient management. The findings will also benefit regulatory bodies worldwide, who might use them to update their guidance on patient follow-up.

# Acknowledgements

First and foremost, I would like to thank my primary supervisor, Professor Alister Hart, for his enthusiasm, support, and the many valuable opportunities he has given me during the past 4 years. I also express my gratitude to my secondary supervisor, Professor Andres Floto, for kindly hosting me in his laboratory, where I learnt a great deal about molecular biology and acquired many new skills.

Appreciation is due to Mr Johann Henckel, for always believing in the project and constantly encouraging me to step out of my “comfort zone”.

I am especially indebted to my collaborators: Professor Frederick W. Mosselmans, Dr Tina Geraki, Mr Shiraz Sabah, Mr Cody Wyles, Dr Joseph Maleszewski, Mr Hugh Apthorp, Nicholas Martin and Dr Barry Sampson. Their immense knowledge and expertise have been instrumental to the success of this PhD.

I would like to thank Catherine Klapholz, Dr Charlotte Passemar, Alex McLatchie, Dr Pawan Dhami, Dr Konstantin Ignatyev and Dr Agata Nyga for scientific advice and technical assistance, which greatly benefitted this thesis. I thank my fellow labmates, and laboratory technicians at the Institute of Orthopaedics and Musculoskeletal Science, for getting me started with cell culture experiments, and always being there when I needed help. I also owe a sincere thanks to Jessica Broni-Tabi, Vandana Luthra and Ufedo Miachi for their guidance during the ethics application process.

My heartfelt appreciation goes to all the study participants and hospital staff, without whom the research studies described in this thesis would not have been possible. Tracy Young deserves a special mention for her dedication and positive energy, which made my time at The Horder Centre a truly amazing experience.

I must acknowledge the academic and moral support of friends and colleagues, who have provided stimulating discussions and pushed me forward in moments of despair. A huge thank you to Akram, Arianna, Laura, Lorenzo, Sean, Betta, Rita, Elena, Kelly, Rob, Reshma, Martin, Vicky, Anna and Harry.

Thanks are also due to Mr Keith Tucker, Gwen Fish Charity, Diamond Light Source, The Horder Centre and the Laboratory of Molecular Biology for their financial support and help in making this research come to life.

I owe a great debt to my family who always believed in me more than I ever did, and supported me in every way they could. In particular, I thank my Grandma, who is the most inspirational person I know.

Most of all, I thank my fiancé, Dom, for his tireless support, understanding, and the ability to see positives in anything that happens. I would not have made it without you.

*Dedicated to my Grandma*

*Zadedykowane dla Babci*

# Contents

<b>ACRONYMS AND ABBREVIATIONS</b> .....	<b>17</b>
<b>LIST OF FIGURES</b> .....	<b>20</b>
<b>LIST OF TABLES</b> .....	<b>27</b>
<b>CHAPTER 1: INTRODUCTION</b> .....	<b>29</b>
1.1    MOTIVATION.....	31
1.2    AIM.....	31
1.3    OBJECTIVES.....	32
1.4    THESIS OUTLINE.....	32
1.5    ETHICAL APPROVAL .....	33
<b>CHAPTER 2: LITERATURE REVIEW</b> .....	<b>35</b>
2.1    THE HIP JOINT .....	37
2.1.1 <i>Common disorders of the hip joint</i> .....	37
2.1.2 <i>Hip replacement surgery</i> .....	39
2.2    IMPLANT BIOMATERIALS .....	41
2.2.1 <i>A brief history of hip implants</i> .....	41
2.2.2 <i>Modern hip replacement</i> .....	42
2.2.3 <i>Metal</i> .....	43
2.2.4 <i>Polyethylene</i> .....	45
2.2.5 <i>Ceramic</i> .....	45
2.2.6 <i>Implant biodegradation</i> .....	45
2.2.7 <i>Metal hypersensitivity</i> .....	47
2.3    COBALT .....	48
2.3.1 <i>Cobalt toxicokinetics</i> .....	49
2.3.2 <i>Local adverse effects</i> .....	50
2.3.3 <i>Remote adverse effects</i> .....	52
2.3.4 <i>Mechanisms of toxicity</i> .....	65
2.3.5 <i>Treatment of cobalt toxicity</i> .....	68
2.4    CHROMIUM.....	69
2.4.1 <i>Chromium toxicokinetics</i> .....	70



2.4.2	<i>Adverse effects</i> .....	72
2.5	TITANIUM.....	73
2.5.1	<i>Titanium toxicokinetics</i> .....	73
2.5.2	<i>Adverse effects</i> .....	74
2.6	CHARACTERISATION OF METAL DEPOSITS IN TISSUE.....	75
2.6.1	<i>Periprosthetic tissue</i> .....	75
2.6.2	<i>Organ tissue</i> .....	77
2.7	ASSESSMENT OF BLOOD METAL LEVELS IN THA PATIENTS .....	78
2.7.1	<i>Cobalt and chromium</i> .....	78
2.7.2	<i>Titanium</i> .....	80
2.7.3	<i>Metal content of different blood fractions</i> .....	81
2.7.4	<i>Inter-laboratory discrepancies</i> .....	82
2.7.5	<i>The units</i> .....	83
2.8	CLINICAL UTILITY OF BLOOD METAL MEASUREMENT IN THA PATIENTS.....	83
2.8.1	<i>Cobalt and chromium</i> .....	83
2.8.2	<i>Titanium</i> .....	90
2.9	INDIVIDUAL SUSCEPTIBILITY TO ADVERSE EFFECTS .....	93
2.9.1	<i>Renal insufficiency</i> .....	93
2.9.2	<i>Malnutrition</i> .....	93
2.9.3	<i>Decreased albumin binding</i> .....	93
2.9.4	<i>Potential genetic vulnerabilities</i> .....	95
2.10	SUMMARY.....	96

**CHAPTER 3: ASSESSING NEUROTOXIC SYMPTOMS IN THA PATIENTS**  
.....**97**

3.1	INTRODUCTION .....	99
3.1.1	<i>Motivation</i> .....	99
3.1.2	<i>Aim</i> .....	99
3.1.3	<i>Objectives</i> .....	100
3.2	PATIENTS AND METHODS.....	100
3.2.1	<i>Patients</i> .....	100
3.2.2	<i>Neurotoxic Symptom Checklist-60 (NSC-60)</i> .....	103
3.2.3	<i>Diabetic Neuropathy Score (DNS)</i> .....	106
3.2.4	<i>Systemic Symptom Checklist (SSC)</i> .....	107

3.2.5	<i>Douleur Neuropathique 10 (DN-10)</i> .....	108
3.2.6	<i>Mini Mental State Examination (MMSE)</i> .....	109
3.2.7	<i>Statistical analysis</i> .....	110
3.2.8	<i>Study design flowchart</i> .....	111
3.3	RESULTS.....	113
3.3.1	<i>NSC-60</i> .....	113
3.3.2	<i>DNS and DN-10</i> .....	114
3.3.3	<i>SSC</i> .....	115
3.3.4	<i>MMSE</i> .....	115
3.4	DISCUSSION.....	115
3.4.1	<i>Study limitations</i> .....	117
3.5	CONCLUSION.....	119

## **CHAPTER 4: ANALYSING METAL DEPOSITS IN VITAL ORGANS OF THA PATIENTS ..... 121**

4.1	BACKGROUND: SYNCHROTRON SPECTROSCOPY.....	123
4.1.1	<i>Synchrotrons</i> .....	123
4.1.2	<i>Diamond Light Source</i> .....	124
4.1.3	<i>I18 beamline</i> .....	125
4.1.4	<i>Micro-X-ray fluorescence (<math>\mu</math>-XRF) spectroscopy</i> .....	126
4.1.5	<i>Microfocus X-ray absorption spectroscopy (<math>\mu</math>-XAS)</i> .....	128
4.2	INTRODUCTION.....	131
4.2.1	<i>Motivation</i> .....	131
4.2.2	<i>Aim</i> .....	131
4.2.3	<i>Objectives</i> .....	132
4.2.4	<i>Study design flowchart</i> .....	132
4.3	MATERIALS AND METHODS.....	132
4.3.1	<i>Patients</i> .....	132
4.3.2	<i>Tissue processing</i> .....	133
4.3.3	<i>Optical microscopy</i> .....	133
4.3.4	<i>Laser ablation ICP-MS (LA ICP-MS)</i> .....	135
4.3.5	<i>Synchrotron X-ray analysis</i> .....	136
4.3.6	<i>Statistical analysis</i> .....	140
4.4	RESULTS.....	141
4.4.1	<i>Histological analysis</i> .....	141
4.4.2	<i>LA ICP-MS</i> .....	141

4.4.3	<i>μ-XRF tissue mapping</i> .....	142
4.4.4	<i>μ-XAS speciation of tissue metal deposits</i> .....	145
4.5	DISCUSSION.....	149
4.5.1	<i>Cardiac cobalt concentration</i> .....	149
4.5.2	<i>μ-XRF tissue mapping</i> .....	149
4.5.3	<i>μ-XAS speciation of tissue metal deposits</i> .....	150
4.5.4	<i>Study limitations</i> .....	154
4.6	CONCLUSION.....	154

**CHAPTER 5: IDENTIFYING COBALT SUSCEPTIBLE GENES: A FEASIBILITY STUDY .....155**

5.1	BACKGROUND: CRISPR/CAS TECHNOLOGY .....	157
5.1.1	<i>CRISPR/Cas systems</i> .....	157
5.1.2	<i>Genome-scale CRISPR/Cas9 knock-out libraries</i> .....	159
5.1.3	<i>Flow cytometry</i> .....	159
5.1.4	<i>DNA sequencing</i> .....	162
5.2	INTRODUCTION .....	165
5.2.1	<i>Motivation</i> .....	165
5.2.2	<i>Aims</i> .....	165
5.2.3	<i>Objectives</i> .....	166
5.3	MATERIALS AND METHODS.....	166
5.3.1	<i>Materials</i> .....	166
5.3.2	<i>THP-1 cells</i> .....	166
5.3.3	<i>Cobalt toxicity assay- establishing lethal conditions</i> .....	166
5.3.4	<i>Toronto KnockOut (TKO) library transduction</i> .....	167
5.3.5	<i>Screening assay and optimisation</i> .....	169
5.3.6	<i>DNA amplification and sample preparation</i> .....	171
5.3.7	<i>Next-generation sequencing and data analysis</i> .....	174
5.3.8	<i>Study design flowchart</i> .....	176
5.4	RESULTS .....	176
5.5	DISCUSSION.....	178
5.5.1	<i>Study limitations</i> .....	179
5.6	CONCLUSION.....	180

**CHAPTER 6: DEFINING A REFERENCE RANGE FOR BLOOD AND PLASMA TITANIUM IN THA PATIENTS.....181**

6.1	INTRODUCTION .....	183
6.1.1	<i>Motivation</i> .....	183
6.1.2	<i>Aim</i> .....	184
6.1.3	<i>Objectives</i> .....	184
6.2	PATIENTS AND METHODS.....	184
6.2.1	<i>Implants</i> .....	185
6.2.2	<i>Radiographs</i> .....	185
6.2.3	<i>Oxford Hip Score</i> .....	186
6.2.4	<i>UCLA activity score</i> .....	187
6.2.5	<i>Blood sampling and trace element analysis</i> .....	188
6.2.6	<i>Statistical analysis</i> .....	190
6.2.7	<i>Study design flowchart</i> .....	191
6.3	RESULTS .....	191
6.3.1	<i>Radiographs</i> .....	192
6.3.2	<i>OHS</i> .....	194
6.3.3	<i>Blood and plasma titanium levels</i> .....	194
6.4	DISCUSSION.....	197
6.4.1	<i>Study limitations</i> .....	198
6.5	CONCLUSION.....	199
<b>CHAPTER 7: CONCLUSIONS AND FUTURE WORK .....</b>		<b>201</b>
<b>APPENDIX A .....</b>		<b>207</b>
A.1.	STUDY DESCRIBED IN CHAPTER 3. ....	209
A.1.1.	<i>Ethical approval</i> .....	209
A.1.2.	<i>Study documentation</i> .....	212
A.2.	STUDY DESCRIBED IN CHAPTER 6. ....	216
A.2.1.	<i>Ethical approval</i> .....	216
A.2.2.	<i>Study documentation</i> .....	219
<b>APPENDIX B .....</b>		<b>223</b>
<b>BIBLIOGRAPHY .....</b>		<b>227</b>

## **Acronyms and Abbreviations**

**ABSU**- absorbance units

**ALTR**- adverse local tissue reaction

**ALVAL**- aseptic lymphocyte-dominated vasculitis associated lesion

**ARMD**- adverse reaction to metal debris

**ASR**- Articular Surface Replacement

**ASTM**- American Society for Testing Materials

**BHR**- Birmingham Hip Resurfacing

**Cas**- CRISPR-associated

**CKD**- chronic kidney disease

**CMR**- cardiac magnetic resonance

**CoC**- ceramic-on-ceramic

**CoM**- ceramic-on-metal

**CoP**- ceramic-on-polyethylene

**CRISPR**- clustered regularly interspaced short palindromic repeats

**DMEM**- Dulbecco's modified eagle medium

**DMT-1**- divalent metal transporter-1

**DN-10**- Douleur Neuropathique-10

**DNA**- deoxyribonucleic acid

**DNS**- Diabetic Neuropathy Score

**DRAQ7**- deep red anthraquinone 7

**EDTA**- ethylenediaminetetraacetic acid

**EF**- ejection fraction

**EKG**- electrocardiogram

**EXAFS**- extended X-ray absorption fine structure

**FACS**- fluorescence-activated cell sorting

**FCS**- foetal calf serum

**FSC**- forward scatter

**FU**- follow-up

**GF AAS**- graphite furnace atomic absorption spectrometry

**HA**- hip arthroplasty

**HDR**- homology-directed repair

**HEK**- human embryonal kidney

**HIF-1**- hypoxia-inducible factor-1

**HR**- hip resurfacing

**HXLPE**- highly cross-linked polyethylene

**IARC**- International Agency for Research on Cancer

**ICP-MS**- inductively-coupled plasma mass spectrometry

**ICP-OES**- inductively-coupled plasma optical emission spectroscopy

**IL**- interleukin

**IMA**- ischaemia-modified albumin

**ISO**- International Organisation for Standardization

**IQR**- interquartile range

**LoD**- limit of detection

**LVAD**- left ventricular assist device

**MMSE**- Mini Mental State Examination

**MoM**- metal-on-metal

**MoP**- metal-on-polyethylene

**NGS**- next generation sequencing

**NHEJ**- non-homologous end joining

**NJR**- National Joint Registry

**NSC-60**- Neurotoxic Symptom Checklist-60

**OA**- osteoarthritis

**OHS**- Oxford Hip Score

**P/S**- penicillin/streptomycin

**PCR**- polymerase chain reaction

**RA**- rheumatoid arthritis

**ROS**- reactive oxygen species

**RBC**- red blood cells

**RPM**- revolutions per minute

**RPMI**- Roswell Park Memorial Institute

**SD**- standard deviation

**sgRNA**- single guide ribonucleic acid

**SNP**- single-nucleotide polymorphism

**SSC**- side scatter

**THA**- total hip arthroplasty

**TKA**- total knee arthroplasty

**TKO**- Toronto KnockOut

**TLR4**- toll-like receptor 4

**TMZF**- titanium-12 molybdenum-6 zirconium-2 iron

**TNF- $\alpha$** - tumour necrosis factor- $\alpha$

**TPE**- therapeutic plasma exchange

**UHMWPE**- ultra-high molecular weight polyethylene

**VEGF**- vascular endothelial growth factor

**XANES**- X-ray absorption near-edge spectroscopy

**XRF**- X-ray fluorescence

**ZTA**- zirconia-toughened alumina

# List of Figures

Figure 2.1. Cross-sectional view of the hip joint (reproduced from stanfordhealth.org). .....	37
Figure 2.2. Movements of the hip joint (adapted from brooksidepress.org). .....	38
Figure 2.3. Total hip replacement (left) <i>versus</i> hip resurfacing (right) (reproduced from adam.com). .....	39
Figure 2.4. The most common hip implant articulations: (from the left) metal-on-metal, ceramic-on-ceramic, metal-on-polyethylene and ceramic-on-polyethylene (reproduced from orthobullets.com). .....	41
Figure 2.5. Components of a conventional THA (adapted from dhallaorthopediccenter.com). .....	43
Figure 2.6. Percentage of primary hip replacements in the UK by bearing type (based on NJR 15 <sup>th</sup> Annual Report 2018). .....	43
Figure 2.7. Summary of the proposed local and systemic adverse effects of hip implant-derived metal debris. ....	46
Figure 2.8. Cellular uptake of cobalt. ....	50
Figure 2.9. Pathways of HIF-1 induction. While HIF-1 signalling is normally induced by low tissue oxygen (hypoxia), cobalt ions can activate this pathway even in times of normal oxygen, leading to transcription of genes that promote cell survival. ....	67
Figure 2.10. Cellular uptake and reduction of different forms of chromium. Pink rectangles represent toxic by-products of Cr <sup>VI</sup> reduction. ....	71
Figure 2.11. Distribution of blood cobalt and chromium levels in a Finnish population of 692 patients with unilateral MoM HR (top) and 1056 patients with unilateral MoM THA (bottom) (reproduced with permission of Coxa Hospital, Finland). .....	84
Figure 3.1. Diabetic Neuropathy Score. ....	107
Figure 3.2. Systemic Symptom Checklist. ....	108



Figure 3.3. The English version of Douleur Neuropathique-10. ....	109
Figure 3.4. Mini Mental State Examination.....	110
Figure 3.5. Flowchart outlining participant enrolment and clinical assessment.....	111
Figure 3.6. Comparison of median total NSC-60 scores (top) and symptom scores (bottom) between the two study groups. Asterisks indicate statistically significant differences.....	113
Figure 3.7. Frequency of systemic toxicity symptoms reported in the two study groups (results are expressed as percentages). Asterisks denote statistically significant differences.....	115
Figure 4.1. The electromagnetic spectrum. Synchrotron light mainly consists of X-ray radiation, which has a sufficiently short wavelength to be used to probe the properties of matter (adapted from kisspng.com). ....	123
Figure 4.2. A schematic summary of the different components of Diamond synchrotron (reproduced from diamond.ac.uk).....	124
Figure 4.3. Experimental hutch of the I18 beamline (reproduced from diamond.ac.uk). ....	125
Figure 4.4. Schematic overview of the I18 beamline, showing the principal optical elements used to focus the beam. The distances given are measured from the beamline extraction point in the storage ring undulator (reproduced from diamond.ac.uk). ..	126
Figure 4.5. Diagram outlining the principles of X-ray fluorescence, using a cobalt-containing sample as an example. The incident X-ray beam has to be set to energy higher than the binding energy of the target electron shell to generate X-ray fluorescence. ....	127
Figure 4.6. The most important X-ray energy lines with their transitions in Siegbahn notation.....	127
Figure 4.7. An XAS spectrum, with the XANES and EXAFS portions identified.	129
Figure 4.8. Flowchart of study design.....	132

Figure 4.9. Schematic overview of the tissue sample preparation process. H&E-haematoxylin and eosin.....	133
Figure 4.10. A laser ablation ICP-MS scan in progress. The laser follows the path of the green lines to ablate tissue material from the selected area. ....	135
Figure 4.11. Schematic bird’s eye view of the experimental setup. The sample was placed on a sample stage, at 45° to both the incoming X-ray beam and the fluorescence detector. Regions of interest were identified with a movable optical microscope. .	137
Figure 4.12. Raw data processing in PyMCA. A representative area in the raw XRF map (top) was viewed in the RGB imaging mode: cobalt, chromium and titanium “hotspots” are shown in red, green and blue, respectively (bottom). Cobalt and chromium appear to be co-localised. ....	138
Figure 4.13. Quantifying metal “hotspots” in PyMCA. A “hotspot” of co-localised cobalt and chromium is shown on the right: the Data Max column displays relative element concentrations as mass fractions. ....	139
Figure 4.14. A representative image of a spleen tissue section (magnification 20x). Arrows indicate fine particulate deposits.....	141
Figure 4.15. Isotope distribution maps of a) spleen, b) liver and c) heart tissue from the current series. Arrows indicate cobalt/chromium deposits. ....	142
Figure 4.16. XRF map of a) spleen (2×4 mm, 5 µm step size), b) liver (2×4 mm, 5 µm step size) and c) heart tissue (2×4 mm, 3 µm step size) from the current series. Co, Cr and Ti deposits are shown in red, green and blue, respectively. Yellow spots indicate highly co-localised cobalt and chromium. In each image, brightness and contrast have been adjusted to improve visibility of the described features (reproduced from Journal of Trace Elements in Medicine and Biology [271]). ....	143
Figure 4.17. Stacked XAS spectra recorded at the K-edge of eight tissue chromium “hotspots”, along with spectra for six chemical standards. The top three traces are Cr <sup>III</sup> -like, fourth one resembles metallic-like Cr, while the bottom four spectra resemble the Cr <sup>VI</sup> standard. Arrows draw attention to the pre-edge peaks (adapted from Journal of Trace Elements in Medicine and Biology [271])......	146

Figure 4.18. Replicate XANES spectra of the different Cr forms found in the tissue samples. The second scan (red line) was performed at the same spot, within 20 min of the initial scan (black line). The pre-edge peaks are emphasised on the right to highlight how their profiles differ between the replicate scans (adapted from Journal of Trace Elements in Medicine and Biology [271]). ..... 146

Figure 4.19. Comparison of  $k^2$ -weighted (left) and Fourier-transformed (right) EXAFS spectra for a chromium species in splenic tissue of Patient 1 (solid line), with that of  $\text{Cr}(\text{H}_2\text{O})_6$  (dashed line). The Cr-O distance is 1.97Å, but the corresponding peak is shifted inward due to phase shift (adapted from Journal of Trace Elements in Medicine and Biology [271]). ..... 147

Figure 4.20. Stacked XAS spectra recorded at the K-edge of six tissue cobalt "hotspots", along with chemical standards. The top two traces correspond to metallic-like cobalt that was oxidised by the beam in the duplicate scan (red line). MPG- N-(2-mercaptopropionyl)glycine (a Co-peptide mimetic) (adapted from Journal of Trace Elements in Medicine and Biology [271]). ..... 148

Figure 4.21. Stacked XAS spectra recorded at the K-edge of thirteen tissue titanium "hotspots", along with chemical standards. All spectra are representative of  $\text{TiO}_2$ - the top nine traces feature rutile-like pre-edge peaks (A2,A3), while the bottom four display anatase-like pre-edge features (A1,A2,A3) (adapted from Journal of Trace Elements in Medicine and Biology [271]). ..... 149

Figure 4.22. Diagram showing a trivalent (left) and a hexavalent (right) chromium complex. The octahedral  $\text{Cr}^{\text{III}}$  has a centre of symmetry, which disallows the  $1s \rightarrow 3d$  electronic transition. Tetrahedral  $\text{Cr}^{\text{VI}}$  is non-centrosymmetric and partially allows this transition, giving rise to a sharp pre-edge absorption in the XANES spectrum. .... 150

Figure 5.1. CRISPR/Cas9 genome editing technology. An RNA "guide" molecule can be synthesised to match any unique DNA sequence in the human genome (top). Combining the guide RNA with Cas9- a specialised DNA-cleaving enzyme- allows the complex to home in on the DNA sequence of interest and cut both strands of the double helix (middle). Repair of the broken DNA results in silencing/modification of the target gene, or introduction of extra DNA (bottom). ..... 158

Figure 5.2. Schematic overview of a typical flow cytometry setup. As the sheath fluid moves, it exerts a drag effect on the central fluid, creating a single file of cells (hydrodynamic focusing). Each individual cell is interrogated by one or more laser beams. Light scattered in the forward and side direction is detected by the corresponding detectors (FSC and SSC, respectively), and provides information about cell size and granularity. Fluorescence measurements taken at different wavelengths (FD1-FD4) inform about fluorochrome-labelled proteins or DNA. .... 160

Figure 5.3. Flow cytometric analysis of bone marrow aspirate, demonstrating the characteristic position of different cell populations. Granulocytes, which are the biggest and most granular while blood cell type, produce the largest forward and side scatter (adapted from Riley and Idowu “Principles and Applications of Flow Cytometry”). ..... 161

Figure 5.4. Principles of fluorescence assisted cell sorting. As cells exit the instrument nozzle, they are charged according to pre-set criteria. Positively and negatively charged voltage plates direct the cells into different containers. .... 161

Figure 5.5. Simplified diagram of DNA structure (adapted from bioninja.com.au). ..... 162

Figure 5.6. Gel electrophoresis of dideoxy-terminated DNA chains. Negatively-charged DNA migrates towards the positively charged end of the electrophoresis plate. Shorter DNA bands are lighter, and travel further, while the longer strands lag behind, resulting in a separation of all the fragments according to their length. Fluorescence emitted by the dideoxynucleotides is detected by the sequencing machine, and the DNA sequence read from the bottom of the plate. .... 163

Figure 5.7. Cluster formation in NGS. Sample DNA is denatured and hybridized to complementary adapter oligonucleotides on the flow cell. Complementary strands are extended, amplified *via* bridge amplification and denatured, resulting in clusters of identical single-stranded library fragments (adapted from Chaitankar *et al.* [424]). ..... 164

Figure 5.8. Cluster sequencing in NGS. Fragments are primed and extended utilising fluorescently-labelled reversible terminator nucleotides. Each newly added nucleotide is interrogated with a laser, and an image of emitted fluorescence captured from each

cluster, so that the identity of each base pair can be recorded (adapted from Chaitankar <i>et al.</i> [424]).....	164
Figure 5.9. Viability of TKO-transduced THP-1-Cas9 cells <i>versus</i> control after lethal Co <sup>II</sup> insult (DRAQ7 stain). The circled area, which was absent in non-TKO transduced cells, might represent surviving cells that are resistant to cobalt-induced cell death. ....	169
Figure 5.10. Validation of the staining protocol: a) fluorescence emitted by DRAQ7 and PI remained stable over a 2-hour period, b) DRAQ7/PI staining did not cause cytotoxicity after a 5-day incubation. ....	170
Figure 5.11. Viability of TKO-transduced THP-1-Cas9 cells after lethal Co <sup>II</sup> insult (DRAQ7+PI stain). ....	170
Figure 5.12. Bioanalyser results for the library and sorted cell DNA samples. The x-axis shows DNA size in base pairs (bp), while y-axis measures DNA fluorescence in fluorescence units (FU). Standards include a 35 bp lower marker (green) and 10,380 bp upper marker (purple). Corresponding gel image for the bioanalyser trace is shown on the right. The average fragment size was 175 and 176 bp for the library and sorted cells, respectively. ....	174
Figure 5.13. Flowchart outlining the principles of the CRISPR/Cas9 cobalt toxicity assay. ....	176
Figure 6.1. The implant design featured in the current study. Reproduced from Journal of Trace Elements in Medicine and Biology [430]. ....	185
Figure 6.2. Oxford Hip Score. ....	187
Figure 6.3. UCLA Activity Score. ....	188
Figure 6.4. Flowchart outlining participant enrolment and clinical assessment. Reproduced from Journal of Trace Elements in Medicine and Biology [430]. ....	191
Figure 6.5. A representative anteroposterior radiographs from the current series, showing a well-fixed hip implant. Reproduced from Journal of Trace Elements in Medicine and Biology [430]. ....	193

Figure 6.6. A radiologically loose stem. The arrow shows a radiolucent line indicative of bone loss at the bone-stem interface. Reproduced from Journal of Trace Elements in Medicine and Biology [430]. ..... 193

Figure 6.7. Histograms showing the spread of a) blood and b) plasma titanium measurements in the current series, with the 75<sup>th</sup> percentile+ 3IQR level marked. Reproduced from Journal of Trace Elements in Medicine and Biology [430]. ..... 194

Figure 6.8. Box plots of titanium concentration in a) blood and b) plasma of study participants. The boundaries of the box represent the 25<sup>th</sup> and 75<sup>th</sup> percentile, with the median line inside the box. The whiskers extend to maximum and minimum values in each data set. Outliers (values more than 1.5IQR from the end of the box) are identified as open circles, while extreme outliers (values more than 3IQR from the end of the box) are denoted as asterisks. Reproduced from Journal of Trace Elements in Medicine and Biology [430]. ..... 195

Figure 6.9. Scatter plot of plasma *versus* blood titanium, showing a moderately strong, positive correlation between the two ( $R^2= 0.58$ ;  $p<0.0001$ ). Reproduced from Journal of Trace Elements in Medicine and Biology [430]. ..... 196

Figure 6.10. Scatter plot showing a weak, negative relationship between plasma titanium and increasing length of follow-up ( $R^2=0.02$ ;  $p=0.002$ ). ..... 196

Figure 7.1. Summary of completed steps (green arrows) and suggested future work (orange arrows). ..... 205

Figure 7.2. Plain radiograph showing a worn polyethylene liner (red circle). The associated blood titanium level ( $6 \mu\text{g L}^{-1}$ ) was elevated with respect to the threshold value derived in this thesis ( $2.2 \mu\text{g L}^{-1}$ ). ..... 206

## List of Tables

Table 2.1. Advantages and drawbacks of the different hip implant bearing couples.	40
Table 2.2. Reported cases of systemic toxicity associated with elevated cobalt levels from hip implants. ....	54
Table 2.3. Examples of techniques used to study metal composition of human tissue samples, and the information they can provide.....	76
Table 2.4. The most important spectral interferences affecting cobalt, chromium and titanium measurement by ICP-MS.....	80
Table 2.5. Blood ion levels measured in patients with different types of well-functioning and malfunctioning hip implants. ....	86
Table 2.6. Proposed blood/serum cobalt threshold levels to warrant systemic toxicity investigations. ....	89
Table 2.7. Blood/serum titanium levels associated with different types of well-functioning hip implants (all measured by high resolution ICP-MS).....	91
Table 2.8. Blood/serum Ti levels associated with different modes of failure of hip implants.....	92
Table 3.1. Implant details (MoM cohort).....	101
Table 3.2. Neurotoxic Symptom Checklist-60 in Dutch (original) and in English.	103
Table 3.3. Summary of participant demographics. ....	112
Table 3.4. Median NSC-60 cluster scores in relation to their clinically important thresholds. ....	114
Table 3.5. Summary of DNS and DN-10 results in the two study groups.....	114
Table 4.1. Characteristic excitation energies for cobalt, chromium and titanium (eV). ....	128

Table 4.2. Characteristic X-ray line energies for cobalt, chromium and titanium (eV). .....	129
Table 4.3. Implant materials and the patients' clinical data. Source: Journal of Trace Elements in Medicine and Biology [271]. .....	134
Table 4.4. LA ICP-MS operating parameters. ....	136
Table 4.5. Relative element counts in the highest intensity spots of the different XRF maps. ....	144
Table 4.6. Cardiac cobalt levels and associated toxicity symptoms (reproduced from the Journal of Trace Elements in Medicine and Biology [271])......	151
Table 5.1. The effect of increasing cobalt ion concentration on THP-1-Cas9 cell viability (24 h/48 h incubation, DRAQ7 stain).....	167
Table 5.2. PCR1 reaction components.....	171
Table 5.3. Thermocycler conditions for PCR1. ....	172
Table 5.4. PCR2 reaction components.....	173
Table 5.5. Thermocycler conditions for PCR2. ....	173
Table 5.6. The ten most highly over-represented genes and the protein products they encode. ....	176
Table 5.7. Depleted genes targeted by three independent guides. ....	177
Table 6.1. Patient demographics. ....	184
Table 6.2. Results submitted by the laboratory to the QMEQAS, the value assigned by QMEQAS, and the range considered acceptable by QMEQAS. The percentage bias of the submitted results compared to the assigned value is also shown.....	189
Table 6.3. Isotopes measured and ICP-MS settings used. ....	190
Table 6.4. Summary of study results.....	192



# **Chapter 1**

## **Introduction**



## 1.1 MOTIVATION

Hip arthroplasty is considered to be the most successful and cost-effective orthopaedic intervention of all time. It relieves arthritic pain and improves the quality of life of hundreds of thousands of patients every year. According to the National Joint Registry (NJR), 100,000 hip replacement procedures are carried out annually in the United Kingdom alone.

The surgery involves removing either part (hip resurfacing), or all (total hip arthroplasty), of the diseased joint surface, and replacing it with synthetic equivalents. Components of hip replacement implants are usually manufactured from cobalt-chromium and titanium alloys. Despite favourable mechanical properties, the metals are not inert and, once implanted, undergo a combination of wear and corrosion (tribocorrosion). Tribocorrosion releases metal particles and ions into the local tissue and blood, which can cause local and systemic/organ toxicity, particularly if the levels are high. There are reports of cardiomyopathy, neurotoxicity, and/or hypothyroidism associated with elevated blood cobalt concentrations, which may not resolve completely even after removal of the implant. Cobalt levels do not always correlate with the severity of reported toxicity symptoms, which could mean that confounding factors and/or genetic factors are involved.

The UK government health regulator, the Medicines and Healthcare products Regulatory Agency (MHRA), advise that blood cobalt/chromium levels of over  $7 \mu\text{g L}^{-1}$  can be indicative of local tissue damage, but there is no threshold to inform on the risk of systemic toxicity. Additionally, a normal reference range hasn't been established for blood titanium.

Constant ageing of the population means that the overall demand for hip replacements is on the rise. Moreover, since indications for hip replacement are increasingly being offered to younger patients (<60 years old), the mean length of exposure to metal debris is also expected to increase.

## 1.2 AIM

To better understand how cobalt, chromium and titanium, derived from hip implants, affect the body's organs, and what blood levels are related to any toxicity symptoms.

### 1.3 OBJECTIVES

- To assess the prevalence of systemic toxicity complaints and cognitive decline in patients with a history of markedly elevated blood cobalt levels, using self-assessment questionnaires and a mental state examination.
- To 1) map cobalt, chromium and titanium deposits in vital organs of hip arthroplasty patients, using micro-X-ray fluorescence, and 2) determine their chemical speciation using micro-X-ray absorption spectroscopy.
- To use CRISPR/Cas9 gene editing technology to carry out a feasibility study into genes that might confer a higher susceptibility to cobalt-induced cell death.
- To 1) accurately measure blood and plasma titanium content in patients with well-functioning hip implants, and 2) correlate the results with patient age, implant time *in situ* and activity level.

### 1.4 THESIS OUTLINE

This thesis begins with a thorough review of cobalt, chromium and titanium in hip arthroplasty, which is followed by four experimental chapters.

Chapter 3 discusses the results of an observational case-control study that aimed to estimate the prevalence of neurotoxicity symptoms and cognitive decline in hip replacement patients with markedly elevated blood cobalt levels.

Chapter 4 is preceded by a background to synchrotron spectroscopy techniques, and details an investigation into the exact chemical form of cobalt, chromium and titanium in the heart, liver and spleen of patients with metal hip implants.

Chapter 5 is preceded by a short background to CRISPR/Cas9 genome editing technology, and describes an exploratory *in vitro* study into genes that could potentially predispose to cobalt-induced adverse reactions.

Chapter 6 reports on a large population study, which aimed to define a reference range for blood and plasma titanium in patients with well-functioning titanium-based implants.

Conclusions and future work are discussed in Chapter 7.

Appendix A contains ethical approvals and study documentation, while Appendix B lists the publications, conferences and awards related to the work presented in this thesis.

## **1.5 ETHICAL APPROVAL**

All investigations were conducted in conformity with ethical principles of research.

The study described in Chapter 3 required a new ethics application, which was prepared entirely by the author of this thesis. The application was approved by Leeds East Research Ethics Committee on 16/07/2018, and by Health Research Authority on 13/08/2018 (18/YH/0245) (see Appendix A.1. for study documentation and ethical approval).

The tissue samples featured in Chapter 4 were obtained from The Mayo Clinic (Rochester, MN, US), and used with approval of their Institutional Review Board (16-005246).

The study described in Chapter 6 required a substantial amendment to existing ethics, to allow for collection of blood samples from subjects with well-functioning hip implants. The amendment was prepared entirely by the author of this thesis, and granted by London-Riverside Research Ethics Committee on 30/07/18 (07/Q0401/25) (see Appendix A.2. for study documentation and ethical approval).

Informed written consent was obtained from all subjects for participation in the study.



# **Chapter 2**

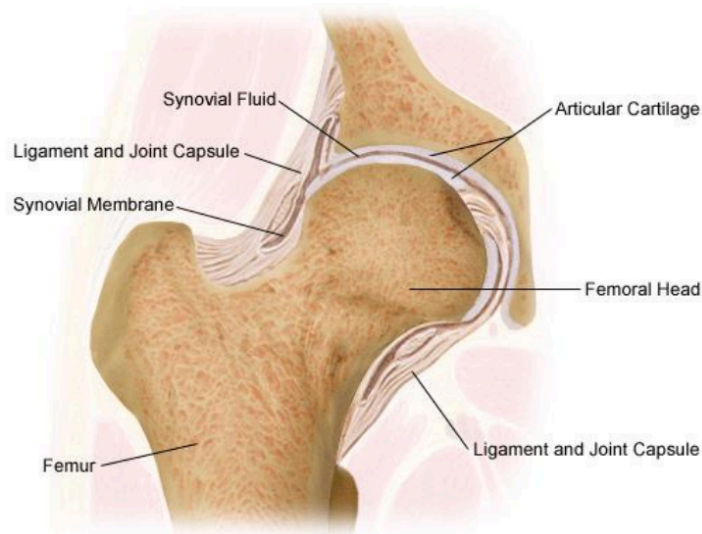
## **Literature review**





## 2.1 THE HIP JOINT

The hip joint forms between the concave structure on the pelvis (acetabulum) and the head of the thigh bone (femur), and is the second largest joint in the human body after the knee (Figure 2.1). Both the femoral head and the acetabulum are lined with articular cartilage, which cushions the ends of the bones, as well as providing a smooth surface for the two components to glide against. The movement is facilitated by synovial fluid (watery, lubricating liquid secreted by synovial membranes), while stability is provided by tough ligaments, tendons and muscles that surround the joint.



**Figure 2.1. Cross-sectional view of the hip joint (reproduced from stanfordhealth.org).**

Blood is supplied to the hip joint primarily by the medial and lateral circumflex femoral arteries (branches of the deep femoral artery) and artery to the head of femur (branch of the obturator artery), while innervation comes from the femoral, obturator, gluteal and sciatic nerves. These same nerves innervate the knee, which explains why hip pain can be referred to the knee, and *vice versa* [1].

The chief function of the hip joint is to weight-bear and maintain balance. The multi-axial ball-and-socket design accommodates a wide range of movement: flexion and extension, abduction and adduction, outward/inward rotation and circumduction (360° movement of the leg), allowing people to walk, run, and carry out a variety of other activities (Figure 2.2).

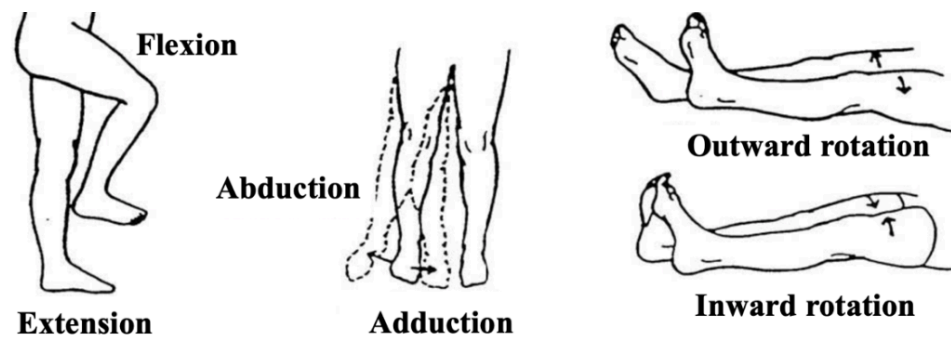


Figure 2.2. Movements of the hip joint (adapted from brooksidepress.org).

### 2.1.1 Common disorders of the hip joint

As a major weight-bearing joint, the hip is prone to osteoarthritis (OA)- a chronic condition that causes the articular cartilage to wear down. Without the protective layer, the bones rub against one another leading to pain, stiffness and reduced range of motion. The exact cause of OA is unclear, but known risk factors include advanced age, obesity, joint overuse and family history.

Rheumatoid arthritis (RA) is an autoimmune disorder characterised by the production of antibodies that attack healthy joint tissue, and is similar to OA in that both diseases produce hip pain and inflammation.

If blood supply to the femoral head is interrupted, the bone tissue can die, causing avascular necrosis. The underlying nature of the disease is poorly understood, but it is thought that several risk factors, including corticosteroid use, alcoholism and trauma, can be implicated in its development [2].

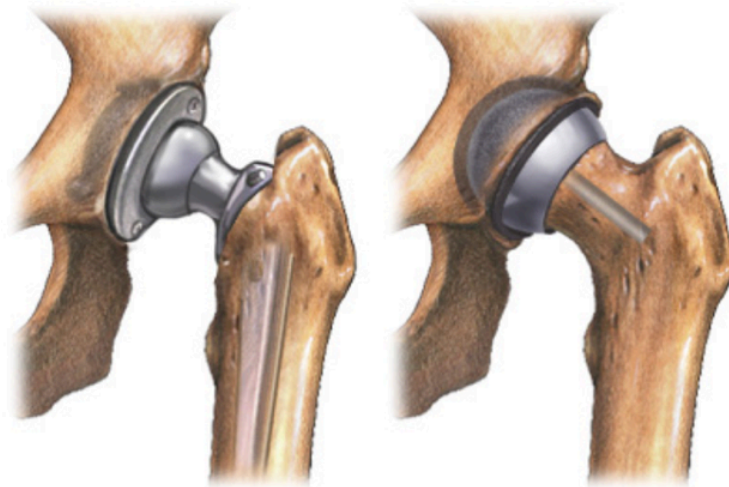
Developmental dysplasia of the hip is an example of a congenital hip disorder, whereby the acetabulum doesn't form properly in babies or young children. The socket is too shallow to fully accommodate the femoral head, resulting in instability and easy dislocation. The altered hip anatomy accelerates joint "wear and tear" and might cause early onset OA.

In addition to arthritis, avascular necrosis and developmental hip dysplasia, femoral neck fractures are the most frequent indications for hip replacement surgery [3].

### 2.1.2 Hip replacement surgery

Hip replacement is one of the most common orthopaedic operations of all time, with over 75,000 procedures performed each year within the National Health Service [4]. It is a safe and effective intervention that helps to alleviate pain and restore hip function, allowing its recipients to regain their former quality of life. During the surgery, either a part, or all of the diseased joint surface, is removed and replaced with synthetic components.

Modern hip implants consist of two basic parts: the ball (femoral head), which can be made from metal or ceramic, and the socket (acetabular cup), which is usually manufactured from metal. In most implant designs, a ceramic or plastic liner is fastened into the metal cup to allow the femoral head to glide easier. In total hip arthroplasty (THA), a long metal stem is introduced into the femur, which links with the femoral head *via* a tapered neck. This is in contrast to hip resurfacing (HR), whereby the patient's femoral head is simply reshaped and capped with a metal covering (Figure 2.3).



**Figure 2.3. Total hip replacement (left) versus hip resurfacing (right) (reproduced from adam.com).**

While both procedures are highly successful, they display unique advantages and disadvantages. By allowing the use of larger diameter femoral components and preserving the femur, HR is believed to reduce the risk of dislocation and the likelihood of post-operative leg length discrepancy. Additionally, the bone-sparing nature of HR makes it a suitable treatment option in younger, more active patients

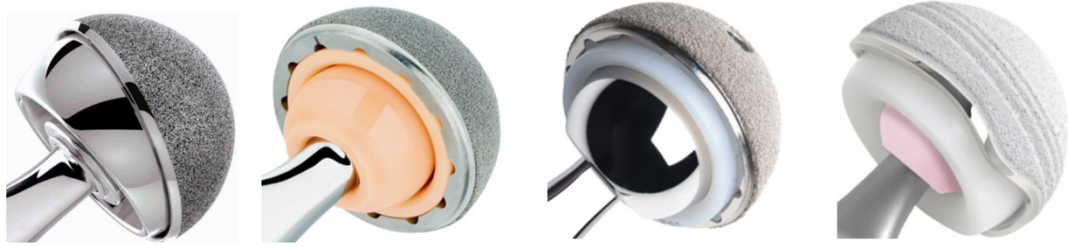
[5,6]. Despite these benefits, HR can increase the risk of femoral neck fracture [7] and adverse reactions to metal debris [8], which has led to a decline in the use of this construct in favour of conventional stemmed THA. According to the NJR, HR accounted for only 4% of all primary hip replacement procedures performed in the UK in 2018 [9].

Depending on the material combination used in the bearing surface (articulation), joint implants are classified as metal-on-metal (MoM), ceramic-on-ceramic (CoC), metal-on-polyethylene (MoP), ceramic-on-polyethylene (CoP) or ceramic-on-metal (CoM) (Figure 2.4). The advantages and drawbacks of each combination are summarised in Table 2.1.

**Table 2.1. Advantages and drawbacks of the different hip implant bearing couples.**

<b>Articulation</b>	<b>Advantages</b>	<b>Drawbacks</b>
<b>MoP (CoCr on HXLPE)</b>	Longest track record Lowest cost	Polyethylene debris linked to osteolysis
<b>MoM (CoCr on CoCr)</b>	Lower volumetric wear rate and potentially longer lifespan than MoP  Use of larger head sizes possible, leading to lower risk of dislocation than MoP	Metal debris linked to local and systemic toxicity symptoms  The highest risk of hypersensitivity (metal allergy) reactions
<b>CoC (ZTA on ZTA)</b>	Best wear properties and longest lifespan  The most biologically inert	Require expert insertion to prevent early damage  Can produce squeaking sounds on movement  The most expensive
<b>CoM (ZTA on CoCr)</b>	Lower wear rate than MoM Lower risk of squeaking than CoC	Elevated blood metal ion level Limited clinical data to support favourable <i>in vitro</i> results
<b>CoP (ZTA on HXLPE)</b>	Lower wear rate than MoP	More expensive than MoP

CoCr- cobalt-chromium alloy, HXLPE- highly cross-linked polyethylene, ZTA- zirconia-toughened alumina.



**Figure 2.4. The most common hip implant articulations: (from the left) metal-on-metal, ceramic-on-ceramic, metal-on-polyethylene and ceramic-on-polyethylene (reproduced from orthobullets.com).**

There are several ways of attaching the implant to the skeleton. Traditionally, quick-drying cement was used to anchor the prosthesis to the remaining bone. Nowadays porous “press-fit” designs made of titanium and its alloys, which encourage bone ingrowth to secure the implants into place, are more widely used.

While generally extremely successful, hip replacement carries a risk of complications including infection, leg length discrepancy, deep vein thrombosis, nerve damage, implant malposition, bone resorption and periprosthetic fractures.

## **2.2 IMPLANT BIOMATERIALS**

### **2.2.1 A brief history of hip implants**

In 1891, a German surgeon, Themistocles Glück, carried out the first documented attempt at a hip arthroplasty using an ivory implant to replace the femoral head [10]. In the 1930s, hip implants made of cobalt-based alloy were introduced, and the first total hip replacements were performed in the 1950s, most notably by George McKee. While a large number of these implants achieved good long-term survival, the high rate of aseptic loosening (loss of implant fixation in the absence of infection) prompted the abandonment of MoM designs in favour of the low friction MoP arthroplasty pioneered by Sir John Charnley [11]. Charnley’s joint, which comprised a stainless steel stem, a small diameter (22 mm) femoral head and an ultra-high molecular weight polyethylene (UHMWPE) liner, was remarkably successful, with reports of excellent patient function after as long as 25 years [12]. However, micrometer-sized UHMWPE wear debris was shown to cause osteolysis and implant failure- particularly in younger, active patients. Introduction of improved, “second-generation” MoM implants in the 1990s was aimed at minimising the incidence of this adverse effect. While bone loss

was rarely seen with these joints, concerns over the release of nanometer-sized metal debris, and its carcinogenic potential, were raised. This led to the rise in popularity of ceramic implants, first introduced by Pierre Boutin in 1970. The tissue reaction to ceramic wear debris was much less damaging to patients than that to MoM or polyethylene wear debris, but brittleness remained the main complication. The first generation of CoC implants displayed a high fracture rate (up to 13%), which was subsequently improved through research into more durable ceramics [13].

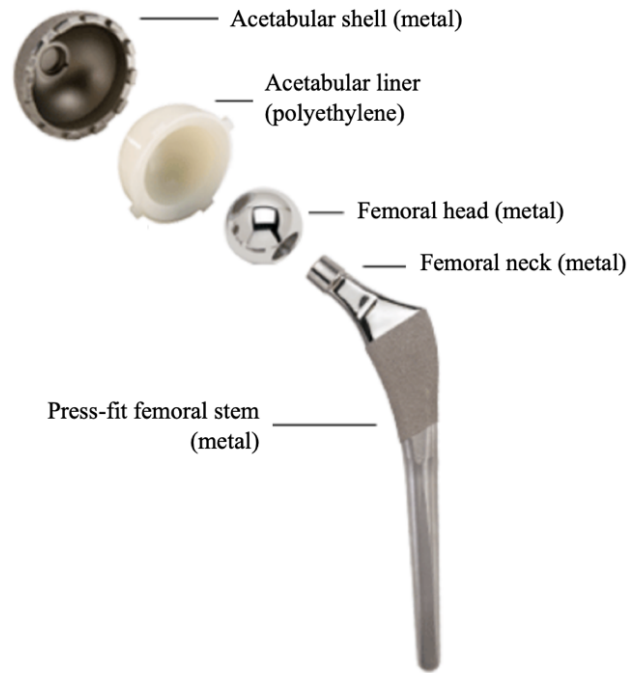
### *Implant modularity*

Early THA implants were of a one-piece design, which, despite reduced risk of breakage, permitted little intraoperative freedom. In the 1960s, the first modular implants became available, whereby the femoral head and stem were separate (head/neck modularity) [14]. This design enabled “mixing and matching” of components, and allowed the surgeons to replace the femoral head independently of the stem and *vice versa*, simplifying the surgical procedure.

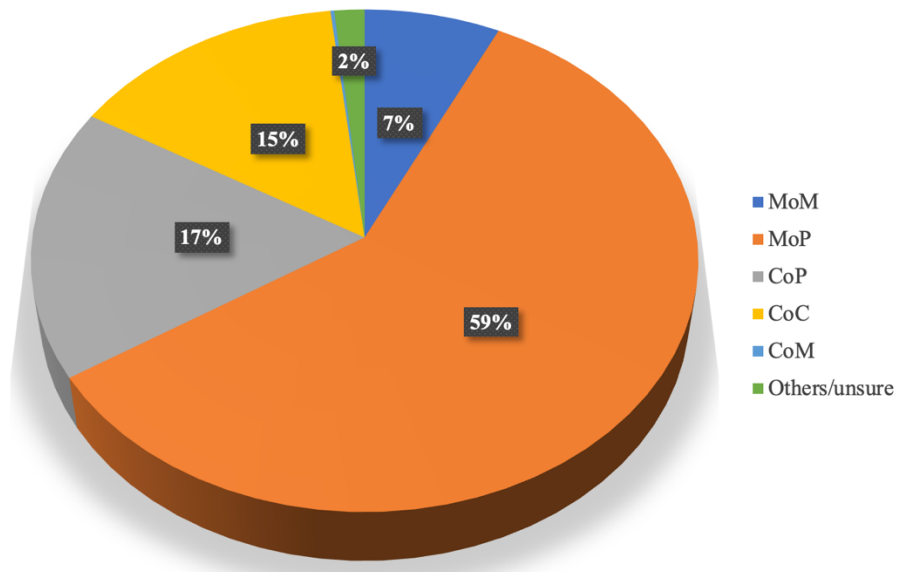
More recently, additional forms of implant modularity, such as dual modular femoral necks, were introduced. Neck/stem modularity allows for intraoperative customisation of leg length, femoral offset and version, with the aim to better reconstruct the natural biomechanics of the hip and enhance implant function [15]. Despite the perceived benefits, the neck/stem junction was particularly vulnerable to metal ion release, and promoted adverse local tissue reactions (ALTR) [16,17]. Cases of severe trunnion corrosion, leading to component dissociation and mechanical failure of the implant, have also been reported [18,19]. As a result of these complications, several authors have recommend against using stems with a modular neck-stem junction [20,21].

### **2.2.2 Modern hip replacement**

Nowadays, MoP implants make up the majority of THA undertaken in the UK (Figure 2.5), while the use of MoM prostheses has all but ceased. Owing to excellent biocompatibility and wear resistance, the use of modern ceramics (mainly zirconia-toughened alumina (ZTA)) is rapidly increasing (Figure 2.6).



**Figure 2.5. Components of a conventional THA (adapted from dhallaorthopediccenter.com).**



**Figure 2.6. Percentage of primary hip replacements in the UK by bearing type (based on NJR 15<sup>th</sup> Annual Report 2018).**

### 2.2.3 Metal

Hip implants are commonly manufactured from metal. Cobalt-based alloys, iron-based alloys and titanium-based alloys are popular because they are strong, elastic, and resistant to fracture and corrosion [22]. Although pure metals are sometimes used in

orthopaedic applications, other metals are usually added to improve the material's mechanical properties. The most important medical alloys are defined by the American Society for Testing Materials (ASTM) or International Organisation for Standardization (ISO).

Cobalt-based alloys contain 26–30% chromium, which facilitates the formation of a protective layer of chromium oxide on the product's surface. Addition of nickel at 3–5%, and molybdenum at 4–6%, serves to increase plasticity, and improve the material's technological properties [23]. The most widely used cobalt-based alloy is cobalt-28 chromium-6 molybdenum (CoCrMo), *i.e.* ASTM F75. The high carbon content (>0.20%) enhances wear-resistance, making it particularly suitable for the manufacture of bearing surfaces and modular necks.

Surgical or orthopaedic stainless steel (ASTM F55 and ASTM F138, respectively) is also used in the manufacture of hip implants. This iron-based alloy, which contains 17–20% chromium, 13–15% nickel and 2–3% molybdenum, is strong and relatively cheap to produce, but its wear characteristics and corrosion resistance are inferior to those of other orthopaedic alloys. Additionally, stainless steel has a marked allergenic potential due to the relatively high nickel content, which has further restricted its use as implant biomaterial [23].

Compared to cobalt and iron, titanium is softer and unsuitable for load-bearing applications. Additionally, it has a higher elastic modulus, which allows it to closely mimic the elasticity of bone. As a result, it is used exclusively in the production of non-moving parts of implants, whose fixation relies on bone integration *i.e.* femoral stems, acetabular cups and screws. Since commercially pure titanium (ASTM F67) is relatively soft, it is often combined with other metals to strengthen its fatigue resistance. The most widely used titanium-based alloys are titanium-6 aluminium-4 vanadium (TiAlV), *i.e.* ASTM F136, titanium-6 aluminium-7 niobium (TiAlNb), *i.e.* ASTM F1295 [24], and titanium-12 molybdenum-6 zirconium-2 iron (TMZF). The latter alloy, which was once a popular femoral stem material, is no longer used commercially due to reports of corrosion at the modular taper junctions when combined with CoCr femoral heads [25].

Despite excellent mechanical properties, metals are susceptible to corrosion once implanted into the body. This poses a risk of metal ion/particle release and ALTR,



which could be more pronounced in patients with a known allergy/hypersensitivity to a particular metal [26] (see Section 2.2.7).

#### **2.2.4 Polyethylene**

Ultra-high molecular weight polyethylene, as introduced by Sir John Charnley, still represents the gold standard as a bearing surface for THA. However, wear and generation of polyethylene particles limit the *in vivo* longevity of these joints. UHMWPE wear debris was linked to periprosthetic osteolysis and implant loosening, necessitating revision surgeries. To reduce the prevalence of this adverse effect, much effort has been made to improve the tribological properties of polyethylene. Irradiation cross-linking, followed by re-melting, increased wear resistance, but diminished the material's fatigue strength.  $\alpha$ -tocopherol (vitamin E) doping is an alternative to post-irradiation thermal processing, and serves to stabilise the highly-crosslinked polymer by protecting it from free radical oxidation [27]. Liners made of highly cross-linked polyethylene (HXLPE) have demonstrated excellent radiographic results and longevity.

#### **2.2.5 Ceramic**

Ceramic materials display increased hardness, improved lubrication and biological inertness compared to metal, making them an attractive choice for younger patient groups. While alumina ( $\text{Al}_2\text{O}_3$ ), zirconia (95%  $\text{ZrO}_2$ , 5%  $\text{Y}_2\text{O}_3$ ) and ZTA (82% alumina, 17% zirconia, trace amounts of strontium aluminate and chromium oxide) are the most commonly used ceramics in THA, other designs are also employed. For example, femoral heads coated with a layer of zirconium-niobium ( $\text{ZrNb}$ ) or silicon nitride ( $\text{Si}_3\text{N}_4$ ) have been developed.

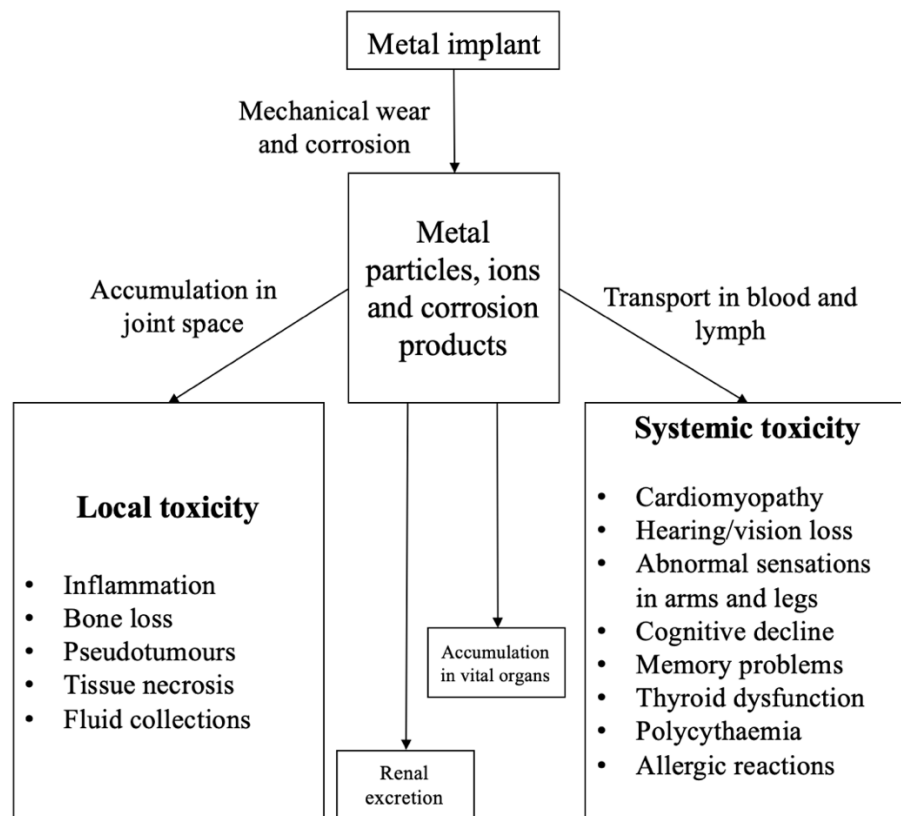
Despite excellent wear resistance, no ceramic material is unbreakable. It follows that correct insertion technique is particularly important with ceramic implants, as malpositioned components exhibit an increased risk of fracture.

#### **2.2.6 Implant biodegradation**

Cobalt-chromium-, titanium- and iron-based alloys are considered biocompatible due to the spontaneous formation of an oxide-rich passivation layer on their surface. This protective film forms a boundary at the interface between the biological medium and the implant, limiting corrosion and increasing the alloy's mechanical stability [28].

Once implanted, friction induces selective fractures of the surface layer, which can lead to high metal particle release and, in turn, local adverse tissue reactions. Moreover, both serum and interstitial fluid are rich in chloride ions and proteins, which cause metal ions and toxic corrosion products to be released from where the protective surface layer had been compromised. Though the film can regenerate itself, the low oxygen content of local tissue impairs the process.

The biodegradation products are complex and can include metal particles, metal-protein complexes, inorganic salts and free ions. These can remain in the joint space and cause local toxicity, or enter the lymphatic or vascular system to exert systemic effects (Figure 2.7). Most metal particles are phagocytosed by tissue-resident macrophages and dissolved in the acidic environment of their endosomes- a process which liberates more metal ions [29]. In cases of high metal debris release, the soft tissue surrounding the implant can take on a dark-grey metallic discolouration, which is commonly referred to as metallosis [30,31].



**Figure 2.7. Summary of the proposed local and systemic adverse effects of hip implant-derived metal debris. Systemic toxicity is only associated with cobalt, except for allergic reactions, which are primarily due to nickel.**

The amount of debris released at the different implant junctions (head/neck, neck/stem, stem/cement etc.), and its physicochemical characteristics, are dependent on several factors, including implant type, its positioning, the exact degradation mechanisms at play, as well as the patient's physical activity and state of health [32,33]. Particles generated through different wear processes can display different elemental composition [34,35], crystal structure [36,37], size [38,39] and shape [40], which might result in differing bioactivity. Particulate wear debris generated by MoM implants has an average particle size range of 30 to 100 nm [41]. Nanoparticles are thought to be generally more dangerous than coarser particles, because they enter cells more easily. The increased surface area-to-volume ratio, which provides a larger surface for ion release, also makes nanoparticles more reactive [42].

It is thought that free metal ions are the most toxicologically-relevant products of implant biodegradation [43], though the ability of different metal ions to exert adverse effects can vary dramatically. For example,  $\text{Ti}^{\text{IV}}$  is very active and readily combines with hydroxyl radicals and anions to form relatively harmless oxides and salts in the body. This means that the ion has little time to react with biomolecules. On the other hand, inactive ions, such as  $\text{Co}^{\text{II}}$ , do not immediately combine with water molecules and inorganic anions. They persist in the ionic state for a relatively long time and are more likely to interact with biomolecule to cause toxicity [44].

The quantity and type of ions released from different metal alloys depends on a multitude of variables, including local pH, protein and salt concentration, the metal's solubility, the quality of its surface oxide film and its regeneration time [45,46]. For example, the higher solubility of cobalt compared to chromium means that the former metal corrodes faster, leading to selective "leaching" of cobalt ions from cobalt-chromium alloys [47]. Titanium, which is the least soluble, and forms the most formidable protective oxide film with the shortest regeneration time, displays the highest corrosion resistance and biocompatibility [46].

### **2.2.7 Metal hypersensitivity**

Metal ions released from the implant can bind to proteins and form complexes that act as antigens for circulating lymphocytes. The resultant immune response may trigger localised inflammation and lead to unexplained implant loosening. It has been proposed that existing metal allergy could contribute to this process [48], but this has been challenged. A correlation of Danish Knee Arthroplasty Register and contact

allergy patch test database revealed that metal allergy was neither a general risk factor for failure of a total knee arthroplasty, nor a major contributor to its etiopathogenesis [49].

While nickel is the most commonly reported allergen, it is estimated that 2.4-3% of the general population is allergic to cobalt, and approximately 1% to chromium [50]. Patients suspected to have a contact allergy to a certain metal may develop joint pain, as well as eczema, urticaria, swelling and effusions, following the insertion of an implant that contains the metal. While skin changes are typically localised to implant site, reports of generalised skin rashes exist [51,52]. Implant-related hypersensitivity is difficult to diagnose and might be underreported. The relationship between contact allergy and deep tissue allergy is not well-defined, as patients testing positive for metal sensitivity pre-operatively often do not react to their metal prostheses [53,54] and *vice versa* [52]. It also remains a subject of debate whether metal hypersensitivity should impact treatment decisions and implant choice in prospective THA recipients.

Patch testing is the most popular test for metal sensitivity [55], though its applicability to the study of immune responses in deep tissue is highly debated, as the skin's antigen-presenting cells (the Langerhans cells) are not present in the periprosthetic environment [56]. The current consensus is that "hypoallergenic" materials (ceramic or ceramic-coated implants) should only be considered in patients with a documented allergy to a metal in the standard implant, e.g. in a metallic watchstrap or costume jewellery [56].

### **2.3 COBALT**

Cobalt is a relatively rare element with the atomic number 27. In its elemental form ( $\text{Co}^0$ ), it is a shiny, ductile, brittle, grey metal that shares many properties with iron and nickel. On account of its durability, high melting point and resistance to oxidation, cobalt is commonly used to make strong, corrosion- and heat-resistant alloys, such as the CoCrMo alloy popular in the manufacture of hip implants. Other uses include permanent magnets, batteries, catalysts, drying agents in paints, diamond polishing, electroplating, radiology and blue-coloured pottery [57]. Outside of the industrial setting, volcanic eruptions, erosions, forest fires, as well as burning of fossil fuels and engine emissions are known sources of cobalt, and give rise to low levels of it in urban air (1-2  $\text{ng/m}^3$ ) [57].

In the body, cobalt occurs primarily in the divalent state ( $\text{Co}^{\text{II}}$ ), but the trivalent form ( $\text{Co}^{\text{III}}$ ) is also found- most notably in vitamin B12 (cobalamin). While inorganic cobalt is not required by mammals, vitamin B<sub>12</sub>, which features a single cobalt ion at the centre of its structure, is an essential micronutrient for humans. The vitamin acts as a cofactor for enzymes involved in DNA synthesis and red blood cell (RBC) production [58], and is obtained primarily from animal-derived foods. If the recommended daily intake of 2-3  $\mu\text{g}$  (approx. 0.01  $\mu\text{g}$  cobalt) [59] is not met, or its absorption is impaired, B<sub>12</sub> deficiency manifests as neuropathy and megaloblastic anaemia [60,61].

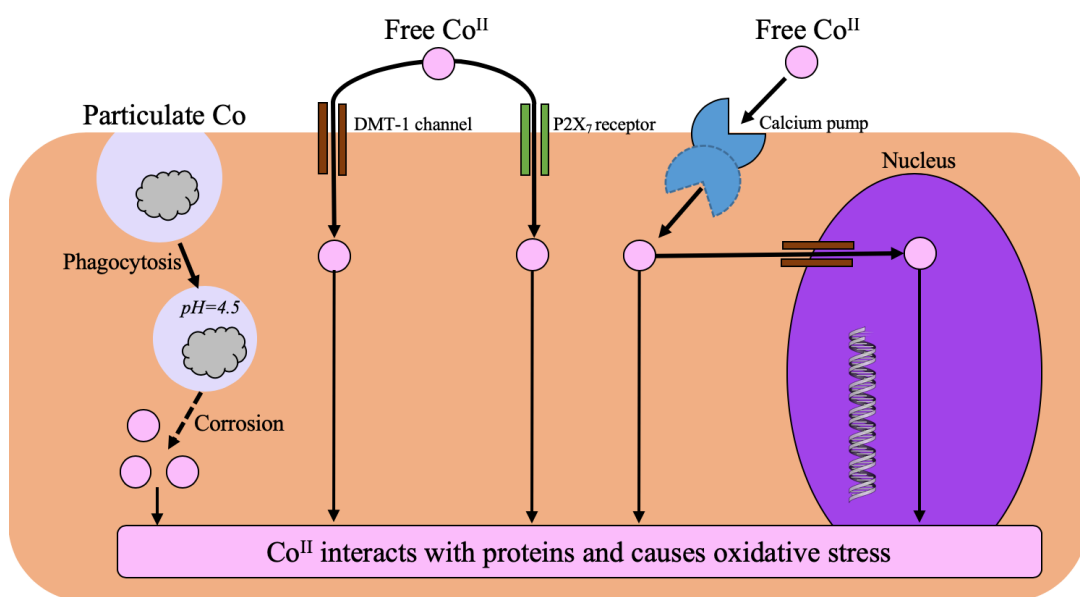
Even though cobalt supplementation has been deemed unnecessary, numerous over-the-counter cobalt-containing products are available in the United States. These supplements are advertised to increase the body's antioxidant defense, reduce inflammation and enhance aerobic performance [62]. The latter claim has made them particularly popular amongst competitive athletes, who use them illicitly to increase red blood cell production and oxygen delivery to the muscle [63].

### 2.3.1 Cobalt toxicokinetics

Following their release from metal implants, cobalt ions bind to proteins in the synovial fluid and surrounding tissue, before entering the circulation. In healthy individuals, approximately 88-95% of blood  $\text{Co}^{\text{II}}$  is bound to serum albumin [64], and much of the remainder is likely complexed with smaller biomolecules, such as lipoic acid and glutathione. The chemical similarity of  $\text{Co}^{\text{II}}$  to other divalent cations allows it to “hijack” their cellular transport mechanisms to gain entry into cells. For example,  $\text{Co}^{\text{II}}$  can enter red blood cells *via* the calcium membrane transporter. The process is essentially irreversible as the metal becomes bound to haemoglobin [65], leading to cobalt accumulation in erythrocytes. Non-protein bound  $\text{Co}^{\text{II}}$  ions can cross cell membranes *via* broad-specificity divalent metal transporters, e.g. the P2X<sub>7</sub> ionotropic receptor or the divalent metal transporter-1 (DMT-1) [66]. DMT-1, which is highly expressed in the neurons, is thought to play a key role in the entry of metal ions into the brain [67]. Additionally, the cellular uptake of cobalt may be mediated both by active transport ion pumps (*i.e.* calcium/magnesium pump) and endocytosis (Figure 2.8).

During short-term exposure, most of the cobalt is found in the serum/plasma, with its red blood cell content two orders of magnitude lower. Long-term exposure leads to a slow, continuous uptake of cobalt into erythrocytes, which reflects the time-averaged

Co<sup>II</sup> exposure during their 120-day lifespan [68]. Total buffering capacity of human red blood cells is approximately 3 g of cobalt for a volume of 2.4 L [69]. A greater distribution of cobalt in whole blood than in plasma may indicate an alteration in the binding of cobalt to plasma proteins, resulting in an increased free ionised Co/bound Co ratio [70]. This is of clinical importance because free cobalt ions, unlike bound cobalt, are able to interact with a variety of biomolecules and cause a range of toxicities [71]. A disproportionately high whole blood Co/plasma Co ratio was proposed to underlie the severe neurotoxic symptoms experienced by a THA patient in Rizzetti *et al.* [72,73].



**Figure 2.8. Cellular uptake of cobalt.**

Cobalt is highly soluble and readily excreted in the urine, and the little that is retained is mainly stored in the liver and kidneys, with smaller amounts in the heart and spleen [74]. High acute doses, or chronic exposure to cobalt, can increase its blood content [75] and lead to accumulation in the periprosthetic tissue and vital organs [65].

### 2.3.2 Local adverse effects

Soluble and particulate wear debris generated *via* wear and corrosion of hip implants can incite a foreign body inflammatory reaction in the periprosthetic tissue, termed “adverse reaction to metal debris” (ARMD). Most CoCr wear particles are phagocytosed by tissue-resident macrophages and dissolved in the acidic environment of their lysosomes to liberate cobalt and chromium ions. Cobalt ions can activate Toll-

like receptor 4 on macrophages and monocytes [76,77], which stimulates the inflammatory cascade by triggering the expression of a wide array of cytokines (tumour necrosis factor  $\alpha$  (TNF- $\alpha$ ), interleukin-1 (IL-1), IL-6, IL-8), growth factors and chemokines, as well as activating a myriad of downstream signalling pathways (nuclear factor- $\kappa$ B, protein kinase B, and mitogen-activated protein kinase) [74]. The interplay between these inflammatory mediators and pathways has not yet been fully elucidated. It is known that TNF- $\alpha$ , IL-1 and IL-6 induce differentiation and maturation of osteoclasts (bone-resorbing cells), while inhibiting osteoblast (bone-forming cells) proliferation and releasing matrix-resorbing enzymes. The net result is periprosthetic osteolysis and, ultimately, aseptic loosening. According to the NJR, aseptic loosening is the number one cause of hip implant failure and was responsible for nearly a quarter of all revision surgeries performed in 2017 [9].

Cobalt ions are cytotoxic to macrophages *in vitro*, with lower doses causing apoptosis (programmed cell death) and higher doses causing necrosis (premature cell death) [78–80]. Histopathological examination of periprosthetic tissue from around failed MoM devices revealed a presence of metal particle-loaded macrophages, juxtaposed with extensive necrosis of connective tissue [8,81]. Expanding necrotic zone, caused by a vicious cycle of necrosis, recruitment of macrophages to clear the necrotic debris and re-phagocytosis of wear debris, could play a role in pseudotumour aetiology [78,82].

Implant wear debris can also induce a hypersensitivity reaction, whereby metal-protein complexes (haptens) capable of acting as antigens for circulating lymphocytes are formed. The immune response is characterized by the formation of antibodies and immune complexes (type I, II, and III hypersensitivity reactions), or, more commonly, activation of CD4<sup>+</sup> T<sub>H1</sub> lymphocytes in the peripheral lymphoid tissues (cell-mediated delayed-type (type IV) hypersensitivity reaction) [56]. Stimulated T-cells generate cytokines that attract macrophages to implant site, and pro-osteoclastogenic factors that can alter bone homeostasis and contribute to bone resorption. Willert *et al.* [83] postulated that the additional presence of B lymphocytes, plasma cells, and massive fibrin exudation in tissue surrounding failed MoM implants distinguished the immunological response from a typical type IV hypersensitivity reaction, and instead referred to it as an aseptic lymphocytic vasculitis-associated lesion (ALVAL). The clinical features of ALVAL are non-specific, but can include a wide spectrum of soft tissue lesions (pseudotumours), including focal inflammatory reactions, fluid collections and cystic or solid periprosthetic soft-tissue masses [8]. In Kwon *et al.* [84],

incidence of pseudotumours in patients with MoM HR was associated with elevated serum metal levels and excessive wear of the femoral component, suggesting that they represent a local biological reaction to high localised concentration of metal debris. Since pseudotumours can also develop in patients with MoP and CoP bearings [85–87], the exact pathophysiology of their formation remains unclear. It has been suggested that in patients with high-wearing implants, the metal debris attracts macrophages and leads to an expanding necrotic zone, while allergic (hypersensitive) patients will react to even low amounts of particles, leading to T-lymphocyte infiltration and ALVAL [82].

### **2.3.3 Remote adverse effects**

Chronic exposure to cobalt can lead to systemic toxicity and deposition of the metal in vital organs [57]. Depending on the route of entry, the adverse effects can affect the lungs (only with inhalation exposure) [88], heart [89,90], nervous system [90], thyroid gland, skin and the immune system. The affected populations include patients on oral cobalt therapy, occupationally-exposed workers and hip replacement recipients [91].

The first report of hip replacement-related systemic cobalt toxicity was published in 2001, in an Italian journal [92]. The patient in question experienced accelerated wear of a revision CoCr femoral head, resulting in a set of generalised complaints, including motor and sensory neuropathy, pericardial tamponade and hypothyroidism. Since that time, over 40 case reports have been published in which patients with CoCr-based hip prostheses presented with elevated levels of cobalt and a constellation of systemic sequelae, including haematological, endocrine, neurological and cardiac effects- a syndrome collectively known as arthroprosthetic cobaltism. The two affected sub-populations were patients with MoM hips, and those with fractured ceramic implants that were subsequently replaced by CoCr-containing ones. The latter group experienced the highest elevations of cobalt, and the most severe adverse effects. It is thought that third-body wear (excessive grinding of residual ceramic particles on the new metal femoral head) was responsible for the catastrophically high systemic cobalt release.

Depending on the wear mechanism, the time from procedure/revision to first symptoms ranged from months to several years. Removal of the offending prosthesis was usually accompanied by resolution of symptoms, though some patients suffered irreversible damage to vision and/or hearing [72,90,93–97], two patients required a



heart transplant [98–100] and at least 7 cases had a fatal outcome (certain cases were reported twice) [89,101–108] (Table 2.2). While majority of the patients underwent formal testing to confirm toxic effects, some reports were based on subjective self-reporting, and were not detailed enough to properly judge the contribution of cobalt to the reported symptoms or identify potential confounding factors. Consequently, a direct cause-and-effect relationship between symptoms and blood cobalt level could not be established.

The use of MoP constructs to replace failed ceramic hips is favoured by some surgeons, as it is thought to decrease the risk of ceramic re-fracture [109]. However, it is now clear that even meticulous synovectomy and extensive joint lavage are unable to completely remove all of the ceramic debris, and that the residual ceramic particles represent a major risk factor for systemic cobalt toxicity (26 out of 45 reported cases of arthroprosthetic cobaltism were linked to this practice). Consequently, it is strongly recommended that fractured ceramic arthroplasties are only revised with new ceramic components [110]. Similarly, the use of large-diameter CoCr femoral heads and hip resurfacing implants, which were associated with high cobalt release and remote adverse effects, has now waned. Nonetheless, approximately a million patients worldwide have a MoM prosthesis, while over 5 million received hip implants with cobalt-containing components. For this reason, it is important to recognise short-term as well as long-term risks of chronic exposure to implant degradation products. Known systemic effects of cobalt are discussed below.

**Table 2.2. Reported cases of systemic toxicity associated with elevated cobalt levels from hip implants.**

Ref.	Age/ Sex	Implant	Co level <sup>a</sup> (µg L <sup>-1</sup> )	Reported toxicity symptoms							Time to first symptoms	Improved after revision?	Co-morbidities	
				C	N	V	H	T	P	Other				
[93]	53/M	CoP→MoP	397,800*	x	x						Progressive dyspnoea, fatigue, nonspecific weakness	N/R	Yes, except leg neuropathy	
[89,101]	46/M	CoC→MoP	1085 <sup>S</sup> 6521 <sup>B</sup>	x	x			x	x		Severe fatigue, anorexia, weight loss, tinnitus, renal and liver failure	6 m	<b>Fatal</b>	
[94]	69/F	CoC→MoP	2696 <sup>B</sup>	x	x	x	x	x			Fatigue, nausea and vomiting, weight loss	10 m	Yes, except lower limb weakness and vision	Hypertension, myocardial infarct, IHD
[111]	61/F	CoP→MoM	2148 <sup>P</sup> 1997 <sup>B</sup>	x	x	x	x	x	x		Dysgeusia, nausea, vomiting, weight loss, gastritis	2 m	Yes	Hyperlipidaemia
[110]	69/F	CoC→MoP	1464 <sup>B</sup>	x		x	x				Fatigue, cognitive decline, memory loss, weight loss, metallic gustation	<1 y	Yes	
[112]	60/M	MoM	1096 <sup>S</sup>		x	x	x	x	x		Tinnitus	16 y	N/R	

[113]	66/M	CoC→MoP	1078 <sup>S</sup>			x	x			Ankle swelling, loss of metal clarity, rash	9 m	Yes	
[114]	50/M	CoC→MoP	1036 <sup>S</sup>	x	x	x	x	x		Fatigue, anorexia, weight loss, loss of smell, anxiety, depression	1 y	Yes	Hypertension, diabetes
[95]	58/M	CoC→MoP	903 <sup>P</sup>	x	x	x	x	x	x	Progressive fatigue, dyspnoea, vertigo, hepatosplenomegaly	9 m	Yes, except hearing	Perforated right eardrum
[115]	55/M	CoC→MoP	885 <sup>P</sup>	x		x	x	x		Enlarged lymph nodes	2 y	Yes, except hearing and vision	
[116]	57/F	CoC→MoP	788	x	x	x		x		Fatigue, memory loss	4 y	Yes	Heavy smoker
[102,103]	63/M	CoC→MoP	779 <sup>S</sup>	x		x	x	x		Progressive dyspnoea, poor appetite, nausea, weight loss	2 y	<b>Fatal</b>	Hypertension, skin cancer, aortic aneurysm
[98]	31/M	CoC→MoP	652 <sup>S</sup>	x							2 y	No- heart transplant required	
[117]	55/M	CoP→MoP	625 <sup>B</sup>	x	x		x	x		Fatigue, headaches, poor concentration, weight loss,	3 m	Yes	

										nail discolouring, eczema, dysgeusia			
[108]	71/M	CoC→MoP	597 <sup>S</sup>	x		x	x	x		Weight loss, vomiting, vertigo	6 m	<b>Fatal</b>	Diabetes, multiple myeloma
[72]	58/F	CoP→MoP	90 <sup>P</sup> ; 549 <sup>B</sup>		x	x	x	x		Fatigue	2 m	Yes, except vision	Diabetes
[90]	56/M	CoC→MoP	506 <sup>S</sup>	x	x		x	x		Weight loss	14 m	Yes, except hearing	Diabetes, hypertension
[31]	52/M	CoC→MoP	490 <sup>S</sup>	x	x		x		x	Fatigue, dyspnoea, muscle weakness	1 y	Yes	Hypertension, alcoholism
[118]	65/M	CoC→MoC	446 <sup>P</sup>	x	x	x			x	General malaise	4 y	Yes	Hypertension, diabetes, obesity
[105]	60/F	CoC→MoP	424 <sup>B</sup>	x			x			Dyspnoea, metallic gustation, weight loss, increased fatigue	10 m	<b>Fatal</b>	
[97]	66/F	CoX→MoP	412 <sup>S</sup>	x	x	x	x	x	x	Recurrent depression, anorexia, weight loss, fatigue	3 y	Yes, except vision	Coronary artery disease, secondary hypothyroidism, heavy smoker

[96]	56/F	CoP→MoP	>400 <sup>B</sup>		x		x	x		Fatigue	2 y	Yes, except hearing	
[51]	53/M	CoC→MoC	398 <sup>S</sup>		x	x	x			Generalised dermatitis	2 y	Yes	
[119]	75/M	CoC→MoM	353 <sup>S</sup>	x							5 y	Yes	
[120]	59/F	2 x MoM	288 <sup>S</sup>	x				x		Progressive dyspnoea, fatigue, foot swelling, heart transplant required	3 y	Yes	
[121]	61/F	MoM	254 <sup>B</sup>		x						3 m	Yes	
[122]	40/M	2 x MoM	246 <sup>S</sup>	x						Exertional dyspnoea	4 y	Yes	Occasional cocaine use
[107]	69/F	2 x MoM	200-300 <sup>S</sup>	x							N/R	<b>Fatal</b>	Hypertension, mild renal insufficiency
[106]	69/F	2 x MoM	199 <sup>S</sup>	x							5 y	<b>Fatal</b>	
[104]	64/F	2 x MoM	192 <sup>S</sup>	x						Dyspnoea, impaired renal function	2 y	<b>Fatal</b>	
[99,100]	54/M	2 x MoM	189 <sup>S</sup>	x	x					Fatigue	6 y	No- LVAD required	Obesity, renal insufficiency

[123]	58/F	MoM HR	169 <sup>S</sup>	x						Acute renal failure, heart transplant required	10 y	Yes	
[112]	56/M	2 x MoM	165 <sup>S</sup>		x					Extreme lethargy	7 y	Yes	
[124]	46/M	2 x MoM	156 <sup>S</sup>	x						LVAD required	2 y	Yes	
[125]	42/M	MoM	156 <sup>S</sup>	x					x	Progressive dyspnoea	Several years	Not revised	
[52,126]	49/M	MoM	122 <sup>S</sup>	x	x	x	x			Fatigue, dyspnoea, headaches, anxiety, tinnitus, cognitive decline, poor memory, lassitude, depression, rash	3 m	Yes, except tinnitus and vision	
[31]	46/M	N/R	112 <sup>S</sup>	x						Dyspnoea, kidney failure, heart transplant required	6 y	Yes	Hypertension, CKD
[127]	39/M	N/R	>100 <sup>S</sup>	x							N/R	Yes	Thyroid cancer, thyroidectomy, low albumin
[128]	N/R	MoM HR	64 <sup>S</sup>		x		x			New onset anxiety and depression, tinnitus, cognitive decline	15 m	Awaiting revision	
[129]	32/M	CoC→MoP	>59 <sup>B</sup>	x			x			Pancreatitis	6 y	No	

[130]	40/M	CoC→MoP	45 <sup>S</sup>	x						Cognitive impairment, poor memory, mood swings, encephalomyelitis	7 y	Yes	
[131]	39/F	2 x MoM	45 <sup>S</sup>			x				Occasional metallic gustation, morning nausea	5 y	Not revised	
[132]	73/F	MoM	24 <sup>S</sup>							Fatigue, cognitive decline, poor memory, depression, weight loss, severe headaches, metallic gustation	5 y	Yes	Stroke
[52,126]	49/M	MoM	23 <sup>S</sup>	x			x			Cognitive decline, mental fog, memory loss, vertigo, rash, dyspnoea	1 y	Yes	
[133]	75/M	MoM	14 <sup>P</sup>	x						Worsening dyspnoea, exertional chest tightness,	6 y	Yes	Diabetes, renal impairment, obesity, prostate cancer
[132]	60/M	MoM	11 <sup>S</sup>							Fatigue, cognitive decline, poor memory, poor exercise tolerance, dyspnoea, painful muscle fatigue	4 y	Yes	Hypertension
[92]	47/M	CoP→MoP	N/R	x	x			x			1 y	Not revised	

<sup>a</sup>Co level measured in: <sup>S</sup>serum, <sup>P</sup>plasma, <sup>B</sup>blood; \*likely to be a reporting error; C-cardiotoxicity, N- peripheral neuropathy, V- visual disturbance, H- hearing disturbance, T- hypothyroidism, P- polycythaemia; LVAD- left ventricular assist device, IHD- ischaemic heart disease, CKD- chronic kidney disease; N/R- not reported.

### **2.3.3.1 Increased red blood cell production (polycythaemia)**

Cobalt has a stimulating effect on red blood cell production [134,135], with increased erythrocyte concentration consistently observed at blood cobalt concentration of 300  $\mu\text{g L}^{-1}$  and higher. For this reason, cobalt salts were historically used to treat certain types of anaemia (primarily those secondary to chronic renal failure and malignancies) [134,136]. Typical adult doses ranged from 25-150 mg cobalt chloride ( $\text{CoCl}_2$ ) per day, although doses as low as 11 mg/day were effective in anephric patients [38,41]. While generally successful, the therapy was associated with adverse effects (cardiomyopathy, thyroid dysfunction and vision and hearing impairment) in children, and adult patients with renal compromise [137,138], and was eventually discontinued.

While the possible impact of occupational exposure to cobalt on red blood cell production is controversial [139,140], haematological effects were observed in heavy drinkers of cobalt-containing beer [141], and in selected case reports of patients with CoCr-based hip replacements, at reported blood/serum cobalt levels exceeding 150  $\mu\text{g L}^{-1}$  [31,71,95,97,101,112,125].

### **2.3.3.2 Hypothyroidism**

Cobalt interferes with thyroid hormone production, resulting in hypothyroidism and symptoms such as goitre, lassitude, lethargy, weakness, poor concentration and diminished reflexes [142]. Reversible thyroid dysfunction has been observed in some patients receiving cobalt chloride treatment [143–145], occupationally-exposed workers [140] as well as in hip replacement patients, at measured blood cobalt levels of 250  $\mu\text{g L}^{-1}$  and higher [72,89,90,94–97,103,108,111,112,115–118,146].

### **2.3.3.3 Neurotoxicity**

The adverse effects of cobalt on the nervous system have been observed in numerous *in vitro* [147,148] and animal studies [149–151]. Rabbits treated with intravenous cobalt showed histopathological evidence of optic nerve damage and loss of retinal and cochlear cells, the severity of which was related to the dosage and time of exposure [150]. Reversible deafness and/or visual deficits were also noted in recipients of  $\text{CoCl}_2$  therapy [145,152,153] and occupationally-exposed subjects [154]. Meecham *et al.* [154] reported on a male factory worker, who developed progressive bilateral deafness with tinnitus, visual failure and occasional vertigo after inhaling cobalt powder for 20 months, working 50 hours a week. His blood cobalt level (234  $\mu\text{g L}^{-1}$  at 3 months after



cessation of exposure) gradually decreased over the subsequent months, which was accompanied by a definite improvement to his hearing and visual acuity.

In THA patients, cobalt neurotoxicity manifests as memory loss, cognitive decline, limb paraesthesia, loss of balance, peripheral neuropathy and altered vision and/or hearing. The adverse effects are usually observed at blood/serum cobalt of around 400  $\mu\text{g L}^{-1}$  and higher [31,51,72,90,96,97,101,105,108,115–118], although levels in the range 23-165  $\mu\text{g L}^{-1}$  were also linked to mild/moderate neurotoxicity [112,126,129,131]. While removal of the prosthesis usually results in complete resolution of the symptoms, several case reports exist where the patient suffered permanent damage [72,90,93–97].

The first longitudinal analysis of systemic neurologic side effects after THA in a large cohort of patients was performed by Bala and colleagues [155]. MoM patients were not found to be at an increased risk of developing neurologic sequelae when compared to age- and gender-matched MoP patients over a 5-year postoperative period. The authors suggested that previously reported cases of neurological side effects after THA could have been caused by metal allergy, and represent a rare scenario. It is difficult to draw any firm conclusions since the study did not track the patients' cobalt levels. Prentice *et al.* [156] did not find any visual/auditory dysfunction in patients with a well-functioning ASR hip resurfacing and normal serum cobalt levels (IQR 0.36-1.05  $\mu\text{g L}^{-1}$ ) at a mean of 10 years after surgery. In contrast, Leyssens *et al.* [157], who subjected 20 MoM recipients with normal plasma cobalt (IQR 0.7-6.3  $\mu\text{g L}^{-1}$ ) to extensive auditory and vestibular testing, reported signs of cobalt-induced deficits to high frequency hearing at a mean of 6 years after surgery, though a clear dose-response relationship could not be established. Moreover, Unsworth-Smith *et al.* [158] detected statistically significant disturbance of retinal electrophysiology in their ASR cohort with elevated serum cobalt (IQR 0.80-8.90  $\mu\text{g L}^{-1}$ ) when compared with non-ASR control groups, at a maximum follow-up of 8 years. The differences did not translate into identifiable clinical visual deficits, and the authors advised against routine visual testing in patients with chronic exposure to mildly (but not excessively) raised cobalt.

In 2013, Leikin *et al.* carried out a retrospective, observational study of 26 MoM patients and 13 controls with a traditional arthroplasty (median blood cobalt 14.1 and 1.5  $\mu\text{g L}^{-1}$ , respectively). One of two patients with demyelinating neuropathy was in the control group and had normal blood cobalt. Tinnitus (ear ringing) and hearing loss

were reported with similar frequency in the two cohorts, suggesting that factors other than cobalt were at play. Notably, peripheral neuropathy and bilateral sensorineural hearing loss was reported in a patient with a CoC implant with a TiAlV stem [159]. The neurological effects diminished following implant revision, and it was proposed that excess vanadium may have been responsible for the observed toxicity.

Collectively, these observations highlight that cobalt can cause neurotoxicity, but that similar symptoms can also occur in the absence of cobalt exposure, and that in many cases advanced age and other patient-specific influencing factors (see Section 2.9) can contribute to the adverse effects [160].

#### **2.3.3.4 Cardiomyopathy**

The link between cobalt and heart damage was first made in the 1950s, when cobalt tablets were commonly prescribed to treat anaemic patients. Little *et al.* [137] and La Grutta *et al.* [161] reported on children presenting with rapid onset cardiomyopathy after treatment with a cobalt-containing supplement. In both cases, the cardiotoxic effects were associated with elevated serum cobalt ( $270 \mu\text{g L}^{-1}$ ), and resolved upon cessation of cobalt therapy. Cardiomyopathy in response to cobalt treatment was also reported in adult anaemic patients [138,162]. Manifold *et al.* [162] described a 17-year-old woman on maintenance haemodialysis who died from rapidly progressing dilated cardiomyopathy after nine months of daily 50 mg cobalt chloride. Post-mortem analysis of the cardiac tissue revealed cobalt concentration 45 times greater than that in control samples. Impaired excretion of cobalt due to severe renal failure was likely a major contributor to the observed outcome (see Section 2.9.1).

In the 1970s, evidence linking occupational exposure to cobalt and myocardial damage began to surface. Barborik and Dusek [163] and Kennedy *et al.* [164] reported on workers who died of acute heart failure after having been exposed to cobalt metal dust for 3-4 years. Myocardial cobalt content was  $1.4$  and  $7 \mu\text{g g}^{-1}$  dry tissue, respectively. In 2004, Linna *et al.* [165] carried out a large cross-sectional study of cardiovascular symptoms in male cobalt plant workers. No major cardiac dysfunction attributable to cumulative cobalt exposure was found at a mean blood cobalt of  $2.5 \mu\text{g L}^{-1}$ , though echocardiographic evidence of altered left ventricular relaxation and early filling was noted. Minor increases in left ventricular wall thickness, which could result from cobalt accumulation in the myocardium [166], concurred with these observations.

In the mid-1960s, breweries in North America and Europe began adding trace amounts of cobalt to their beer, in order to promote and stabilise foam formation. This practice resulted in an endemic of subacute cardiomyopathy in heavy beer drinkers [141,167–169]. The disease was characterised by rapid-onset heart failure with pericardial effusion, polycythaemia and thyroid abnormalities, and often had a fast clinical progression to death (10-40% of cases) [170]. Post-mortem examination of the victims' cardiac tissue revealed a grossly enlarged heart, with increases in left ventricular wall thickness [171]. At the ultrastructural level, the cardiac mitochondria were swollen and disorganised, and contained osmophilic particles considered to represent cobalt-protein complexes [172]. Histological features of “beer-drinkers' cardiomyopathy” were similar to those of cobalt chloride supplementation and industrial cobalt exposure, and readily distinguishable from those of typical alcoholic cardiomyopathy. However, it seemed that cobalt and alcohol were not the only factors contributing to the disease, and that coexistence of a protein-poor diet was required to induce the adverse effects. Well-nourished beer drinkers did not experience any toxicity at an estimated dose of  $0.09 \text{ mg Co kg}^{-1} \text{ d}^{-1}$ , while those with a long-standing malnutrition suffered severe cardiomyopathy and death with an identical estimated cobalt dose [169]. Available evidence suggests that the cause of “beer drinkers' cardiomyopathy” was multifactorial, resulting from a combination of cobalt's depressant action on the heart, direct effects of alcohol and a coexisting protein and thiamine deficiency [172,173].

As the clinical/industrial use of cobalt salts has waned, and measures to reduce occupational exposure in cobalt plant workers have been implemented, the incidence of subacute cobalt-related cardiomyopathy has plummeted. Recent years have seen a resurgence of reports describing classical features of the disease among THA patients, with over 30 published reports linking cobalt release from hip prostheses to cardiotoxic effects. The patients typically present with shortness of breath, palpitations and exertional chest tightness [142], and exhibit elevated blood/serum cobalt levels (14 to  $6521 \mu\text{g L}^{-1}$ ).

The body of knowledge pertaining to THA-associated cardiomyopathy is largely limited to individual case reports, but the recent finding of a three-fold increase in hospital admissions from cardiac failure in men with an ASR XL MoM prosthesis (now recalled from the market) has fuelled concerns [174]. Reassuringly, large-scale epidemiological studies consistently show that MoM implants are not associated with

an increased risk of cardiac failure [175,176]. It is unclear whether chronic exposure to low circulating concentrations of cobalt could lead to an increased risk of cardiomyopathy. A post-mortem tissue study reported significantly higher median myocardial cobalt concentration in individuals with THA, compared with non-arthroplasty controls (0.12 *versus* 0.06  $\mu\text{g g}^{-1}$  dry tissue), which was associated with an increased incidence of cardiomegaly and interstitial fibrosis, and a 10% lower ejection fraction. None of these characteristics were significantly correlated with myocardial cobalt level.

Several groups have used cardiac magnetic resonance (CMR) and electrocardiograms (EKG) to look for subclinical functional and structural cardiac abnormalities and associations with cobalt levels [177–180]. Generally, asymptomatic patients with well-functioning MoM hips exhibited subtle changes in myocardial structure/function compared to controls (median follow-up 7-9 years), but the differences were not clinically significant, and a dose-effect relationship could not be established [181]. The current recommendation is that routine cardiac screening of MoM patients is unnecessary unless blood cobalt levels are very high [182].

#### **2.3.3.5 Cancer**

*In vitro* studies have shown that cobalt metal and its salts are genotoxic [183,184]. They induce DNA strand breaks and cross-links [185], and interfere with DNA repair mechanisms [186], which may play an important role in the initiation of cancer. Indeed, cobalt-induced tumours have been observed in animal models [187], albeit at doses markedly higher than those experienced by THA patients. While an increased incidence of lung cancer was noted in workers exposed to cobalt dust, the finding was deemed inconclusive because of co-exposure to other carcinogenic substances [188].

A significant increase in DNA aberrations (aneuploidy and chromosomal translocations) was revealed in peripheral lymphocytes of patients with MoM implants [189], and those undergoing revision of cobalt-chromium hip implants [190]. Clinically relevant consequences of these findings have not been demonstrated. Similar effects were noted in patients with CoC implants, which are not associated with elevated systemic metal ion levels. Based on this finding, Christian *et al.* proposed that the observed DNA aberrations were not due to raised blood cobalt/chromium levels, but to a non-specific inflammatory response caused by the presence of the implant [191].

Large-scale epidemiological analyses have not shown a causal link between hip replacement and increased overall cancer risk [192–197]. In contrast, it has been reported that TJA recipients have a lower mortality from all causes, and a lower incidence of cancer than the general population [198]. While several studies point to an elevated incidence of prostate cancer [196,199–201], bladder cancer [200], endometrial cancer [201], melanoma [196,200,202] and hematopoietic cancers [201] in THA patients compared to the general population, these excess risks are likely a result of various biases and lack of information on confounding comorbidities in the studied cohorts [192,199,203]. That said, it is well-known that particle-mediated cancers can have long latency times [204], with some solid malignant tumours requiring between 20 to 40 years to develop. It is possible that the relatively short follow-up time in the previous studies (up to 25 years) was not long enough to detect any malignant changes. As a result, it might not be possible to extrapolate these findings to young patients, who are expected to use their THA prostheses for over 30 years.

Due to a lack of convincing *in vivo* evidence in humans, cobalt is currently classified as a Group 2B substance (possibly carcinogenic to humans) by the International Agency for Research on Cancer [205].

### **2.3.4 Mechanisms of toxicity**

The local and systemic adverse effects of cobalt are likely caused by a combination of several mechanisms.

#### **2.3.4.1 Disruption of cellular energy production**

Cellular respiration is a tightly regulated metabolic pathway that turns glucose into usable cellular energy. The process consists of three main stages- glycolysis, citric acid cycle and oxidative phosphorylation- and relies on a number of enzymes and co-factors to run smoothly. Cobalt ions bind to one of the co-factors (lipoic acid), hindering its function and inhibiting the reactions that rely on it, which effectively interrupts the citric acid cycle and depletes the cell's energy source [206]. Build-up of metabolic intermediates in the mitochondria increases osmotic pressure, resulting in oedema and structural disruption [172]. Apoptogenic factors released in response to disturbed cellular respiration can lead to cell death.

In the heart, interference with cellular energy production leads to oxygen deprivation, reduction in contraction rate and myocardial dysfunction. The nervous system is another target for this toxicity mechanism due to its inherent reliance on oxidative metabolism. The retina, being one of the highest oxygen consuming tissues of the body, is particularly vulnerable [150].

#### **2.3.4.2 Interference with calcium signalling**

Cobalt ions compete with calcium ions for binding sites on enzymes, and can “hijack” calcium channels to gain entry into cells. Displacement of calcium binding in the peripheral nervous system blocks synaptic transmission. Suppressed communication between neurons can result in neurotoxic symptoms including weakness, paraesthesia, hearing loss and vision loss [121]. A similar effect is seen in patients who ingest large amounts of magnesium and suffer weakness due to the displacement of calcium.

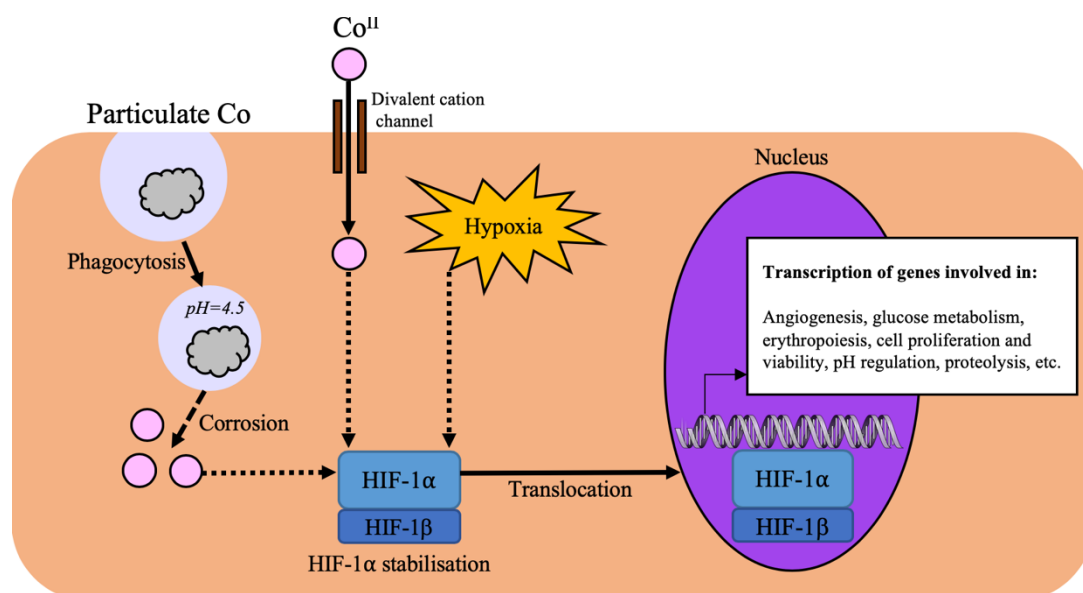
#### **2.3.4.3 Stimulation of a hypoxia-like state in cells**

Cobalt ions induce a hypoxia-like state in the cell, even in the presence of normal molecular oxygen pressure [207]. The underlying mechanism involves the stabilisation of hypoxia-inducible factor 1 (HIF-1)- a transcription factor that is usually degraded when sufficient oxygen is present. HIF-1 directs transcription of an array of genes that promote cell survival during times of low oxygen, including those encoding angiogenic growth factors, glucose transporters, glycolytic enzymes and proteins involved in the regulation of cell proliferation and apoptosis (Figure 2.9) [208].

Polycythaemia seen in anaemic patients treated with cobalt tablets is likely caused by HIF-1-mediated stimulation of the erythropoietin gene, and consequent overproduction of red blood cells. Another result of HIF-1 activation is enhanced expression of vascular endothelial growth factor (VEGF)- a key player in angiogenesis (formation of new blood vessels) and tissue/bone remodelling. VEGF has been linked to bone resorption/aseptic loosening [209] and development of pseudotumours [210] around hip implants.

While HIF-1-mediated responses serve to increase cell survival in times of low oxygen perfusion, they can have tumourigenic consequences in tissues with normal oxygen supply. HIF-1 signalling is known to inhibit p53 (an important tumour suppressor) [211], as well as stimulating cell proliferation and neovascularisation. These adaptations are important for neoplastic growth and tumour progression. It follows that

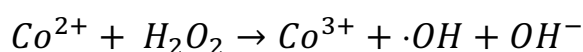
cobalt may generate a series of potentially carcinogenic responses, though their clinical relevance in human cancers is unclear. A recent review of the topic concluded that “*in vitro* cobalt-stimulated HIF-1 overexpression does not correlate with cancer risk from cobalt exposure in humans” [212].



**Figure 2.9. Pathways of HIF-1 induction. While HIF-1 signalling is normally induced by low tissue oxygen (hypoxia), cobalt ions can activate this pathway even in times of normal oxygen, leading to transcription of genes that promote cell survival.**

#### 2.3.4.4 Induction of oxidative stress

Co<sup>II</sup> catalyses the generation of highly toxic hydroxyl radicals ( $\cdot\text{OH}$ ) from hydrogen peroxide ( $\text{H}_2\text{O}_2$ ), in a Fenton-like reaction [213]. Reactive oxygen species (ROS), such as  $\cdot\text{OH}$ , promote protein, lipid, carbohydrate and DNA oxidation, which can lead to cell death.



Though Fenton chemistry occurs naturally *in vivo*, its impact is generally negligible thanks to the work of antioxidants and specialised enzymes that are designed to “mop up” excess ROS. When metal ions are present at an increased concentration, as is the case in THA patients, the rate of  $\cdot\text{OH}$  formation can overwhelm the protective mechanisms- a condition known as oxidative stress [214].

The brain is a prime target for oxidative injury, because it contains high concentrations of readily oxidisable polyunsaturated fatty acids, and a relatively modest antioxidant level [186]. In the nervous system, excess ROS can induce demyelination, axonal loss and toxic damage to oligodendrocytes, which are particularly vulnerable to oxidative stress [142]. Local tissue necrosis and pseudotumour formation observed in MoM patients are also thought to be caused by ROS activity [29]. Additionally, ROS-mediated DNA damage might translate into an increased risk of cancer.

#### **2.3.4.1 Displacement of other divalent metal ions from metalloproteins**

Co<sup>II</sup> can displace other divalent ions from their enzymatic active sites, leading to inhibition, or modification, of enzyme function. Most notably, substitution of Co<sup>II</sup> for Zn<sup>II</sup> in the zinc finger domain of transcription factors, and for Mg<sup>II</sup> in magnesium-dependent DNA repair proteins, has been postulated to contribute to cobalt-induced DNA damage [215].

#### **2.3.4.2 Inhibition of iodine uptake**

The main function of the thyroid gland is the synthesis of thyroid hormones, thyroxine (T4) and triiodothyronine (T3). The process relies on an efficient uptake of iodine and the amino acid tyrosine, and their subsequent reaction. Cobalt ions hinder this process—possibly by inhibiting iodine uptake by the thyroid, or by binding to enzymes or co-factors necessary for tyrosine iodination. When insufficient quantities of T3 and T4 are generated, the growth of the thyroid gland is stimulated as a means of increasing hormone production. When iodine binding is inhibited, the thyroid is unable to produce more T3 and T4, and the gland continues to grow, forming a goitre.

#### **2.3.4.3 Stimulation of oestrogen signalling**

Cobalt ions can bind to cellular oestrogen receptors and mimic the action of physiological oestrogens [216]. Stimulation of oestrogen signalling facilitates both synthesis and secretion of prolactin, whose overproduction may lead to pathologies in the breast and prostate tissue [217]. These effects have been proposed to underlie the observed higher incidence of prostate cancer in THA patients compared to the general population [199].

#### **2.3.5 Treatment of cobalt toxicity**

Treatment of cobalt toxicity usually relies on a prompt removal of the offending prosthesis. In cases where blood cobalt concentration is extremely elevated, metal



chelators, such as ethylenediaminetetraacetic acid (EDTA) or N-acetylcysteine might be additionally employed [94,101,127].

Pazzaglia and *et al.* [218] used long-term EDTA chelation to reduce cobalt levels in a patient with severe vision and hearing loss associated with third-body wear of a MoP prosthesis. The authors noted that cobalt concentration in whole blood was twice as high as that in the plasma, and that decrements induced by the chelating treatment were more evident in the plasma. Interestingly, after each chelating treatment there was a re-equilibration, with a passage of cobalt ions from the red cell fraction to the serum.

A significant disadvantage of metal chelators is that they depend on renal excretion, which makes them unsuitable for patients with impaired kidney function. Instead, clinicians may be forced to explore alternative therapies in patients with renal compromise. Recently, therapeutic plasma exchange (TPE) was used to rapidly reduce plasma cobalt in a THA patient with extreme levels ( $1500 \mu\text{g L}^{-1}$ ) and pronounced systemic toxicity symptoms [111]. Though initially successful, the effect was short-lived as the cobalt concentration rebounded to pre-TPE values 8 hours later. It was only after revision operation that cobalt levels stably decreased and clinical symptoms improved.

In summary, without the elimination of the metal source, chelation and TPE treatments may be futile as metal ions that are removed from the plasma are replaced by those accumulated in RBC or tissue stores, as a new equilibrium is reached [111].

## 2.4 CHROMIUM

Chromium is a metallic element with the atomic number 24. In its elemental form ( $\text{Cr}^0$ ), chromium is a hard, brittle, silvery metal with a high melting point ( $2000^\circ\text{C}$ ). It is used extensively within the chemical, metallurgical and refractory industries, where it has found applications as a corrosion inhibitor, catalyst and fungicide, as well as being used for stainless steel, pigments, wood preservatives and leather tanning [219]. Industrial use can contaminate the atmosphere, groundwater and soil with chromium, resulting in human exposure to the metal. Food products, such as brewer's yeast, calf liver, cheese, and wheat germ also contain considerable amounts of chromium [219].

Chromium has a number of valence states, ranging from  $\text{Cr}^I$  to  $\text{Cr}^{VI}$ , out of which trivalent ( $\text{Cr}^{III}$ ) and hexavalent ( $\text{Cr}^{VI}$ ) are the most stable.  $\text{Cr}^{III}$  occurs naturally in the environment, while  $\text{Cr}^{VI}$  typically originates from anthropogenic (man-made) activity. The oxidation state of chromium is intimately related to its solubility and biochemical activity in humans.  $\text{Cr}^{VI}$ , which is readily soluble, is a known human carcinogen and one of the most commonly encountered occupational hazards [220]. On the other hand,  $\text{Cr}^{III}$  which is sparingly soluble, is considered to be fairly innocuous. In fact, there is evidence suggesting that trivalent chromium plays a role in glucose, protein and fat metabolism, and many nutritionists regard it as an essential micronutrient for humans (although this is controversial [221]). Chromium supplements, such as  $\text{Cr}^{III}$  picolinate and  $\text{Cr}^{III}$  propionate, are widely used to treat insulin resistance and Type 2 diabetes [222]. Their purported beneficial effects on lean body mass, muscle growth and athletic performance, though not backed by scientific research [223], have also made them popular amongst athletes.

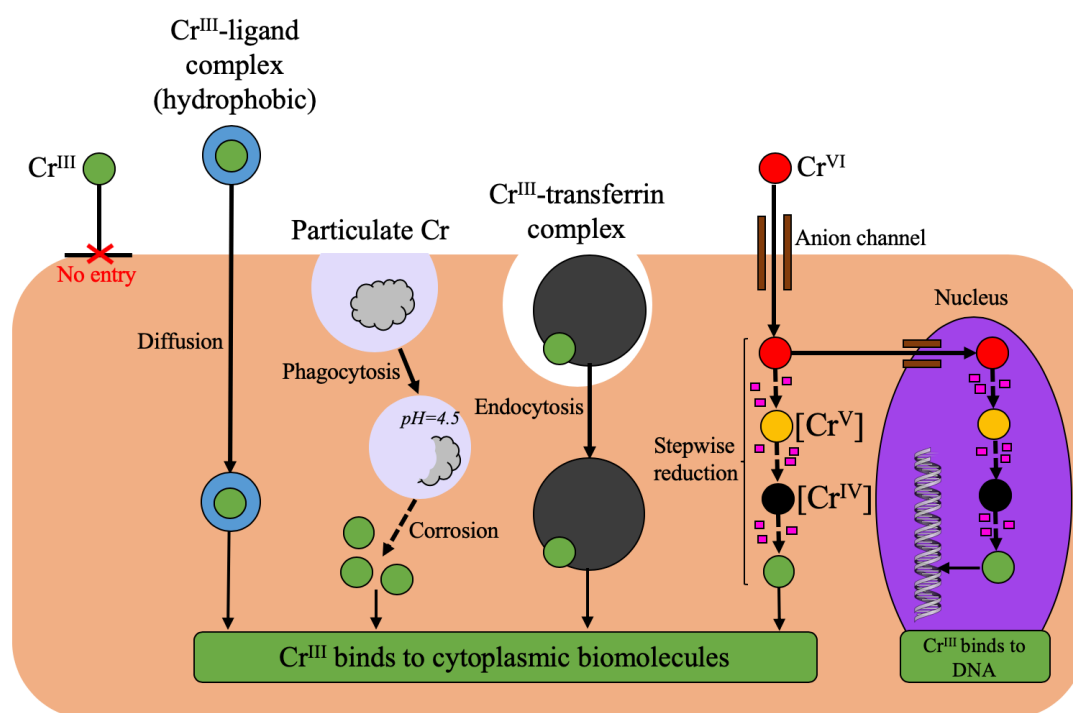
#### 2.4.1 Chromium toxicokinetics

Cell membranes are relatively impermeable to free  $\text{Cr}^{III}$ . Moreover,  $\text{Cr}^{III}$  ions are kinetically inert and form complexes with surrounding ligands very slowly [219]. As a result, trivalent chromium released from hip implants tends to combine with ubiquitous phosphate ions, and accumulate in periprosthetic tissue as chromium phosphate ( $\text{CrPO}_4$ ) [224,225]. Synthetic  $\text{Cr}^{III}$  supplements often contain hydrophobic ligands, which facilitate the permeation of chromium through plasma membranes.

Insoluble particles of chromium oxide ( $\text{Cr}_2\text{O}_3$ ) or CoCr alloy are taken up by macrophages and sequestered in lysosomes. The particles are gradually dissolved, releasing free  $\text{Cr}^{III}$  ions inside the cell. The  $\text{Cr}^{III}$  ions bind to intracellular biomolecules, which can impair their function. In intestinal epithelial cells,  $\text{Cr}^{III}$ -transferrin complexes can be taken up by endocytosis [184,226].

In physiological environments,  $\text{Cr}^{VI}$  exists as chromate anion,  $[\text{CrO}_4]^{2-}$ , and readily crosses cellular and nuclear membranes *via* non-specific anionic channels, such as the phosphate and sulphate exchange pathway. Once inside the cell,  $\text{Cr}^{VI}$  undergoes metabolic reduction to  $\text{Cr}^{III}$  by intracellular reductants, including glutathione, ascorbate and cysteine. The reduction process generates short-lived  $\text{Cr}^V$  and  $\text{Cr}^{IV}$  intermediates and ROS, which can damage cellular components. If  $\text{Cr}^{VI}$  reduction takes place inside the nucleus, the reactive intermediates, as well as the final  $\text{Cr}^{III}$

species, can induce potentially genotoxic DNA modifications, including Cr-DNA adducts, strand breaks, crosslinks, oxidised bases and abasic sites (Figure 2.10).



**Figure 2.10. Cellular uptake and reduction of different forms of chromium. Pink rectangles represent toxic by-products of  $\text{Cr}^{\text{VI}}$  reduction.**

In the blood,  $\text{Cr}^{\text{III}}$  is transported by serum transferrin, while  $\text{Cr}^{\text{VI}}$  accumulates in red blood cells. Since cellular uptake of chromium is an indication of its valence, increased chromium concentration in red blood cells could be taken as indirect evidence of  $\text{Cr}^{\text{VI}}$  exposure [68]. When workers of a dichromate-producing factory were divided into those mainly exposed to  $\text{Cr}^{\text{III}}$ , and those mainly exposed to  $\text{Cr}^{\text{VI}}$ , chromium erythrocyte content was 7-fold higher in the latter group [227]. RBC Cr/serum Cr ratio was also measured in THA patients to infer whether orthopaedic implants could be a source of hexavalent chromium [68,228–230]. A recent study by Finley *et al.* [231] showed that chromium released from MoM hip implants preferentially distributed into the serum, with no associated increase in RBC chromium concentration, indicating that the metal was in the non-toxic trivalent state.

## 2.4.2 Adverse effects

### 2.4.2.1 Kidney damage

Since chromium is primarily excreted by the kidney, it also exhibits nephrotoxic activity. Both trivalent and hexavalent chromium compounds are selectively accumulated in the renal cortex where, in large dosage, they cause kidney damage [232]. Acute tubular necrosis, renal failure and chronic interstitial nephritis are reported following accidental ingestion of chromic acid [232]. Increased urinary excretion of enzymes and low molecular weight proteins observed in chromate workers suggests that chronic exposure to airborne chromium can also cause tubular dysfunction and contribute to the development of renal failure [233]. It is unclear whether chromium released from surgical devices carries the same risks.

### 2.4.2.2 Cancer

The main toxicological hazard related to chromium is the carcinogenicity of its hexavalent form. Intracellular reduction of  $\text{Cr}^{\text{VI}}$  to  $\text{Cr}^{\text{III}}$  generates reactive intermediates, including  $\text{Cr}^{\text{VI}}$  esters,  $\text{Cr}^{\text{V}}$  and  $\text{Cr}^{\text{IV}}$  complexes, free radicals and ROS, which can all induce genotoxic DNA modifications. The final  $\text{Cr}^{\text{III}}$  species cannot leave the cell and is effectively trapped, usually bound to intracellular proteins or DNA. It has been proposed that the stable  $\text{Cr}^{\text{III}}$ -protein/peptide complexes can be re-oxidised to the genotoxic  $\text{Cr}^{\text{V/VI}}$  species by cellular oxidants. The resulting oxidation-reduction cycle, and continuous generation of toxic intermediates, could explain the long-term toxicity caused by exposure to  $\text{Cr}^{\text{VI}}$  [234]. Besides directly causing DNA damage, ROS generated during  $\text{Cr}^{\text{VI}}$  reduction have been shown to activate various mitogen-activated protein kinases and mitogenic transcription factors, with an overall pro-inflammatory and oncogenic effect. It follows that carcinogenicity of hexavalent chromium involves both direct and indirect mutagenesis [184].

Breathing hexavalent chromium can cause a range of toxicities in the respiratory tract, including perforation of the nasal septum, laryngitis, asthma, bronchitis, pneumonitis and lung tissue damage. Chronic inhalational exposure to hexavalent chromium has been linked to an increased risk of lung cancer in factory workers [235]. Interestingly, only relatively insoluble particulate chromates, such as lead chromate and zinc chromate, exhibit tumorigenic activity *in vitro*. This is likely caused by adherence of the particles to the lining of the respiratory tract, and slow release of  $\text{Cr}^{\text{VI}}$  ions, leading to a sustained genotoxic insult to the surrounding tissue [235]. Hexavalent chromium

is also toxic by ingestion. Oral exposure to hexavalent chromium is associated with increased incidence of stomach, lung and liver cancer in areas where drinking water is contaminated with the metal [220,236,237].

While there is insufficient evidence in humans for the carcinogenicity of chromium metal and trivalent chromium, Cr<sup>VI</sup> is classified as a Group 1 human carcinogen by the International Agency for Research on Cancer (IARC). It is not known whether hip implants are a source of hexavalent chromium *in vivo*, and there is limited epidemiological evidence for carcinogenic outcomes in THA patients (see Section 2.3.3.5) [192,193].

## 2.5 TITANIUM

Titanium is a metallic element with the atomic number 22. It is the 9<sup>th</sup> most abundant element in the Earth's crust, and the 7<sup>th</sup> most abundant metal overall [238]. Its most stable oxidation state is Ti<sup>IV</sup>, but Ti<sup>III</sup> compounds are also common. Human exposure to titanium is largely *via* titanium dioxide (TiO<sub>2</sub>)- an important industrial material which can exist in three main forms: rutile, anatase and brookite (only the first two are produced commercially). TiO<sub>2</sub> is used in a range of applications, such as paints, tattoo inks, solar panels, catalysts, personal care products and cosmetics, as well as being added to processed foods, nutritional supplements and sweets, where it serves as a flavour enhancer and white colourant (additive E171) [239,240]. Exposure to titanium, *via* ingestion of pigment grade TiO<sub>2</sub>, is particularly commonplace in westernised populations. In the UK, the median daily adult intake is approximately 2.5 mg [241].

Unlike for cobalt, a biological role for titanium in the human body is still uncertain, as no titanium requiring biomolecules have been identified. Nevertheless, 10–20 mg of titanium are found in the human body, making it more abundant than some of the essential elements [242].

### 2.5.1 Titanium toxicokinetics

Implant-derived soluble titanium ions (Ti<sup>IV</sup>) bind to serum transferrin, which allows them to be transported to different parts of the body [243]. The transferrin-titanium complex can enter cells *via* endocytosis, though the intracellular activities of Ti<sup>IV</sup>, and how it exerts its effects, remain largely unknown [226]. The low molecular mass (non-protein-bound) fraction of implant-derived Ti<sup>IV</sup> is likely complexed with small

molecular anions, such as citrate [244]. At the pH of blood (pH 7.4) many  $Ti^{IV}$  compounds dissociate and transform into  $TiO_2$  [226].

Titanium is not readily excreted in the urine, and tends to accumulate in tissue [245], which could explain why blood titanium levels generally decrease with time since implantation [246,247]. The fate of the metal deposits in remote tissues is unclear. It is likely that the particles are retained for many years, and act as a sustained source of metal ions as they undergo gradual dissolution [248]. The clinical implications of chronic low-level exposure to titanium ions are yet to be established.

## **2.5.2 Adverse effects**

It is widely held that titanium and its alloys are biologically inert. As a result, the potential toxicity of hip implant-derived titanium has received relatively little attention. Nevertheless, recent studies and case reports link titanium ions to inflammation [249], pain [250], cytotoxicity [251,252], metal allergy [46,253], genotoxicity [254] and implant failure [255]. Soluble and particulate titanium is known to affect bone homeostasis, leading to increased bone resorption and implant loosening, which often necessitates revision surgery [39,255–257]. Additionally, formation of pseudotumours in periprosthetic tissue, originally thought to be an immune response unique to CoCr alloy, was recently seen with titanium-based implants [26,85,258]. While the exact pathogenesis of pseudotumor development is unknown, it is thought to involve both chronic inflammation and a delayed hypersensitivity response to ultrafine titanium particles [258].

Hip implants are a source of  $TiO_2$  particles, which were linked to cardiac inflammation [259,260], brain damage [261], impairment of spatial recognition memory [262] and learning abilities [263] in mice. Titanium deposits have been revealed in distal organs in both animal and human experiments [248,264,265]. Even though the metal concentration was relatively low and without apparent pathological importance, cases of titanium-related organ injury have been reported [248,259,266–268].

### **2.5.2.1 Cancer**

Titanium is a redox-active metal that can enhance ROS production and induce oxidative stress [269], which is implicated in many degenerative diseases including cancer. Mouse studies have shown that  $TiO_2$  nanoparticles have the potential to convert benign tumour cells to malignant ones through the generation of ROS [270].

Particulate debris from a titanium-based metal prosthesis induced chromosomal instability and reproductive failure in cell culture [271]. Based on experimental evidence from animal inhalation studies, TiO<sub>2</sub> nanoparticles are classified as a Group 2B substance (possibly carcinogenic to humans) by the IARC [272], and as “occupational carcinogen” by the National Institute for Occupational Safety and Health [273]. It is unclear if these results can be extrapolated to human exposure and implanted titanium is currently non-classifiable as to its carcinogenicity to humans.

## **2.6 CHARACTERISATION OF METAL DEPOSITS IN TISSUE**

Wear and corrosion of metal implants releases metal debris, which, depending on its physicochemical properties, can become incorporated into the periprosthetic tissue or enter the circulation and accumulate in systemic organs. Probing the distribution and chemical form of the metal deposits can shed light on implant degradation mode [34], as well as providing clues as to how the debris is metabolised, and the likely toxicity mechanisms at play. While several methods can be used to look at metals in tissue (Table 2.3), synchrotron techniques, such as X-ray fluorescence (XRF) and X-ray absorption (XAS), are preferred due to their low limits of detection (LoD), non-destructive nature, and requirement for minimal sample preparation (for an overview of synchrotron techniques see Section 4.1).

### **2.6.1 Periprosthetic tissue**

Samples of tissue surrounding failed metal implants can be harvested during revision operation and analysed for metal content. Synchrotron analysis of periprosthetic tissue revealed that its metal composition does not mirror the composition of the source hip (ASTM F75 alloy typically 60% cobalt, 28% chromium and 6% molybdenum). Hart *et al.* [43,225,274] reported that the predominant species found in tissues adjacent to MoM implants was chromium phosphate, with cobalt present occasionally in areas of high chromium concentration (mainly as Co or CoCr particles). The higher solubility of cobalt compared to chromium means that it corrodes faster, and the resultant cobalt ions readily enter the bloodstream to be disseminated around the body. The process tends to leave chromium ions behind, which precipitate out as insoluble particles of CrPO<sub>4</sub>, or corrode to form Cr<sub>2</sub>O<sub>3</sub> [34,40]. Although chromium phosphate and oxide have potential for ROS production, it is thought that free cobalt ions are mainly responsible for periprosthetic tissue reactions in patients with MoM hips [43].

**Table 2.3. Examples of techniques used to study metal composition of human tissue samples, and the information they can provide.**

<b>Technique</b>	<b>Metal mapping in tissue</b>	<b>Metal mapping in cells</b>	<b>Type of metal</b>	<b>Oxidation state</b>	<b>Surrounding atoms</b>	<b>Sample preparation protocol</b>	<b>Destructive?</b>	<b>Reference</b>
<b>Light microscopy</b>	+	+	-	-	-	H&E staining	No	[34,225,275]
<b>Laser ablation ICP-MS</b>	+	-	+	-	-	Dewaxing	Yes	[276]
<b>TEM</b>	-	+	+	+	+	Fixation, dehydration, resin embedding, semithin sectioning, staining	Yes	[40,277]
<b>SEM/EDXA</b>	-	+	+	-	-	Fixation, dehydration, drying, metal coating	Yes	[275,278]
<b>μ-XRF</b>	+	-	+	-	-	Dewaxing	No	[43,225,279]
<b>μ-XAS</b>	-	-	+	+	+	Dewaxing	No	[32,221,279]

ICP-MS- inductively-coupled plasma mass spectrometry, TEM- transmission electron microscopy, SEM/EDXA- scanning electron microscopy with energy dispersive X-ray analysis, μ-XRF- micro X-ray fluorescence, μ-XAS- microfocus X-ray absorption spectroscopy.



Although previous *in vitro* studies suggested that Cr<sup>VI</sup> may also be a corrosion product of MoM hips, multiple studies utilising synchrotron radiation failed to detect it in periprosthetic tissue [43,225]. This is of clinical relevance as Cr<sup>III</sup> is relatively benign, while Cr<sup>VI</sup> is an established human carcinogen.

Particulate titanium derived from wear and corrosion of hip implants can exist in several forms, which might differ in toxicity. *In vitro* studies have shown that nano-anatase is 100 times more toxic than nano-rutile- possibly due to an increased capacity for ROS production [36]. X-ray analysis of periprosthetic tissue revealed presence of TiO<sub>2</sub> particles, in either anatase, rutile [280] or amorphous form [34].

### **2.6.2 Organ tissue**

Metal wear debris is ingested by tissue-resident macrophages before entering the lymph and blood. Post-mortem studies using electron microscopy detected increased metal levels in lymph nodes, spleen and liver tissue samples of THA patients, with the highest metal loads in patients with loose or worn prostheses, and those having undergone multiple revision surgeries [277,278]. Case *et al.* [277] showed that heavy accumulation of wear debris caused fibrotic and necrotic changes in the lymph nodes, but similar effect was not seen in the spleen or liver- possibly due to the larger size of these organs.

To date, only one study attempted to determine the exact chemical form of metal debris in vital organs of THA patients [279]. The authors reported on a 44-year old individual with catastrophic third-body wear of a CoCr alloy femoral head, and highly elevated blood cobalt and chromium (587.9 and 20.4 µg L<sup>-1</sup>, respectively). Synchrotron analysis of his liver biopsy revealed an abundance of highly co-localised cobalt and chromium (possibly particles of CoCr alloy) in hepatic macrophages. Despite the high particulate load, liver function tests were normal, suggesting that the deposits were well-tolerated- at least at the time of assessment. The effects of chronic accumulation of metallic debris over several decades are unknown.

## **2.7 ASSESSMENT OF BLOOD METAL LEVELS IN THA PATIENTS**

While tissue metal deposition is difficult to quantify without an invasive biopsy or access to post-mortem samples, determination of blood metal concentration is relatively straightforward. It is well-documented that increased implant wear leads to elevated blood metal levels. It has been suggested that measurement of blood cobalt and chromium should be a part of routine follow-up of patients with metal hip prostheses, as a means of monitoring implant function and the risk of adverse biological reactions [281]. The choice of specimen type, sample preparation protocol and analytical methodology can heavily influence the reliability and clinical interpretation of the results, and needs to be carefully considered [282,283]. The most important pre- and post-analytical challenges associated with the determination of metal content of biological samples are discussed below.

### **2.7.1 Cobalt and chromium**

Historically, atomic absorption spectrometry (AAS) was used to determine blood cobalt/chromium levels in THA patients [284]. In this technique, a flame or a high temperature graphite furnace (GF) is used to atomise the sample, which is then irradiated with light of a wavelength specific to the element to be analysed. Within certain limits, the amount of light energy absorbed by the atoms can be linearly correlated to analyte concentration in the sample, allowing analyte quantification [285]. More recently, quadrupole inductively-coupled plasma mass spectrometry (ICP-MS) was introduced. In this technique, the sample is transformed into a fine aerosol, which is carried by an inert gas (argon or helium) to the inductively-coupled plasma. The high temperature of the plasma (8000-10,000°C) turns the atoms into ions, before a vacuum system accelerates them towards a collection of electrostatic discs that extract positively charged ions. The ions are sorted according to their mass-to-charge ratio and detected [285].

Due to its ability to analyse multiple elements/isotopes at the same time, high throughput, shorter run times and lower LoD, quadrupole ICP-MS has now nearly completely replaced GF AAS in analytical laboratories. However, the technique is not without its limitations. ICP-MS instruments fitted with a quadrupole mass filter (resolving power (R)=300) are susceptible to atomic and polyatomic interferences

(species having the same nominal mass-to-charge ratio as the measured isotope), which can overestimate analyte concentration. The interferences originate from the plasma gas, the surrounding atmosphere and solvents, and are very common in biological samples, which naturally contain high levels of inorganic salts and organic compounds (Table 2.4). Several methods have been reported that minimise these interferences, with cell-based technology (reaction/collision cell) being the most general approach [246].

A reaction cell is filled with a reactive gas that changes interfering species to a new form with a different mass-to-charge ratio, while collision cell uses an inert gas at varying flow rates to lower kinetic energy of the polyatomics, and prevent them from reaching the detector [286]. An alternative way to deal with interferences is to use a high resolution ICP-MS instrument. The machine separates ions using electric or magnetic fields instead of quadrupoles, allowing for a significant increase in resolving power ( $R > 3000$ ). High resolution ICP-MS can also be operated in low resolution mode (e.g.  $R = 300$ ), which offers LoD one order of magnitude lower than those obtained with quadrupole ICP-MS [287].

Irrespective of the interference minimisation strategy used, ICP-MS measures the total cobalt load, including particulate cobalt and bound/unbound cobalt ions [288]. Several authors suggested that since only unbound ions are associated with toxic manifestations, measuring them directly might be more useful in understanding the effects and variability of cobalt toxicity in THA patients. In 2013, Kerger *et al.* [289] described a new analytical method that allows for a separate quantification of large molecular cobalt (Co bound to albumin and other large proteins  $> 50$  kDa), cyanocobalamin and low molecular cobalt (Co bound to small proteins  $< 1.3$  kDa and free  $\text{Co}^{\text{II}}$  ions) in human serum, by utilising size exclusion chromatography with ICP-MS detection. The technique boasted a short run time, a low LoD ( $0.037 \mu\text{g L}^{-1}$ ) and was highly specific for cobalt. Application of the assay to serum samples from participants of a  $\text{CoCl}_2$  dosing study, and patients with CoCr implants, revealed that the large molecular Co species comprised 94.3% of total serum cobalt. Development of chromatography methods that might successfully separate free  $\text{Co}^{\text{II}}$  from the low molecular cobalt fraction is currently underway. If successful, the technique could be useful for identifying individuals with diminished larger protein-binding capacity, and presumed higher susceptibility to free  $\text{Co}^{\text{II}}$ -mediated toxicity.

**Table 2.4. The most important spectral interferences affecting cobalt, chromium and titanium measurement by ICP-MS.**

Analyte	Abundance	Interferences
$^{59}\text{Co}^+$	100	Polyatomic: $^{43}\text{Ca}^{16}\text{O}$ , $^{40}\text{Ar}^{19}\text{F}$
$^{52}\text{Cr}^+$	83.79	Polyatomic: $^{40}\text{Ar}^{12}\text{C}$ , $^{35}\text{Cl}^{16}\text{O}^1\text{H}$
$^{46}\text{Ti}^+$	7.99	Polyatomic: $^{32}\text{S}^{14}\text{N}^+$ , $^{14}\text{N}^{16}\text{O}_2^+$ , $^{15}\text{N}_2^{16}\text{O}^+$ Isobaric: $^{46}\text{Ca}$
$^{47}\text{Ti}^+$	7.32	Polyatomic: $^{32}\text{S}^{14}\text{N}^1\text{H}^+$ , $^{30}\text{Si}^{16}\text{O}^1\text{H}^+$ , $^{32}\text{S}^{15}\text{N}^+$ , $^{33}\text{S}^{14}\text{N}^+$ , $^{33}\text{S}^{14}\text{N}^+$ , $^{15}\text{N}^{16}\text{O}_2^+$ , $^{14}\text{N}^{16}\text{O}_2^1\text{H}^+$ , $^{12}\text{C}^{35}\text{Cl}^+$ , $^{31}\text{P}^{16}\text{O}^+$
$^{48}\text{Ti}^+$	73.98	Polyatomic: $^{32}\text{S}^{16}\text{O}^+$ , $^{34}\text{S}^{14}\text{N}^+$ , $^{33}\text{S}^{15}\text{N}^+$ , $^{14}\text{N}^{16}\text{O}^{18}\text{O}^+$ , $^{14}\text{N}^{17}\text{N}_2^+$ , $^{12}\text{C}_4^+$ , $^{36}\text{Ar}^{12}\text{C}^+$ Isobaric: $^{48}\text{Ca}$
$^{49}\text{Ti}^+$	5.46	Polyatomic: $^{32}\text{S}^{17}\text{O}^+$ , $^{32}\text{S}^{16}\text{O}^1\text{H}^+$ , $^{35}\text{Cl}^{14}\text{N}^+$ , $^{34}\text{S}^{15}\text{N}^+$ , $^{33}\text{S}^{16}\text{O}^+$ , $^{14}\text{N}^{17}\text{O}_2^1\text{H}^+$ , $^{14}\text{N}^{35}\text{Cl}^+$ , $^{36}\text{Ar}^{13}\text{C}^+$ , $^{36}\text{Ar}^{12}\text{C}^1\text{H}^+$ , $^{12}\text{C}^{37}\text{Cl}^+$ , $^{31}\text{P}^{18}\text{O}^+$
$^{50}\text{Ti}^+$	5.25	Polyatomic: $^{32}\text{S}^{18}\text{O}^+$ , $^{32}\text{S}^{17}\text{O}^1\text{H}^+$ , $^{36}\text{Ar}^{14}\text{N}^+$ , $^{35}\text{Cl}^{15}\text{N}^+$ , $^{36}\text{S}^{14}\text{N}^+$ , $^{33}\text{S}^{17}\text{O}^+$ , $^{34}\text{S}^{16}\text{O}^+$ , $^1\text{H}^{14}\text{N}^{35}\text{Cl}^+$ , $^{34}\text{S}^{15}\text{O}^1\text{H}^+$ Isobaric: $^{50}\text{Ca}$ , $^{50}\text{V}$

### 2.7.2 Titanium

Historically, GF AAS was the method of choice for blood titanium determination [290–293]. It is now known that the technique is not sensitive and/or selective enough to reliably quantify trace levels of titanium in complex matrices, such as blood or serum. Titanium levels cannot be successfully determined using quadrupole ICP-MS either, due to a range of polyatomic and isobaric interferences affecting all of its isotopes (Table 2.4). Even with the use of typical collision/reaction cells, these interferences produce positively biased results, which are pronounced when measuring low metal concentrations that are close to the instrument's LoD.

High resolution ICP-MS is the method of choice for the determination of titanium content of blood and serum of THA patients and non-arthroplasty subjects. Though successful at minimising polyatomic interferences, the instrument cannot remove isobaric interferences (elements whose isotopes share a common mass with the analyte), meaning that only isotopes that do not suffer from isobaric interferences ( $^{47}\text{Ti}$

and  $^{49}\text{Ti}$ ) can be detected [282]. Balcaen *et al.* [294] demonstrated that reliable determination of titanium levels in clinical samples can also be achieved with triple quadrupole ICP-MS (ICP-MS/MS). The technique, which used a mixture of ammonia and helium gas to convert  $^{48}\text{Ti}^+$  to  $[\text{Ti}(\text{NH}_3)_6]^+$  cluster ions, provided an interference-free conditions and low limits of detection ( $3 \text{ ng L}^{-1}$ ). Inductively coupled plasma optical emission spectroscopy (ICP-OES)- a technique related to ICP-MS, but which uses emission lines from the analyte of interest rather than the ions generated in the plasma- displayed a low LoD for the determination of titanium concentration in the serum ( $0.6 \text{ } \mu\text{g L}^{-1}$ ) [295] and plasma ( $1.6 \text{ } \mu\text{g L}^{-1}$ ) [296], but it was not sensitive enough for whole blood specimens [295].

The accuracy and precision of high resolution ICP-MS and ICP-MS/MS come at a price, as both machines incur high running costs and require highly trained operators. As a result, they are not widely available in routine clinical laboratories.

### **2.7.3 Metal content of different blood fractions**

There is little consensus regarding the optimal blood fragment for the monitoring of metal concentration in THA patients. As a result, in some studies whole blood is assayed, while others quote serum, plasma or erythrocyte values.

In oral cobalt dosing studies, serum cobalt concentrations displayed high variability, while whole blood measurements tended to be more stable, potentially offering a better indication of the long-term average cobalt exposure [297]. Similar findings were reported in MoM patients. It appears that serum reflects the more recent cobalt exposure (past few months), which can vary depending on the patient's physical activity level and bearing surface wear [65]. Several authors agreed that serum cobalt concentration was a poor surrogate of systemic cobalt exposure, and advocated measuring cobalt content of whole blood [298,299] or erythrocytes [65]. This view was not uniformly shared [68]. Due to the complexity of blood matrix components, whole blood analysis tends to be more difficult, and display higher LoD. Additionally, digestion protocols used to improve the recovery of the metal from RBC may theoretically contaminate the sample [300]. The large quantity of iron in the RBC could also interfere with the results [288].

Another point to consider is that metal ions with different valence states might distribute into different blood fractions. For example, Cr<sup>VI</sup> typically accumulates in red blood cells, with a much smaller amount found in the serum. Measuring chromium concentration only in the serum would therefore be an incomplete assessment.

Despite early evidence to the contrary [301], cobalt and chromium concentrations in different blood fractions cannot be used interchangeably [302,303]. Moreover, the plasma/whole blood ratio appears to be concentration-dependent, making it impossible to derive a constant conversion factor [302]. This is further confounded by inaccuracies in reporting of the blood fractions used for analysis, and the different methodologies employed by different laboratories.

In the UK, the MHRA calls for the measurement of cobalt and chromium in whole blood (collected in K<sub>2</sub>EDTA-coated tubes), though the analytical protocol is not standardised. There are no guidelines concerning titanium measurement in biological samples. Most groups prefer serum analysis, because the matrix is less complex and contains a higher concentration of titanium compared to whole blood. The main downside is that serum requires more processing and poses a greater contamination risk [304].

#### **2.7.4 Inter-laboratory discrepancies**

Lack of protocol standardisation across laboratories may result in discrepancies between measurements, and lead to different clinical interpretation of the results. Koller and colleagues [282] have recently shown that when the same blood samples were analysed for titanium by seven different laboratories, the results spanned an unacceptably wide range (from below LoD up to 25 µg L<sup>-1</sup>), depending on how the samples were prepared and what analytical instrument/methodology was employed [282]. Rahme *et al.* [305] highlighted that the choice of blood collection tube might also potentially impact the measurements. In their study, paired blood samples from MoM patients were analysed for cobalt and chromium content in two different laboratories, using either lavender top tubes (7.2 mg K<sub>2</sub>EDTA) or royal blue top tubes (10.8 mg K<sub>2</sub>EDTA). The lower anticoagulant content was associated with significantly higher mean blood cobalt (4.51 vs 3.98 µg L<sup>-1</sup>) and chromium (3.04 vs 2.27 µg L<sup>-1</sup>). Importantly, the two laboratories also employed a different sample preparation protocol (simple dilution vs acid digestion). In line with these findings, other studies

reported that simple dilution was associated with numerically higher serum cobalt values when compared to digestion methods [306]. Rahme *et al.* concluded that even though the inter-laboratory discrepancies were relatively small, in a third of the patients they were significant enough to risk clinical misinterpretation, e.g. when decisions on implant performance and revision for surgery are to be made [305].

In light of these results, it would be advisable to use a single laboratory for sequential metal ion testing, as values generated from different laboratories may not be directly comparable.

### **2.7.5 The units**

An additional source of confusion when interpreting the results of trace metal analyses is the variety of units used to report the values. Blood/serum metal concentrations are usually given in micrograms per litre ( $\mu\text{g L}^{-1}$ ), parts per billion (ppb) or nanograms per millilitre ( $\text{ng mL}^{-1}$ ), all of which are equivalent. Some authors choose to use nanomoles per litre ( $\text{nmol L}^{-1}$ ), which cannot be used interchangeably with the other units. The following formula can be used to convert between  $\text{nmol L}^{-1}$  and  $\mu\text{g L}^{-1}/\text{ng mL}^{-1}/\text{ppb}$ :

$$x = \frac{Ay}{1000}$$

Where x is the metal ion concentration in  $\mu\text{g L}^{-1}/\text{ng mL}^{-1}/\text{ppb}$ , y is the measured metal ion concentration in  $\text{nmol L}^{-1}$ , and A is the element's atomic weight (58.993 for cobalt, 51.996 for chromium and 47.867 for titanium) [288].

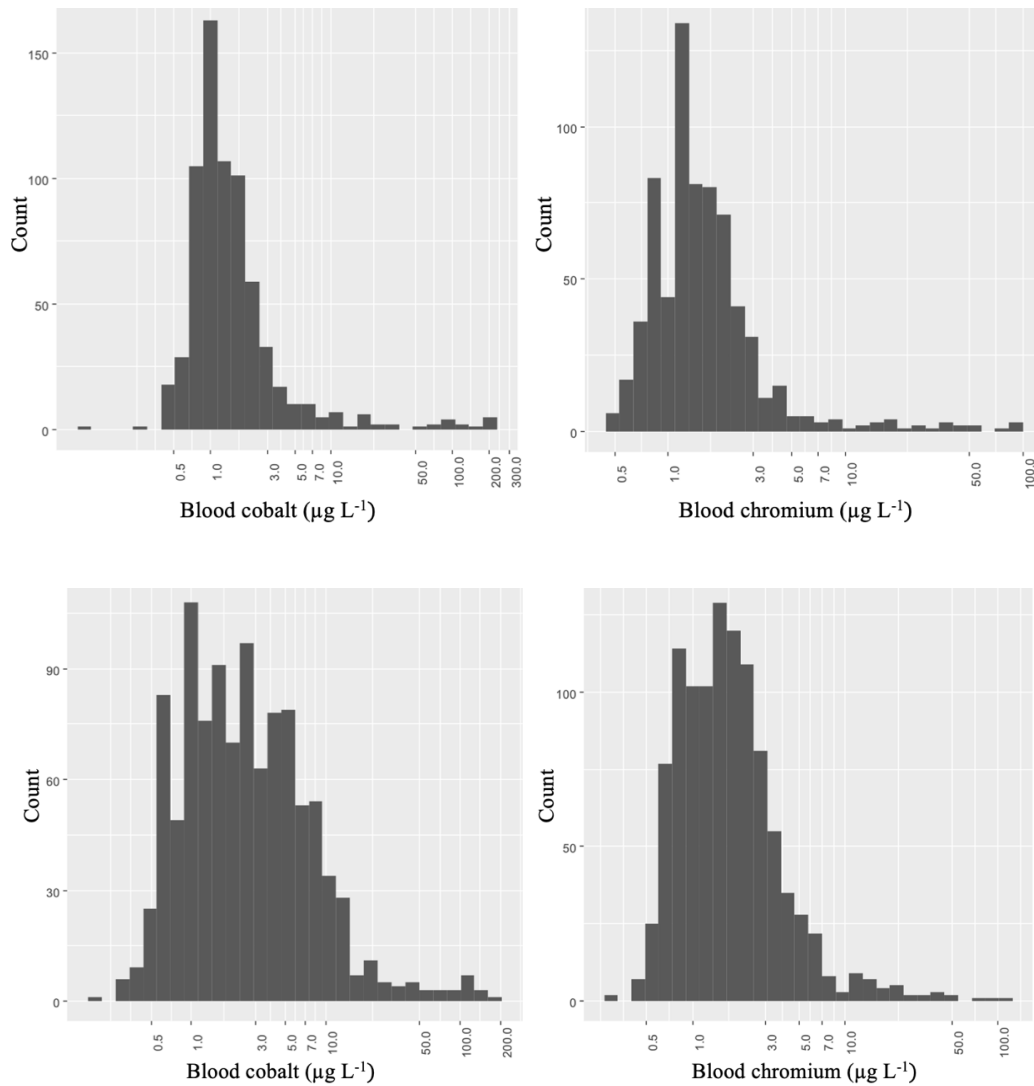
## **2.8 CLINICAL UTILITY OF BLOOD METAL MEASUREMENT IN THA PATIENTS**

### **2.8.1 Cobalt and chromium**

#### **2.8.1.1 Normal levels**

In non-occupationally exposed subjects without hip implants, blood cobalt and chromium levels are less than  $1 \mu\text{g L}^{-1}$  [307,308]. After implantation, they often increase due to a combination of wear and corrosion. The most wear occurs during the first 1-2 years after surgery (the “bedding-in” phase) [74], which is followed by a low, but steady, rate of wear over the subsequent years. In the majority of individuals with

MoM implants, blood cobalt and chromium concentrations range between 0.2 to 10  $\mu\text{g L}^{-1}$  (Figure 2.11), with steady-state median concentrations between 1.5 and 2.3  $\mu\text{g L}^{-1}$  [178,309], and reported levels as high as 23  $\mu\text{g L}^{-1}$  in some asymptomatic MoM recipients [310].



**Figure 2.11. Distribution of blood cobalt and chromium levels in a Finnish population of 692 patients with unilateral MoM HR (top) and 1056 patients with unilateral MoM THA (bottom) (reproduced with permission of Coxa Hospital, Finland).**

In general, patients with MoP arthroplasties exhibit approximately ten-fold lower metal ion levels than those with MoM bearings [121]. Previous studies of metal release from CoC and CoP implants reported that associated cobalt/chromium concentrations were always  $<1 \mu\text{g L}^{-1}$ , and in many cases undetectable (Table 2.5) [311–313].



### 2.8.1.2 Local toxicity and implant failure

In 2010, the MHRA advised that whole blood cobalt/chromium levels exceeding  $7 \mu\text{g L}^{-1}$  ( $119 \text{ nmol L}^{-1}$  for cobalt and for  $134.5 \text{ nmol L}^{-1}$  chromium) indicate potential for adverse soft tissue reactions, and an increased risk of MoM implant failure [314]. This threshold has a relatively high specificity (89%), but poor sensitivity (52%) for detecting failed hip replacements. A cut-off of  $4.97 \mu\text{g L}^{-1}$  ( $84.5 \text{ nmol L}^{-1}$  for cobalt and  $95.5 \text{ nmol L}^{-1}$  for chromium) was subsequently found to provide optimal balance between sensitivity (63%) and specificity (86%) [315].

More recently, Van der Straeten and colleagues [316] proposed that well-functioning unilateral HR should produce serum cobalt and chromium levels of up to  $4.0$  and  $4.6 \mu\text{g L}^{-1}$ , respectively, while a well-functioning bilateral HR should give rise to serum levels up to  $5.0$  and  $7.4 \mu\text{g L}^{-1}$ , respectively. These thresholds are associated with higher specificity (95% and 93% for unilateral and bilateral HR, respectively), but lower sensitivity (25% and 43% for unilateral and bilateral HR, respectively) than the MHRA cut-off. The authors supported the use of serum metal ion measurements as a surrogate parameter of wear severity and proposed that early recognition of increased wear of the articulating surfaces leads to a better outcome of revision surgery [316,317]. There are no official alerts pertaining to blood/serum ion levels with MoP constructs, but a recent study suggested a threshold of  $1 \mu\text{g L}^{-1}$  as cut-off for identification of adverse local tissue reactions in such patients [318].

According to these information, the European Consensus stated that for MoM hips “blood cobalt levels of under  $2 \mu\text{g L}^{-1}$  are probably devoid of clinical concern, while the threshold value for clinical concern is expected to be within the range of  $2\text{-}7 \mu\text{g L}^{-1}$ ” [319]. In contrast, The Mayo Clinic advise that patients with serum cobalt and chromium exceeding  $10$  and  $15 \mu\text{g L}^{-1}$ , respectively, are likely to display “significant implant deterioration”. They also note that while elevated metal ion concentrations may indicate implant wear, they are not considered a health hazard (Mayo Clinic, 2012). Similarly, US Food and Drug Administration (FDA) concluded that “there is insufficient evidence to correlate the presence of localised lesions, clinical outcomes, and/or the need for revision with specific metal ion levels for individual patients” [320].

While blood metal ion concentrations might be useful in discriminating between malfunctioning and well-functioning implants, they were found to poorly correlate with local histopathological changes related to ARMD [321,322]- possibly due to high variability in individual patient susceptibility to metal ions. Consequently, it is not advised to use raised metal ion levels in isolation as a trigger for revision [323]. Patient history, clinical examination, functional outcome measures, plain radiographs, ultrasound and/or Metal Artefact Reduction Sequence MRI results should all be taken into account before considering surgical intervention.

**Table 2.5. Blood ion levels measured in patients with different types of well-functioning and malfunctioning hip implants.**

Ref.	Implant	Technique	Mean blood level ( $\mu\text{g L}^{-1}$ )		Mean follow-up
			Co	Cr	
[299]	Well-functioning MoM HR	High resolution ICP-MS	0.2 1.3 1.2	0.3 2.4 1.1	Pre-op 1 y 4 y
[324]	Well-functioning implants -MoM HR -MoM THA -MoP THA	ICP-MS with DRC	2.4 2.6 1.7	0.5 0.6 0.1	1 y
[325]	Well-functioning THA -MoM -MoP	Not stated	5.2 1.6	2.8 0.8	2 y
[312]	Well-functioning THA -MoM -MoP -CoP	EA AAS	1.55* <sup>S</sup> 0.26* <sup>S</sup> 0.15* <sup>S</sup>	2.83* <sup>S</sup> 0.84* <sup>S</sup> 0.07* <sup>S</sup>	6 y 6 y 11 y
[313]	Well-functioning THA -MoP  -CoP	High resolution ICP-MS	0.2 0.2 0.7 0.4 0.1	0.9 0.7 0.5 1.0 0.6	Pre-op 1 y 2 y 5 y Pre-op

			0.1	0.6	1 y
			0.2	0.4	2 y
			0.2	0.5	5 y
[326]	Well-functioning MoP THA -ø28 mm head -ø36mm head -ø40 mm head	Not stated	0.1 1.0 0.8	0.2 0.3 0.2	36.5 m
[310]	Well-functioning MoM THA	ICP-MS	22.9	19.4	37 y
[316]	Unilateral MoM HR -Well-functioning -Poorly-functioning Bilateral MoM HR -Well-functioning -Poorly-functioning	ICP-MS	1.8 <sup>S</sup> 6.6 <sup>S</sup> 2.8 <sup>S</sup> 8.5 <sup>S</sup>	2.0 <sup>S</sup> 7.3 <sup>S</sup> 3.8 <sup>S</sup> 10.7 <sup>S</sup>	4.3 y 5 y
[281]	Failed MoM HR -Without metallosis -With metallosis	ICP-MS	3.2* <sup>S</sup> 33.8* <sup>S</sup>	3.4* <sup>S</sup> 33.9* <sup>S</sup>	0.5-8.4 y
[327]	Painful MoM HR -Unilateral -Bilateral	ICP-MS with DRC	4.5* 10.6*	3.0* 7.9*	27 m*
[328]	MoM THA and HR -Well-functioning -Failed -Non-pseudotumour -Pseudotumour	ICP-MS with DRC	1.7* 6.9* 1.9* 9.2*	2.3* 5.0* 2.1* 12.0*	39-42 m
[329]	MoM THA and HR -Non-pseudotumour -Pseudotumour	ICP-MS with DRC	2.9 11.0	3.2 6.7	39 m*
[330]	MoM HR -Well-functioning ASR -Well-functioning BHR -Adverse reactions	ICP-MS	2.7 1.8 69.0	4.2 4.2 29.3	≥12 m

<sup>S</sup>Metal concentration in serum, \*median value; ASR- Articular Surface Replacement, BHR- Birmingham Hip Resurfacing, ICP-MS- inductively coupled plasma mass spectrometry, DRC- dynamic reaction cell, EA AAS- electrothermal atomization atomic absorption spectrophotometry.

### 2.8.1.3 Systemic toxicity

To date, there is no universally accepted threshold level to guide investigations for systemic sequelae in arthroplasty patients (Table 2.6). This is largely due to little historical concern regarding the issue, and scarcity of data relating specific blood cobalt levels to different adverse effects. In order to bridge this data gap, researchers from the consultancy group Cardno ChemRisk carried out a series of cobalt supplementation studies that aimed to better define blood cobalt kinetics [297,331,332]. One of the studies [332], which also assessed clinical outcomes, concluded that blood cobalt averaging 10-70  $\mu\text{g L}^{-1}$  (max 117  $\mu\text{g L}^{-1}$ ) was not associated with clinically significant changes in vision, hearing, cardiac/neurological function or haematological parameters after short-term (90-day) supplementation with 1 mg/day  $\text{CoCl}_2$ .

Using the collected pharmacokinetics data, Unice *et al.* [333,334] developed a biokinetic model to estimate tissue cobalt levels in MoM patients exposed to sustained blood cobalt of 10  $\mu\text{g L}^{-1}$  for 10 years. The authors reported that the estimated peak cardiac, kidney and liver cobalt concentrations in these patients (0.04, 0.31 and 0.17  $\mu\text{g g}^{-1}$ , respectively) were similar to those estimated following 90-day cobalt supplementation, and concluded that most MoM recipients are unlikely to suffer from systemic health effects. Paustenbach *et al.* [160] used the biokinetic model to estimate the blood cobalt concentration as a function of oral cobalt dose used in previous human/animal dosing studies. According to their calculations, hypothyroidism and polycythaemia occurred at blood cobalt  $\geq 300 \mu\text{g L}^{-1}$ , while cardiotoxic and neurotoxic effects were only observed at much higher levels (range 420-1087  $\mu\text{g L}^{-1}$ ). These thresholds do not agree with multiple case reports, where systemic sequelae were associated with significantly lower blood/serum cobalt levels (Table 2.2).

**Table 2.6. Proposed blood/serum cobalt threshold levels to warrant systemic toxicity investigations.**

<b>Ref.</b>	<b>Proposed cut-off (<math>\mu\text{g L}^{-1}</math>)</b>	<b>Basis</b>	<b>Recommended action</b>
[160,206]	100 (blood)	Review of 122 studies and case reports involving Co-exposed subjects (not including hip implant patients); cobalt oral dosing studies [297,331,332]; cobalt biokinetic model [333]  The proposed threshold includes an uncertainty factor of 3 to account for the fact that persons in the various studies were exposed to cobalt for less than a year	Monitor for signs of hypothyroidism and polycythaemia
[316]	20 (serum)	Existing case reports of neurological, ototoxic, and cardiac symptoms in THA patients	Consider revision even with minor clinical symptoms
[126,335]	7 (serum)	MHRA cut-off; two Alaskan case reports of arthroprosthetic cobaltism [52]	Assess possible cardiac and neurological symptoms

The most widely employed protocol for the determination of blood cobalt levels in THA patients measures the total cobalt load, including particulate cobalt and bound/unbound cobalt ions [288]. This might be the reason why cobalt levels quoted in the case reports of systemic cobalt toxicity often do not correlate well with the observed toxicity symptoms. The issue was recently highlighted by Olmedo-Garcia *et al.* [129], who reported on two cases of severe complications after a MoP prosthesis was used to replace a fractured ceramic hip implant. Abrasion from small ceramic particles embedded in the polyethylene liner led to a catastrophic wear of the CoCr femoral head. Even though both patients had markedly elevated blood cobalt 10 years after the revision operation (60-100  $\mu\text{g L}^{-1}$ ), one suffered severe symptoms of cobalt poisoning (cardiomyopathy and hearing loss) for years without suspicion of a relationship with the prosthesis, while the other did not present with any systemic complaints. In the case described by Moniz *et al.* [123], a patient with a high-wearing MoM implant and serum cobalt of 169  $\mu\text{g L}^{-1}$  presented with heart failure symptoms that necessitated a heart transplant. A direct measurement of free cobalt might prove

more useful in understanding effects and variability of cobalt toxicity, and allow for correlations between free cobalt and certain adverse effects to be made [289].

### **2.8.2 Titanium**

Titanium levels could potentially also be used to monitor implant biodegradation [336]. High resolution ICP-MS analyses of blood and serum titanium in non-arthroplasty subjects consistently point to values lower than  $1 \mu\text{g L}^{-1}$  [246,294,337–341]. Well-functioning hip implants are associated with values ranging from less than 1 to  $9 \mu\text{g L}^{-1}$  (Table 2.7), while implants with loose or failed titanium components generally give rise to raised titanium at the time of implant failure, with the available data ranging from 1.5 to  $602 \mu\text{g L}^{-1}$  (Table 2.8). Marked variations in the reported results are likely caused by a combination of factors, including inter-study differences in implant design and stability, number of titanium components implanted [247,295], severity of wear, follow-up time, blood fraction used for analysis, analytical approach, as well as the patient's health status and environmental exposure to titanium [239]. No universally accepted cut-off values for “normal” and “abnormal” blood titanium in THA patients are in place.

**Table 2.7. Blood/serum titanium levels associated with different types of well-functioning hip implants (all measured by high resolution ICP-MS).**

Ref.	Blood Ti ( $\mu\text{g L}^{-1}$ ) <sup>a</sup>	Serum Ti ( $\mu\text{g L}^{-1}$ ) <sup>a</sup>	Implant fixation/ clinical function	Follow-up
[246]	2.306 (n=11) 1.519 (n=11)	n/a n/a	Not assessed	14-22 m 70-106 m
[339]	3.0 (n=9 males), 2.2 (n=6 females)	n/a	Not assessed	n/a
[342]	3.74; 1.40-8.80 (n=34) 2.75; 1.40-4.10 (n=33) 1.83; 0.90-4.60 (n=31) 1.30; 0.35-2.40 (n=24)	n/a n/a n/a n/a	X-Ray/ WOMAC, Merle D'Aubigne and Postel scores	3 m 6 m 1 y 2 y
[343]	n/a	2.7; 1.1-7.0 (n=6)	Not assessed	7-13 m
[247]	n/a	1.8; 1.7-1.9 (n=8)	X-Ray/ Harris Hip Score	10 y
[344]	n/a n/a	2.54; 2.17-3.10 (n=23) 2.70; 2.11-3.25 (n=23)	Not assessed	1 y 2 y
[313]	2.165 (n=15) 1.359 (n=15) 2.160 (n=15)	n/a n/a n/a	X-ray/ Short-Form 12, WOMAC, Harris Hip Score	1 y 2 y 5 y
[304]	n/a	2.28 (n=74)	X-ray/ WOMAC, Harris Hip Score	50 m

<sup>a</sup>Results are reported as mean/median; range (sample size); WOMAC- Western Ontario and McMaster Universities Osteoarthritis Index.

**Table 2.8. Blood/serum Ti levels associated with different modes of failure of hip implants.**

<b>Failure mechanism</b>	<b>Analytical technique</b>	<b>Blood Ti (<math>\mu\text{g L}^{-1}</math>)<sup>a</sup></b>	<b>Serum Ti (<math>\mu\text{g L}^{-1}</math>)<sup>a</sup></b>
<b>Loosening of a titanium component</b>	GF AAS	38-602 (n=22) [345]	n/a
	GF AAS	n/a	<LoD- 17.2 (n=21) [290]
	High resolution ICP-MS	1.5-1.8 (n=2) [341]	n/a
	ICP-OES	n/a	9.1-61 (n=2) [296]
	Not specified	n/a	15 (n=1) [346]
	High resolution ICP-MS	n/a	11.3 <sup>b</sup> (n=1) [343]
<b>Breakage of modular neck related to manufacturing error</b>	High resolution ICP-MS	n/a	4.5 <sup>b</sup> (n=1) [343]
<b>Wear, osteolysis and/or loosening</b>	High resolution ICP-MS	LoD-140 (n=23) [347]	n/a
<b>Polyethylene wear-through leading to secondary wear of titanium acetabular shell</b>	Not specified	n/a	280 <sup>b</sup> (n=1) [348]
<b>Corrosion at the neck-stem junction</b>	Not specified	n/a	1.6-5.8 (n=11) [224]
<b>Pseudotumour formation in local tissue</b>	ICP-OES	n/a	30 (n=1) [258]
<b>Fracture of ceramic liner leading to abrasive wear of titanium cup</b>	High resolution ICP-MS	21.5 <sup>c</sup> (n=1)	n/a

<sup>a</sup>Results are expressed as "range (sample size)"; <sup>b</sup>sample drawn post-revision of failed implant; <sup>c</sup>unpublished result; ICP-OES- inductively coupled plasma optical emission spectroscopy, LoD- limit of detection.



## 2.9 INDIVIDUAL SUSCEPTIBILITY TO ADVERSE EFFECTS

### 2.9.1 Renal insufficiency

The kidneys are integral to the filtration of waste, including excess metals, from the body. It follows that poor renal function can cause metal ions generated from hip implants to be retained, increasing their systemic levels [349]. This is especially important for cobalt, which is more soluble and reliant on urinary excretion than chromium and titanium. Indeed, THA patients with renal insufficiency exhibit higher blood/serum cobalt levels compared to patients with normal renal function. In Hur *et al.* [284], a group of renal failure patients displayed a mean serum cobalt level two orders of magnitude higher than a group of healthy individuals matched for implant type and time *in situ*. Notably, chromium levels were comparable in the two groups.

When cobalt was used to treat anaemia, adult patients with renal failure tended to develop symptoms of systemic cobalt toxicity (hypothyroidism, vision and hearing impairment and cardiomyopathy [138,162]) at doses that were well-tolerated by other patients, presumably due to increased accumulation of cobalt in the blood. Curtis *et al.* [138], who investigated two haemodialysis patients and one healthy subject receiving 50 mg of cobalt chloride for 2 weeks, found that the former patients displayed significantly higher blood cobalt levels than the healthy patient (approximately 400 and 800  $\mu\text{g L}^{-1}$  *versus* approximately 100  $\mu\text{g L}^{-1}$ , respectively).

THA patients with kidney insufficiency, as well as elderly patients, who often have a degree of renal compromise, might be more vulnerable to the potential deleterious effects of cobalt compared to younger, healthy patient groups. For this reason, MoM bearings are contraindicated in patients with chronic renal disease [350].

### 2.9.2 Malnutrition

Amino acids and proteins bind free cobalt ions, providing partial protection from their toxicity [172]. This helps to explain why malnourished beer drinkers displayed increased susceptibility to the cardiotoxic effects of cobalt beer fortification compared to well-nourished beer drinkers, with the identical estimated cobalt dose (0.09 mg/kg/day) (see Section 2.3.3.4) [169].

### **2.9.3 Decreased albumin binding**

Albumin, being the “managing protein” of divalent metal ions, has been identified as a possible marker of individual susceptibility to released cobalt, and onset of systemic symptoms in patients with MoM prostheses [160]. Reduced albumin binding, and the resultant increase in the proportion of free  $\text{Co}^{\text{II}}$ , could render an individual susceptible to the adverse effects at blood cobalt concentrations that would normally not pose a risk to a healthy individual. This situation might arise in a number of ways, which are discussed below.

#### **2.9.3.1 Generation of ischaemia-modified albumin**

Pathologic events, such as trauma, infections, end-stage renal disease, diabetes, hypertension, liver cirrhosis, brain/myocardial ischaemia, peripheral arterial disease, obesity and cancer can induce post-translational mutations in the N-terminus of albumin and generate ischaemia-modified albumin (IMA) [351]. This deformed variant of albumin has a lower metal binding capacity, leading to elevated concentration of free metal ions in blood and urine.

The concentration of IMA in blood can be measured by a colorimetric assay [352]. An inverse relationship exists between the amount of albumin-bound cobalt and the intensity of the colour formation, reported in absorbance units (ABSU). Piwowar *et al.* [353] demonstrated that diabetic patients, who have significantly higher IMA levels than healthy subjects (0.561 ABSU vs 0.328 ABSU), exhibit a reduced albumin-cobalt binding. It is thought that chronic hypoxia conditions, provoked mainly by hyperglycaemia and oxidative stress, are responsible for the observed effect.

Importantly, a number of chronic illnesses, including diabetes, are themselves associated with neurological and cardiovascular complaints, which can confound investigations for systemic cobalt toxicity.

#### **2.9.3.2 Displacement of cobalt from albumin**

Three of the major cobalt binding sites on albumin also bind divalent cadmium, zinc, copper and nickel ions. An appreciable increase in concentration of any of these ions could prevent binding of cobalt to the protein [354], or displace it from its albumin binding sites, resulting in an increased proportion of free  $\text{Co}^{\text{II}}$ . This effect might be pronounced in heavy smokers, as cigarette smoke is a major source of cadmium.

### **2.9.3.3 Too little albumin in the blood**

Normal albumin concentration in the serum is between 35 to 50 g L<sup>-1</sup> and remains fairly stable, though inadequate protein intake and certain pathological conditions can result in decreased levels. Besides analbuminaemia- a rare congenital disease- the main pathological situation known to lower albumin concentration is the nephrotic syndrome [355]. In addition, it has been reported that serum albumin decreases with age and cigarette smoking [356].

### **2.9.4 Potential genetic vulnerabilities**

Single nucleotide polymorphisms (SNP), which are normal genetic variations found in >1% of the population, may contribute towards inter-individual susceptibility to certain pathological conditions. SNP in the albumin gene can cause missense mutations in the amino acid sequence, generating an immature form of the protein with a compromised ability to bind metal ions [357]. It is estimated that such mutations occur with a frequency of 1:1000 to 1:3000 in the population [358].

Toll-like receptors (TLR) are required for the induction of innate immune responses to microbial ligands, and their polymorphism has been shown to influence pathogenesis and outcome of various diseases, including asthma, malaria, atherosclerosis and inflammatory bowel disease [359]. TLR4 is a key target for cobalt. It is possible that TLR4 variants exist that confer a higher susceptibility to cobalt-mediated inflammation, which might contribute to the variability of inflammatory pseudotumour formation and premature failure of MoM hips [360].

The effects of SNP in genes encoding various inflammatory mediators, enzymes, proteins and receptors have been explored in THA recipients [361]. Mihalko *et al.* [362] compared patients who had been revised because of high cobalt levels and/or ALTR, with asymptomatic MoM patients with normal cobalt levels. There was a strong genetic relationship in one cytokine gene (designated MS1), whose heterozygous or recessive isoform was preferentially found in the revision patients, while the dominant isoform was typical of the control cohort. Bachman *et al.* [363] investigated the T393C polymorphism of GNAS1 (gene coding for a protein involved in bone physiology and development of aseptic loosening) in 57 patients undergoing revision surgery for aseptic loosening. Compared with a reference group of TT individuals, TC and CC patients had a 6.25-fold and 11-fold lower risk of loosening,

respectively. Even though SNPs of a number of genes (e.g. IL6, MMP-1, MMP-2, TGF $\beta$  and OPG-163) were found to be overexpressed in patients with aseptic loosening and osteolysis, a direct relationship could not be established [361].

More recently, Langton *et al.* [364] used a genome-wide DNA sequencing strategy to assess genetic predisposition to ALVAL in THA patients with or without the condition. The authors noted that DQA1/DQAB (cell surface receptors involved in recognising and presenting foreign antigens) combinations with greater affinity for albumin-derived peptides (e.g. albumin-cobalt complex) were positively associated with ALVAL, possibly due to a higher ability to mount an immune response.

## 2.10 SUMMARY

In this literature review, the toxicological aspects of hip implant degradation, and the potential utility of blood metal measurement to monitor implant performance, have been discussed. Several gaps in the knowledge have been identified:

1. The potential risk of generalised toxicity associated with high-wearing CoCr implants is not well-recognised. There are no validated protocols or questionnaires relating to the management of patients with raised blood cobalt levels, and the diagnosis of possible systemic adverse effects. The true prevalence of arthroprosthetic cobaltism among THA recipients is unknown.
2. Implant debris can accumulate in remote organs. Since the biological activity and toxicity of metals are often determined by their oxidation state, a detailed characterisation of tissue metal deposits is warranted. While the metal composition of periprosthetic tissue has been determined, data on the distribution, and exact chemical form, of wear debris in vital organs of THA patients is scarce.
3. While alcoholism, protein-poor diet, renal compromise and chronic diseases are known to predispose to metal toxicity, genetic susceptibility to cobalt is a relatively under-researched area. Several authors explored the effects of gene SNPs on risk of osteolysis and aseptic loosening, but analyses that focus on adverse effects mediated specifically by cobalt are lacking.
4. Blood titanium concentration is an emerging biomarker of implant wear. To put measured levels into context, a laboratory reference range is needed. The existing guidelines concerning blood titanium levels in patients with well-functioning hip implants have been derived from small studies involving Q-ICP-MS or GF AAS, and are unreliable.

# **Chapter 3**

## **Assessing neurotoxic symptoms in THA patients**

The work presented in this chapter has been submitted for publication.



## **3.1 INTRODUCTION**

Patients with high-wearing CoCr hip implants can experience generalised toxicity symptoms, including peripheral neuropathy, cognitive decline, hypothyroidism and cardiomyopathy, which are associated with elevated blood metal levels (see Section 2.3.3). While both cobalt and chromium are often raised in such cases, cobalt is the more important contributor to the observed symptoms. Its ability to disturb cellular energy production and kill many different cell types is known [148]. Additionally, analogous adverse reactions resulting from occupational exposure, accidental ingestion and medicinal use are well-documented for cobalt [141,145,154], but not for chromium.

While measured blood cobalt concentrations exceeding  $7 \mu\text{g L}^{-1}$  indicate potential for adverse local tissue reactions and implant failure [314], there is no universally accepted threshold above which cobalt is likely to lead to systemic toxicity in HA patients (see Section 2.8.1.3). It has been proposed that serious symptoms, such as heart failure or blindness, do not generally occur at levels below  $100 \mu\text{g L}^{-1}$  [206], but cognitive decline, memory problems, tremor, vertigo, decreased exercise tolerance, hearing loss and cardiomyopathy were reported in association with serum cobalt as low as  $15\text{-}50 \mu\text{g L}^{-1}$  [52,130–133]. Even lower concentrations can lead to subtle changes in brain structure and function after prolonged exposure [365]. Removal of the offending prosthesis usually leads to a sharp drop in blood cobalt concentration, and to reversal of any health effects, though a few patients are known to have suffered irreversible damage [90,117,129].

### **3.1.1 Motivation**

Even though metal bearing hip replacements are no longer in widespread use, over a million patients worldwide have a MoM prosthesis. It is important to understand the consequences of long-term exposure to highly elevated blood cobalt, and raise awareness of the dangers involved, to facilitate the management of patients with high metal ion levels, but no local symptoms.

### **3.1.2 Aim**

To assess the potential long-term effects of prolonged exposure to highly elevated blood cobalt levels.

### 3.1.3 Objectives

To compare cognitive function, and the prevalence of neurotoxicity and other systemic symptoms, in patients with high blood cobalt *versus* those with low blood cobalt, using a set of self-assessment questionnaires and a mental state examination.

## 3.2 PATIENTS AND METHODS

### 3.2.1 Patients

From our hospital database, we retrospectively identified 81 patients with a hip resurfacing, or a MoM THA (either indwelling or revised), *in situ* for  $\geq 12$  months, with a history of blood cobalt  $\geq 20 \mu\text{g L}^{-1}$ . The rationale behind the  $20 \mu\text{g L}^{-1}$  threshold was that systemic toxicity symptoms were seldom reported in association with lower blood cobalt concentrations (1 published case [132]), and that this particular patient group was underrepresented in previous studies [366–368]. The control group consisted of 81 age-matched patients with CoC hip implants.

The blood samples were collected during normal patient follow-up, following a recommended protocol [288], and analysed on an ICP-MS instrument before the commencement of the study. The median peak blood cobalt level in the MoM cohort was  $48 \mu\text{g L}^{-1}$ —an order of magnitude higher than that observed in 95% of MoM population (Figure 2.11).

The clinical assessment involved 1) a set of questionnaires (Neurotoxic Symptom Checklist-60, Diabetic Neuropathy Symptom Score and Systemic Symptom Checklist); 2) a physical examination (Douleur Neuropathique-10); 3) Mini Mental State Examination, and 4) a short interview. Participants were questioned about their current medications (certain pharmaceuticals, such as platinum-based drugs and aminoglycoside antibiotics, have a known ototoxic effect [157]), intake of oral supplements, their state of health, and whether they had been involved in litigation against metal hip implant manufacturers. Since heavy alcohol use and malnutrition are risk factors for systemic cobalt toxicity [169], the participants were also asked about their diet and alcohol intake.

Diabetic patients were excluded due to peripheral neuropathy and vision/hearing disturbances, which are commonly associated with the disease [369,370]. One MoM



patient with advanced dementia was excluded due to her inability to give informed consent. After exclusions, there were 53 patients in each group.

In the MoM cohort, there were 40 patients with unilateral (16 male, 24 female) and 13 with bilateral (2 male, 11 female) implants, out of which 28 (53%) were revised to a non-MoM bearing at a median time of 38 months (IQR 26-62) before assessment. In each case, the indication for revision was high metal ions associated with unexplained pain and/or ARMD. MoM patients were exposed to blood cobalt  $\geq 20 \mu\text{g L}^{-1}$  for a median of 3 years (IQR 2-5). Implant details are listed in Table 3.1.

In the control group, blood cobalt measurements were available for 13 of the participants (25%). Since the remaining subjects had no other metal implants, and disclosed no occupational, dietary or previous implant exposure to cobalt, it was assumed that they displayed similarly low concentrations ( $\text{Co} < 1 \mu\text{g L}^{-1}$ ).

**Table 3.1. Implant details (MoM cohort).**

<b>Patient ID</b>	<b>Implant type</b>	<b>Revised before assessment?</b>	<b>MoM implant time <i>in situ</i> (years)</b>
1	THA (brand unknown)	No	13
2	BHR	Yes <sup>a</sup>	18
3	Cormet HR	No	11
4	Birmingham/Synergy THA	Yes <sup>a</sup>	8
5	2 x BHR	No	16; 14
6	BHR	No	18
7	Magnum/Taperloc THA	No	8
8	BHR	No	10
9	2 x BHR	No	20
10	BHR	Yes <sup>a</sup>	15
11	ASR XL/Corail THA	Yes <sup>a</sup>	10
12	2 x BHR	Yes <sup>a</sup>	5; 5
13	2 x BHR	Yes (one hip) <sup>a</sup>	11
14	Muller THA	Yes <sup>a</sup>	6
15	Pinnacle/Corail THA	Yes <sup>a</sup>	9
16	Adept/CLS Spotorno THA	No	13
17	ASR/Corail THA	Yes <sup>a</sup>	11
18	BHR	Yes <sup>a</sup>	8

19	2 x Cormet HR	No	13
20	Birmingham/Synergy THA	No	9
21	BHR	Yes <sup>a</sup>	12
22	2 x BHR	No	14
23	ASR HR	No	13
24	BHR	No	15
25	Ultima C-stem THA;ASR/Corail THA	No	12; 12
26	ASR HR	Yes <sup>a</sup>	10
27	Magnum/Recap HR	Yes <sup>a</sup>	7
28	BHR	Yes <sup>a</sup>	16
29	Magnum/Taperloc THA	Yes <sup>a</sup>	6
30	Magnum/Taperloc THA	Yes <sup>a</sup>	9
31	2 x BHR	No	11; 6
32	BHR	Yes <sup>a</sup>	12
33	Magnum/Taperloc THA	No	11
34	HR (brand unknown)	Yes <sup>a</sup>	7
35	Cormet THA	Yes <sup>a</sup>	6
36	2 x Pinnacle/Corail THA	Yes (one hip) <sup>a</sup>	9
37	Trident/Accolade THA	Yes <sup>a</sup>	3
38	BHR	No	11
39	BHR	Yes <sup>a</sup>	10
40	Cormet HR	No	12
41	HR (brand unknown)	Yes <sup>a</sup>	14
42	BHR	No	6
43	ASR HR	Yes <sup>a</sup>	7
44	THA (brand unknown), BHR	No	11; 9
45	2 x BHR	No	11
46	BHR	Yes <sup>a</sup>	4
47	THA (brand unknown)	Yes <sup>a</sup>	7
48	ReCap Magnum/Stanmore THA	No	11
49	2 x BHR revised to MoM THA in 2013/2015	No	12; 11
50	MITCH/Accolade THA	Yes <sup>a</sup>	9
51	ReCap Magnum/Stanmore THA	Yes <sup>a</sup>	9
52	BHR	Yes <sup>a</sup>	9
53	BHR, Cormet HR	Yes (one hip) <sup>a</sup>	12

<sup>a</sup>Indication for revision surgery was high metal ions with unexplained pain and/or ARMD; ASR- articular surface replacement, BHR- Birmingham hip resurfacing.

### 3.2.2 Neurotoxic Symptom Checklist-60 (NSC-60)

NSC-60 is a Dutch questionnaire developed by TNO and Arbouw- the Dutch expertise and service centre for working conditions in the construction industry- as a screening tool for chronic neurotoxic symptoms of occupational exposure to organic solvents and heavy metals [371,372]. Since neurobehavioural sequelae described in case reports of arthroprosthetic cobaltism were often similar to those experienced by painters and heavy metal workers (fatigue, poor memory and concentration, depression, irritability, mood changes, headaches, paraesthesia, sleep disturbances and vertigo), NSC-60 has been extended to evaluating neurotoxicity in hip replacement patients [366,367].

The questionnaire, adapted from Hooisma and Emmen *et al.* [373], lists 53 symptoms and 7 personality items, which are scored on a four-point scale: “Never” (1 point), “Seldom” (2 points), “Sometimes” (3 points) or “Often” (4 points). The 53 questions are grouped into 9 different categories (clusters): cognitive defects/absentmindedness, chest complaints, balance (equilibrium) disturbances, sleeping difficulties, mood disturbances, sensorimotor complaints, physical complaints, fatigue and organic solvent-specific neurotoxicity (Table 3.2). The personality questions are relatively independent of neurotoxic symptoms and designed to reflect the attitude of answering, with high cluster scores indicating a tendency to report more/more severe symptoms [374].

The total score, and mean category scores, were recorded for each participant, before median total and category scores were calculated for each cohort. The median category scores were compared against category-specific clinical thresholds.

**Table 3.2. Neurotoxic Symptom Checklist-60 in Dutch (original) and in English.**

<b>Dutch</b>	<b>English<sup>a</sup></b>
Valt u moeilijk in slaap?	Do you find it difficult to fall asleep?
Vindt u het moeilijk om de inhoud van kranten of boeken te begrijpen?	Do you find it difficult to understand the content of newspapers or books?
Heeft u krachtverlies in uw benen?	Do you lose strength in your legs?
Bent u duizelig?	Do you get dizzy?
Voelt u zich terneergeslagen?	Do you feel depressed?

Heeft u last van uw maag?	Do you have problems with your stomach?
Heeft u nachtmerries?	Do you have nightmares?
Heeft u moeilijkheden bij het bewegen van uw handen als uw werk nauwkeurigheid vraagt	Do you have trouble making fine movements with your hands when precision is required?
Bent u wel eens misselijk?	Do you ever get nauseous?
Voelt u zich 's morgens wel eens abnormaal moe?	Do you feel abnormally tired in the morning?
Bent u vergeetachtig?	Are you forgetful?
Heeft u last van hartkloppingen?	Do you suffer from heart palpitations?
Vindt u het moeilijk u te concentreren	Do you find it hard to concentrate?
Bent u ongeduldig?	Are you impatient?
Gebruikt u "spiekbriefjes" om dingen te onthouden?	Do you use little notes to help you remember things?
Valt u wel eens in slap terwijl u niet in bed ligt?	Do you fall asleep while you're not in bed?
Verandert uw stemming wel eens zonder directe aanleiding?	Do you experience sudden changes of mood without reason?
Heeft u last van trillende handen?	Do you suffer from trembling hands?
Wordt u vaak wakker in uw slaap?	Do you wake up in the night?
Heeft u een verdoofd of tintelend gevoel in uw handen?	Do you have a numb or tingling sensation in your hands?
Voelt u zich rusteloos?	Do you feel restless?
Bent u wel eens plotseling angstig, zonder dat daarvoor een reden is	Do you get scared all of a sudden without reason?
Gebeurt het dat als u iets wilt zeggen of doen, dat u vergeten bent wat u wilde?	Do you ever want to say or do something, but forget what it was?
Ziet u het wel eens niet meer zitten?	Do you feel listless/fed up with life?
Heeft u wel eens krachtverlies in uw handen en armen?	Do you ever lose strength in your hands and arms?
Voelt u zich 's avonds wel eens abnormaal moe?	Do you feel abnormally tired in the evenings?
Laat u wel eens dingen uit uw handen vallen?	Do you drop things out of your hands?

Moet u wel eens terug gaan om te controleren of u bijv. het gas heeft uitgedaan of de deur heeft afgesloten?	Do you have to go back to check if you have, for example, turned off the gas or locked the front door?
Voelt u zich rusteloos?	Do you feel restless?
Droomt u weg in uw eigen gedachten?	Do you daydream?
Heeft u moeilijkheden bij het bewegen van uw handen als uw werk kracht vraagt?	Do you have difficulty moving your hands when force is required?
Heeft u last van oorsuizingen?	Do you suffer from ringing in your ears?
Bent u slaperig?	Do you get sleepy?
Bent u zenuwachtig als u zich moet haasten?	Are you nervous when you have to hurry?
Heeft u een verdoofd of tintelend gevoel in uw benen?	Do you have a numb or tingling sensation in your legs?
Voelt u zich geïrriteerd?	Do you feel irritated?
Heeft u last van evenwichtsstoornissen?	Do you suffer from disturbances of balance?
Hebben anderen geklaagd over uw geheugen?	Do others complain about your memory?
Merkt u veranderingen in uw reukvermogen?	Do you notice changes in your sense of smell?
Vindt u uzelf nu eens vol energie end dan weer lui?	Do you find yourself full of energy and then lazy again?
Heeft u pijnlijke tintelingen ergens in uw lichaam?	Do you have painful tingling anywhere on your body?
Zweet u abnormaal vaak?	Do you sweat abnormally often?
Heeft u hoofdpijn?	Do you have headaches?
Voelt u zich ongelukkig?	Do you feel unhappy?
Heeft u het gevoel iets in uw keel te hebben waardoor u moeilijk kunt slikken?	Do you feel like you have something in your throat, which makes it difficult for you to swallow?
Heeft u last van ademhalingsproblemen?	Do you suffer from breathing problems?
Bent u gevoelig voor lawaai?	Are you sensitive to noise?
Vermoeit het u als u in een groep mensen bent?	Do you get tired when you're in a group of people?
Heeft u het koud?	Are you cold?

Voelt u zich wel eens dronken zonder dat u alcohol heeft gedronken?	Do you ever feel drunk without having drunk any alcohol?
Bent u wel eens afwezig?	Are you ever absent-minded?
Voelt u wel eens druk op uw borst?	Do you ever feel pain or pressure in your chest?
Als u een onbekende ontmoet, vindt u het dan moeilijk om een gesprek te beginnen?	When you meet a stranger, do you find it difficult to start a conversation?
Vindt u het moeilijk om snel te werken?	Do you find it difficult to work quickly?
Vindt u uzelf neerslachtig?	Are you “down in the dumps”?
Vindt u het onplezierig om onbekenden te ontmoeten?	Do you find it unpleasant to meet new people?
Vindt u het moeilijk om vrienden te maken?	Do you find it difficult to make friends?
Voelt u zich geremd bij vreemden?	Are you inhibited by strangers?
Vindt u het vervelend als men u haast?	Do you find it annoying when somebody hurries you?
Vindt u het moeilijk om beslissingen te nemen?	Do you find it difficult to make decisions?

<sup>a</sup>Partial English translation was provided by the authors of the questionnaire [372]; \*this category was not considered in the current study.

### 3.2.3 Diabetic Neuropathy Symptom Score (DNS)

DNS is a scoring system validated to detect symptoms of diabetic polyneuropathy [375], which has recently been used to screen for neuropathy in hip replacement patients [367]. The questionnaire consists of 4 questions scored as “Present” (1 point) or “Absent” (0 points), with a total score  $\geq 1$  suggesting distal diabetic neuropathy with 64% sensitivity and 81% specificity [376] (Figure 3.1).

**In the past two weeks:**

- 1) Did you suffer unsteadiness in walking? (*Need for visual control/walking like a drunken man/lack of contact with floor*)
- 2) Did you have a burning, aching pain or tenderness at your legs or feet? (*Occurring at rest or at night- NOT related to exercise*)
- 3) Did you have a prickling sensations at your legs and feet? (*Occurring at rest or at night*)
- 4) Did you have places of numbness on your legs or feet?

**Figure 3.1. Diabetic Neuropathy Score.**

### **3.2.4 Systemic Symptom Checklist (SSC)**

SSC is a questionnaire written by the author of this thesis. It covers 12 of the most commonly reported symptoms associated with elevated blood cobalt levels, and is prefaced by asking whether the patient had been told that they had high metal ion levels, to assess for bias (Figure 3.2). The answers to the questions (“Yes”- 1 point; “No”-0 points) were analysed separately for frequency of reporting.

<b>Preliminary questions:</b>	
1. Do you know your blood metal level?	<input type="checkbox"/>
2. Have you been told that you have high blood metal ion level?	<input type="checkbox"/>
<b>Since the day your implant was inserted:</b>	
1. Have you noticed any face swelling (particularly around the eyes)?	<input type="checkbox"/>
2. Do you feel cold when others feel warm?	<input type="checkbox"/>
3. Have you experienced:	
a) Significant unexplained weight loss?	<input type="checkbox"/>
b) Significant unexplained weight gain?	<input type="checkbox"/>
4. Do you have a metallic taste in your mouth?	<input type="checkbox"/>
5. Have you noticed that your eyesight has worsened significantly?	<input type="checkbox"/>
6. Have you noticed that your hearing has worsened significantly?	<input type="checkbox"/>
7. Are you often out of breath:	
a) On exertion?	<input type="checkbox"/>
b) When lying flat?	<input type="checkbox"/>
8. Are your ankles swollen?	<input type="checkbox"/>
9. Have you developed any permanent skin changes (e.g. rash or eczema):	
a) Localized to the implant site?	<input type="checkbox"/>
b) Not localized to the implant site (anywhere on your body)?	<input type="checkbox"/>

**Figure 3.2. Systemic Symptom Checklist.**

### **3.2.5 Douleur Neuropathique 10 (DN-10)**

DN-10 is a validated French questionnaire that is used in the clinical setting to distinguish between neuropathic pain (pain resulting from injury to the nervous system) and that caused by other somatic lesions. It consists of 10 questions answered “Yes” (1 point) or “No” (0 points), which aim to establish how the pain feels to the patient (Figure 3.3). A physical examination is needed to assess whether there is reduced sensation to touch or pinprick, and whether brushing increases or causes pain. English version of the survey [377] was administered if the participant reported presence of chronic pain. A total score of  $\geq 4$  indicates neuropathic pain with 90% specificity and 83% sensitivity [377].




Tick the box when patient answers “Yes”:

1. Does the pain have one of more of the following characteristics?
  - Burning
  - Painful Cold
  - Electric Shocks
2. Is the pain associated with one or more of the following symptoms in the same area?
  - Tingling
  - Pins and Needles
  - Numbness
  - Itching
3. Is the pain located in an area where the physical examination may reveal one or more of the following characteristics?
  - Touch Hypoaesthesia
  - Prickling Hypoaesthesia
4. In the painful area, can the pain be caused or increased by:
  - Brushing

**Figure 3.3. The English version of Douleur Neuropathique-10.**

### **3.2.6 Mini Mental State Examination (MMSE)**

Following recent reporting of neurocognitive deficits in MoM patients [378], each participant underwent the MMSE [379] (Figure 3.4). The examination, which is a validated test for cognitive function in adults, consists of 30 questions that test the participant’s orientation, memory, language, ability to follow verbal commands, attention and visual-spatial skills. A total score of  $\geq 28$  was considered normal for the studied population, with  $< 25$  indicating possible dementia [379].

Maximum Score	Patient's Score	Questions
5		"What is the year? Season? Date? Day? Month?"
5		"Where are we now? State? County? Town/city? Hospital? Floor?"
3		The examiner names three unrelated objects clearly and slowly, then the instructor asks the patient to name all three of them. The patient's response is used for scoring. The examiner repeats them until patient learns all of them, if possible.
5		"I would like you to count backward from 100 by sevens." (93, 86, 79, 72, 65, ...) Alternative: "Spell WORLD backwards." (D-L-R-O-W)
3		"Earlier I told you the names of three things. Can you tell me what those were?"
2		Show the patient two simple objects, such as a wristwatch and a pencil, and ask the patient to name them.
1		"Repeat the phrase: 'No ifs, ands, or buts.'"
3		"Take the paper in your right hand, fold it in half, and put it on the floor." (The examiner gives the patient a piece of blank paper.)
1		"Please read this and do what it says." (Written instruction is "Close your eyes.")
1		"Make up and write a sentence about anything." (This sentence must contain a noun and a verb.)
1		"Please copy this picture." (The examiner gives the patient a blank piece of paper and asks him/her to draw the symbol below. All 10 angles must be present and two must intersect.) 
30		TOTAL

**Figure 3.4. Mini Mental State Examination.**

### 3.2.7 Statistical analysis

Before statistical tests were performed, the data was checked for normality with the Shapiro-Wilk test. Total and mean cluster symptom scores of the NSC-60 questionnaire followed a skewed distribution, and were compared between cohorts with Mann-Whitney U test, while the mean MMSE scores, which were normally distributed, were analysed using the independent samples T-test. The prevalence of abnormal DNS and DN-10 scores was compared with Pearson's Chi Squared test. Answers to the SSC questionnaire were analysed separately using Pearson's Chi Squared test or, if expected frequencies fell below 5, two-tailed Fisher's Exact test.

IBM SPSS (version 25) was employed for all statistical analyses, with p-values <0.05 considered statistically significant. All graphs and charts were produced in SPSS or Microsoft Excel (version 16.22).

### 3.2.8 Study design flowchart

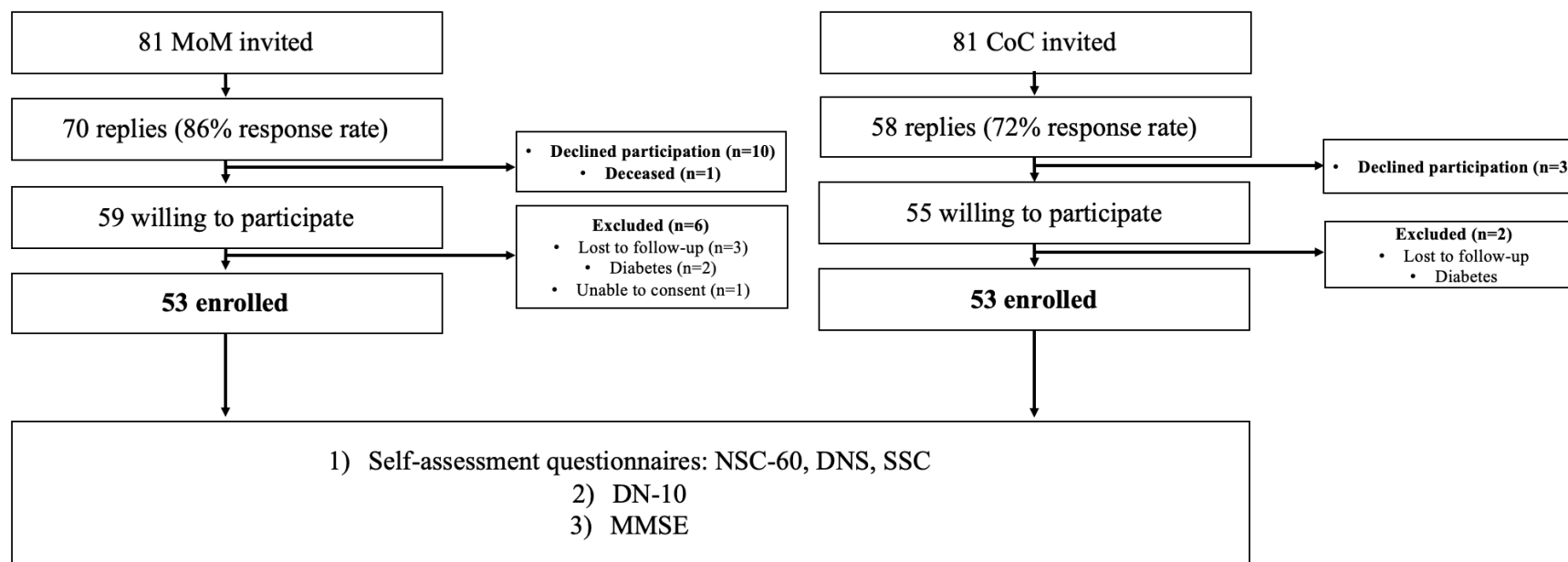


Figure 3.5. Flowchart outlining participant enrolment and clinical assessment.

**Table 3.3. Summary of participant demographics.**

		Age <sup>a</sup>			Max recorded blood cobalt ( $\mu\text{g L}^{-1}$ )			Blood cobalt at last follow-up ( $\mu\text{g L}^{-1}$ )		
		Overall (n=53)	Males (n=18) <sup>b</sup>	Females (n=35) <sup>b</sup>	Overall (n=53)	Males (n=18) <sup>d</sup>	Females (n=35) <sup>d</sup>	Overall (n=53)	Males (n=18) <sup>e</sup>	Females (n=35) <sup>e</sup>
<b>MoM</b>	<b>Mean</b>	66	62	68	69.7	81.1	63.9	22.4	25.4	20.9
	<b>Median</b>	67	62	69	48.0	40.9	54.2	14.6	18.8	9.1
	<b>Range</b>	38-85	38-76	43-85	20.6-587.9	21.0-597.9	20.6-193.0	0.2-124.0	0.2-124.0	0.6-86.7
	<b>IQR</b>	60-74	53-73	61-74	26.9-78.8	25.8-69.5	27.2-84.3	1.6-30.4	2.85-36.4	1.4-29.3
		<b>Overall (n=53)</b>	<b>Males (n=23)<sup>c</sup></b>	<b>Females (n=30)<sup>c</sup></b>	<b>Overall (n=13)</b>	<b>Males (n=2)</b>	<b>Females (n=11)</b>	<b>Overall (n=13)</b>	<b>Males (n=2)</b>	<b>Females (n=11)</b>
<b>CoC</b>	<b>Mean</b>	68	67	69	0.2	0.2	0.2	0.2	0.2	0.2
	<b>Median</b>	70	69	71	0.2	0.2	0.2	0.2	0.2	0.2
	<b>Range</b>	33-86	33-86	51-82	0.1-0.5	0.1-0.2	0.1-0.5	0.1-0.5	0.1-0.2	0.1-0.5
	<b>IQR</b>	64-74	62-74	65-74	0.1-0.2	n/a	0.1-0.2	0.1-0.2	n/a	0.1-0.2

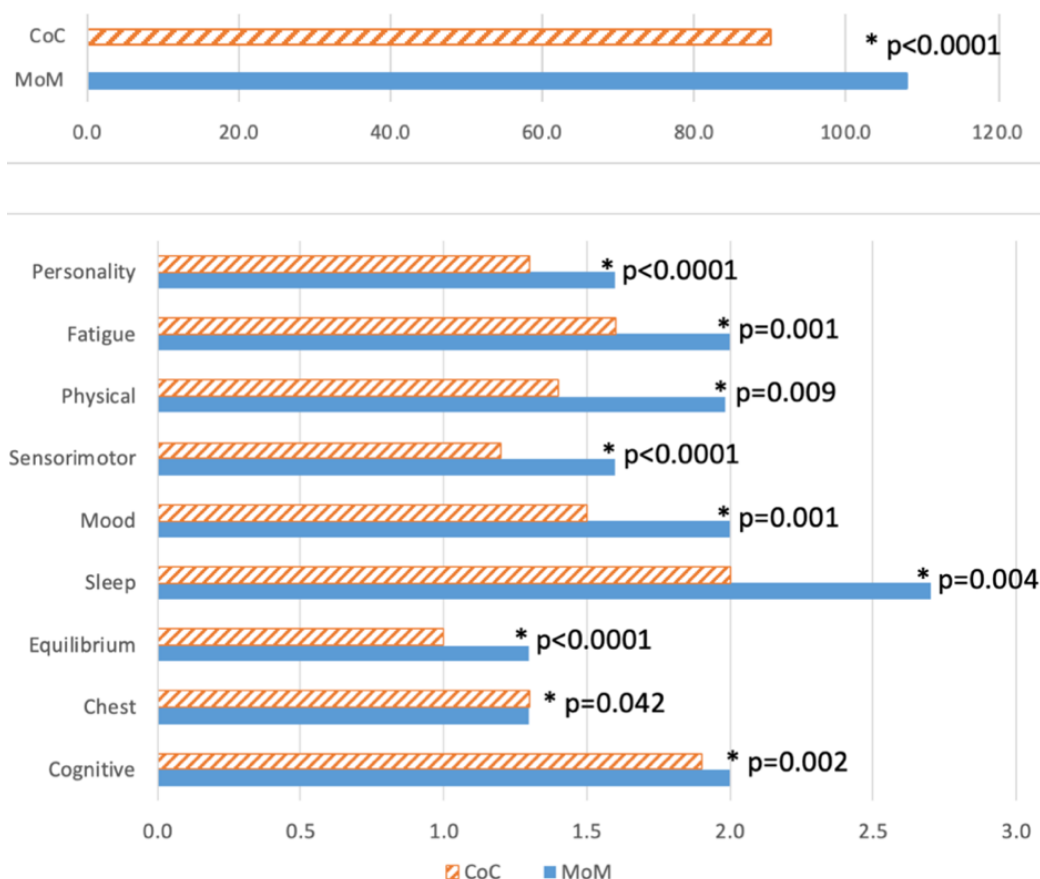
<sup>a</sup>No significant difference between cohorts (p=0.306); <sup>b</sup>Significant gender difference (p=0.03); <sup>c</sup>No significant gender difference (p=0.47); <sup>d</sup>No significant gender difference (p=0.34); <sup>e</sup>No significant gender difference (p=0.62).

### 3.3 RESULTS

Baseline patient characteristics are summarised in Table 3.3.

#### 3.3.1 NSC-60

We observed a significantly higher prevalence of cognitive problems, chest complaints, balance disturbances, sleep disorders, mood changes, sensorimotor disorders, physical complaints and fatigue in the high cobalt group compared to control. The median total score was also higher at 108 (IQR 92.5-136.5), compared to 90 (IQR 79.5-105.0) in the CoC group (Figure 3.6). Median personality score, which aimed to measure the participants' tendency to overreport symptoms, was significantly higher in the MoM group. Total and cluster scores did not differ between current MoM patients, and those whose implants had been revised prior to commencement of the study.



**Figure 3.6. Comparison of median total NSC-60 scores (top) and symptom scores (bottom) between the two study groups. Asterisks indicate statistically significant differences.**

Despite the higher scores and higher frequency of abnormal results in the MoM group, median cluster scores, including the personality score, never exceeded their respective clinically important cut-offs. (Table 3.4).

**Table 3.4. Median NSC-60 cluster scores in relation to their clinically important thresholds. The frequency of abnormal scores is shown in brackets.**

<b>NSC-60 cluster</b>	<b>Cut-off value (abnormal if &gt;...)</b>	<b>MoM</b>	<b>CoC</b>
<b>Cognitive</b>	2.9	2.0 (17)	1.9 (0)
<b>Chest</b>	2.1	1.3 (17)	1.3 (2)
<b>Equilibrium</b>	2.0	1.3 (19)	1.0 (4)
<b>Sleep</b>	2.7	2.7 (32)	2.0 (19)
<b>Mood</b>	2.7	2.0 (19)	1.5 (12)
<b>Sensorimotor</b>	2.8	1.6 (13)	1.2 (0)
<b>Physical</b>	2.5	2.0 (23)	1.4 (0)
<b>Fatigue</b>	3.1	2.0 (9)	1.6 (0)
<b>Personality</b>	2.9	1.6 (4)	1.3 (0)

### 3.3.2 DNS and DN-10

The case cohort displayed a significantly higher frequency of abnormal DNS ( $p < 0.0001$ ) and DN-10 ( $p = 0.028$ ) scores compared to control (Table 3.5). In three MoM patients and the one CoC patient, the chronic pain was likely caused or confounded by other comorbidities (carpal tunnel syndrome, spina bifida, lupus and lower extremity bypass).

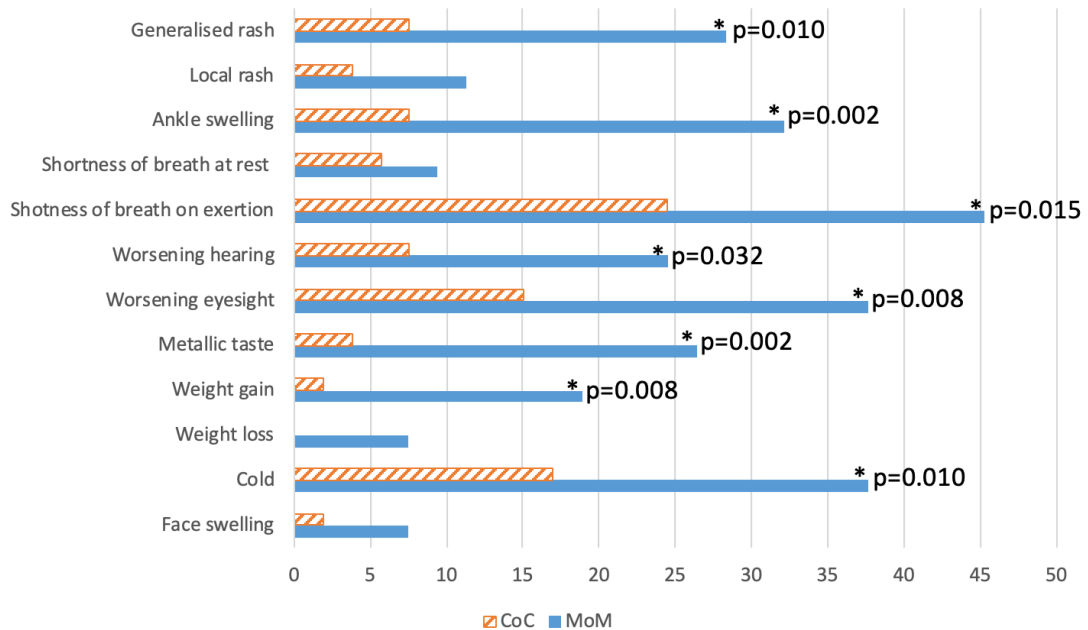
**Table 3.5. Summary of DNS and DN-10 results in the two study groups.**

	<b>MoM (n=53)</b>	<b>CoC (n=53)</b>
<b>N abnormal DNS scores (%)</b>	32 (60.3)	13 (24.5)
<b>N abnormal DN-10 scores (%)*</b>	7 (13.2)	1 (1.9)

\*DN-10 was administered to 9 MoM and 1 CoC patients.

### 3.3.3 SSC

There were significant differences in the frequency of reporting of 8 out of 12 symptoms (Figure 3.7). The total score was also significantly higher in the MoM group compared to control (88 and 37, respectively;  $p < 0.0001$ ). Symptom reporting frequency was similar in current MoM patients, and those whose implant had been revised prior to the commencement of the study.



**Figure 3.7. Frequency of systemic toxicity symptoms reported in the two study groups (results are expressed as percentages). Asterisks denote statistically significant differences.**

### 3.3.4 MMSE

We observed a small, but statistically significant ( $p=0.017$ ), difference in cognitive function between high cobalt patients and controls, with a median score of 29 (IQR 29-30) and 30 (IQR 29-30), respectively. There was one abnormal score (27) in the case group, and none in the control group. There were no significant gender differences.

## 3.4 DISCUSSION

The prevalence of systemic cobalt toxicity in Dutch MoM patients was previously assessed using NSC-60, DNS and DN-10 [366,367]. Van der Straeten and colleagues

[366] noted a significant correlation between increasing blood cobalt levels and frequency of neurotoxic symptoms. The highest prevalence of adverse effects was found in the  $\text{Co} > 20 \mu\text{g L}^{-1}$  group, with female gender and age  $< 50$  years acting as confounding factors. In contrast, van Lingen *et al.* [367] found no relationship between whole blood cobalt levels and neurotoxic symptoms in their cohort. The latter study only included 1 male and 18 females with blood  $\text{Co} > 20 \mu\text{g L}^{-1}$ , and might have been underpowered to detect neurotoxic symptoms in that group. A more recent study by Jelsma and co-workers [368] showed a trend, but no significance, in systemic complaints from patients with high cobalt concentrations, with neuro-ocular toxicity being the most commonly reported. The high cobalt group was, again, underrepresented (9 hips compared to 52 patients in the control group). We found that the prevalence and severity of neurotoxic complaints (as assessed with the NSC-60 questionnaire), and the frequency of abnormal DN-10 scores, were higher in the MoM group. This is in line with Van der Straeten's observations [366]. Additionally, we noted a significantly higher frequency of abnormal DNS scores in the case cohort, which is a novel finding.

The MMSE was previously used to assess the cognitive state of 10 recipients of the now-recalled ASR total hip replacement [378]. The participants, with a mean age of 60.5 years and mean implant time *in situ* of 4.4 years, had toxic levels of cobalt and chromium in the blood (mean 39.5 and 17.6  $\mu\text{g L}^{-1}$  respectively) before revision. A mean MMSE score of 24.2 was noted, with short-term memory deficit in 70% of the sample. The assessment took place several years after revision surgery, when the blood metal levels were expected to have normalised, so the scores were found to be unexpectedly low. The authors concluded that elevated blood metal levels might exert a long-term impact on cognitive function, which “could have major, as yet unrecognised, implications for public health” [378]. A similar effect was not observed in our series. Even though there was a significant difference between mean group MMSE scores, all participants but one passed the test (total score  $\geq 28$ ). Mental state testing can be affected by a number of factors, such as age, education, cultural background and certain disease states [380], which might explain the conflicting findings. Additionally, Green's study had a much smaller sample size, and might have been more prone to selection bias and random error than our investigation.



Three patients in the MoM cohort sought neurological opinion prior to our assessment, out of which two were diagnosed with new-onset tremor. In the third case, the patient (indwelling bilateral HR with peak blood Co of  $21.5 \mu\text{g L}^{-1}$ ) complained of mental fog and significant memory loss since surgery, but neurological evaluation found no abnormalities. Notably, when 10 patients from Van Lingen's cohort (mean blood cobalt  $46.8 \mu\text{g L}^{-1}$ ; range  $18\text{--}153 \mu\text{g L}^{-1}$ ) underwent clinical testing, no symptoms of neurological dysfunction, cardiomyopathy or thyroid insufficiency could be identified after 3-6 years follow-up [381].

One patient with advanced dementia was excluded from the study due to her inability to give informed consent. This particular patient underwent hip replacement surgery after the onset of the condition, so it is not thought that dementia was related to the elevated blood cobalt.

### 3.4.1 Study limitations

The participants were required to attend a clinic visit, so that DN-10 and MMSE could be administered. The advantage of the face-to-face approach over postal questionnaires is that the patients could have the meaning of the questions explained, which helped to ensure that they were interpreted the same, and that the forms were completed fully. The requirement for an outpatient visit reduced the number of participants we were able to assess. Despite relatively small sample size, the current study is the largest neurobehavioural investigation of HA patients with highly elevated blood cobalt levels to date.

There are no validated protocols or questionnaires relating to the diagnosis of systemic toxicity in HA patients. The self-assessment questionnaires we employed, with the exception of the SSC, were not designed for cobalt toxicity. Interestingly, the NSC-60 cluster scores, including personality items, were consistent with those of 42 cadmium-exposed workers and 47 controls investigated by Viaene *at al.* [374]. Cadmium and cobalt ions are both divalent and act *via* similar toxicity mechanisms (ROS and free radical generation, inhibition of cellular respiration and disruption of calcium signalling and homeostasis [382]) to produce similar neurotoxic symptoms. The finding suggests that, despite not having been validated for the screening of cobalt neurotoxicity in HA patients, NSC-60 could be successfully extended to this scenario. Notwithstanding, the questionnaires include a number of non-specific symptoms that

could be caused by other factors, such as advanced age or chronic diseases [121]. We addressed this by excluding diabetic patients from the study and ensuring that the two cohorts were matched for age. .

Another limitation of our study is the heterogeneity of the case group. Since MoM constructs are no longer widely utilised, any new case-control studies of arthroprosthetic cobaltism have to rely on a finite existing pool of patients with MoM implants. These patients will have been exposed to varying blood cobalt levels for varying lengths of time, with 95% of the population displaying a steady-state blood cobalt concentration  $<5 \mu\text{g L}^{-1}$ . It follows that the number of patients with blood cobalt content high enough to raise systemic toxicity concerns ( $>20 \mu\text{g L}^{-1}$ ) is very limited, and it is difficult to draw a homogenous sample of current MoM recipients that is large enough to be sufficiently powered. Our study aimed to recruit all patients with a history of elevated blood cobalt levels at our institution to study potential long-term adverse effects of cobalt exposure. This approach was intended to reduce selection bias and maximise sample size.

11 patients did not reply to the invitation letter while 10 declined participation for undisclosed reasons, which could have distorted the sample population. For example, patients who thought they may have been harmed by metal implants could have been more drawn to taking part in a study investigating the effects of cobalt exposure. 2 patients (4%) in the MoM group admitted they had been involved in litigation against MoM implant manufacturers. Median personality scores, though not exceeding the clinically-relevant threshold, were also significantly higher in MoM patients ( $p<0.0001$ ), possibly contributing to the higher symptom scores.

A further limitation of our study is the subjective nature of self-assessment questionnaires, and potential for bias. The MoM cohort knew that they were being evaluated for adverse effects of cobalt exposure, and 79% of the group were aware of their history of high blood metal levels, which possibly influenced their answers. This was unavoidable, as not explaining the study to the participants, or not informing them of their blood cobalt levels, would have been unethical.

### 3.5 CONCLUSION

The current study is the largest investigation of potential systemic toxicity symptoms in HA patients with markedly elevated blood cobalt ( $\geq 20 \mu\text{g L}^{-1}$ ) to date. We detected an increase in a range of self-reported neurotoxic symptoms, and a small decrease in cognitive function, in the high cobalt group compared to control. However, the differences fell below the clinically significant thresholds and patients were generally well-functioning. While these findings do not support the need for regular systemic health check-ups in asymptomatic patients with highly (but not extremely) elevated blood cobalt, those with high blood cobalt levels should be questioned about possible systemic health complaints at follow-up visits. Further studies employing formal cardiac, audiometric, ophthalmologic, neuro-cognitive, nerve conduction studies and thyroid testing are needed to assess the sensitivity of the questionnaires, and their usefulness as a screening tool in the MoM population.



# Chapter 4

## **Analysing metal deposits in vital organs of THA patients**

The work presented in this chapter has been published.\*

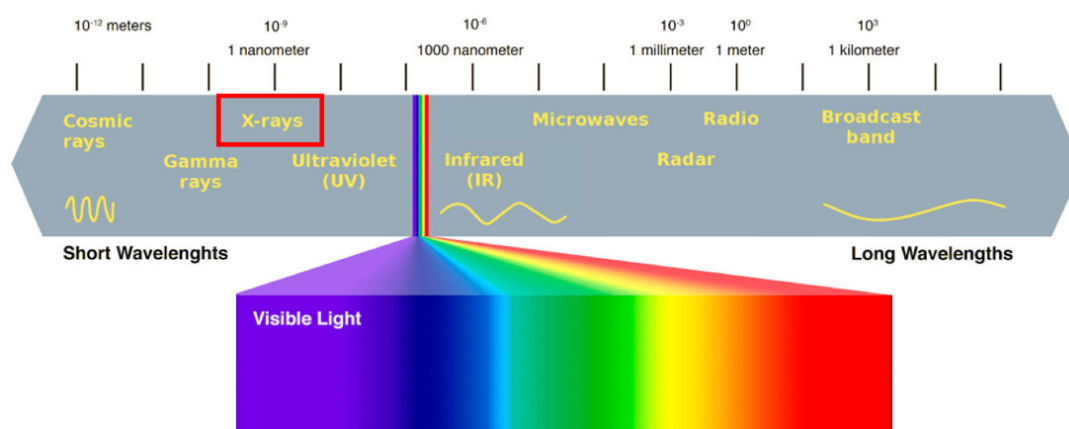
\*Swiatkowska I, Mosselmans J. F.W, Geraki T, Wyles C.C, Maleszewski J.J, Henckel J, Sampson B, Potter D.B, Osman I, Trousdale R.T, Hart A.J. Synchrotron analysis of human organ tissue exposed to implant material. *Journal of Trace Metals in Medicine and Biology* 46 (2018) 128–137.



## 4.1 BACKGROUND: SYNCHROTRON SPECTROSCOPY

### 4.1.1 Synchrotrons

Every time the path of an electron beam is bent, light is emitted. Synchrotrons are powerful scientific machines that utilise this simple principle in order to generate intense light beams that span a wide frequency range- from infrared to the highest energy X-rays (Figure 4.1). They achieve this by accelerating electrons to very high speeds before bending their trajectory with a series of magnets. The resultant radiation is directed off into a number of laboratories, where it is focused and used to conduct different experiments. Synchrotron light is millions of times brighter than that from conventional excitation sources (X-ray tubes and gamma-emitting radioisotopes), and can be 10 billion times brighter than the sun. The high brightness and tunability make it ideal for the study of individual molecules and atoms in a sample.

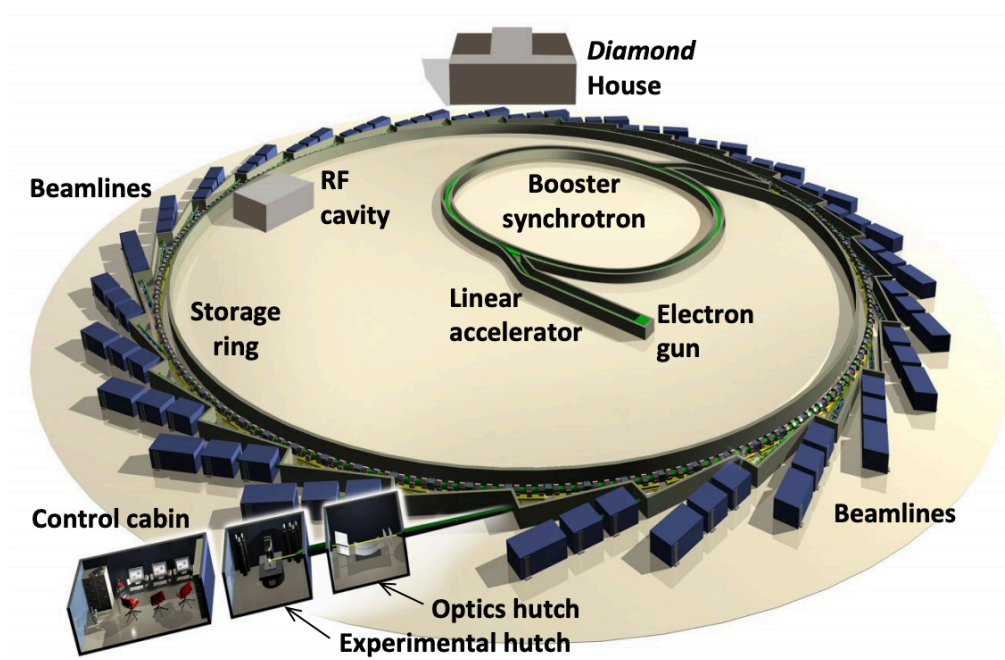


**Figure 4.1. The electromagnetic spectrum. Synchrotron light mainly consists of X-ray radiation, which has a sufficiently short wavelength to be used to probe the properties of matter (adapted from kisspng.com).**

There are over 70 synchrotrons in various stages of development around the world. Access to these facilities can be gained *via* a competitive proposal process, whereby experiments of the greatest scientific value are selected by a panel of external scientific advisors. Successful applicants are allocated beamtime, which is free of charge for academics.

### 4.1.2 Diamond Light Source

Diamond Light Source, located in Didcot in Oxfordshire, is the UK's national synchrotron facility. It was established in 2002 and funded as a joint venture by the Science & Technology Facilities Council (STFC) and the Wellcome Trust. A diagram showing the different parts of Diamond synchrotron is shown in Figure 4.2.



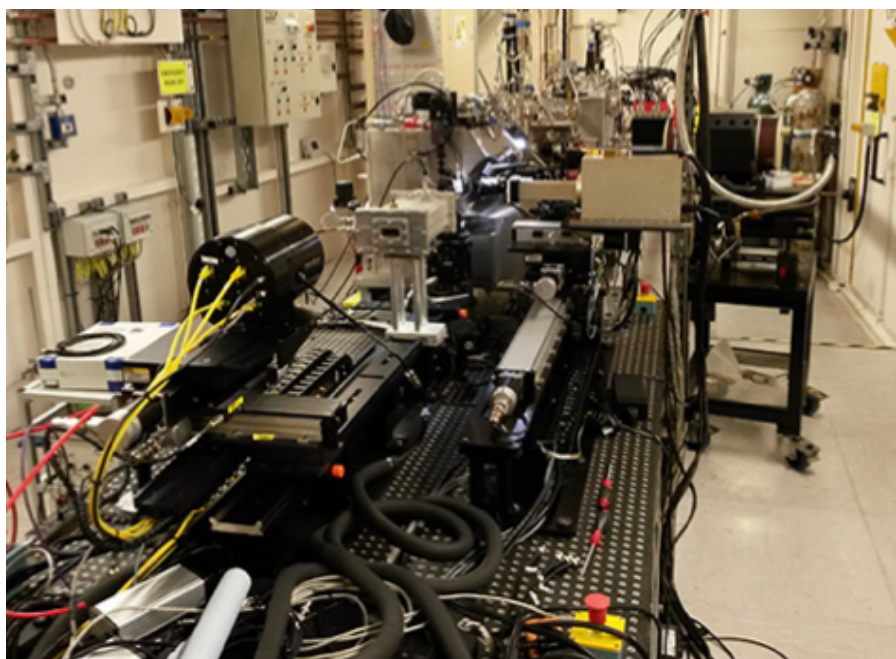
**Figure 4.2.** A schematic summary of the different components of Diamond synchrotron (reproduced from [diamond.ac.uk](http://diamond.ac.uk)).

The electrons are generated in a high voltage cathode electron gun, which is heated under vacuum. The linear accelerator and booster synchrotron use radiofrequency (RF) cavities and bending magnets to accelerate the electrons to near-light speed, before they enter the storage ring- a long stainless steel vacuum chamber. The storage ring is a large polygon made of 50 straight sections angled together to form a closed loop 562 m in circumference. The ring is fitted with dipole magnets and insertion devices (magnet arrays inserted into the straight sections of the storage ring) to bend the electron beam and generate the synchrotron radiation, which is channelled into 32 beamlines for use in different experiments. Each beamline has the same general design, comprising: 1) an optics hutch, where the light is filtered and focussed, 2) experiment hutch where the sample is introduced, and 3) control cabin where the researchers monitor their experiment.



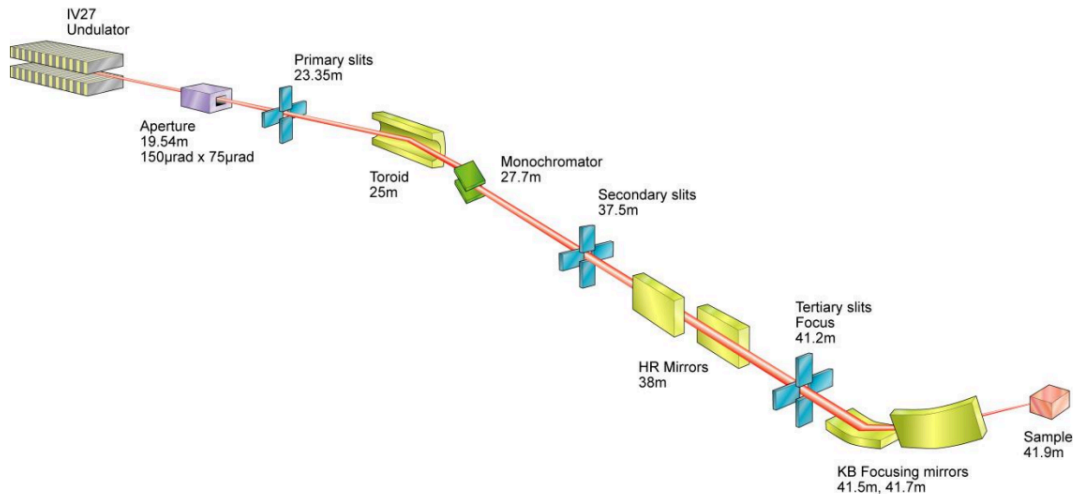
### 4.1.3 I18 beamline

The I18 Microfocus Spectroscopy beamline was used to conduct the experiments discussed in this chapter (Figure 4.3). A schematic overview of the beamline is shown in Figure 4.4.



**Figure 4.3. Experimental hutch of the I18 beamline (reproduced from [diamond.ac.uk](http://diamond.ac.uk)).**

The X-ray beam enters the beamline from an undulating insertion device. The light is defined with an aperture and primary slits, while the rhodium-coated silicon toroid mirror focuses the beam horizontally and collimates it in the vertical plane. Monochromators, which are located downstream of the mirror, are used to select light with energy in a particular range (2.0-20.7 keV). The final focussing is achieved by KirkpatrickBaez (KB) mirrors, and results in a typical beam spot size of  $3 \times 3 \mu\text{m}$ , which gives resolution at a length scale similar to that of individual cells. The resultant high energy, monochromatic light can be used to detect elements ranging from phosphorus to plutonium [383], and support a broad range of experiments- from analysis of extra-terrestrial materials to human tissue samples. In particular, the beamline has proven to be highly successful for the investigation of elemental composition of tissues surrounding metal implants, using micro-X-ray fluorescence and microfocus X-ray absorption spectroscopy techniques [43,225,280].

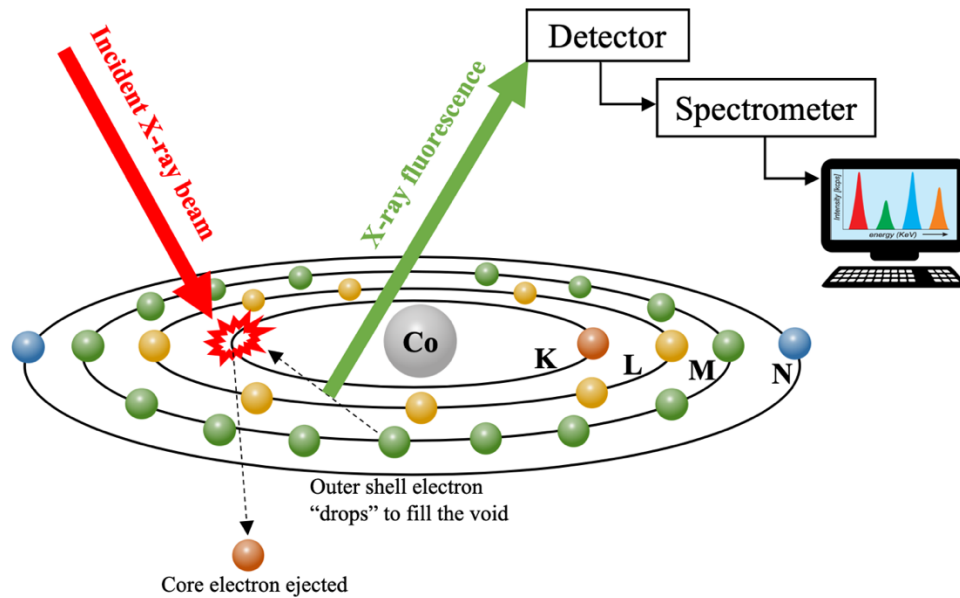


**Figure 4.4. Schematic overview of the I18 beamline, showing the principal optical elements used to focus the beam. The distances given are measured from the beamline extraction point in the storage ring undulator (reproduced from diamond.ac.uk).**

#### **4.1.4 Micro-X-ray fluorescence ( $\mu$ -XRF) spectroscopy**

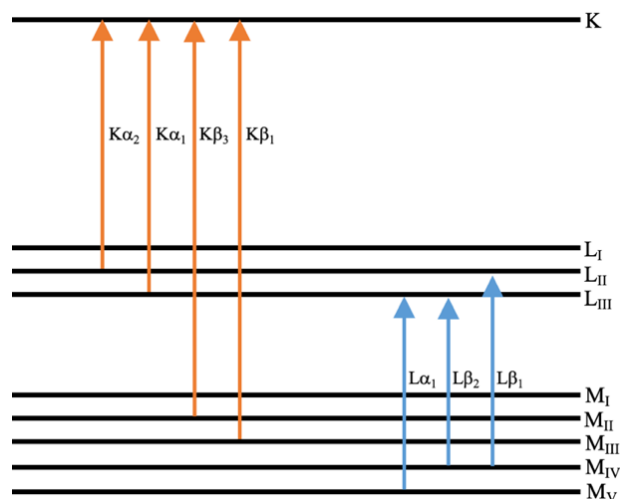
$\mu$ -XRF is a versatile analytical technique that can characterise the elemental composition and distribution of a wide range of samples [225,384,385], offering fast identification of most elements in the periodic table. The method involves irradiating the sample with X-rays and detecting the X-ray fluorescence that is emitted.

More specifically, the incident X-ray beam removes one of the element's core electrons (shell K or L), resulting in a high energy, unstable configuration for the atom. To restore equilibrium, an electron from one of the higher energy shells fills the void. The excess energy from this process is released in the form of fluorescent X-ray radiation, which is equal to the difference in binding energies of the shells with the 'initial' and 'final' vacancies (Figure 4.5).



**Figure 4.5. Diagram outlining the principles of X-ray fluorescence, using a cobalt-containing sample as an example. The incident X-ray beam has to be set to energy higher than the binding energy of the target electron shell to generate X-ray fluorescence.**

The energy and wavelength of the emitted photon are unique to the studied element and the specific electronic transition from which it originated (Figure 4.6), permitting the determination of the source atom. By measuring the intensities of the emitted fluorescence is it also possible to determine how much of each element is present in the sample.



**Figure 4.6. The most important X-ray energy lines with their transitions in Siegbahn notation.**

Spectrometer systems are generally divided into two main groups: energy dispersive (ED) and wavelength dispersive (WD). The former type uses a semiconductor-type detector that registers the energy of every photon that strikes it, effectively “decoding” the sample into its constituent elements. The main advantage of this approach is that accurate quantitative data on the entire mass spectrum can be obtained in a matter of minutes. WD spectrometers use an analysing crystal to diffract the emitted photons based on their wavelength, and place the detector in the correct physical location to receive X-rays of a given energy, one wavelength at a time. Compared to ED spectrometers, WD instruments boast lower LoD, and detector outputs that are easier to deconvolute. The main drawback is that they are incapable of quick multi-element analyses and incur higher hardware costs.

The I18 beamline uses an ED spectrometer, which allows for relatively rapid sample analysis that covers multiple elements, and offers LoD in the ppm to ppb range.

#### 4.1.5 Microfocus X-ray absorption spectroscopy ( $\mu$ -XAS)

$\mu$ -XAS is a versatile tool used for determining the local electronic, structural and magnetic properties of matter. The fundamental principle underlying the technique is that every element will absorb X-rays at distinct energies, which are unique to the type of absorber atom and the specific electronic transition. It follows that each element has a characteristic set of excitation energies, with the greatest absorption occurring at the so-called absorption edge. Edge energies and X-ray line energies for cobalt, chromium and titanium are listed in Table 4.1 and Table 4.2, respectively [386].

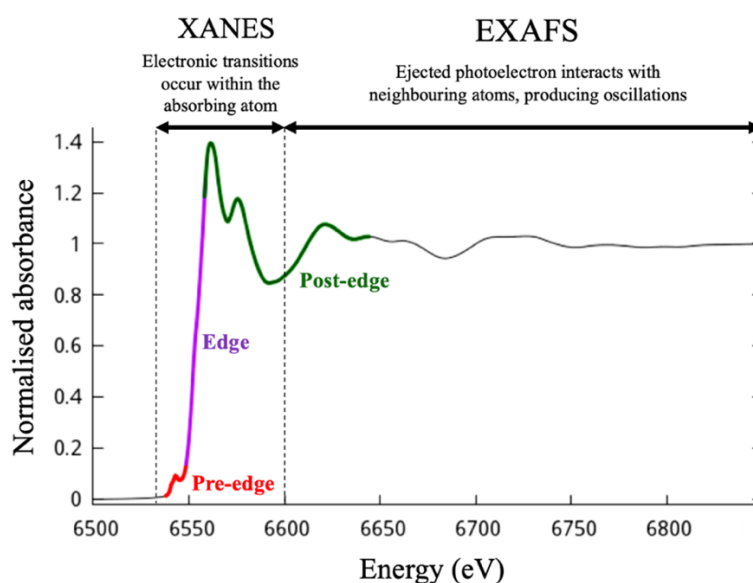
**Table 4.1. Characteristic excitation energies for cobalt, chromium and titanium (eV).**

	<b>Cobalt</b>	<b>Chromium</b>	<b>Titanium</b>
<b>K-edge</b>	7712	5987	4965
<b>L<sub>I</sub>-edge</b>	929	694	529
<b>L<sub>II</sub>-edge</b>	797	582	460
<b>L<sub>III</sub>-edge</b>	782	572	454

**Table 4.2. Characteristic X-ray line energies for cobalt, chromium and titanium (eV).**

Energy line	Transition	Cobalt	Chromium	Titanium
$K_{\beta 1}, K_{\beta 3}$	$KM_{III}, KM_{II}$	7649	5947	4932
$K_{\alpha 1}$	$KL_{III}$	6930	5415	4511
$K_{\alpha 2}$	$KL_{II}$	6915	5405	4505
$L_{\beta 3}, L_{\beta 4}$	$L_{I}M_{III}, L_{I}M_{II}$	870	654	-
$L_{\beta 1}$	$L_{II}M_{IV}$	791	583	458
$L_{\alpha 1}, L_{\alpha 2}$	$L_{III}M_{V}, L_{I}M_{IV}$	870	573	452

The sample is kept static, while the beam energy increases in small increments through the selected energy range (from just under the edge energy of the element of interest, to approximately 500 eV above it). The spectrum is built from the measurements of X-ray absorption coefficient,  $\mu(E)$ , at each increment. The region from approximately 30 eV below and up to 50 eV above the edge is referred to as the X-ray absorption near edge structure (XANES), while the ongoing spectral features are called extended X-ray absorption fine structure (EXAFS) (Figure 4.7). XANES is sensitive to formal oxidation state and coordination environment of the absorbing atom, whereas information on bond distances, coordination number and type of nearest neighbouring atoms (up to about 4 Å) can be found in the EXAFS [387].



**Figure 4.7. An XAS spectrum, with the XANES and EXAFS portions identified.**

$\mu$ -XAS is a direct method of speciation that necessitates minimum sample processing, though the requirement for long, intense irradiation of the same sample region is a major drawback, as it can induce beam damage and alter the oxidation state of the very chemical species being measured. Moreover, if the analyte concentration is not high enough, the technique is limited to the XANES regime, and/or the resultant spectra are very noisy.

$\mu$ -XAS is usually performed by measuring the photons transmitted through the sample to calculate the  $\mu(E)$ :

$$\mu(E)t = -\ln\left(\frac{I}{I_0}\right)$$

Where  $I_0$  is the intensity of the incident beam,  $I$  is the transmitted beam intensity and  $t$  is sample thickness.

If the analyte concentration is low (as is often the case in trace metal analysis),  $\mu$ -XAS spectra are acquired in the more sensitive fluorescence detection mode:

$$\mu(E)t = -\ln\left[1 - \frac{I_f}{I_0}\right] \propto I_f/I_0$$

Where  $I_f$  is the fluorescence intensity,  $I_0$  is the initial beam intensity and  $t$  is sample thickness.

The  $\mu(E)$  depends on sample density ( $\rho$ ), atomic number ( $Z$ ) and mass ( $A$ ) of the absorbing atom, and on the incident X-ray energy ( $E$ ):

$$\mu(E) \propto \frac{\rho Z^4}{AE^3}$$

Due to the  $Z^4$  dependence, the absorption coefficient varies greatly for different elements, making it possible to distinguish between them by adjusting X-ray energy.

## 4.2 INTRODUCTION

Wear and corrosion of CoCr and Ti alloys leads to the release of their constituent metals into surrounding tissue and blood. Accumulation of metal debris in vital organs can lead to tissue damage, and is of particular concern [101,123,266]. Deposition of metal in systemic organs of THA patients is hard to quantify without an invasive biopsy, meaning that currently available evidence is not always robust. Organ samples obtained at necropsy are ideal specimens for this purpose.

In the body, implant-derived cobalt can be found in two predominant forms: metallic ( $\text{Co}^0$ ) or divalent ( $\text{Co}^{\text{II}}$ )- the latter being the toxicologically relevant species [65] (see Section 2.3.1). The most stable states of chromium are metallic ( $\text{Cr}^0$ ), trivalent ( $\text{Cr}^{\text{III}}$ ) or hexavalent ( $\text{Cr}^{\text{VI}}$ ). While  $\text{Cr}^{\text{III}}$  is considered relatively non-toxic,  $\text{Cr}^{\text{VI}}$  compounds are potent human carcinogens [388] (see Section 2.4.1). Release of  $\text{Cr}^{\text{VI}}$  from hip implants is highly debated, with some reports supporting the idea [228,389] and others opposing it [68,390,391]. Titanium is considered the most biocompatible out of the three metals, though recent reports indicate that it may also have a significant potential for eliciting a pathologic response in tissues [26,258,259] (see Section 2.5.2).

### 4.2.1 Motivation

Deposition of chromium, particularly in the  $\text{Cr}^{\text{VI}}$  form, in vital organs is of concern due to the carcinogenic nature of the metal. The extent to which cobalt accumulates in the organs is also of interest. Elevated cardiac cobalt loads have been linked to cardiac dysfunction and several cases of fatal cardiomyopathy [71,105,123]. Previous analyses of periprosthetic tissue revealed an abundance of  $\text{CrPO}_4$  and  $\text{Cr}_2\text{O}_3$ , but no evidence of  $\text{Cr}^{\text{VI}}$  [34,43]. Organs of THA patients have also been probed for metal content [248,277,392], but chemical speciation of the metal deposits was rarely investigated [279] (see Section 2.6). Detailed characterisation of the physicochemical properties of implant-derived debris is crucial to assess the possible long-term systemic implications posed by medical biomaterials, and to identify patient groups that might be at an increased risk of adverse effects.

### 4.2.2 Aim

To determine the exact chemical form of cobalt, chromium and titanium deposits in vital organs of THA patients.

### 4.2.3 Objectives

To employ a systematic approach including optical microscopy, laser ablation ICP-MS and  $\mu$ -XRF to: 1) map cobalt, chromium and titanium deposits in the spleen, liver and heart tissue of THA patients, and 2) use  $\mu$ -XAS to speciate them.

### 4.2.4 Study design flowchart

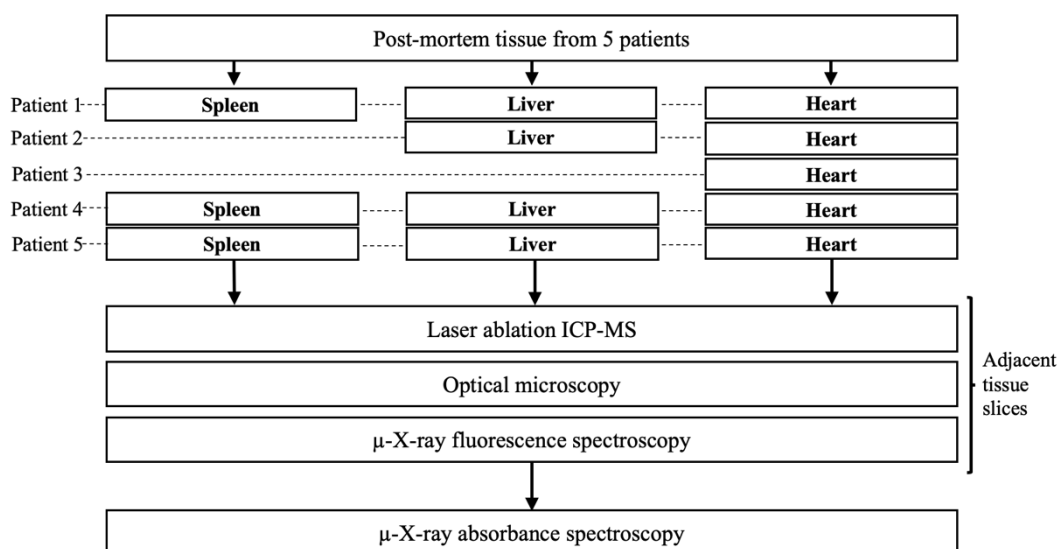


Figure 4.8. Flowchart of study design.

## 4.3 MATERIALS AND METHODS

### 4.3.1 Patients

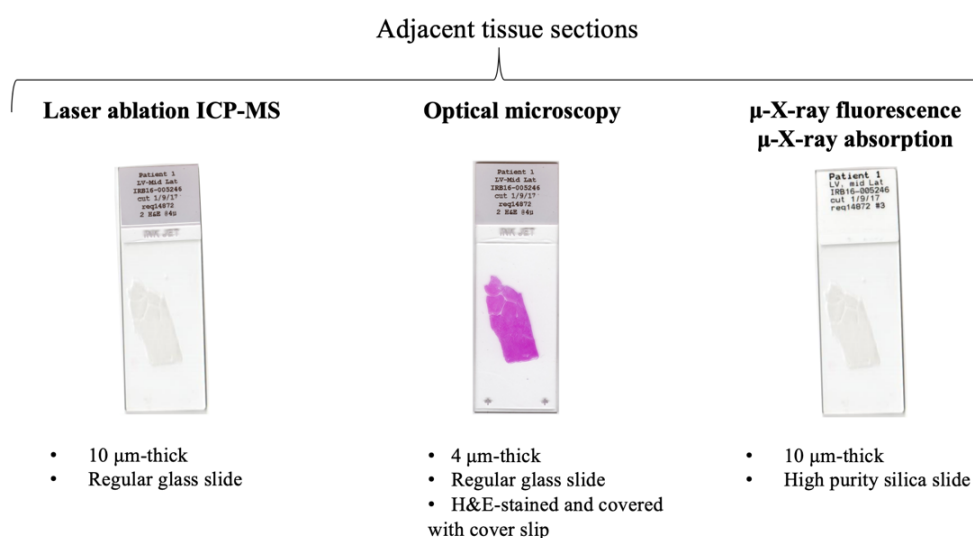
Consented tissue was obtained from The Mayo Clinic (Rochester, MN, US) and used with approval of their Institutional Review Board (ref. number 16-005246).

The Mayo Clinic Tissue Registry was queried for autopsies of individuals who had undergone THA between 1990 and 2013. Samples of left ventricular tissue were acquired from five subjects with the highest cardiac cobalt concentration (determined on an ICP-MS instrument as part of a previous study [106]). Hepatic tissue was available from four, and splenic tissue from three of the five patients. The patients' clinical data and implant details are listed in Table 4.3.



### 4.3.2 Tissue processing

The tissue samples were excised using polytetrafluoroethylene (PTFE)-coated blades, to reduce potential metal contamination. The specimens were fixed in 10% neutral buffered formaldehyde solution (Solmedia Ltd., UK) and embedded in paraffin wax, before three sections were cut and mounted on either regular, or high purity UV-fused silica slides (UQG Optics, Cambridge, UK) (Figure 4.9). The specimens were packaged into standard microscope slide storage boxes and shipped to our laboratory.



**Figure 4.9. Schematic overview of the tissue sample preparation process. H&E-haematoxylin and eosin.**

The samples were dewaxed (sequential immersion in 3 changes of xylene and 1 change each of 100%, 95% and 70% ethanol) and air-dried in a dust-free environment. One tissue section was stained with haematoxylin and eosin (H&E) for histological examination. The staining allows key cell features to be identified, but it can interfere with laser ablation ICP-MS and synchrotron analysis, due to the metal contaminants in contains. Similarly, the destructive nature of laser ablation ICP-MS meant that the tissue section could not be reused for X-ray spectroscopy. For these reasons, separate, adjacent tissue sections were used for each of the three techniques.

### 4.3.3 Optical microscopy

The H&E-stained tissue slices were investigated for visible metal debris and associated tissue irregularities under a digital optical microscope. Images of “areas of interest” were acquired in AxioCam software (version 4.4, Carl Zeiss).

**Table 4.3. Implant materials and the patients' clinical data. Source: Journal of Trace Elements in Medicine and Biology [276].**

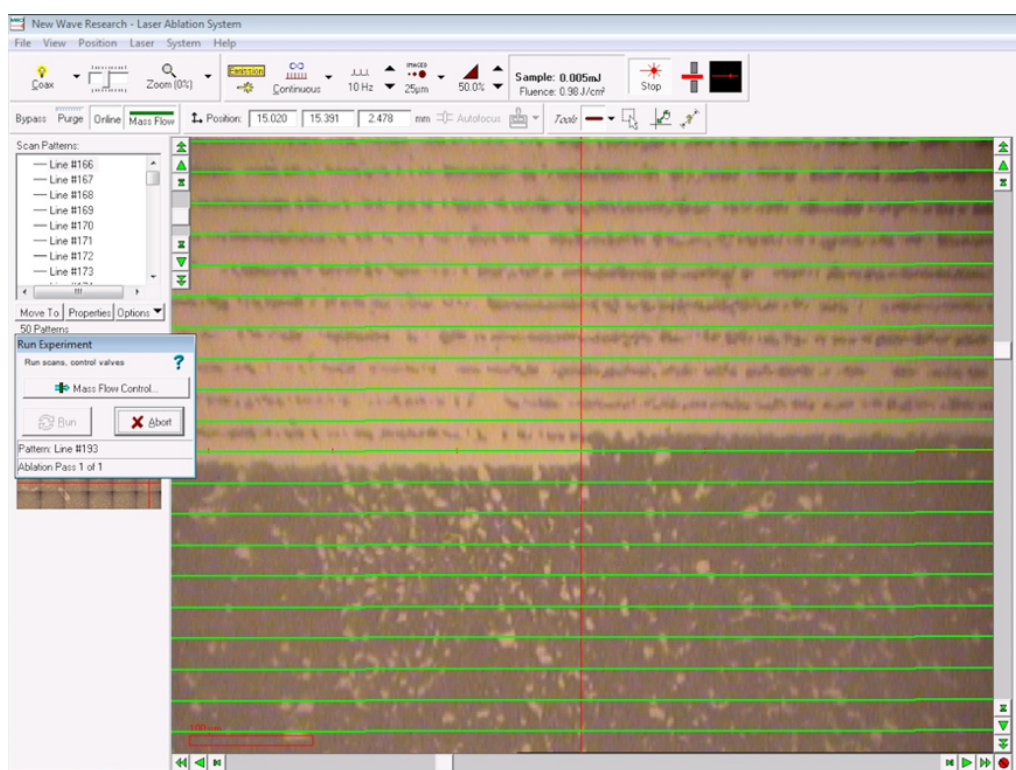
#	Gender Age at death	Implant materials <sup>a</sup>	Cumulative implant years <sup>b</sup>	Cause of death <sup>c</sup>	Cardiac Co, Cr ( $\mu\text{g g}^{-1}$ )	Necropsy findings
1	Male 79	Bilateral THA- 32 mm CoCr head, CoCr stem (cemented), Ti cup; Unilateral TKA (CoCr)	28.6	Probable sepsis, diabetes mellitus, reactive hyper cellular bone marrow (mild)	0.91, 0.30	Cardiomegaly <sup>d</sup> , interstitial fibrosis
2	Male 82	Bilateral THA- 28 and 32 mm CoCr head, Ti stems (uncemented), CoCr modular neck, Ti cup; Bilateral TKA (CoCr)	52.3	Acute bronchopneumonia	0.59, 0.08	Cardiomegaly <sup>d</sup> , interstitial fibrosis
3	Male 49	Unilateral THA- 36 mm CoCr head, CoCr stem (uncemented), CoCr modular neck, Ti cup	1.7	Brain death, acute subdural hematoma, seizure disorder, papillary thyroid cancer	0.35, 0.06	Cardiomegaly <sup>d</sup>
4	Female 87	Unilateral THA- 36 mm CoCr head, CoCr stem (uncemented), Ti cup	5.7	1. Acute/ongoing myocardial infarction secondary to atherosclerotic ischemic heart disease, coronary atherosclerosis; 2. Anaemia, diabetes mellitus (type II)	0.34, 0.14	Interstitial fibrosis
5	Female 79	Bilateral THA- 28 and 32 mm CoCr heads, CoCr stem (cemented), CoCr modular neck, Ti cup	17.9	1. Subdural hematoma, fall at home; 2. Remote heart transplantation, end stage renal disease	0.31, 0.16	Cardiomegaly <sup>d</sup>

<sup>a</sup>All CoCr components were made of ASTM F75 alloy with cobalt content of 60-65% and chromium content of 26-30%, <sup>b</sup>defined as sum of individual implant years, <sup>c</sup>causes of death were not thought to be related to the joint prostheses, <sup>d</sup>heart weight >50% above the expected mean based on the patient's body size. TKA- total knee arthroplasty.

#### 4.3.4 Laser ablation ICP-MS

Laser ablation (LA) ICP-MS is a powerful technique that enables highly sensitive elemental and isotopic analysis to be performed directly on solid samples. It employs a high power ultraviolet laser beam (output from a frequency-quintupled neodymium-doped yttrium aluminium garnet crystal) to “burn” a small amount of sample surface. A stream of inert gas carries the ablated material into the argon inductively-coupled plasma. The extremely high temperature of the plasma converts the sample particles into ions, which are extracted in the ultrahigh vacuum mass spectrometer. The ions are separated according to their mass-to-charge ( $m/z$ ) ratio, and detected by an ion detector. In this way, the spatial distribution of major and trace elements can be established in a variety of samples.

For this study, a quadrupole-based ICP-MS (Agilent 7900, Agilent, Stockport, UK) was coupled to a laser ablation system (New Wave UP213, ESI, Huntingdon, UK). The laser beam was programmed to scan the material in a series of 40-60 lines, each about 2-3000  $\mu\text{m}$  long, giving a total ablated area of up to 3000x3000  $\mu\text{m}$  (Figure 4.10). Operating parameters of the machine are listed in Table 4.4.



**Figure 4.10.** A laser ablation ICP-MS scan in progress. The laser follows the path of the green lines to ablate tissue material from the selected area.

Raw data was imported into Origin2017 software (OriginLab, Northampton, MA, US) to generate isotope distribution maps for Co<sup>59</sup> and Cr<sup>52</sup>. The relatively low resolution of the ICP-MS instrument used in the present study meant that mapping of titanium in the tissue was not possible.

Data capture and analysis was performed by Dr Barry Sampson in the Trace Element Laboratory at Charing Cross Hospital.

**Table 4.4. LA ICP-MS operating parameters.**

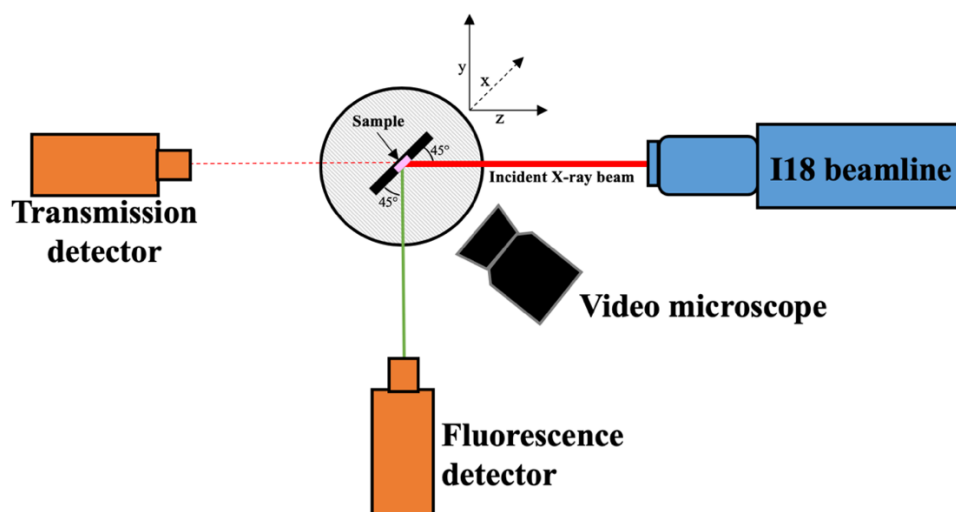
<b>Laser ablation operating parameters</b>	
<b>Wavelength</b>	193 nm
<b>Spot size</b>	25-40 µm
<b>Frequency</b>	10 Hz
<b>Scan speed</b>	20 nm sec <sup>-1</sup>
<b>Energy</b>	40-50%, 0.12 mJ
<b>Inert gas (helium) flow rate</b>	600 mL min <sup>-1</sup>
<b>ICP-MS operating parameters</b>	
<b>Power</b>	1250 Watts
<b>Collision gas (helium)</b>	2 mL min <sup>-1</sup>
<b>Nebuliser gas flow</b>	1.0 L min <sup>-1</sup>
<b>Plasma gas flow</b>	15 L min <sup>-1</sup>
<b>Dwell time</b>	0.25 ms (Co <sup>59</sup> ), 0.2 ms (Cr <sup>52</sup> )

#### **4.3.5 Synchrotron X-ray analysis**

The synchrotron work was conducted at the I18 Microfocus Spectroscopy beamline of Diamond Light Source, between the 10<sup>th</sup>-14<sup>th</sup> March 2017 (proposal number sp15034). Two types of experiments were performed: micro-X-ray fluorescence elemental mapping and microfocus X-ray absorption spectroscopy.

#### 4.3.5.1 Micro-X-ray fluorescence ( $\mu$ -XRF) spectroscopy

The sample was mounted on a holder plate and inserted vertically on the stage, at  $45^\circ$  to the incident X-ray beam. The fluorescence detector was positioned at  $45^\circ$  to the sample (Figure 4.11). The sample stage could be controlled remotely and shifted in three dimensions: x (left-right), y (up-down) and z (away-towards), relative to the beam. The video microscope, which was aimed at the sample, fed into the control hutch computer, allowing the beam position to be visualised and adjusted before analysis.



**Figure 4.11. Schematic bird's eye view of the experimental setup. The sample was placed on a sample stage, at  $45^\circ$  to both the incoming X-ray beam and the fluorescence detector. Regions of interest were identified with a movable optical microscope.**

Large tissue areas (typically 3 x 2 mm) were scanned at room temperature, by incident X-ray beam at a fixed energy (8.5 keV). The data were recorded using the four-element silicon drift Vortex ME4 detector (Hitachi Hi-Technologies Science America) with Xspress-3 processing electronics, at a fixed sample-detector distance (75 mm).

The choice of tissue areas was guided by optical microscopy and LA ICP-MS findings. In cases where sample pre-screening did not highlight any regions of increased metal concentration, areas for XRF analysis were chosen at random. 1-3 areas per tissue section were scanned to increase the probability of finding metal deposits.

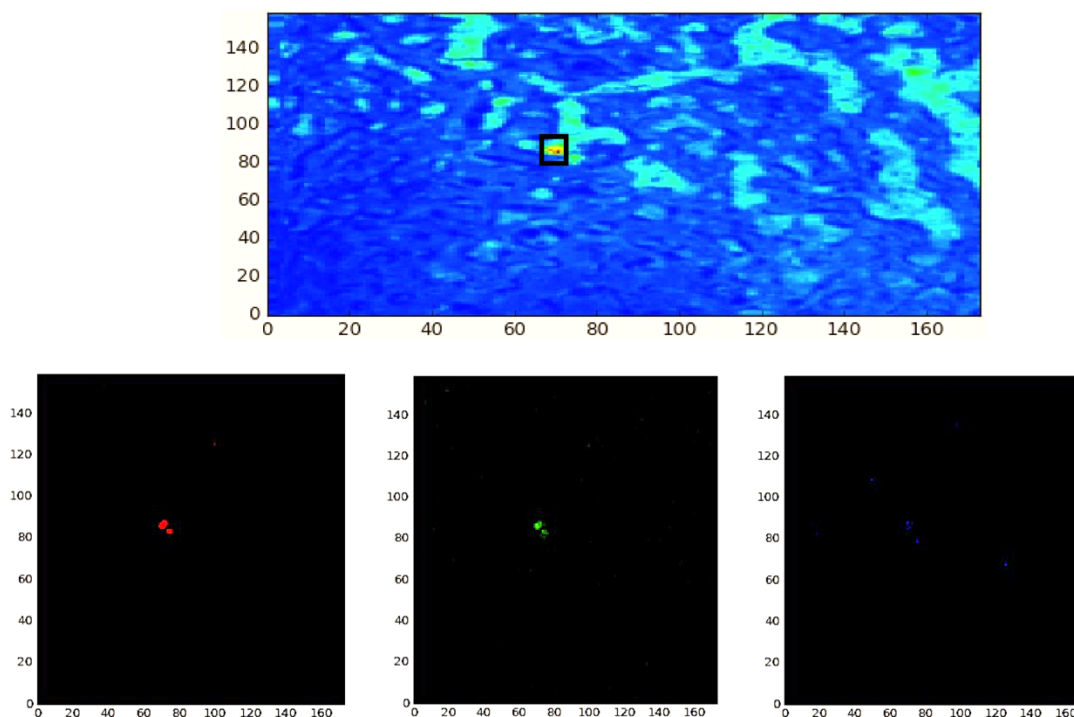
During the scan, the sample was moved in discrete steps under the X-ray beam, remaining at each position for a fixed dwell time of 50 ms. This allowed for the

elemental composition at each point to be determined. The initial fluorescence maps were collected using a slightly defocused beam (20  $\mu\text{m}$  step in each direction), before regions of interest were scanned with a 3-5  $\mu\text{m}$  step to locate metal deposits to within a few microns.

The raw data was analysed in PyMCA software (version 5.1.4, European Synchrotron Radiation Facility) [393].

### *Qualitative analysis*

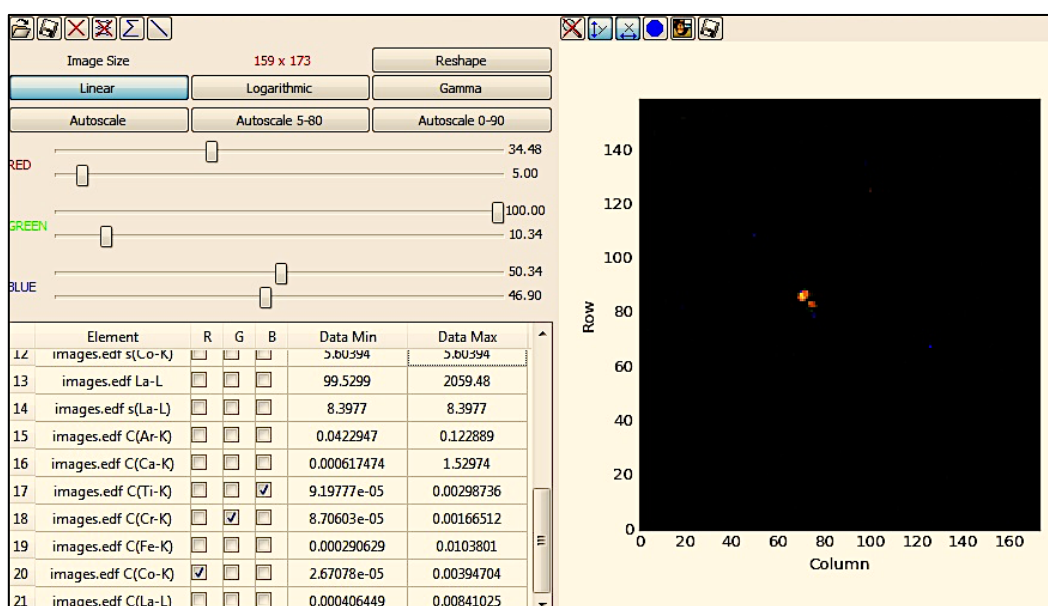
The “ROI Imaging” tool in PyMCA was used to present the raw XRF data as multichannel analyser (mca) spectra, which displayed all the elements, and the specific electronic transitions, detected during the scan. From the mca spectrum, it was possible to isolate the peaks of interest and view them as two-dimensional distribution maps with “hotspots” of increased cobalt, chromium and titanium counts. The RGB imaging mode was used to assign a different colour to each of the studied elements for ease of viewing (Figure 4.12).



**Figure 4.12. Raw data processing in PyMCA. A representative area in the raw XRF map (top) was viewed in the RGB imaging mode: cobalt, chromium and titanium “hotspots” are shown in red, green and blue, respectively (bottom). Cobalt and chromium appear to be co-localised.**

## Quantification

Representative spots in each XRF map were quantified for cobalt, chromium and titanium concentration using the “Fast XRF stack fitting → Calculate concentrations” tool in PyMCA (Figure 4.13). The results, which were expressed in mass fractions, can be converted to ppm by multiplying the values by 1,000,000. Importantly, this method assumes that the particles are 1  $\mu\text{m}$  in size, and cannot be used reliably to quantify nanoparticles.



**Figure 4.13. Quantifying metal “hotspots” in PyMCA. A “hotspot” of co-localised cobalt and chromium is shown on the right: the Data Max column displays relative element concentrations as mass fractions.**

### 4.3.5.2 Microfocus X-ray absorption spectroscopy ( $\mu$ -XAS)

The highest intensity “hotspot” in each elemental XRF map was selected by double-clicking on the pixel. The spot was irradiated with an incident X-ray beam tuned to the K-edge of cobalt, chromium or titanium (Table 4.1), and the resultant fluorescence recorded. The majority of  $\mu$ -XAS measurements were done in duplicate (repeated twice at the same spot) to improve data quality and investigate possible beam damage to the sample. Spectra were also collected in transmission mode from cobalt (7709 eV), chromium (5989 eV) and titanium (4966 eV) metal foils, to serve for energy calibration.

On the resultant spectra, the XANES region was used to infer the oxidation state and geometry of the metal. Information on atoms surrounding the X-ray absorbing atom was gleaned from both comparisons of the XANES with standard spectra and, in one case, the EXAFS portion of the spectrum, which, although short, was of sufficient quality to analyse.

#### *XANES and EXAFS analysis*

The XANES curves were normalised in Athena software (version 0.9.25, Demeter) [394] by Prof. J. Frederick W. Mosselmans at Diamond Light Source.

A smooth pre-edge line was fitted and subtracted from the measured data, in order to remove instrumental background and absorption from other edges. The “jump” in the edge ( $\Delta\mu_0$ ) was normalised to go from 0 to 1, to represent the absorption of one X-ray. The resulting spectra were compared with those of reference materials, and re-plotted in Origin2017 (OriginLab, Northampton, MA, US).

EXAFS fitting was performed by Prof. J. Frederick W. Mosselmans in Artemis software (version 0.9.25, Demeter).

Briefly, a smooth post-edge background function was removed from the data to approximate the absorption from an isolated atom. The EXAFS wavefunction,  $\chi(k)$ , was isolated and  $k^2$ -weighted to amplify the oscillations at high  $k$  (the wave number of the ejected photoelectron). The data was then Fourier transformed into R-space, which provided information on coordination number and bond distance to the nearest neighbouring atoms. EXAFS spectra of “model” compounds were fitted to the Fourier-transformed spectra to find the best fit.

#### **4.3.6 Statistical analysis**

No statistical analysis of data was applied due to the small sample size.

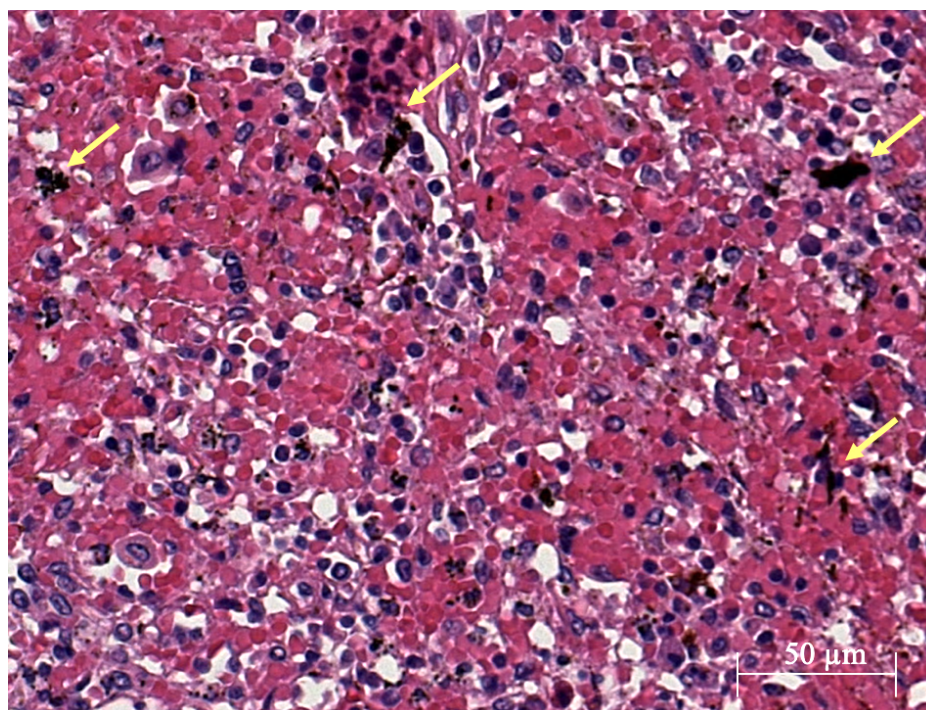


## 4.4 RESULTS

### 4.4.1 Histological analysis

Investigation of H&E-stained tissue indicated presence of fine particulate matter in all three spleen samples, and one of the liver tissue sections (Figure 4.14). The particles were not associated with any structural irregularities and appeared to be of little toxicological relevance.

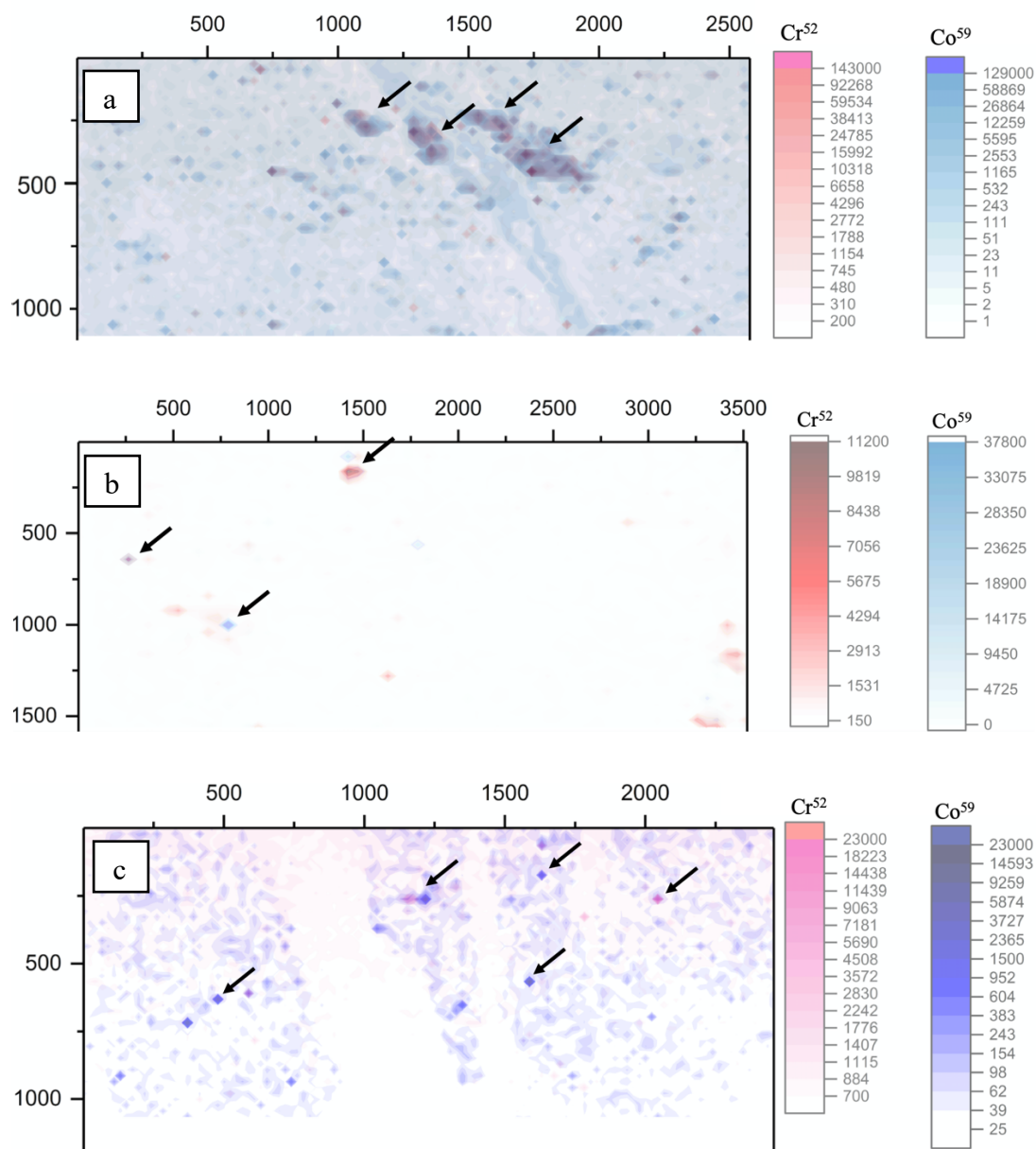
Assuming that the tissue samples were representative of the particle burden of the organ as a whole, the absence of visible particles in most tissue sections suggests that they were too small to be seen ( $<1\ \mu\text{m}$ ), or had already corroded and dissolved.



**Figure 4.14.** A representative image of a spleen tissue section (magnification 20x). Arrows indicate fine particulate deposits.

### 4.4.2 Laser ablation ICP-MS

LA ICP-MS analysis revealed the presence of cobalt and chromium in most tissue samples. Their levels varied greatly, with the highest relative counts in splenic tissue, followed by hepatic and cardiac tissue. In Patient 1 spleen, the cobalt and chromium deposits were found to be highly co-localised, which could be indicative of CoCr alloy particles (Figure 4.15).



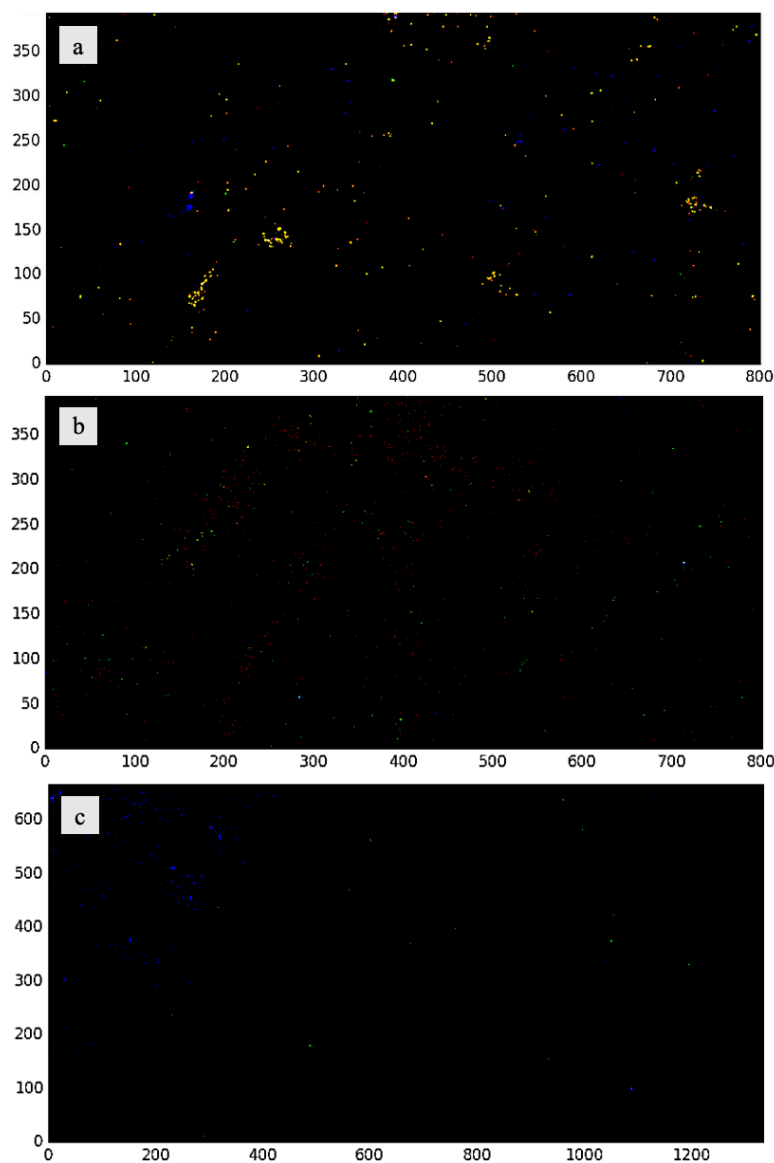
**Figure 4.15. Isotope distribution maps of a) spleen, b) liver and c) heart tissue from the current series. Arrows indicate cobalt/chromium deposits.**

#### 4.4.3 $\mu$ -XRF tissue mapping

##### *Qualitative analysis*

In total, 25 areas from 5 cardiac, 4 hepatic and 3 splenic tissue samples were mapped. Cobalt and chromium were highly co-localised in all splenic XRF maps (n=8). A small number of spots with co-localised cobalt and chromium were identified in hepatic tissue of Patients 1, 4 and 5, and in cardiac tissue of Patient 5. A few spots with co-localised chromium and titanium, and two with co-localised cobalt and titanium, were

also recognised. In general, splenic tissue displayed the highest relative counts of metal in the XRF maps, followed by hepatic and cardiac tissue (Figure 4.16).



**Figure 4.16. XRF map of a) spleen (2×4 mm, 5 µm step size), b) liver (2×4 mm, 5 µm step size) and c) heart tissue (2×4 mm, 3 µm step size) from the current series. Co, Cr and Ti deposits are shown in red, green and blue, respectively. Yellow spots indicate highly co-localised cobalt and chromium. In each image, brightness and contrast have been adjusted to improve visibility of the described features (reproduced from *Journal of Trace Elements in Medicine and Biology* [276]).**

### *Quantification*

Results of quantitative analysis of the XRF maps are presented in Table 4.5.

**Table 4.5. Relative element counts in the highest intensity spots of the different XRF maps.**

Patient	Organ	XRF map	Relative counts in the brightest pixel			Co/Cr ratio
			Co	Cr	Ti	
1	Heart	1	0.0007	0.024	0.04	0.29
		2				
	Liver	1	0.0013	0.0026	0.0035	0.50
		2	0.0036	0.0031	0.0073	1.16
		3	0.0039	0.0017	0.003	2.37
		4	0.002	0.01	0.002	0.20
	Spleen	1	0.0097	0.004	0.003	2.43
		2	0.17	0.07	0.01	2.38
3		0.095	0.039	0.198	2.44	
4		0.11	0.079	0.063	1.35	
2	Heart	1	0.0003	0.0001	0.002	0.25
		2	0.0002	0.0097	0.15	0.02
	Liver	1	0.0009	0.003	0.025	0.30
		2	0.0015	0.042	0.0097	0.04
		3	0.0005	0.0044	0.0027	0.11
3	Heart	1	0.0006	0.0005	0.04	1.20
		2	0.0002	0.0003	0.004	0.67
4	Heart	1	0.0002	0.008	0.05	0.03
		2				
	Liver	1	0.0006	0.0005	0.032	1.20
		2	0.0006	0.0009	0.068	0.70
	Spleen	1	0.003	0.001	0.0016	2.11
2		0.0007	0.0004	0.001	1.75	
5	Heart	1	0.0005	0.0007	0.04	0.71
		2	0.0002	0.001	0.0008	0.20
	Liver	1	0.0009	0.0006	0.0029	1.59
		2	0.0006	0.0004	0.0024	1.49
	Spleen	1	0.003	0.002	0.0006	1.64
		2	0.0004	0.0003	0.001	1.36

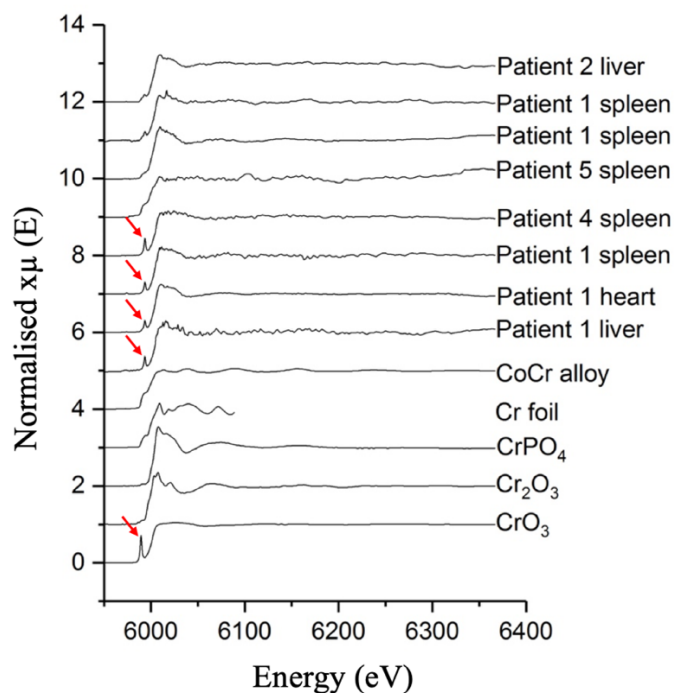
The absolute concentrations calculated by the software were extremely high and deemed unreliable. The size of the investigated particles was expected to be much smaller than 1  $\mu\text{m}$ , so this was anticipated. The results were used to calculate Co/Cr ratios instead, which provided clues as to whether particles of the bulk CoCr alloy were likely to be present in any of the studied organs. The cobalt and chromium content of the patients' hip implants ranged from 60-65% and 26-30%, respectively, which translates into a Co/Cr ratio of 2.0-2.5. Ratios in this range were found in the spleen and liver of Patient 1, and in the spleen of Patient 5.

#### **4.4.4 $\mu$ -XAS speciation of tissue metal deposits**

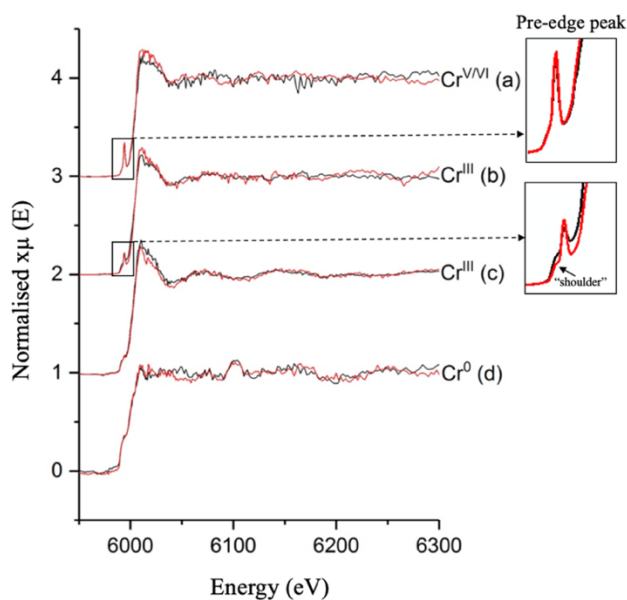
##### **4.4.4.1 Chromium**

Chromium K-edge XAS spectra were recorded at 12 separate points from 2 cardiac, 2 hepatic and 3 splenic tissue samples. Four points generated unusable data, likely due to the particle size being too small. Where better quality data was obtained, chromium could be found in either a metallic-like form ( $\text{Cr}^0$ ), in the  $\text{Cr}^{\text{III}}$  form, or in a more highly oxidised state characterised by a sharp pre-edge peak in the XANES region of the spectrum. The latter species was identified in all three organs from Patient 1, as well as in Patient 4 spleen (Figure 4.17).

The spectrum recorded at a chromium "hotspot" in Patient 2 liver also displayed a pre-edge peak, albeit of a different profile. The peak featured a "shoulder" and became more pronounced in the duplicate scan, suggesting that the chromium species was originally in the trivalent state, but underwent oxidation due to prolonged X-ray beam exposure (b in Figure 4.18).

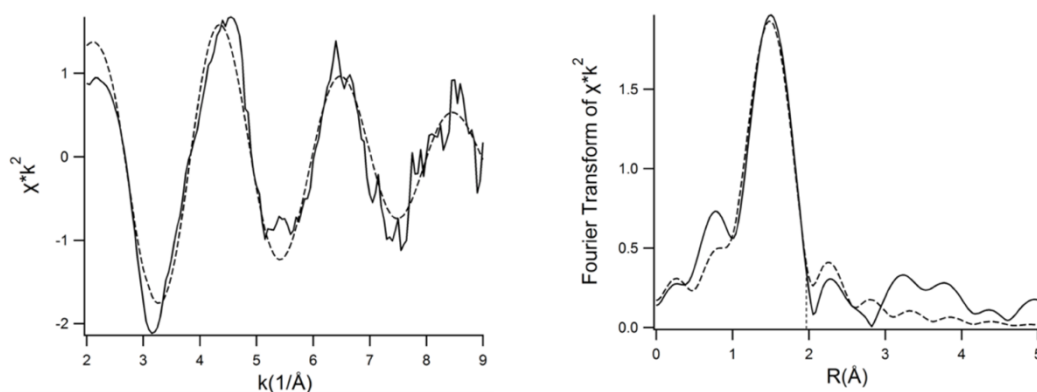


**Figure 4.17.** Stacked XAS spectra recorded at the K-edge of eight tissue chromium “hotspots”, along with spectra for six chemical standards. The top three traces are  $\text{Cr}^{\text{III}}$ -like, fourth one resembles metallic-like Cr, while the bottom four spectra resemble the  $\text{Cr}^{\text{VI}}$  standard. Arrows draw attention to the pre-edge peaks (adapted from *Journal of Trace Elements in Medicine and Biology* [276]).



**Figure 4.18.** Replicate XANES spectra of the different Cr forms found in the tissue samples. The second scan (red line) was performed at the same spot, within 20 min of the initial scan (black line). The pre-edge peaks are emphasised on the right to highlight how their profiles differ between the replicate scans (adapted from *Journal of Trace Elements in Medicine and Biology* [276]).

In one case only the data was of sufficient quality to warrant EXAFS analysis. For the Patient 1 splenic tissue point, six oxygens could be fitted at a distance of  $1.97 \pm 0.02$  Å, suggesting the presence of a hydrated  $\text{Cr}^{\text{III}}$  species, *i.e.*  $\text{Cr}^{\text{III}}(\text{H}_2\text{O})_6$  (Figure 4.19).

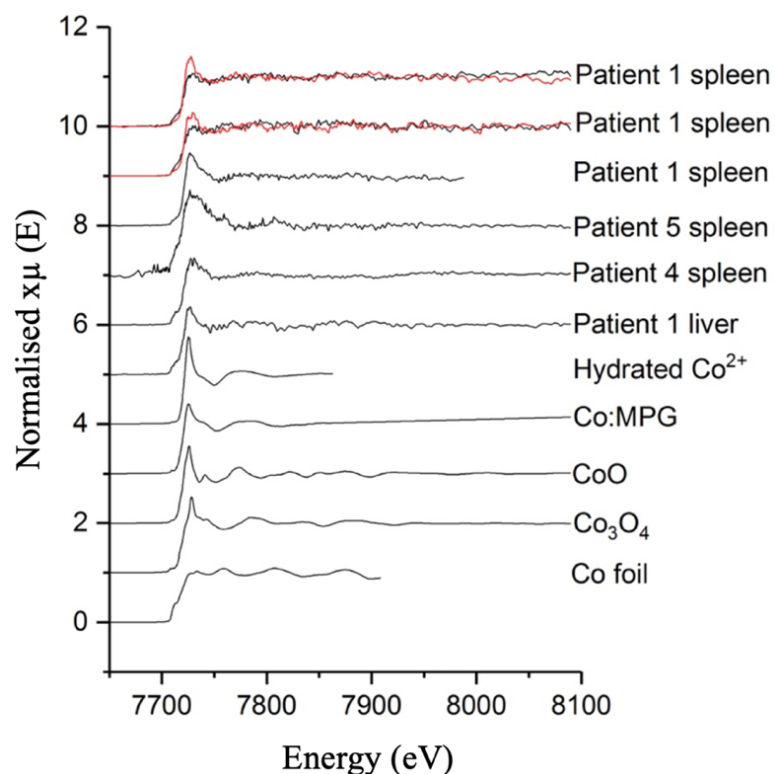


**Figure 4.19. Comparison of  $k^2$ -weighted (left) and Fourier-transformed (right) EXAFS spectra for a chromium species in splenic tissue of Patient 1 (solid line), with that of  $\text{Cr}(\text{H}_2\text{O})_6$  (dashed line). The Cr-O distance is  $1.97\text{Å}$ , but the corresponding peak is shifted inward due to phase shift (adapted from Journal of Trace Elements in Medicine and Biology [276]).**

#### 4.4.4.2 Cobalt

Cobalt K-edge XAS spectra were acquired at 9 separate points from 1 cardiac, 1 hepatic and 3 splenic tissue samples (Figure 4.20). Absorption edge was not observed in three cases, indicating that the cobalt concentration was below the machine's LoD. In the remaining cases, the low signal-to-noise ratio complicated analysis. Overall, most of the spectra resembled the  $\text{Co}^{\text{II}}$  state, with two exceptions from Patient 1 spleen. At those two points, the cobalt appeared to have been originally in the metallic form (either pure metal or CoCr alloy), which was oxidised in the duplicate scan due to beam exposure. Similar effect was observed in previous work investigating cobalt speciation in tissues surrounding metal hip implants [225].



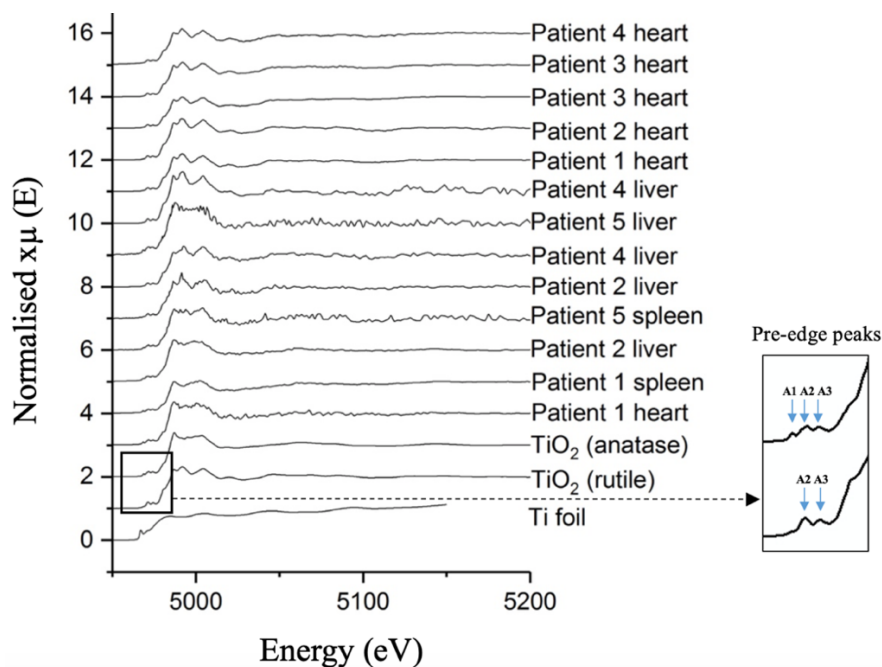


**Figure 4.20. Stacked XAS spectra recorded at the K-edge of six tissue cobalt "hotspots", along with chemical standards. The top two traces correspond to metallic-like cobalt that was oxidised by the beam in the duplicate scan (red line). MPG- N-(2-mercaptopropionyl)glycine (a Co-peptide mimetic) (adapted from Journal of Trace Elements in Medicine and Biology [276]).**

#### 4.4.4.3 Titanium

Comparison of standard spectra with spectra taken at areas of high relative titanium fluorescence intensity revealed that the metal was present exclusively in the oxide form, with six-fold coordination state akin to anatase and rutile. Both crystal structures generate characteristic pre-edge features in the XANES spectrum, with anatase displaying three prominent peaks and rutile displaying two main absorptions [395] (Figure 4.21). Rutile was the predominant crystal structure in our samples, with anatase present in 4 out of the 13 points scanned. There was no relationship between TiO<sub>2</sub> crystal structure and tissue type in which it was detected.





**Figure 4.21. Stacked XAS spectra recorded at the K-edge of thirteen tissue titanium "hotspots", along with chemical standards. All spectra are representative of  $\text{TiO}_2$ - the top nine traces feature rutile-like pre-edge peaks (A2,A3), while the bottom four display anatase-like pre-edge features (A1,A2,A3) (adapted from Journal of Trace Elements in Medicine and Biology [276]).**

## 4.5 DISCUSSION

### 4.5.1 Cardiac cobalt concentration

Cobalt accumulation in the heart has been linked to cardiac dysfunction and several cases of fatal cardiomyopathy (Table 4.6). In our series, even though the concentration of cobalt in the heart was only mildly increased (normal  $0.05\text{-}0.4 \mu\text{g g}^{-1}$  dry tissue [164]), 4 patients exhibited cardiomegaly and 3 displayed severe interstitial fibrosis at necropsy. It is not known if these features were directly caused by the cobalt deposits.

### 4.5.2 $\mu$ -XRF tissue mapping

Dissemination of metal debris to the liver, spleen and heart is a common occurrence in TKA and THA patients [248,396]. In line with these findings, laser ablation ICP-MS and XRF mapping detected varying levels of cobalt, chromium and titanium in most of our spleen, liver and heart tissue samples. It was not possible to calculate absolute metal concentrations, though there was a relative decrease in the number and intensity of metal "hotspots", and in the Co/Cr ratio, in the cardiac XRF maps compared to splenic maps. For example, while the Co/Cr ratio in Patient 1 spleen was

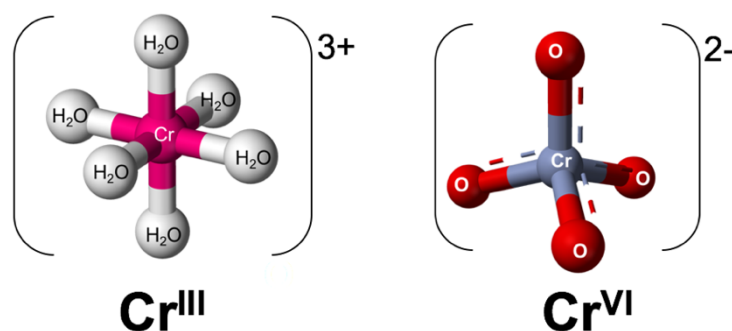
2.4, *i.e.* similar to that in bulk alloy, in the liver it decreased to 1, and further down to 0.3 in the heart. Cobalt is more soluble and corrodes faster than chromium, leading to selective “leaching” of cobalt from CoCr alloy particles [397] (see Section 2.2.6). The process leaves chromium aggregates behind, which tend to accumulate in tissue [398]. While it is likely that spots in which cobalt and chromium were co-localised represented particles of CoCr alloy, it was impossible to discern whether the metals were chemically bound together, or if they were separate metal particles that happened to be near each other in the tissue. Co-localisation of titanium with cobalt or chromium likely occurred within macrophages.

### 4.5.3 $\mu$ -XAS speciation of tissue metal deposits

#### 4.5.3.1 Chromium

XANES spectra acquired at four different tissue points in samples from two different patients detected the presence of a highly oxidised chromium species *i.e.*  $\text{Cr}^{\text{IV/V/VI}}$ . This is the first time synchrotron analysis revealed the presence of a chromium species more highly oxidised than  $\text{Cr}^{\text{III}}$  in human tissue.

All four spectra featured a sharp pre-edge peak that is characteristic of  $\text{Cr}^{\text{VI}}$ , and completely absent from  $\text{Cr}^{\text{III}}$  spectra. The absorbance, which is caused by a  $1s \rightarrow 3d$  electronic transition, is partially allowed in the case of tetrahedral  $[\text{Cr}^{\text{VI}}\text{O}_4]^{2-}$ , due to mixing of the metal’s empty 3d orbitals with 2p orbitals of the oxygen ligands [399] (Figure 4.22). In centrosymmetric molecules, including octahedral  $\text{Cr}^{\text{III}}$  complexes, such mixing is not possible, and pre-edge features do not manifest in the same way.



**Figure 4.22. Diagram showing a trivalent (left) and a hexavalent (right) chromium complex. The octahedral  $\text{Cr}^{\text{III}}$  has a centre of symmetry, which disallows the  $1s \rightarrow 3d$  electronic transition. Tetrahedral  $\text{Cr}^{\text{VI}}$  is non-centrosymmetric and partially allows this transition, giving rise to a sharp pre-edge absorption in the XANES spectrum.**

**Table 4.6. Cardiac cobalt levels and associated toxicity symptoms (reproduced from the Journal of Trace Elements in Medicine and Biology [276]).**

<b>Ref.</b>	<b>Cardiac Co (<math>\mu\text{g g}^{-1}</math>)</b>	<b>Source of cobalt</b>	<b>Associated toxicity symptoms</b>
[61]	0.48 <sup>a</sup>	Cobalt additive in beer combined with malnutrition	Acute onset heart failure with hypotension, pericardial effusion and progressive dyspnoea; fatal cardiomyopathy
[62]	0.37 <sup>a</sup> ; 1.4 <sup>b</sup>	Occupational cobalt exposure for 4 years	Cardiomegaly with fatal cardiomyopathy
[63]	1.65 <sup>b</sup>	3-month cobalt chloride therapy with haemodialysis	Cardiomegaly with fatal cardiomyopathy
[64]	8.9	9-month cobalt chloride therapy with haemodialysis	Cardiomegaly with pericardial effusion and fatal cardiomyopathy
[65]	7	Occupational cobalt exposure for 4 years	Changes consistent with cobalt cardiomyopathy
[7]	3.85	Revision of a fractured ceramic implant to MoP THA	Pericardial effusion, fatal cardiomyopathy with EF of 30%
[66]	8.32	Catastrophic wear of bilateral MoM hip replacement	Pericardial effusion, cardiomyopathy with EF of 10%; heart transplantation
[67]	4.75	Catastrophic wear of bilateral MoM hip replacement	Fatal cardiomyopathy with EF of 10-15%
[68]	2.5	Revision of a fractured ceramic implant to MoP THA	Fatal cardiomyopathy with EF of 35-40%
[23]	3.76 <sup>b</sup>	Catastrophic wear of bilateral MoM hip replacement	Fatal biventricular heart failure with EF of 16%
Current series	0.31-0.91 <sup>b</sup>	Wear and corrosion of metal joint implants	Cardiomegaly (80%) and/or severe interstitial fibrosis (60%)

<sup>a</sup>Wet tissue, <sup>b</sup>dry tissue; EF- ejection fraction.

The exact chemical form of these complexes could not be elucidated. The pre-edge peak was not as intense as that of pure Cr<sup>VI</sup>, nor that of Cr<sup>VI</sup>-glutathione complex (likely intermediate formed during the cellular metabolism of Cr<sup>VI</sup>) [400]. It is well-established that the height of the pre-edge absorbance can offer quantitative information on the proportion of Cr<sup>VI</sup> in a mixture of Cr<sup>III</sup> and Cr<sup>VI</sup> oxides. Several groups have used XANES to determine the Cr<sup>VI</sup> content in a range of environmental samples, and found that the intensity of the peak increased in proportion to increasing percentage of Cr<sup>VI</sup> in the sample [399,401–403]. Based on their striking resemblance to a 36/64 mixture of Na<sub>2</sub>CrO<sub>4</sub> and Cr<sub>2</sub>O<sub>3</sub> described by Bajt and colleagues [399], we propose that our XANES spectra correspond to a mixture of Cr<sup>III</sup> and Cr<sup>VI</sup> oxides.

XANES spectrum of a Cr<sup>V</sup>-carbohydrato intermediate, that is thought to form in biological systems exposed to Cr<sup>VI</sup>, features a pre-edge peak of a similar intensity [404]. Even though certain carbohydrates can stabilise the reactive Cr<sup>V</sup> intermediate *in vivo* [405], the resultant complexes would be expected to decompose under the X-ray beam, which was not observed in our case. The replicate XANES scan acquired at the same spot looked nearly identical, with the pre-edge absorption intensity and the edge position largely unchanged. For this reason, it is much less probable that our spectra correspond to a Cr<sup>V</sup> species. We exclude that the species is a Cr<sup>IV</sup> complex, as those are notoriously unstable [400]. Moreover, pre-edge peak energies of model Cr<sup>IV</sup> complexes [406] are considerably different to those recorded in the current study.

It is unlikely that the highly oxidised chromium species was released directly from the orthopaedic implants, as no evidence of Cr<sup>VI</sup> has ever been found in periprosthetic tissue [43,225]. The high sequestering and reducing capacity of blood means that if any hexavalent chromium was to be liberated, it would have been reduced before it had the chance to reach organ tissue [407]. Re-oxidation of Cr<sup>III</sup> to Cr<sup>VI</sup> under physiologically relevant conditions is possible [408]. Despite early claims to the contrary, it is now experimentally established that Cr<sup>III</sup> complexes can be oxidised to Cr<sup>VI</sup> in neutral aqueous solutions at ambient conditions by H<sub>2</sub>O<sub>2</sub> or H<sub>2</sub>O<sub>2</sub>-producing enzymatic systems [409]. More recent considerations highlight that oxygen, and its partially reduced intermediates, can also oxidise chromium to the hexavalent state [410]. Although intracellular environments are generally reducing [411–414], significant local concentrations of strong oxidants are formed during normal cell signalling, and in pathological inflammatory conditions such as diabetes (Patient 1 and

Patient 4 in our series were diabetic) [415,416]. In fact, evidence is mounting that insulin-enhancing activity of Cr<sup>III</sup> supplements is mediated by their *in vivo* oxidation to Cr<sup>V/VI</sup> complexes [417].

There is limited evidence for carcinogenic outcomes in THA patients [192,193]. However, chromium-produced cancers could take between 10-40 years to develop, which is much longer than the follow-up time in previous studies. Reduction of Cr<sup>VI</sup> to Cr<sup>III</sup> generates a plethora of noxious species, including Cr<sup>V</sup> and Cr<sup>IV</sup> intermediates, ROS and free radicals that damage cellular proteins, lipids and DNA. Even in absence of malignancy, repeated reduction-oxidation cycles, and chronic production of reactive species, could induce functional failure of the affected organ (see Section 2.4.1).

#### 4.5.3.2 Cobalt

Previous studies investigating chemical composition of tissues surrounding MoM and MoP hip implants reported on the presence of Co<sup>II</sup> complexed with organic ligands, in an octahedral environment [34,43,225]. In the current study, most cobalt XANES spectra resembled Co<sup>II</sup>, but we were unable to establish the exact chemical form of the metal due to poor data quality.

#### 4.5.3.3 Titanium

Previous studies found that tissues surrounding titanium alloy implants contain TiO<sub>2</sub> particles, in either anatase, rutile [280] or amorphous form [34]. Our investigation identified TiO<sub>2</sub> in most of the systemic tissue samples. All of the titanium XANES spectra featured small pre-edge peaks that represent transitions to d orbitals in anatase and rutile crystal structures. We detected no metallic titanium particles, which could mean that the hip implants did not undergo significant wear, or that any particles of titanium metal released from the implants underwent oxidation before depositing in the organs. It is also possible that the particles originated from external sources. TiO<sub>2</sub> is a common additive in many food and personal care products [239]. Biodistribution experiments showed that oral intake of TiO<sub>2</sub> nanoparticles could lead to their deposition in the spleen and the liver, and result in accumulation in tissues upon repeated exposure [418].

#### 4.5.4 Study limitations

Chief limitations of our study are its *ex vivo* nature, and small sample size (5 cadavers). Synchrotron technology has a limited availability, which means that the number of specimens that can be analysed will always be much smaller than with other techniques. It is also impractical to scan the whole sample. Instead, selected tissue areas are mapped, which might not be representative of the sample as a whole. Due to time constraints, our investigation did not include a control group. As a result, we were unable to ascertain whether highly oxidised chromium forms could also be found in tissue of non-arthroplasty subjects.

The spectroscopy techniques we utilised are not destructive, have a low LoD and enable mapping of large tissue areas, followed by repeated analysis of element valency and its nearest atomic neighbours, that is widely accepted as precise and accurate. However, if the concentration of the element of interest is not high enough,  $\mu$ -XAS is limited to the XANES regime and/or the resulting spectra are very noisy. This was the case in the present study, and meant that in many cases we were unable to determine the exact chemical form of the metal “hotspots”. It is likely that systemic dissemination of metal debris is greater with MoM implants compared to that with well-functioning MoP articulations [180]. A higher concentration of cobalt and chromium in the organs would have allowed for a more thorough elemental analysis.

#### 4.6 CONCLUSION

The absence of  $\text{Cr}^{\text{VI}}$  from periprosthetic tissue is regarded as evidence that  $\text{Cr}^{\text{VI}}$  generation does not occur during biocorrosion of CoCr alloy joint implants. Our novel finding of highly oxidised chromium species in cadaveric samples of heart, liver and spleen tissue derived from donors with MoP implants uncovers the possibility that these forms of chromium might arise in vital organs of TJA patients. Low concentrations of  $\text{Cr}^{\text{VI}}$  are unlikely to pose serious issues, as the built-in detoxification mechanisms prevent the movement of the genotoxin into the cell nucleus. Oxidation of  $\text{Cr}^{\text{III}}$  to  $\text{Cr}^{\text{VI}}$  might present a greater health hazard if the protective mechanisms are overtaken by high chromium release from failing MoM prostheses [411]. Larger, controlled studies are needed to determine if these findings can be generalised to the *in vivo* conditions, and whether  $\text{Cr}^{\text{VI}}$  can arise in organ tissue in the absence of metal implants.

# **Chapter 5**

## **Identifying cobalt susceptible genes: a feasibility study**



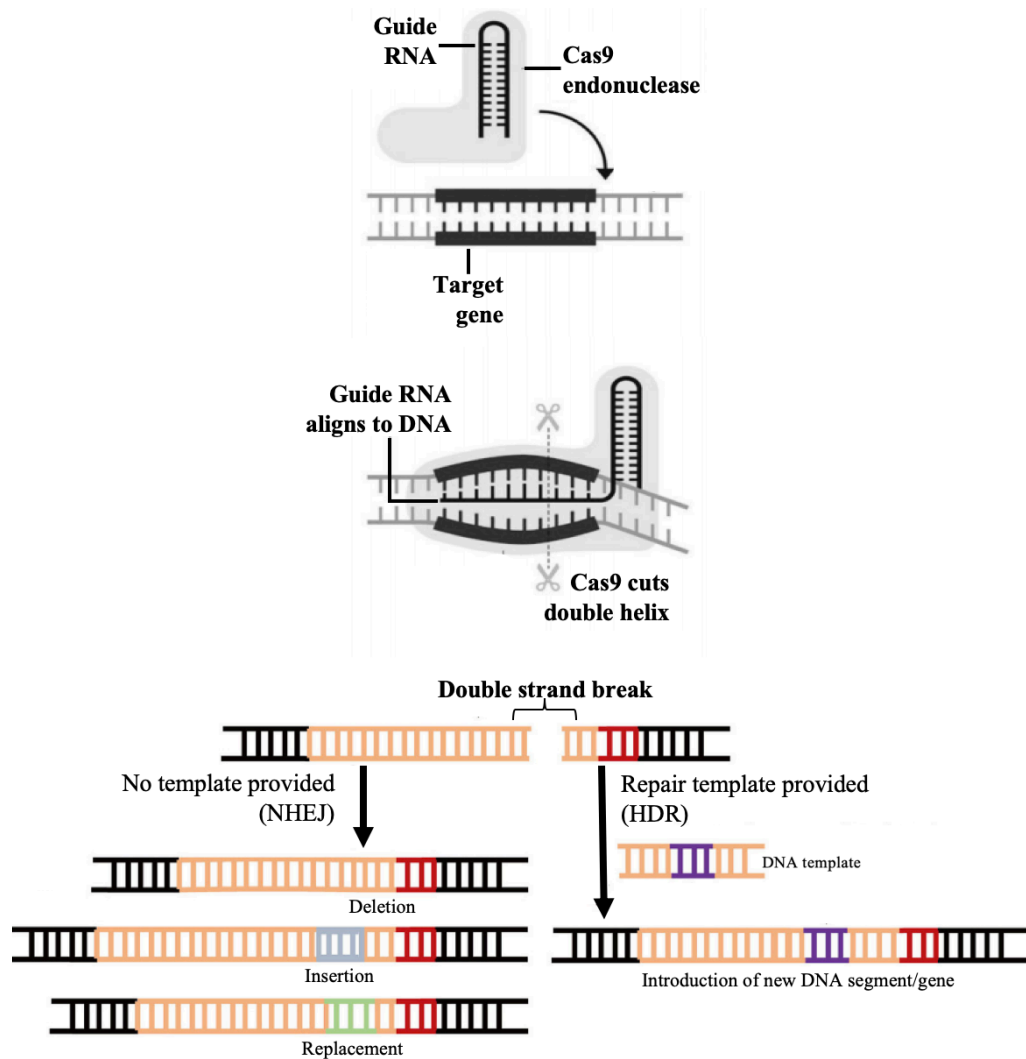


## 5.1 BACKGROUND: CRISPR/CAS TECHNOLOGY

### 5.1.1 CRISPR/Cas systems

Viruses infect cells by injecting their DNA. Bacteria are able to “pluck out” segments of viral DNA and insert them into their own chromosome, at specific sites called CRISPR (Clustered Regularly Interspaced Short Palindromic Repeats). This allows them to produce an RNA transcript of the incorporated DNA, and associate it with a specialised endonuclease (DNA-cleaving enzyme). The RNA guides the enzyme to a complementary sequence on invading DNA, and prompts it to cut the double helix at a specific site. Essentially, CRISPR and CRISPR-associated (Cas) endonucleases constitute an adaptive immune system that serves to protect the organism against viral attack. In 2012, the Doudna-Charpentier team at the University of California, Berkeley, found a way to harness this bacterial defense mechanism to modify or delete specific regions of DNA in bacterial cells [419]. Since then, CRISPR/Cas technology has been applied to a multitude of systems, including fruit flies, mice, monkeys, crops and human cells [420].

Although three different types of CRISPR/Cas system have been discovered, type II system featuring Cas9 endonuclease is the most commonly used in research [419]. In brief, target cells are transfected with a DNA plasmid expressing both the Cas9 protein and a fragment of single guide RNA (sgRNA) which has been programmed to direct the enzyme to a gene of interest. As the enzyme cuts the DNA at the desired locus, one of two cellular DNA repair pathways is activated. The more dominant mechanism-non-homologous end joining (NHEJ)- is notoriously error-prone and leads to insertions, deletions and frame shift mutations that often disable the target gene. Alternatively, the nick can be repaired by insertion of extra DNA *via* homology directed repair (HDR). In this pathway, a “repair template” is supplied, which directs introduction of a new DNA segment, or a whole new gene. The latter mechanism can also be utilised to “correct” point mutations in the target gene (Figure 5.1).



**Figure 5.1. CRISPR/Cas9 genome editing technology. An RNA “guide” molecule can be synthesised to match any unique DNA sequence in the human genome (top). Combining the guide RNA with Cas9- a specialised DNA-cleaving enzyme- allows the complex to home in on the DNA sequence of interest and cut both strands of the double helix (middle). Repair of the broken DNA results in silencing/modification of the target gene, or introduction of extra DNA (bottom).**

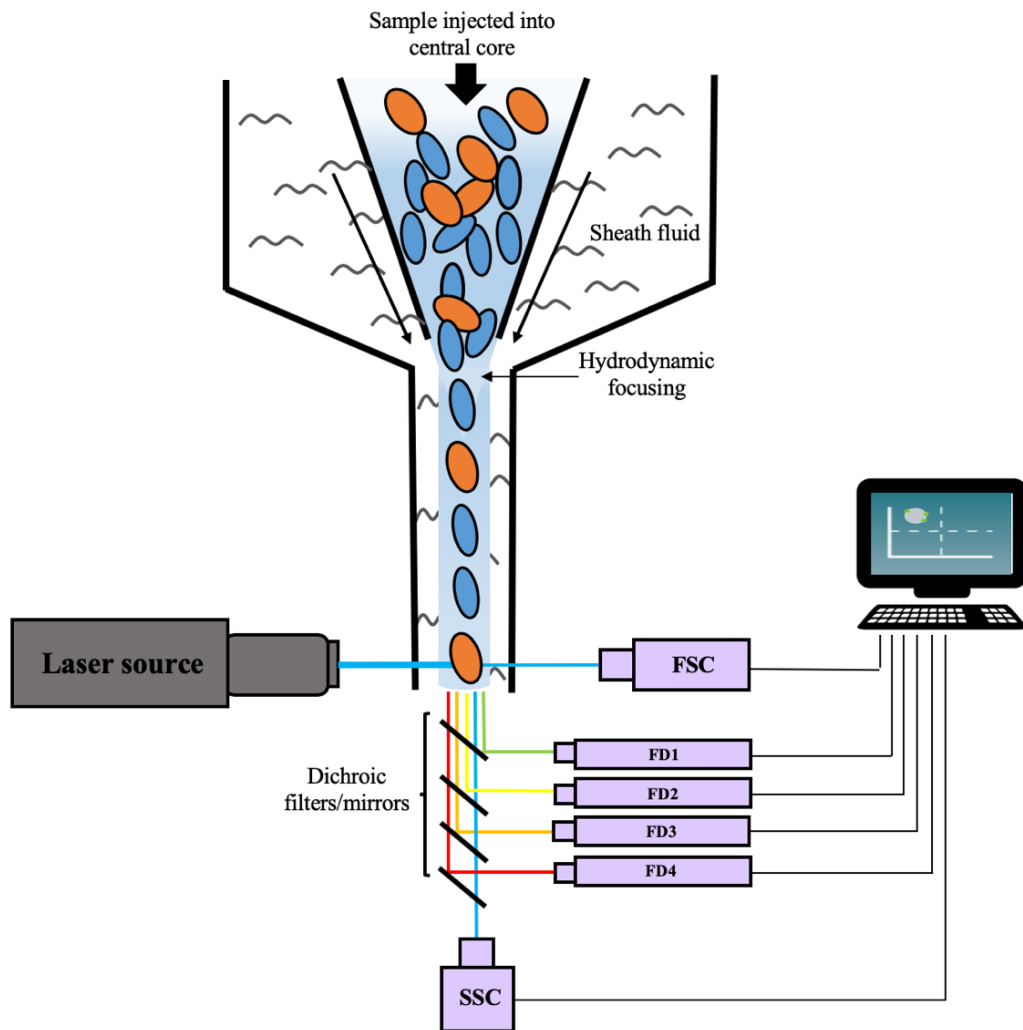
High precision, versatility, simplicity and ability to target virtually any gene have made CRISPR/Cas9 the tool of choice for modern DNA editing. The technique has created exciting yet controversial opportunities, including genetic modification of crops to boost food production [421], eradication of malaria-carrying mosquitos [422] and treatment of human genetic diseases [423]. However, if the pairing between DNA and guide RNA is not perfect, Cas9 can induce off-target mutations when, which could have unforeseen consequences [424]. Moreover, the efficiency of CRISPR/Cas9 delivery into different target cells can vary.

### **5.1.2 Genome-scale CRISPR/Cas9 knock-out libraries**

Genome-scale CRISPR/Cas9 knock-out libraries targeting  $1 \times 10^2$ - $10^4$  genes are now commercially available. Their transduction into cell lines results in pools of cells, in which different genes had been inactivated, enabling cost-effective large-scale perturbation screens in mammalian cells. Toronto KnockOut (TKO) library, developed by Jason Moffat's group, was originally used to pinpoint 1580 genes essential for growth and proliferation in healthy cells and tumour cell lines (core fitness genes) [425]. This system has since been shown to be highly effective at identifying drug resistant genes [426,427], and genes that confer susceptibility to certain toxins [428]. In the latter case, library-transfected cells are subjected to a toxic concentration of the drug of choice, before the surviving cells are harvested (usually by flow cytometry) and their DNA sequenced to reveal which genes had been knocked-out.

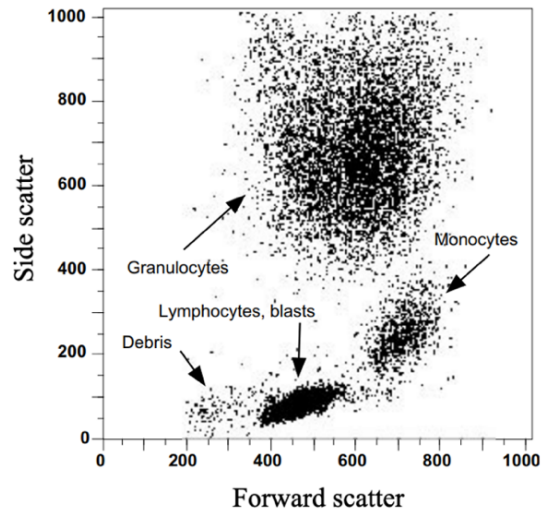
### **5.1.3 Flow cytometry**

Flow cytometry is a technique that can be used to differentiate between different cell types in a mixture. After the sample is injected into the machine, the fluidics system orders it into a stream of single cells, allowing each to be interrogated by light at a particular wavelength (Figure 5.2). The amount of light scattered by the cell in the forward direction is positively correlated with particle size, and can be used to distinguish between live cells and cell debris (the latter is much smaller). Light measured at approximately  $90^\circ$  to the excitation line (side scatter) is proportional to the granularity of the cell. Forward and side scatter are unique for each cell type, which helps to distinguish different cell populations, and estimate their proportions in a sample (Figure 5.3).



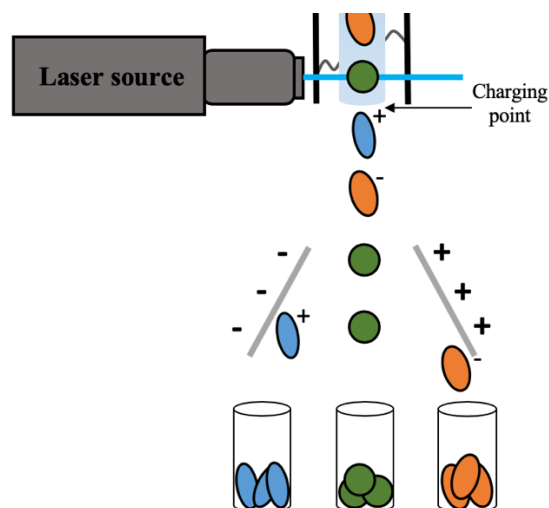
**Figure 5.2. Schematic overview of a typical flow cytometry setup. As the sheath fluid moves, it exerts a drag effect on the central fluid, creating a single file of cells (hydrodynamic focusing). Each individual cell is interrogated by one or more laser beams. Light scattered in the forward and side direction is detected by the corresponding detectors (FSC and SSC, respectively), and provides information about cell size and granularity. Fluorescence measurements taken at different wavelengths (FD1-FD4) inform about fluorochrome-labelled proteins or DNA.**

To better characterise the sample, the cells can be stained with different fluorescent dyes prior to analysis. For example, calcein AM only fluoresces inside metabolically active cells, while deep red anthraquinone 7 (DRAQ7) and propidium iodide (PI) fluoresce upon binding to DNA of dead or permeabilised cells. Depending on the dye used, the amount of fluorescence emitted by stained cells allows their viability to be estimated, or inform on expression of particular cell surface receptors or cytokines.



**Figure 5.3. Flow cytometric analysis of bone marrow aspirate, demonstrating the characteristic position of different cell populations. Granulocytes, which are the biggest and most granular while blood cell type, produce the largest forward and side scatter (adapted from Riley and Idowu “Principles and Applications of Flow Cytometry”).**

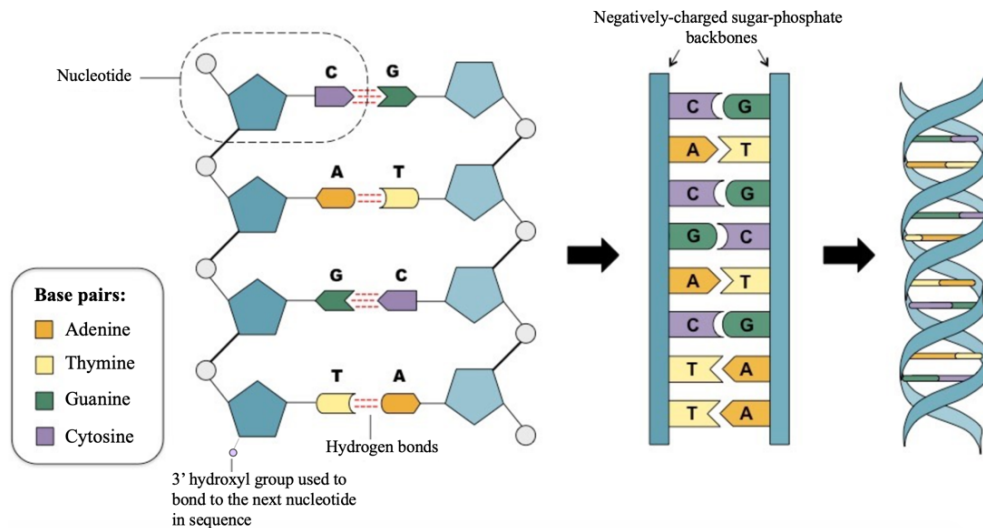
Fluorescence-activated cell sorting (FACS) is an application of flow cytometry, which allows different cell populations to be separated for further biological studies. Separation is achieved by comparing scatter and fluorescence signals of each individual cell against specific pre-set criteria, and applying an electrostatic charge to cells that match them. A strong electrostatic field deflects the cells depending on their charge, directing them into different containers (Figure 5.4).



**Figure 5.4. Principles of fluorescence assisted cell sorting. As cells exit the instrument nozzle, they are charged according to pre-set criteria. Positively and negatively charged voltage plates direct the cells into different containers.**

### 5.1.4 DNA sequencing

DNA sequencing is the process of “decoding” the precise order of base pairs in a DNA molecule (Figure 5.5), used to further our understanding of evolution and genetic function.

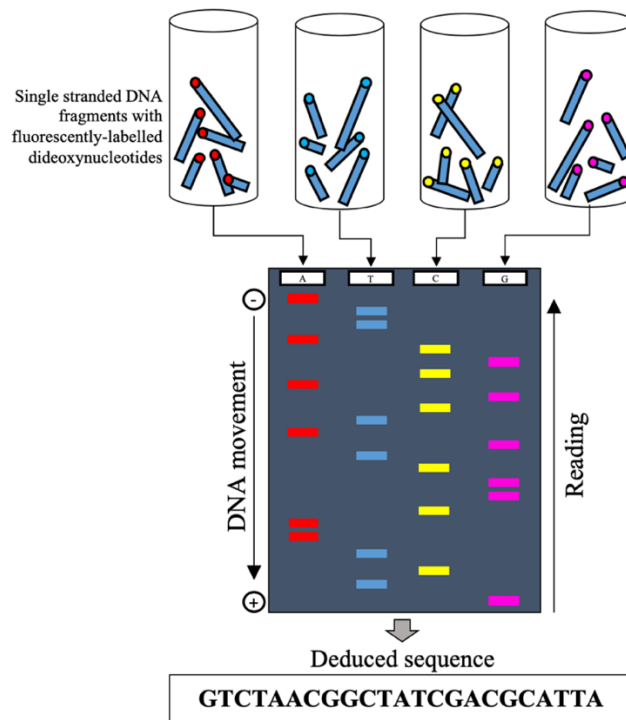


**Figure 5.5. Simplified diagram of DNA structure showing the antiparallel complementary polynucleotide strands, the DNA “ladder” and the DNA double helix (adapted from bioninja.com.au).**

#### 5.1.4.1 Sanger sequencing

The “dideoxy method”, developed in the 1970s by Frederick Sanger, remains the gold standard for routine DNA sequencing applications [429]. In this approach, the sample is denatured into single strands and divided between four reaction vessels, each containing DNA polymerase, a set of DNA building blocks (nucleotides), and a low concentration of a fluorescently-labelled dideoxynucleotide (either ddATP, ddCTP, ddGTP or ddTTP). In each test tube, a complementary chain is synthesised. Nucleotides are added one after the other, according to base pairing rules, until a dideoxynucleotide is incorporated. Dideoxynucleotides lack the 3' hydroxyl group and are unable to form a bond with the subsequent nucleotide, leading to chain termination. The process generates many copies of different-length DNA fragments terminated at all the possible positions by one of the dideoxynucleotides. The double-stranded molecules are heat denatured and separated according to size by electrophoresis. The sequence of the new strand is recorded from fluorescent emission of the

dideoxynucleotides as it flows through the gel, and the original template sequence is deduced (Figure 5.6).



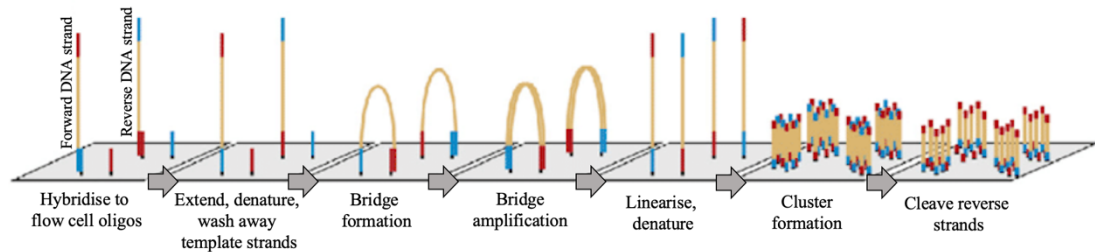
**Figure 5.6. Gel electrophoresis of dideoxy-terminated DNA chains. Negatively-charged DNA migrates towards the positively charged end of the electrophoresis plate. Shorter DNA bands are lighter, and travel further, while the longer strands lag behind, resulting in a separation of all the fragments according to their length. Fluorescence emitted by the dideoxynucleotides is detected by the sequencing machine, and the DNA sequence read from the bottom of the plate.**

#### 5.1.4.2 Next-generation sequencing (NGS)

NGS instruments sequence millions of DNA templates simultaneously in a single reaction, permitting large-scale automated genome analyses at a fraction of the time and cost of Sanger sequencing.

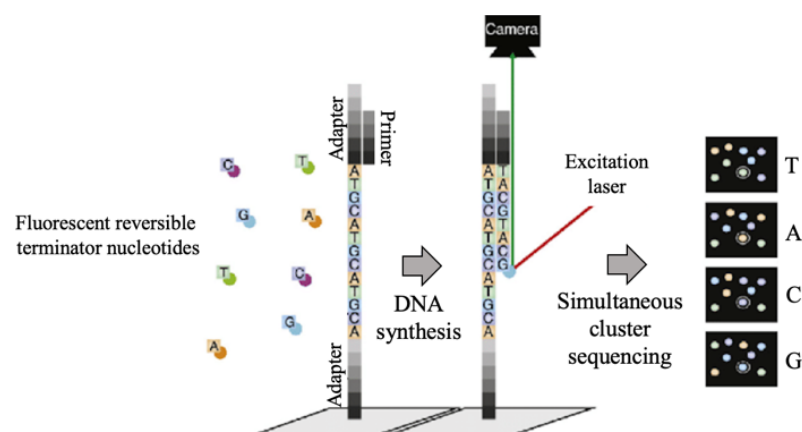
While several different types of NGS sequencers exist, which differ in technical specifications, the key element of every NGS instrument is the flow cell- a glass slide lined with two types of oligonucleotide adapters (short sequences of single-stranded DNA) that serve as tethering points for both ends of single-stranded sample DNA. Once the forward and reverse strands are captured by the flow cell, DNA polymerase and nucleotides are added, and the extension reaction is initiated from a customised primer. Once complete, the double-stranded molecules are denatured and the template

strands washed away, leaving the complementary strands covalently attached to the flow cell. Each DNA fragment forms a bridge with another flow cell adapter through its 5' end, and a second round of DNA synthesis proceeds. The process is repeated several hundred times for a given fragment of sample DNA, resulting in clusters containing many identical copies of each unique DNA fragment (Figure 5.7).



**Figure 5.7. Cluster formation in NGS.** Sample DNA is denatured and hybridized to complementary adapter oligonucleotides on the flow cell. Complementary strands are extended, amplified *via* bridge amplification and denatured, resulting in clusters of identical single-stranded library fragments (adapted from Chaitankar *et al.* [430]).

Complementary chains are synthesised using fluorescently-labelled nucleotides, which have the 3' hydroxyl group reversibly blocked. After each base pair addition, fluorescence emitted from each cluster is captured and the blocking group removed to allow chain elongation (Figure 5.8). Once all DNA fragments have been sequenced, the reads are sorted, aligned and compared with a reference genome to identify sequence differences.



**Figure 5.8. Cluster sequencing in NGS.** Fragments are primed and extended utilising fluorescently-labelled reversible terminator nucleotides. Each newly added nucleotide is interrogated with a laser, and an image of emitted fluorescence captured from each cluster, so that the identity of each base pair can be recorded (adapted from Chaitankar *et al.* [430]).



## 5.2 INTRODUCTION

Cobalt ions are the most toxic species released from CoCr alloy-based orthopaedic implants. They are known to cause death of many different cell types *in vitro*, as well as promoting periprosthetic inflammation and systemic toxicity in some THA patients. A dose-response relationship between cobalt and *in vivo* toxic effects has not been established. In case reports of local and systemic toxicity, the reported adverse symptoms often do not correlate with blood/serum cobalt concentrations (Table 2.2), prompting the hypothesis that some patients might be inherently more prone to the adverse effects of cobalt. Although several predisposing factors have been identified (see Section 2.9), it is possible that there are genes that confer increased susceptibility to cobalt-induced toxicity.

Innate immunity, mediated by monocytes, macrophages and dendritic cells, is the first line of defense against foreign antigens. A large proportion of hip implant debris is phagocytosed by tissue-resident macrophages. The particles are gradually dissolved in the acidic environment of the lysosome, releasing free  $\text{Co}^{\text{II}}$  ions inside the cell. The high cobalt ion concentration inside macrophages can cause them to die, leading to the recruitment of more macrophages, and an expanding necrotic zone. THP-1 is an immortalised monocyte cell line derived from the peripheral blood of a childhood case of acute monocytic leukaemia. The cell line is a popular model of primary human monocytes and macrophages, and is often used to mimic their responses to pathogens and toxins [431].

### 5.2.1 Motivation

Several authors attempted to find genetic relationships in THA patients with bone loss and implant failure, and identified particular SNPs that are commonly overexpressed in those with aseptic loosening and ALTR (see Section 2.9.4). As SNP analyses are broad and unspecific in nature, it is impossible to infer whether the genetic differences are caused by the hip implants. Studies focusing on toxic effects mediated directly by cobalt are warranted.

### 5.2.2 Aims

To carry out a feasibility study into identifying genes that might mediate susceptibility to cobalt toxicity.

### **5.2.3 Objectives**

To 1) establish conditions (Co<sup>II</sup> dose and incubation time) needed to kill the entire cell population and 2) combine CRISPR/Cas9 technology with NGS sequencing to pinpoint genes that are absent in cells that survive the lethal Co<sup>II</sup> insult.

## **5.3 MATERIALS AND METHODS**

### **5.3.1 Cell culture materials**

Roswell Park Memorial Institute (RPMI) 1640 medium with L-glutamine (Lonza, Belgium), foetal calf serum (FCS; Sigma, UK), penicillin/streptomycin (P/S; Thermo Fisher Scientific, Germany), blasticidin S HCl (Gibco™, UK), DRAQ7 (abcam, UK), PI (Sigma, UK), haemocytometer (Glasstic®, KOVA International), 25 cm<sup>2</sup>, 75 cm<sup>2</sup> and 175 cm<sup>2</sup> cell culture flasks (Thermo Fisher Scientific, Germany) and Corning® Costar® 6 and 12-well tissue culture plates.

### **5.3.2 THP-1 cells**

The monocytic THP-1 cell line (kindly provided by Prof. Andres Floto of the Laboratory of Molecular Biology) was cultured in RPMI 1640 media supplemented with 10% FCS and 1% P/S, in a humidified atmosphere of 5% CO<sub>2</sub>, at 37 °C. Cells were assessed under a light microscope, and counted using a haemocytometer until they reached approximately 80% confluency.

In order to induce Cas9 expression, THP-1 cells were transduced with a virus carrying the Cas9-2A-Blasticidin vector (Addgene plasmid #73310). Since the vector conferred blasticidin resistance, Cas-9-expressing cells were selected with blasticidin (20 µg mL<sup>-1</sup>) [425]. THP-1-Cas9 cells (clone 3) were cultured in RPMI and maintained with 10 µg mL<sup>-1</sup> blasticidin.

### **5.3.3 Cobalt toxicity assay- establishing lethal conditions**

Solution of cobalt ions was prepared from cobalt (II) chloride hexahydrate (CoCl<sub>2</sub>.6H<sub>2</sub>O MW= 237.93; Sigma, UK). CoCl<sub>2</sub>.6H<sub>2</sub>O was diluted in distilled water to a concentration of 10 mM, and then further diluted in cell culture medium to achieve desired concentrations.

THP-1-Cas9 cells were plated at a density of  $1 \times 10^6$  cells/well in two 12-well plates (3.8 cm<sup>2</sup> growth area, cell medium volume: 1.5 mL). Cobalt ion solution was added at either 2, 3, 4 or 8 mM before the cells were incubated. The percentage of surviving cells at 24 and 48 hours was established using flow cytometry and DRAQ7 staining. DRAQ7 is a far-red fluorescent dye that stains the DNA of membrane-compromised (dead) cells only, with an excitation at 647 nm and emission at 670 nm. The cells were stained with 5  $\mu$ L DRAQ7 (1% v/v), incubated for 40 minutes at 37 °C in the dark, and acquired on a LSRFortessa cell analyser (BD Sciences, US). The results were analysed in FlowJo software (version 10.5.3) (Table 5.1).

A two-day incubation with either 4 or 8 mM Co<sup>II</sup> was able to kill the entire cell population. 4 mM, which killed the cells more gently, and was less likely to induce morphological/functional alterations in the surviving cells, was chosen for subsequent experiments.

**Table 5.1. The effect of increasing cobalt ion concentration on THP-1-Cas9 cell viability (24 h/48 h incubation, DRAQ7 stain).**

Co <sup>II</sup> concentration (mM)	Mean % live cells	
	24 h	48 h
0	96.2	68.1
2	55.2	3.66
3	51.8	1.82
4	42.5	1.20
8	30.4	1.02

### 5.3.4 Toronto KnockOut (TKO) library transduction

TKO (Addgene, pooled library #1000000069) is a human CRISPR library with 176,500 sgRNAs that target silencing of 17,661 different protein-coding genes. The library is split into two sub-libraries with 6 sgRNAs on average per gene in each: the “90k” library contains 91,320 sequences and does not allow any off-target activity, while the supplemental library contains 85,180 sequences and authorises one off-target

“hit”. The sgRNAs are contained within viral plasmids, which have to be assembled into lentivirus before being transduced into target cells. This is achieved by co-transfecting the library and lentiviral packaging mix into human embryonal kidney (HEK) 293FT cell line. The cells produce viral RNA and proteins, which are released into cell culture medium as viral particles.

#### *Making the lentiviral library*

HEK 293FT cells ( $22 \times 10^6$ ) were seeded in DMEM medium (Thermo Fisher Scientific, US) supplemented with 10% FCS and  $10 \mu\text{g mL}^{-1}$  lysostaphin (Sigma, UK), in a T75 flask. Once at ~80% confluency, the cells were co-transfected with  $16 \mu\text{g}$  PAX2,  $1.56 \mu\text{g}$  pMD2 and  $14 \mu\text{g}$  TKO library, using Invitrogen™ Lipofectamine™ 3000 Transfection Reagent (Thermo Fisher Scientific, US), and incubated at  $37^\circ\text{C}$  in 5%  $\text{CO}_2$ . The supernatant was collected and replaced with fresh media 24 hours later, and again at the 48 hour mark. The collected virus was pooled, centrifuged at 2200 revolutions per minute (RPM) for 5 min to remove cellular debris, filtered ( $0.22 \mu\text{M}$ ), and stored at  $-80^\circ\text{C}$  until needed.

#### *Library transduction*

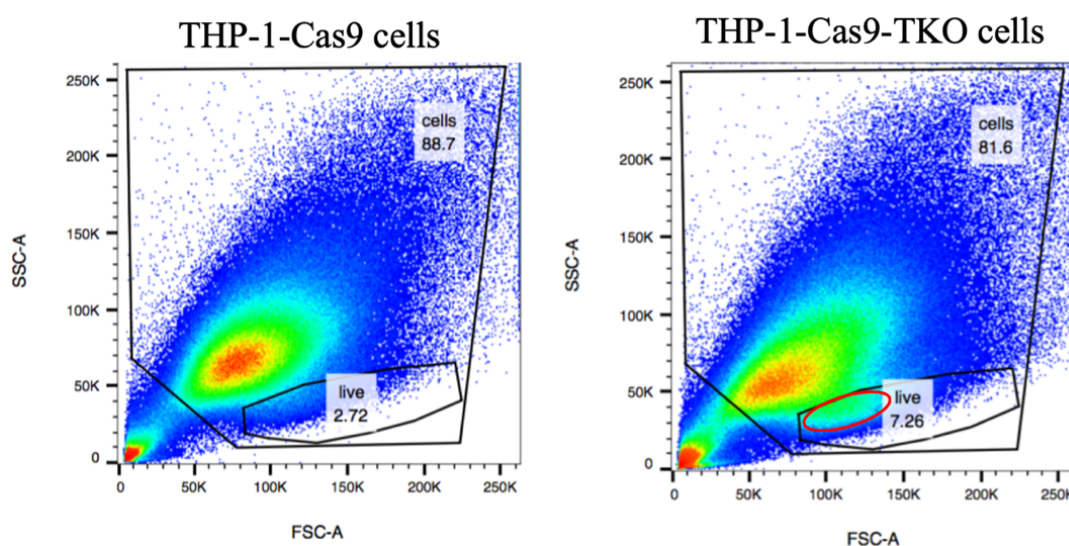
THP-1-Cas9 cells ( $1 \times 10^8$ ) were seeded in 12-well plates and transduced with the lentiviral library at a low multiplicity of infection (0.35:1), *i.e.* 0.3 mL of virus per  $1 \times 10^6$  cells in 1 mL total medium [425]. This helped to ensure that most cells received only 1 viral construct with high probability. The cells were spun at 1800 RPM for 2 hours at  $37^\circ\text{C}$ , with media change 24 hours later.

48 hours post-transduction, cells were re-suspended in fresh media with puromycin ( $1 \mu\text{g mL}^{-1}$ ) and blasticidin ( $10 \mu\text{g mL}^{-1}$ ), to ensure that only cells with stable viral integration were selected. Although 2-3 days of puromycin treatment is generally enough to successfully select transduced cells, we chose to incubate for 14 days to allow more time for Cas9 genome modification. The THP-1-Cas9-TKO cells were kept in T175 flasks to enable proliferation.

Generation of the lentiviral library, transduction and selection were performed by Ms Catherine Klapholz at the Laboratory of Molecular Biology (LMB).

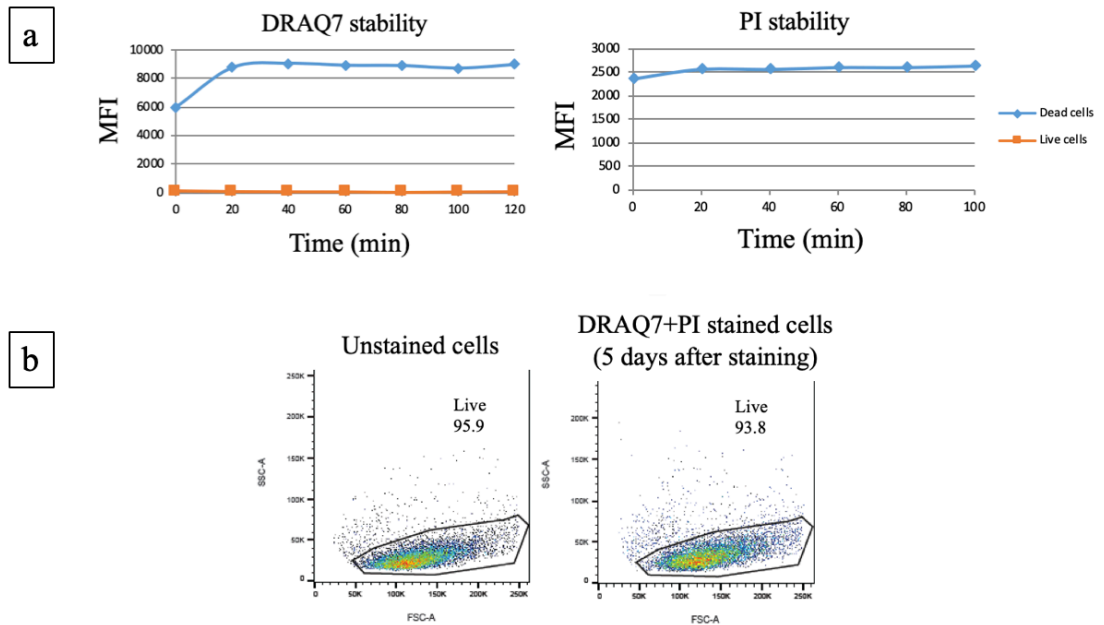
### 5.3.5 Screening assay and optimisation

THP-1-Cas9-TKO cells and THP-1-Cas9 cells were seeded at a density of  $5 \times 10^6$  in two T25 flasks (25 cm<sup>2</sup> growth area, cell medium volume: 7.5 mL). The cells were exposed to 4 mM Co<sup>II</sup> for 48 hours. At the end of incubation time, cell viability was assessed by flow cytometry, using the same staining protocol as before (Figure 5.9).



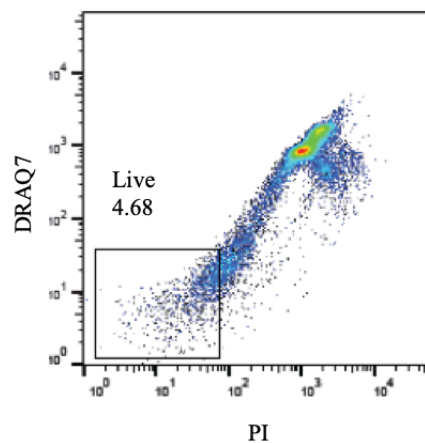
**Figure 5.9. Viability of TKO-transduced THP-1-Cas9 cells *versus* control after lethal Co<sup>II</sup> insult (DRAQ7 stain). The circled area, which was absent in non-TKO transduced cells, might represent surviving cells that are resistant to cobalt-induced cell death.**

Flow cytometry results revealed that the live cell population was enriched in TKO-transduced cells (red circle in Figure 5.9), which was encouraging, though it appeared that approximately 3% of dead cells failed to take up the DRAQ7 stain and masqueraded as live cells. In order to improve dead cell staining, a second DNA dye (PI; excitation at 535nm, emission at 615 nm) was added, which, similarly to DRAQ7, is excluded by cells that have their plasma membrane integrity preserved (live or early apoptotic cells). The cells were first incubated with DRAQ7 (40 min, 37 °C) then PI (15 min, 4 °C), and acquired on a LSRFortessa cell analyser (BD Sciences, US). This staining protocol was shown to be stable, and it did not cause cell death, even after prolonged incubation (Figure 5.10).



**Figure 5.10. Validation of the staining protocol: a) fluorescence emitted by DRAQ7 and PI remained stable over a 2-hour period, b) DRAQ7/PI staining did not cause cytotoxicity after a 5-day incubation.**

The toxicity assay was repeated with  $20 \times 10^6$  cells, using the optimised staining protocol (Figure 5.11).



**Figure 5.11. Viability of TKO-transduced THP-1-Cas9 cells after lethal  $\text{Co}^{\text{II}}$  insult (DRAQ7+PI stain).**

Live cells (negative for both DRAQ7 and PI) were sorted on an LSRFortessa machine (BD Sciences, US), yielding 35,000 survivors.

Cell sorting was performed by Ms Catherine Klapholz at the LMB.

### 5.3.6 DNA amplification and sample preparation

DNA of library (THP-1-Cas9-TKO before cobalt insult) and sorted cells (surviving THP-1-Cas9-TKO after cobalt insult) was extracted using the QIAamp<sup>®</sup> DNA Mini Kit (QIAGEN, Germany) (5 x 10<sup>6</sup> cells per column), yielding 1130  $\mu$ L (142  $\mu$ g) and 770  $\mu$ L (81.6  $\mu$ g) DNA, respectively.

Regions containing the sgRNAs were amplified to increase sample concentration for sequencing. This was done by primary polymerase chain reaction (PCR1), using the Q5<sup>®</sup> Hot Start High-Fidelity DNA polymerase with GC enhancer (New England BioLabs, UK) and the following primers:

Forward PCR1 primer (Sigma, UK) : 5'-AGGGCCTATTTCCCATGATTCCTT-3'

Reverse PCR1 primer (Sigma, UK): 5'-TCAAAAAGCACCGACTCGG-3'

The components were assembled in clean 15 mL tubes, mixed well, and distributed between 71 and 41 wells of two 96-well plates (50  $\mu$ L total volume in each well) (Table 5.2).

**Table 5.2. PCR1 reaction components.**

Component	Quantity ( $\mu$ L)	
	Library	Sorted cells
5X Q5 Reaction Buffer	710	410
10 mM dNTPs	71	41
100 $\mu$ M Forward Primer	17.75	10.25
100 $\mu$ M Reverse Primer	17.75	10.25
Extracted DNA	1130 (142 $\mu$ g)	770 (81.6 $\mu$ g)
Q5 High-Fidelity DNA Polymerase	35.5	20.5
5X Q5 High GC Enhancer <sup>a</sup>	710	410
Nuclease-free water	fill to 3550	fill to 2050

<sup>a</sup>Since template DNA is poor in GC base pairs, GC enhancer is needed to ensure balanced proportion of base pairs in the sequencing run; dNTP- deoxyribonucleotide triphosphate.

The reactions were transferred to a thermocycler and processed according to Table 5.3.

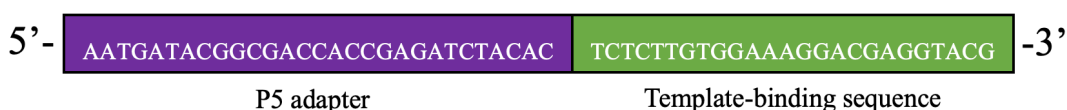
**Table 5.3. Thermocycler conditions for PCR1.**

Step	Temperature (°C)	Time (s)
Initial denaturation	98	30
18 cycles	98, 64, 72	10, 20, 20
Final extension	72	120
Hold	4	∞

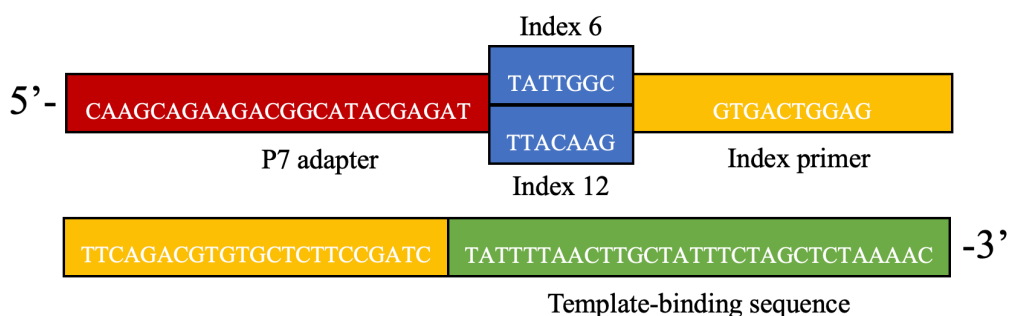
The reactions were pooled into fresh 15 mL tubes. 0.5 mL of library and sorted cell DNA was purified with QIAquick® PCR Purification kit (QIAGEN, Germany) and eluted in 50 µL dH<sub>2</sub>O. The eluate was quantified by NanoDrop™ 1000 spectrophotometer (Thermo Fisher Scientific, UK), and the samples diluted to 100 ng µL<sup>-1</sup>.

A secondary PCR (PCR2) was performed to further amplify the pooled amplicons and prepare the sample for sequencing. Sequencing adapters (P5/P7) were added to both ends of the DNA template to enable it to hybridise to the surface of the flow cell (Table 5.4). Library DNA and sorted cell DNA was tagged with Index 6 and Index 12, respectively, to facilitate their recognition by the DNA sequencer. The following primers were used:

Forward PCR2 primer (Sigma, UK):



Reverse PCR2 primer (Sigma, UK):





**Table 5.4. PCR2 reaction components.**

Component	Quantity ( $\mu\text{L}$ )	
	Library	Sorted cells
5X Q5 Reaction Buffer	20	20
10 mM dNTPs	2	2
100 $\mu\text{M}$ Forward Primer	0.5	0.5
100 $\mu\text{M}$ Reverse Primer (Index 6 for library and Index 12 for sorted cells)	0.5	0.5
PCR1 product	2 (200 ng)	2 (200 ng)
Q5 High-Fidelity DNA Polymerase	1	1
5X Q5 High GC Enhancer <sup>a</sup>	20	20
Nuclease-free water	fill to 100	fill to 100

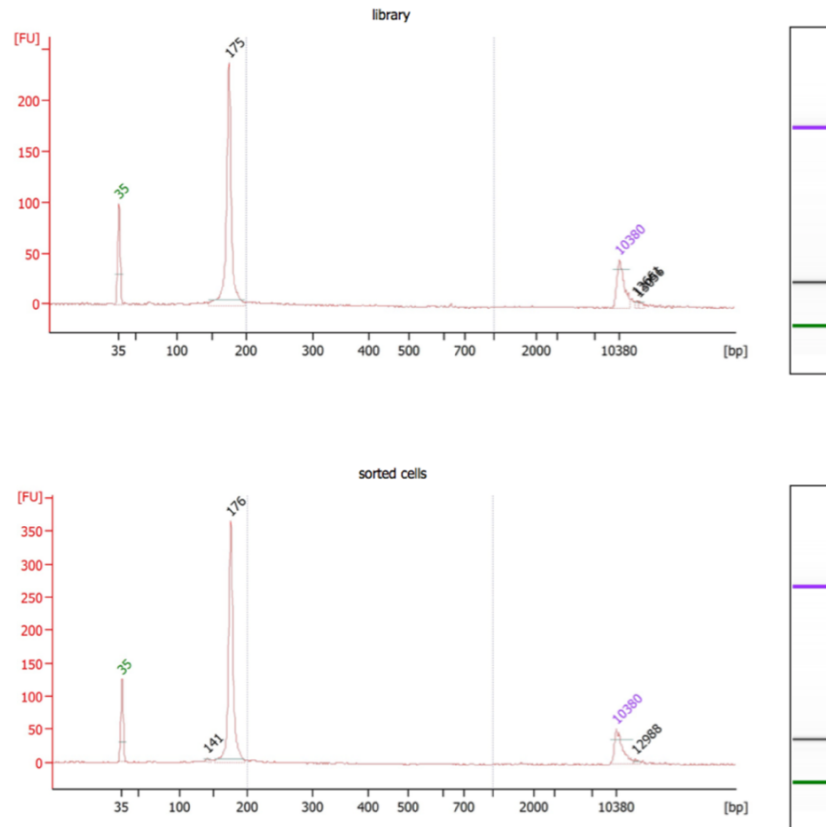
<sup>a</sup>Since template DNA is poor in GC base pairs, GC enhancer is needed to ensure balanced proportion of base pairs in the sequencing run; dNTP- deoxyribonucleotide triphosphate

The reaction was transferred to a thermocycler and processed according to Table 5.5.

**Table 5.5. Thermocycler conditions for PCR2.**

Step	Temperature ( $^{\circ}\text{C}$ )	Time (s)
Initial denaturation	98	30
24 cycles	98, 64, 72	10, 20, 20
Final extension	72	120
Hold	4	$\infty$

The reaction was purified with QIAquick<sup>®</sup> PCR purification kit (QIAGEN, Germany) and eluted in 32  $\mu\text{L}$  dH<sub>2</sub>O. The eluate was analysed on Agilent 2100 Bioanalyser, using Agilent High Sensitivity DNA kit (Agilent Technologies, US), according to the manufacturer's instructions (Figure 5.12).



**Figure 5.12. Bioanalyser results for the library and sorted cell DNA samples. The x-axis shows DNA size in base pairs (bp), while y-axis measures DNA fluorescence in fluorescence units (FU). Standards include a 35 bp lower marker (green) and 10,380 bp upper marker (purple). Corresponding gel image for the bioanalyser trace is shown on the right. The average fragment size was 175 and 176 bp for the library and sorted cells, respectively.**

Any remaining low molecular weight contaminants were removed using Agencourt AMPure XP bead purification (Beckman Coulter, US) in a DNA-to-bead ratio of 1:1.6. The product was washed twice in 70% ethanol and eluted with 35  $\mu$ L dH<sub>2</sub>O (only 30  $\mu$ L was recovered to avoid any bead contamination). The final PCR2 product contained the sgRNA sequence, flanked by P5 adapter on 5' end, and P7 adapter and index 6/12 on 3' end. The samples were stored at  $-20$  °C until sequencing.

### 5.3.7 Next-generation sequencing and data analysis

The DNA samples were transferred to UCL Cancer Institute, where sample preparation and sequencing took place under the supervision of Mr Alex McLatchie.

First, the PCR2 products were quantified on Invitrogen Qubit 4 Fluorometer (Thermo-Fisher, US). The DNA concentration of library and sorted cells was 0.354 and 0.342

ng  $\mu\text{L}^{-1}$ , respectively. Using the formula below, with average library size of 175 bp, the results translated to 3.12 and 3.01 nM, respectively.

$$\frac{\text{DNA concentration in ng } \mu\text{L}^{-1}}{660 \text{ g mol}^{-1} \cdot \text{average library size in bp}} \cdot 10^6 = \text{DNA concentration in nM}$$

The samples were sequenced on an Illumina MiSeq instrument, using the single-end sequencing mode. Briefly, the samples were diluted to 2 nM in  $\text{H}_2\text{O}$  (5  $\mu\text{L}$  total volume each) then pooled. The pooled sample was denatured with 10  $\mu\text{L}$  of 0.2 N sodium hydroxide solution, centrifuged at 280 g for 1 minute, then incubated at room temperature for 5 minutes. Pre-chilled hybridization buffer 1 (HT1, 980  $\mu\text{L}$ ) was added to make up a 10 pM stock solution, which was further diluted with HT1 to 6 pM final concentration.

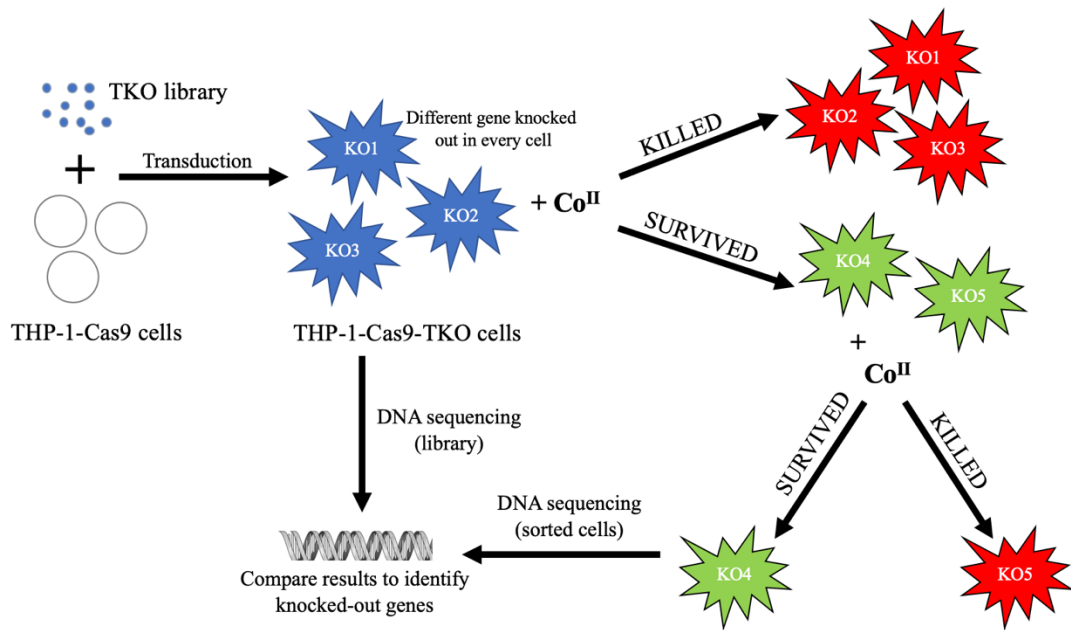
PhiX Control v3 (Illumina, US) is a concentrated Illumina library (10 nM in 10  $\mu\text{L}$ ) derived from a well-characterised bacteriophage genome. It has an average size of 500 bp with a balanced base composition (~45% GC and ~55% AT), and can serve as a sequencing control in NGS. PhiX was diluted to 10 pM with HT-1, before 0.2 N NaOH was added to denature the library. The mixture was further diluted to 6 pM and added at 5% to the pooled library.

The following custom primer (Eurofins Scientific, Belgium) was used to read the sequence: 5'-ACACTCTCTTGTGGAAAGGACGAGGTACCG-3'

The primer was resuspended in 482  $\mu\text{L}$  DNA-ase RNA-ase-free water, to make up a working concentration of 100 pmol  $\mu\text{L}^{-1}$ .

The library mix, and 3  $\mu\text{L}$  of the custom primer, were loaded onto the reagent cartridge in the designated reservoirs, and a 27-cycle run was set up. The raw sequencing data was demultiplexed (sorted to separate reads tagged with different indices) with MiSeq Reporter software (Illumina), and converted to the universally used .fastq format. FastQ files were quality checked using the FastQC tool, before they were analysed with the open-access bioinformatics pipeline located at GenePattern. The software uses MAGECK algorithm [432] to identify positively selected genes.

### 5.3.8 Study design flowchart



**Figure 5.13.** Flowchart outlining the principles of the CRISPR/Cas9 cobalt toxicity assay.

## 5.4 RESULTS

Index 12 (sorted cells) generated 1.2 million reads, of which 87575 mapped to the TKO CRISPR guide reference library. Genes corresponding to the 10 most highly overrepresented sequences are listed in Table 5.6.

3362, 270 and 10 of the depleted genes had one, two or three independent guides mapping to them, respectively. The latter are listed in Table 5.7.

**Table 5.6.** The ten most highly overrepresented genes and the protein products they encode.

Gene	Count	Product	Role
INS	1154	Insulin	Regulates blood glucose level
ENTPD2	202	Ectonucleoside triphosphate diphosphohydrolase 2	Regulates purinergic neurotransmission
LAMP1	171	Lysosome-associated membrane glycoprotein 1	Receptor
IQGAP2	170	Ras GTP-ase-activating-like protein	Binds calmodulin

UBTD1	166	Ubiquitin domain-containing protein 1	May be involved in regulation of cell senescence
C7orf65	165	Uncharacterised protein	N/A
SPDYA	153	Speedy protein A	Regulates the G1/S phase transition of the cell cycle
MOCOS	147	Molybdenum cofactor sulfurase	Sulfurates the molybdenum cofactor in xanthine dehydrogenase and aldehyde oxidase
WDYHV1	147	Protein N-terminal glutamine amidohydrolase	Involved in protein degradation
ARL3	146	ADP-ribosylation factor-like protein 3	Involved in cellular transport

**Table 5.7. Depleted genes targeted by three independent guides.**

<b>Gene</b>	<b>Count</b>	<b>Product</b>	<b>Role</b>
DDX60L	137	Probable ATP-dependent RNA helicase DDX60-like	Mediates ATP binding, ATP hydrolysis, nucleic acid binding and RNA unwinding
HBE1	137	Haemoglobin subunit epsilon	Beta-type chain of early embryonic haemoglobin
SFRP4	122	Secreted frizzled-related protein 4	Involved in regulation of cell growth and differentiation in specific cell types
FIGF	75	Vascular endothelial growth factor D	Involved in endothelial cell growth, angiogenesis and lymphangiogenesis
ZNF12	72	Zinc finger protein 12	Transcriptional repressor
MYL2	53	Myosin regulatory light chain 2	Contractile protein with a role in heart development and function
PHYHIPL	49	Phytanoyl-CoA 2-hydroxylase interacting protein-like	Enzyme with a likely role in central nervous system development
CDKN1A	28	Cyclin-dependent kinase inhibitor-1	May be involved in inhibition of cellular proliferation in response to DNA damage
POU3F4	20	POU domain, class 3, transcription factor 4	Neural transcription factor involved in inner ear development

HSDL1	19	Inactive hydroxysteroid dehydrogenase-like protein 1	Might be involved in oxidation-reduction processes
-------	----	--	--

## 5.5 DISCUSSION

The application of CRISPR/Cas9 technology to induce targeted, genome-wide DNA mutations has made it possible to study the effects of systematic gene knockout in human and animal cells. The mutated cell pool can be exposed to a toxin of interest to identify host factors that modulate the adverse effects [428]. In the present study, TKO-transduced THP-1 cells were subjected to a lethal dose of cobalt ions, and the sgRNAs of the surviving cells were sequenced, in order to identify depleted genes.

The TKO CRISPR library has 12 independent sgRNAs targeting every gene. Such an approach is intended to overcome the noise introduced by variable reagent effectiveness, and allow for fine-scale analysis of gene function [433]. 92% of the pinpointed genes, including the highest counting ones, such as INS and ENTPD2, were each targeted by one type of sgRNA. There are several possible explanations for this phenomenon. “True” susceptibility genes could have been hit by only one of the guides, sorted cells could have had multiple lentiviral integrations, or they could have survived the cobalt insult by chance (without a resistant phenotype) [428]. It could also be that the sgRNAs in this group were derived from PCR contamination.

Gene candidates that are expressed in THP-1, and have two or more independent sgRNA mapping to them, are less likely to have arisen by chance [428]. Considering the large proportion of likely false-positive results, we applied an even more stringent cut-off of three independent sgRNAs, and identified 10 “genes of interest”. It was interesting to see that DMT-1 channel (encoded by SLC11A2) and P2X7 receptor (encoded by P2RX7), which are both involved in Co<sup>II</sup> entry into cells, were not significantly depleted in the surviving cells. This suggests that there are multiple ways in which cobalt ions can cross cell membrane, and knockout of one type of ion channel is not enough to prevent cobalt entry into the cell and confer resistance to the cytotoxic effect.

Even though the TKO library has been designed to allow only one off-target “hit”, the occurrence of unintended effects cannot be completely excluded. Recent studies have shown evidence of off-target cleavages using the CRISPR-Cas9 system in mammalian

cells [424]. Off-target activity can happen due to imperfect hybridisation between guide RNA and DNA template, which prevents the enzyme from cleaving at the desired genomic locus, or prompts it to cleave at an undesired site. The former situation can arise if there are mutations in the gene of interest. Human cell lines have a homogeneous genetic background, which minimises the degree of variability in the cell phenotype. Oncogenic cell lines, such as THP-1, had to have undergone significant number of mutations to become immortalised. Moreover, the cellular response to Cas9 delivery and activity is unknown, and might induce mutagenesis. Specificity of Cas9 in human cells, and the mutations that cause off-target DNA cleavage, or abolish on-target cleavage, are not well-characterised in mammalian cells [424].

### 5.5.1 Study limitations

Millimolar cobalt ion concentration was necessary to ensure complete death of non-transduced cells, as basis for the CRISP/Cas9 knock-out screen. Studies have shown that cobalt levels in the fluid surrounding MoM joints can range from less than 0.04 mM (well-functioning implants) to 6 mM (malpositioned or failing implants), with lower content in the blood and distant tissues [360]. The majority of MoM patients exhibit blood cobalt concentrations below 2  $\mu$ M (Figure 2.11), while those with third-body wear following ceramic fracture can reach up to 1.6 mM [101]. It follows that  $\text{Co}^{\text{II}}$  concentration used in the killing assay (4 mM) was comparable to synovial content in some malfunctioning MoM joints, but 2-3 orders of magnitude higher than typical blood cobalt readings in THA patients. It has been proposed that the lack of complex physiological processes, and interaction with other cell types, means that *in vitro* cultures of isolated cell lines require higher concentrations of a toxic agent to produce the effects seen *in vivo* [434].

Subjecting THP-1-Cas9 and THP-1-Cas9-TKO cells to a deadly  $\text{Co}^{\text{II}}$  concentration killed the entire control population while leaving a small number of survivors in the TKO-transduced population. It is likely that this surviving population contained sgRNAs that mapped to “true” cobalt susceptibility genes, but also a number of false positives. For this reason, it is important that the sorted cells are subsequently expanded and the killing assay is repeated at least once more. We were unable to do so as the sorted cells died after 48 hours of incubation. It is possible that the extremely high cobalt concentration used in the screen induced functional alterations in the surviving cells, eventually leading to their death. The DNA extracted from surviving

cells straight after sorting might also be altered in some way, potentially biasing the NGS results.

## **5.6 CONCLUSION**

The results demonstrate the potential for efficient loss-of-function screening using the CRISPR/Cas9-based approach in the investigation of genetic differences underlying susceptibility to cobalt-induced cell death. Our feasibility study identified several “genes of interest”, which now require validation in targeted knock-out screens (for discussion of future work see Chapter 7). Further work is required to ascertain whether results obtained with millimolar concentration of  $\text{Co}^{\text{II}}$  can be extrapolated to



# Chapter 6

## **Defining a reference range for blood and plasma titanium in THA patients**

The work presented in this chapter has been published.\*

\*Swiatkowska I, Martin, N, Henckel, J, Apthorp, A, Hamshere, J, Hart A.J. Blood and plasma titanium levels associated with well-functioning hip implants. *Journal of Trace Metals in Medicine and Biology* 57 (2020) 9-17.



## 6.1 INTRODUCTION

Titanium displays an enhanced capacity for bone integration, which makes it a popular material choice for uncemented joint arthroplasties. The rising popularity of uncemented designs is associated with a growing use of titanium in implant manufacture. Despite the metal's perceived corrosion resistance, titanium-based prostheses were shown to biodegrade following implantation, leading to elevated circulating titanium levels (Table 2.7). Since titanium is relatively slowly transported in the body, a modest increase in systemic concentration likely reflects a massive release of titanium into the local joint space.

In the case of cobalt and chromium, a blood level of up to  $2 \mu\text{g L}^{-1}$  is thought to indicate a well-functioning MoM prosthesis, while concentrations exceeding  $7 \mu\text{g L}^{-1}$  suggest an increased risk of local toxicity and implant failure [328] (see Section 2.8). Elevated blood titanium content could also potentially serve as a biomarker for wear or corrosion, and inform on the risk of local adverse effects and eventual revision surgery [248,336,346,435]. Despite an increasing clinical interest in this biomarker, and growing use of titanium in orthopaedics, normal and pathological ranges for titanium levels remain to be defined. This is partly due to technical challenges relating to the measurement of titanium in biological samples (see Section 2.7.2).

### 6.1.1 Motivation

Several groups have reported blood/serum titanium levels associated with different types of well-functioning and malfunctioning prostheses [224,246,292,293,312,339,343,347,436]. Aside from small sample size, the analytical techniques used in most of these studies- namely GF AAS and quadrupole ICP-MS- have since been shown to lack the required level of accuracy and precision. High resolution ICP-MS, as one of the most sensitive and versatile techniques available for trace metal analysis, is perfectly suited to the measurement of minute levels of titanium in complex biological samples. An updated laboratory reference range, derived from high resolution ICP-MS analyses, is urgently needed.

### 6.1.2 Aim

To define a reliable upper reference level for blood and plasma titanium in patients with well-functioning titanium-based implants, taking into account as much clinical data as possible.

### 6.1.3 Objectives

1) To assess implant positioning and fixation using radiographs; 2) to assess pain and clinical function using Oxford Hip Score; 3) to measure blood and plasma titanium content on a high resolution ICP-MS.

## 6.2 PATIENTS AND METHODS

Patients who received one type of titanium alloy femoral stem (see Section 6.2.1 for details) between 2007-2014 at a participating institution were identified using the NJR database (n=1036). Inclusion criteria stipulated a unilateral, primary, uncemented CoC hip implant inserted by the same surgeon. The eligible patients (n=199) were contacted, and those willing to take part invited to attend an outpatients appointment. The clinical assessment involved 1) a pelvis X-ray; 2) Oxford Hip Score; 3) UCLA Activity Score; 4) a blood test and 5) a short interview. A complete set of data was obtained for 95 subjects (42 males and 53 females). The underlying diagnoses leading to the primary surgery were OA (98%) or developmental hip dysplasia (2%). Patient demographics are summarised in Table 6.1.

**Table 6.1. Patient demographics.**

	<b>Male (n=42)</b>	<b>Female (n=53)</b>	<b>Overall (n=95)</b>	<b>Gender difference?</b>
<b>Age (years)</b>				
<b>Median</b>	73	71	71	No (p=0.44) <sup>a</sup>
<b>IQR</b>	66-77	67-75	67-76	
<b>Implant time in situ (months)</b>				
<b>Median</b>	92	107	102	Yes (p=0.009) <sup>b</sup>
<b>IQR</b>	81-111	90-121	86-118	

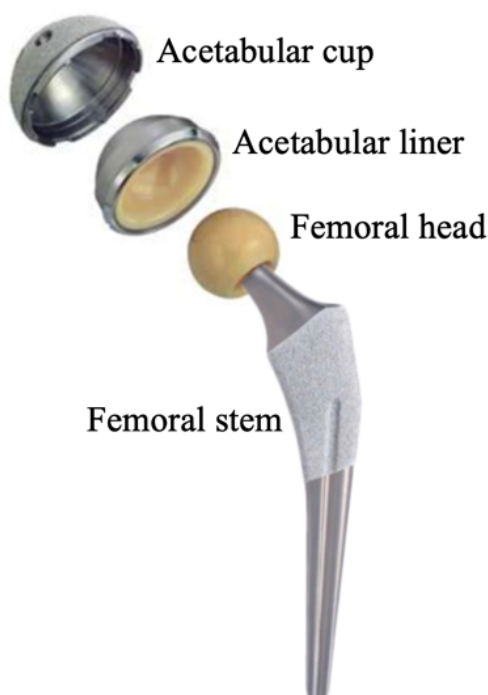
<sup>a</sup>Student's T-test, <sup>b</sup>Mann-Whitney U test; IQR-interquartile range (25<sup>th</sup> percentile-75<sup>th</sup> percentile).

### 6.2.1 Implants

All 95 participants received the same implant type. The articulation comprised a V40  $\varnothing$ 32 mm alumina femoral head, and a Trident<sup>®</sup> titanium-backed alumina insert. Trident<sup>®</sup> PSL commercially-pure titanium acetabular cup and a TMZF Accolade<sup>®</sup> I femoral stem, which were both inserted without cement, completed the design (Figure 6.1). TMZF stems are no longer used commercially due to high failure rates when combined with CoCr femoral heads [25].

All the components were manufactured by Stryker Orthopaedics (Mahwah, NJ). In several cases, the acetabular component was fixed to the pelvis with a varying number of Ti-6Al-4V screws.

11 (12%) participants had CoCrMo knee replacement implants in addition to the hip implant. Since these did not contain titanium, the patients were included in the study.



**Figure 6.1. The implant design featured in the current study. Reproduced from Journal of Trace Elements in Medicine and Biology [437].**

### 6.2.2 Radiographs

Standardized anteroposterior radiographs were taken by Ms Jane Hamshere at The Horder Centre, using the Proteus X-ray machine (GE Healthcare).

The films were pseudo-anonymised and reviewed by two observers (senior orthopaedic surgeons) for evidence of poor implant positioning and signs of acetabular cup/femoral stem loosening. Parameters, such as acetabular cup abduction/anteversion angle and femoral offset, do not influence blood titanium levels [304,438], so they were not quantified in the current study.

### **6.2.3 Oxford Hip Score**

The participants were asked to complete the Oxford Hip Score (OHS) to assess pain and the ease with which they can perform daily activities [439] (Figure 6.2).

The OHS has been developed and validated specifically to assess hip function and pain in patients prior to the THA, and has since been extended to the assessment of surgery outcomes [440,441]. The original version of the questionnaire, developed in 1996 by Dawson and co-workers [442], consisted of 12 items graded from 1 (no symptoms) through to 5 (most severe symptoms). Individual question scores were summed to give an overall score of between 12 to 60, with 12 being the best possible outcome. This scoring system was found unintuitive by surgeons, and was later replaced by a new one, whereby answers to each question range from 0 (worst outcome) to 4 (best outcome). A total score  $\geq 42$  is considered excellent, 41-34 good, 33-27 fair, while  $\leq 26$  indicates poor implant function [443]. Participants with excellent and good total scores ( $\geq 34$ ) were included in the study, while those with poor scores ( $\leq 26$ ) were excluded.

The OHS is short, reproducible, sensitive to clinically important changes, and widely used to assess hip function and pain in THA patients. Despite having been designed as a site-specific measure, responses to certain questions can be influenced by existing co-morbidities, such as pain and/or disability at other joints [444]. For this reason, participants with fair scores (33-27), who volunteered the existence of a co-morbidity affecting the score, were also included in the current study.

During the past 4 weeks...	
<p><b>1. How would you describe the pain you usually have in your hip?</b></p> <p>4) None 3) Very mild 2) Mild 1) Moderate 0) Severe</p>	<input type="text"/>
<p><b>2. Have you been troubled by pain from your hip in bed at night?</b></p> <p>4) No nights 3) Only 1 or 2 nights 2) Some nights 1) Most nights 0) Every night</p>	<input type="text"/>
<p><b>3. Have you had any sudden, severe pain-' shooting', 'stabbing', or 'spasms' from your affected hip?</b></p> <p>4) No days 3) Only 1 or 2 days 2) Some days 1) Most days 0) Every day</p>	<input type="text"/>
<p><b>4. Have you been limping when walking because of your hip?</b></p> <p>4) Rarely/never 3) Sometimes or just at first 2) Often, not just at first 1) Most of the time 0) All of the time</p>	<input type="text"/>
<p><b>5. For how long have you been able to walk before the pain in your hip becomes severe (with or without a walking aid)?</b></p> <p>4) No pain for 30 minutes or more. 3) 16 to 30 minutes 2) 5 to 15 minutes 1) Around the house only 0) Not at all</p>	<input type="text"/>
<p><b>6. Have you been able to climb a flight of stairs?</b></p> <p>4) Yes, easily 3) With little difficulty 2) With moderate difficulty 1) With extreme difficulty 0) No, impossible</p>	<input type="text"/>
<p><b>7. Have you been able to put on a pair of socks, stockings or tights?</b></p> <p>4) Yes, easily 3) With little difficulty 2) With moderate difficulty 1) With extreme difficulty 0) No, impossible</p>	<input type="text"/>
<p><b>8. After a meal (sat at a table), how painful has it been for you to stand up from a chair because of your hip?</b></p> <p>4) Not at all painful 3) Slightly painful 2) Moderately painful 1) Very painful 0) Unbearable</p>	<input type="text"/>
<p><b>9. Have you had any trouble getting in and out of a car or using public transportation because of your hip?</b></p> <p>4) No trouble at all 3) Very little trouble 2) Moderate trouble 1) Extreme difficulty 0) Impossible to do</p>	<input type="text"/>
<p><b>10. Have you had any trouble with washing and drying yourself (all over) because of your hip?</b></p> <p>4) No trouble at all 3) Very little trouble 2) Moderate trouble 1) Extreme difficulty 0) Impossible to do</p>	<input type="text"/>
<p><b>11. Could you do the household shopping on your own?</b></p> <p>4) Yes, easily 3) With little difficulty 2) With moderate difficulty 1) With extreme difficulty 0) No, impossible</p>	<input type="text"/>
<p><b>12. How much has pain from your hip interfered with your usual work, including housework?</b></p> <p>4) Not at all 3) A little bit 2) Moderately 1) Greatly 0) Totally</p>	<input type="text"/>
<p><b>TOTAL =        /    48</b></p>	

Figure 6.2. Oxford Hip Score.

### 6.2.4 UCLA activity score

Since increased physical activity has the potential to accelerate implant wear and raise blood metal levels [445], the participants were classified using the University of California Los Angeles (UCLA) activity score (Figure 6.3).

**Check the box that best describes your current activity level.**

- 1. Wholly inactive, dependent on others and cannot leave residence
- 2. Mostly inactive or restricted to minimum activities of daily living
- 3. Sometimes participates in mild activities, such as walking, limited housework and limited shopping
- 4. Regularly participates in mild activities
- 5. Sometimes participates in moderate activities, such as swimming, or could do unlimited housework or shopping
- 6. Regularly participates in moderate activities
- 7. Regularly participates in active events, such cycling
- 8. Regularly participates in active events, such as golf or bowling
- 9. Sometimes participates in impact sports, such as jogging, tennis, skiing, acrobatics, ballet, heavy labour or backpacking
- 10. Regularly participates in impact sports

**Figure 6.3. UCLA Activity Score.**

### **6.2.5 Blood sampling and trace element analysis**

Blood was withdrawn from a forearm vein by a certified phlebotomist, using a stainless steel needle surrounded by an inert plastic cannula. In order to minimise any potential contamination from the metal needle, the first 5 mL of blood drawn was used to rinse the system and then discarded. The subsequent 5 mL of blood were collected into royal blue top Vacuette® PREMIUM Trace Elements tubes (Greiner Bio-One International), which were coated with sodium heparin as anticoagulant. It is worth noting that, currently, no blood tubes are certified for titanium, but it is reasonable to assume that trace element tubes are “cleaner” than standard tubes.

The specimens were delivered to the Trace Element Laboratory at the Charing Cross Hospital on collection day, where they were processed and analysed by laboratory technicians under the supervision of Mr Nicholas Martin.

The samples were mixed by inversion and 2.5 mL of whole blood was aliquoted. The remaining 2.5 mL of blood was centrifuged at 2500 RPM for 10 minutes in a bench-



top centrifuge, to separate the plasma. The samples were refrigerated until analysis (typically within 3-7 days of taking the sample). Of note, stability of metal ions is 28 days when the sample is stored at 4°C [446].

Whole blood and plasma samples were quantified for titanium content on an Element 2 high resolution ICP-MS instrument (Thermo Fisher Scientific GmbH, Bremen, Germany), which had a LoD of 0.77  $\mu\text{g L}^{-1}$  for titanium (calculated as 3SD of the blank readings [447]). Two levels of ClinChek Plasma (Recipe, Germany) Internal Quality Control (IQC) and two levels of Custom Whole Blood IQC (UTAK, US) material were included in each batch. To ensure high quality of analysis, the laboratory was enrolled in the Quebec Multielement External Quality Assessment Scheme (QMEQAS) at the time this study was conducted (see Table 6.2 for the results).

**Table 6.2. Results submitted by the laboratory to the QMEQAS, the value assigned by QMEQAS, and the range considered acceptable by QMEQAS. The percentage bias of the submitted results compared to the assigned value is also shown.**

Sample	Assigned Ti concentration ( $\text{nmol L}^{-1}$ )	Submitted Ti concentration ( $\text{nmol L}^{-1}$ )	Acceptable range ( $\text{nmol L}^{-1}$ )	Bias (%)
QM-B-Q1901	207	196	123 - 291	-5.3
QM-B-Q1902	307	319	181 - 433	+3.9
QM-B-Q1903	246	247	143 - 349	+0.4

150  $\mu\text{L}$  of each sample or IQC were dispensed into polystyrene assay tubes with 150  $\mu\text{L}$  of water and 4.5 mL of assay diluent (0.5% (v/v) tetramethylammonium hydroxide (Electronics grade, Alpha Aesar, US) and 0.005% (v/v) Triton X-100 (Romil, UK) with 2.5  $\mu\text{g L}^{-1}$  gallium (Alpha Aesar, US) as internal standard).

Calibration standards were prepared by dilution from a custom stock solution (Qmx Laboratories Limited, Thaxted, UK) with a titanium concentration traceable to NIST SRM 3162a Lot 130925. The standard concentrations were: 0.00, 1.00, 4.00, 9.99, 39.96, 99.90 and 249.75  $\mu\text{g L}^{-1}$ . Whole blood and serum/plasma matrix-matched calibrations were prepared by dispensing 150  $\mu\text{L}$  of each standard into polystyrene assay tubes with 4.5 mL of assay diluent and 150  $\mu\text{L}$  of either defibrinated horse blood (TSC Biosciences, Buckingham, UK) or foetal bovine serum (Sigma-Aldrich, UK).

The diluted samples, calibration standards and IQC were sequentially sampled using an ESI-SC FAST autosampler (Elemental Scientific, US) and introduced to the high resolution ICP-MS with a PTFE nebulizer (Elemental Scientific, US) and cyclonic spray chamber (Thermo Scientific, US). The counts per second (cps) data for Ti<sup>47</sup> were normalised to Ga<sup>71</sup> cps, and a calibration curve was plotted using ordinary linear regression in Microsoft Excel. The regression equation was applied to the normalised Ti<sup>47</sup> cps for each sample and IQC, to give the titanium concentration. See Table 6.3 for the ICP-MS settings used for each isotope.

Two blank royal blue top Vacuette<sup>®</sup> PREMIUM Trace Elements tubes were run to estimate the background titanium concentration. The mean blank result (0.6 µg L<sup>-1</sup>) was subtracted from all sample measurements.

**Table 6.3. Isotopes measured and ICP-MS settings used.**

<b>Isotope</b>	Ti47	Ga71
<b>Mass range</b>	46.948 - 46.954	70.921 - 70.928
<b>Mass window</b>	50	40
<b>Settling time</b>	0.300	0.050
<b>Sample time</b>	0.7500	0.0500
<b>Samples per peak</b>	25	20
<b>Search window</b>	50	40
<b>Integration window</b>	50	40
<b>Scan type</b>	EScan	EScan
<b>Resolution mode</b>	Medium	Medium
<b>Runs</b>	4	4
<b>Passes</b>	1	1

### 6.2.6 Statistical analysis

Before statistical tests were performed, the normality of the data was evaluated (Shapiro-Wilk test and inspection of histograms and boxplots). The results revealed

that age was the only normally-distributed variable in the dataset. Based on this, the independent samples T-test was used to assess gender differences in age, while Mann-Whitney U test was used to assess gender differences in implant time *in situ*, OHS, activity score and titanium levels. A Spearman's correlation was ran to determine the influence of age, follow-up time, OHS and activity score on titanium levels, and to correlate the titanium content of blood and plasma.

IBM SPSS (version 25) was employed for all statistical analyses, with p values<0.05 considered statistically significant. All graphs and charts were produced in SPSS.

### 6.2.7 Study design flowchart

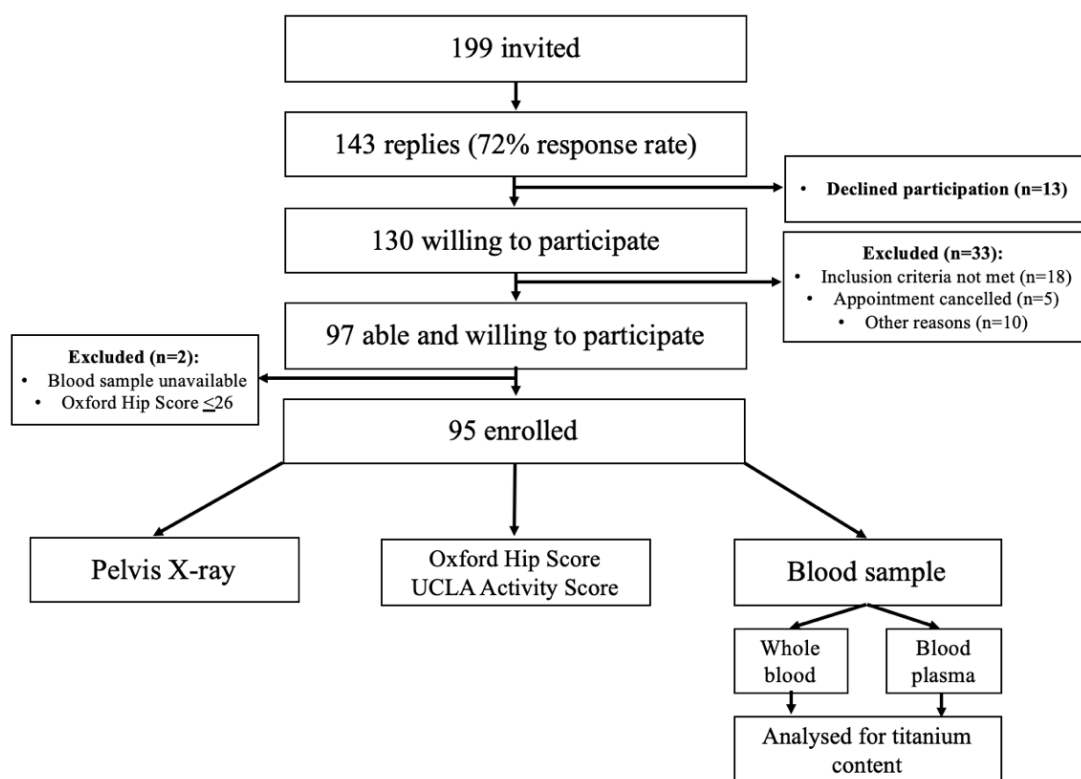


Figure 6.4. Flowchart outlining participant enrolment and clinical assessment. Reproduced from *Journal of Trace Elements in Medicine and Biology* [437].

## 6.3 RESULTS

Study results are summarised in Table 6.4.

**Table 6.4. Summary of study results.**

	<b>Male (n=42)</b>	<b>Female (n=53)</b>	<b>Overall</b>	<b>Gender difference?</b>
<b>Oxford Hip Score (48 being the best possible score)</b>				
<b>Median</b>	46	47	47	No (p=0.22) <sup>a</sup>
<b>IQR</b>	43-48	45-48	45-48	
<b>UCLA activity score (10 being the most physically active)</b>				
<b>Median</b>	7	6	6	No (p=0.21) <sup>a</sup>
<b>IQR</b>	5-8	6-7	6-8	
<b>Blood titanium (<math>\mu\text{g L}^{-1}</math>)</b>				
<b>Median</b>	1.20	1.20	1.20	No (p=0.69) <sup>a</sup>
<b>IQR</b>	1.00-1.50	1.10-1.60	1.00-1.50	
<b>Plasma titanium (<math>\mu\text{g L}^{-1}</math>)</b>				
<b>Median</b>	1.70	1.70	1.70	No (p=0.36) <sup>a</sup>
<b>IQR</b>	1.38-2.13	1.55-2.15	1.40-2.10	

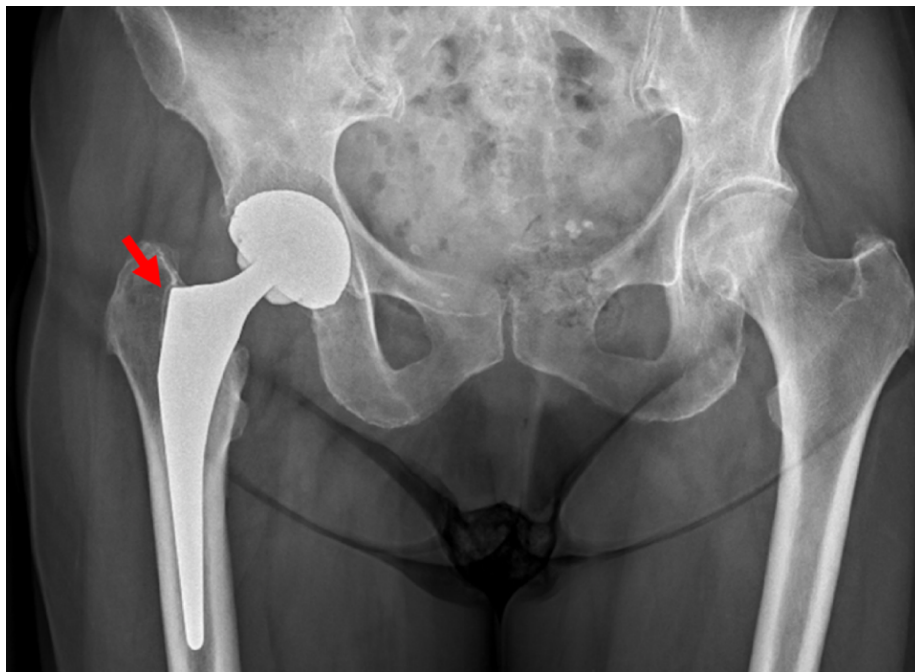
<sup>a</sup>Mann-Whitney U test; IQR-interquartile range (25<sup>th</sup> percentile-75<sup>th</sup> percentile).

### **6.3.1 Radiographs**

Radiological inspection revealed that all the hip implants were well-positioned, with no signs of cup loosening (Figure 6.5). Two femoral stems (2%) were radiologically loose, but clinically asymptomatic (Figure 6.6).



**Figure 6.5.** A representative anteroposterior radiographs from the current series, showing a well-fixed hip implant. Reproduced from *Journal of Trace Elements in Medicine and Biology* [437].



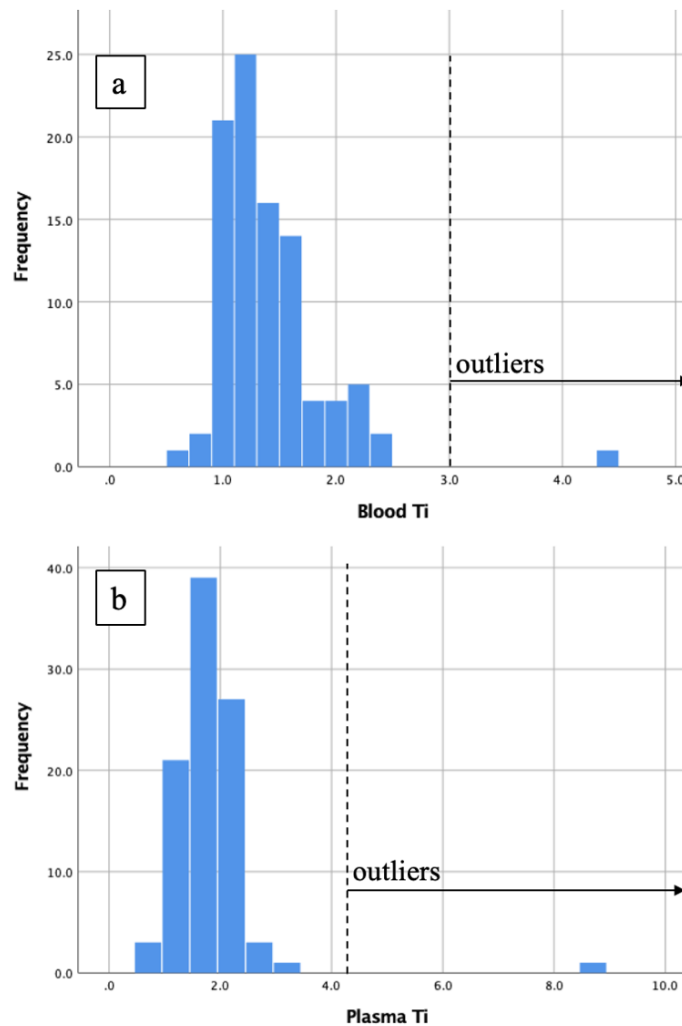
**Figure 6.6.** A radiologically loose stem. The arrow shows a radiolucent line indicative of bone loss at the bone-stem interface. Reproduced from *Journal of Trace Elements in Medicine and Biology* [437].

### 6.3.2 OHS

According to the OHS, 84 (88%) patients had excellent, and 8 patients (8%) had good hip function. The remaining 3 participants reporting fair scores (range 28-32) volunteered the existence of co-morbidities (severe arthritis in other joints or spinal stenosis) that affected the outcome. One patient with unexplained pain in the replaced hip, and OHS score of 16, was excluded from the study.

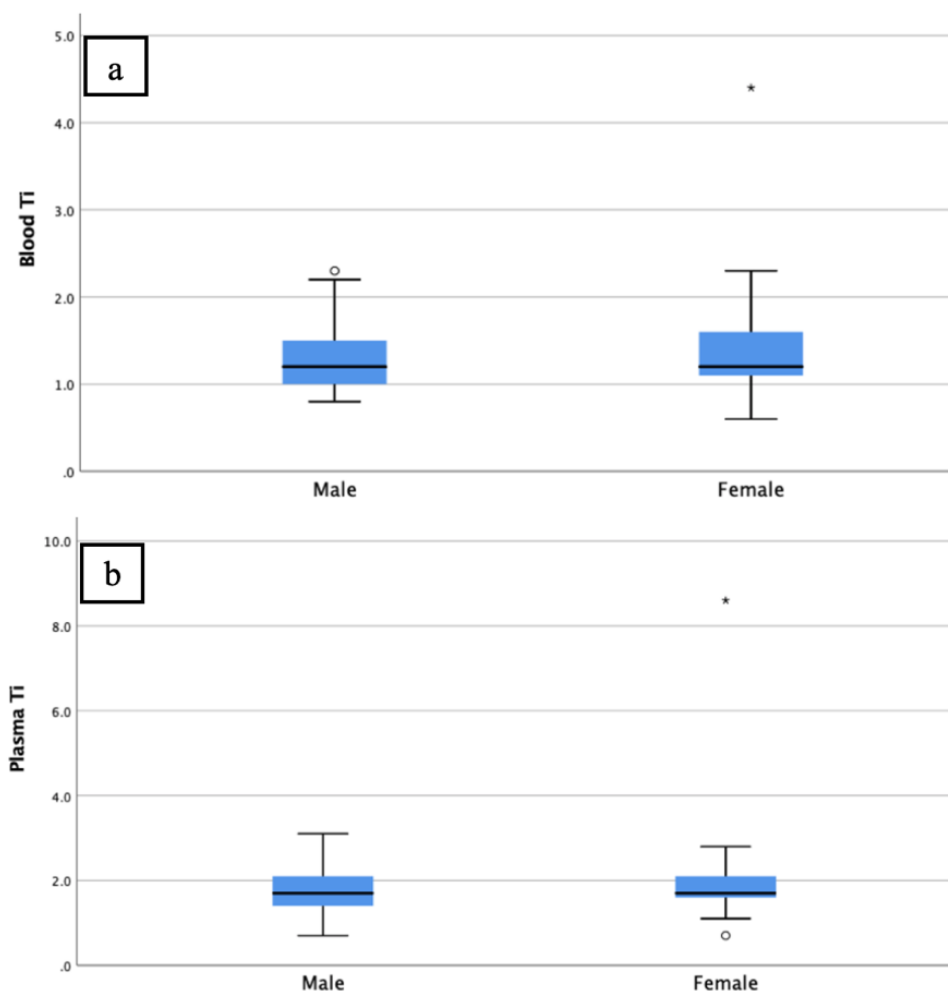
### 6.3.3 Blood and plasma titanium levels

Blood and plasma titanium measurements were non-normally distributed, with one outlier (value larger than 3IQR from the 75<sup>th</sup> percentile), which was included in the statistical analysis. The spread of data is shown in Figure 6.7.

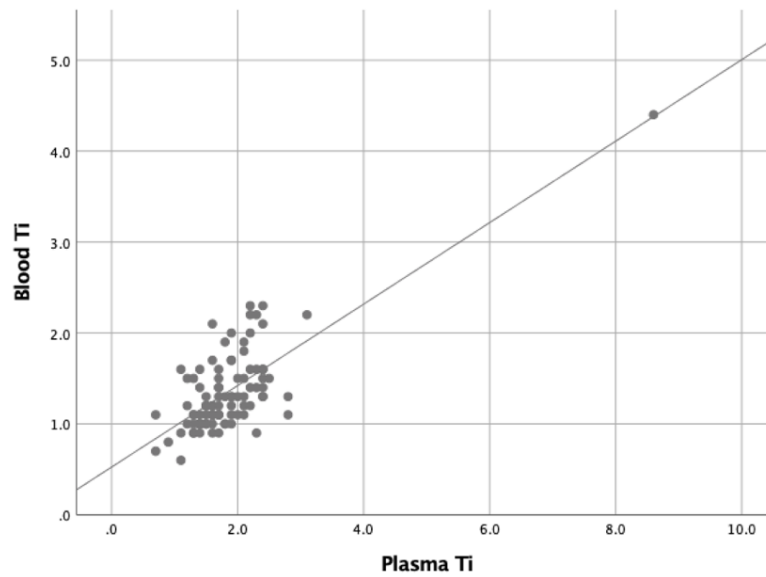


**Figure 6.7. Histograms showing the spread of a) blood and b) plasma titanium measurements in the current series, with the 75<sup>th</sup> percentile+ 3IQR level marked. Reproduced from Journal of Trace Elements in Medicine and Biology [437].**

The upper normal titanium level (95<sup>th</sup> percentile) was 2.20 and 2.56  $\mu\text{g L}^{-1}$  in whole blood and plasma, respectively. Even though there was a significant difference in the follow-up time between males and females, blood and plasma titanium did not differ between the two groups (Figure 6.8). Titanium levels in the blood and plasma were positively correlated ( $r_s=0.571$ ;  $p<0.0001$ ) (Figure 6.9).

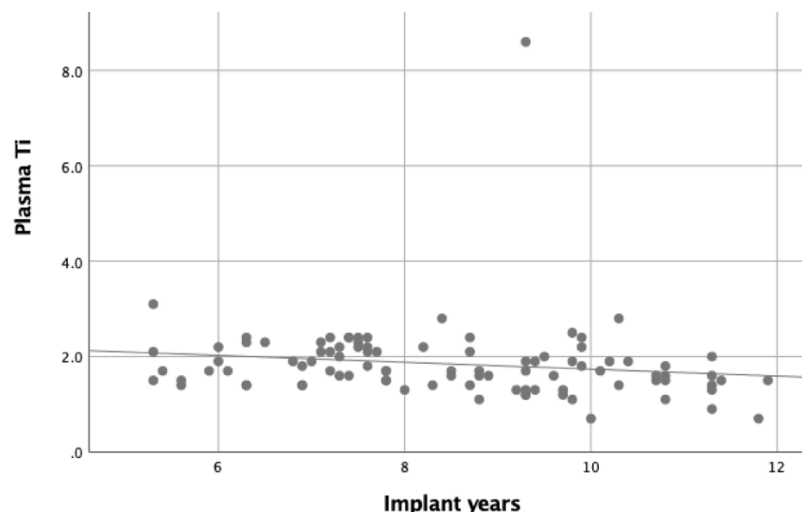


**Figure 6.8.** Box plots of titanium concentration in a) blood and b) plasma of study participants. The boundaries of the box represent the 25<sup>th</sup> and 75<sup>th</sup> percentile, with the median line inside the box. The whiskers extend to maximum and minimum values in each data set. Outliers (values more than 1.5IQR from the end of the box) are identified as open circles, while extreme outliers (values more than 3IQR from the end of the box) are denoted as asterisks. Reproduced from *Journal of Trace Elements in Medicine and Biology* [437].



**Figure 6.9.** Scatter plot of plasma *versus* blood titanium, showing a moderately strong, positive correlation between the two ( $R^2= 0.58$ ;  $p<0.0001$ ). Reproduced from *Journal of Trace Elements in Medicine and Biology* [437].

No significant correlations between blood titanium and age ( $r_s=0.056$ ;  $p=0.59$ ), OHS ( $r_s=-0.01$ ;  $p=0.92$ ), UCLA activity score ( $r_s= -0.012$ ;  $p=0.91$ ) or implant years *in situ* ( $r_s=-0.151$ ;  $p=0.14$ ) were detected. There were no significant correlations between plasma titanium and age ( $r_s=0.077$ ;  $p=0.46$ ), OHS ( $r_s= -0.058$ ;  $p=0.58$ ) or activity score ( $r_s=-0.033$ ;  $p=0.75$ ), either. There was a weak, negative monotonic association between plasma titanium and implant years *in situ* ( $r_s= -0.313$ ;  $p=0.002$ ) (Figure 6.10).



**Figure 6.10.** Scatter plot showing a weak, negative relationship between plasma titanium and increasing length of follow-up ( $R^2=0.02$ ;  $p=0.002$ ).



## 6.4 DISCUSSION

While there are no official guidelines pertaining to “normal” blood titanium levels in THA patients, several groups have attempted to set “cut-off” values for well-functioning implants. For example, the Mayo Clinic Laboratory recommends that serum titanium between 1-3  $\mu\text{g L}^{-1}$  should be taken as a sign of a prosthetic device in good condition, while concentrations exceeding 10  $\mu\text{g L}^{-1}$  are suggestive of implant wear. These values are based on two small-scale studies (55 and 5 participants) from 1998. Both used GF AAS for trace metal analysis [291,448], which puts the validity of their conclusions into question.

More recently, Jacobs *et al.* [336] suggested that well-functioning, unilateral hip implants should correspond to serum titanium levels of approximately 4  $\mu\text{g L}^{-1}$ , while levels exceeding 8  $\mu\text{g L}^{-1}$  should prompt further investigation, such as radiological review of implant positioning and fixation. This was in agreement with the work of Savarino and colleagues, who proposed the upper normal reference limit to be 5.13  $\mu\text{g L}^{-1}$  in the medium term (2-7-year follow-up) [449], and 4.5  $\mu\text{g L}^{-1}$  in the long term (10-year follow-up) [293]. Since GF AAS was used for trace metal analysis, these thresholds are likely overestimated. Highlighting this point is the fact that 98% of our plasma titanium measurements fell below the instrumental LoD reported by Savarino *et al.* (2.91  $\mu\text{g L}^{-1}$ ). Analyses employing high resolution ICP-MS, which boasts a much lower LoD than GF AAS, point to lower values, which generally decrease with increasing length of follow-up (Table 2.7).

The mean titanium level in the current series was 1.35  $\mu\text{g L}^{-1}$  in whole blood and 1.85  $\mu\text{g L}^{-1}$  in the plasma, at a mean follow-up of 8.5 years (range 5-12). This is consistent with the work of Sarmiento-Gonzalez *et al.* [246] and Levine *et al.* [247]. The former study investigated 11 patients with titanium-based hip implants, and reported a mean blood level of 1.52  $\mu\text{g L}^{-1}$  at a mean 6.5 years after surgery (range 6-9). The latter group measured serum titanium in 8 patients with well-functioning implants and reported a mean serum titanium level of 1.8  $\mu\text{g L}^{-1}$  9 years after the surgery. The authors added that the plasma titanium content peaked at the 3-year follow-up, before gradually declining until after the 9-year interval. A decreasing tendency of plasma titanium values over time was also detected in the present study, and could reflect excretion of the metal by the kidneys and liver, and/or decreased rate of implant

degradation. It has been suggested that gradual accumulation of titanium debris in local and/or systemic tissue could contribute to the observed trend [248]. The clinical implications of titanium deposition, and chronic low-level exposure to titanium ions, are yet to be established.

Titanium concentration was higher in the plasma compared to whole blood in 85 out of 95 participants (89%). This could be accounted for by the fact that the metal associates with plasma proteins, such as transferrin [450]. Titanium content of blood or plasma was not confounded by age, gender or OHS. Activity level did not seem to influence the systemic titanium load either. Similar observation was made by Vendittoli *et al.* [342]. Since titanium was not present in the articulation, and the implants were well-fixed, it is assumed that majority of the titanium debris originated from passive corrosion of the acetabular cup and/or the femoral stem, rather than from wear [344]. Corrosion, unlike bearing wear, is unlikely to be affected by physical activity, which helps to explain these findings.

#### **6.4.1 Study limitations**

The present study has a number of limitations.

First, pre-operative blood/plasma titanium measurements were unavailable, so that true influence of the hip implant on the systemic titanium load could not be assessed. While it is believed that the prosthesis was the main source of the measured titanium, it is likely that other sources contributed to it. TiO<sub>2</sub> is a common additive found in food and personal care products [239], as well as being present in ambient air (see Section 2.5). High resolution ICP-MS quantifies both ionic and particulate titanium [282], and is unable to discriminate between the two forms of the metal. Because the study was conducted in a hospital, it was difficult to account for the influence of environmental contamination on the results. None of the participants disclosed occupational exposure to titanium, but dietary intake, and the use of titanium-containing products, were impossible to control for. Additionally, we did not account for potential dental implants and fillings, which are commonly made from titanium. Owing to the relatively small surface area, metal debris has rarely been observed around oral implants [451], and it is reasonable to assume that any contribution to the systemic titanium load would have been negligible.

Secondly, participants' kidney function could not be estimated due to the lack of recent creatinine clearance data. Though impaired excretion could lead to retention of certain metals in the body [308], titanium is highly insoluble and tends to accumulate in tissue rather than being excreted in the urine [452,453]. It follows that reduced urinary output is unlikely to influence blood titanium levels to a great extent.

## **6.5 CONCLUSION**

Given the rising demand for hip replacement, and the recent surge in the use of titanium in implant manufacture, postoperative measurement of circulating titanium in THA patients is of increasing clinical interest. Analytical constraints and lack of protocol standardisation have long precluded the validation and incorporation of this potential biomarker into routine patient monitoring.

The current study is the largest investigation of systemic titanium levels in THA patients to date. Large sample size, combined with the clean data set and a state-of-the-art analytical technique, allowed for a reliable upper reference limit for blood ( $2.20 \mu\text{g L}^{-1}$ ) and plasma ( $2.56 \mu\text{g L}^{-1}$ ) titanium to be defined in patients with well-functioning titanium-based hip implants. The range could be used to monitor implant function and guide patient management decisions.



# **Chapter 7**

## **Conclusions and future work**



Every year, 100,000 people undergo hip replacement in the United Kingdom, while worldwide the number is over 2 million. This figure is on the rise due to the ageing of the population. It is predicted that by 2030, hip arthroplasty procedures will reach 4 million per year in the United States alone. Additionally, the surgery is increasingly being offered to younger patients (<60 years old), leading to a longer mean exposure time to metal debris. In addition to local adverse effects, generalised toxicity symptoms, such as cardiomyopathy and neurotoxicity, have been reported in HA patients with highly elevated blood cobalt. A growing number of hip implant recipients, combined with a higher activity level and increased life expectancy, means that the pool of patients at risk of local and systemic toxicity is expanding. For this reason, it is important to recognise not only short-term, but also long-term risks of chronic exposure to implant degradation products, and develop sensitive biomarkers to facilitate early diagnosis and timely revision operation.

The aim of this thesis was to better understand how cobalt, chromium and titanium debris affects the body's organs, and what blood metal levels are related to any toxicity symptoms.

The prevalence of a number of self-reported systemic toxicity symptoms was assessed in hip replacement patients with markedly elevated, or normal, blood cobalt. Despite a number of statistically significant differences between the groups, the results generally fell below clinically significant thresholds, and the patients were well-functioning. While our findings do not support the need for neurological examinations in asymptomatic patients with markedly (but not extremely) elevated blood cobalt, patients with high blood cobalt levels should be questioned about possible systemic health complaints at follow-up visits. Further studies employing formal cardiac, audiometric, ophthalmologic, neuro-cognitive and thyroid testing in this patient population are needed.

Implant debris enters the blood and accumulates in vital organs, where it might cause toxicity. The oxidation state of the metal deposits is an important determinant of their biological effects. Our finding of a highly oxidised chromium species in *ex vivo* samples of heart, liver and spleen tissue from TJA donors could mean that oxidation of Cr<sup>III</sup> to the hexavalent form can occur. It is important to stress that our study involved cadaveric tissue, and it is not known if the findings can be extrapolated to the *in vivo* situation. Larger studies involving biopsy specimens are warranted.

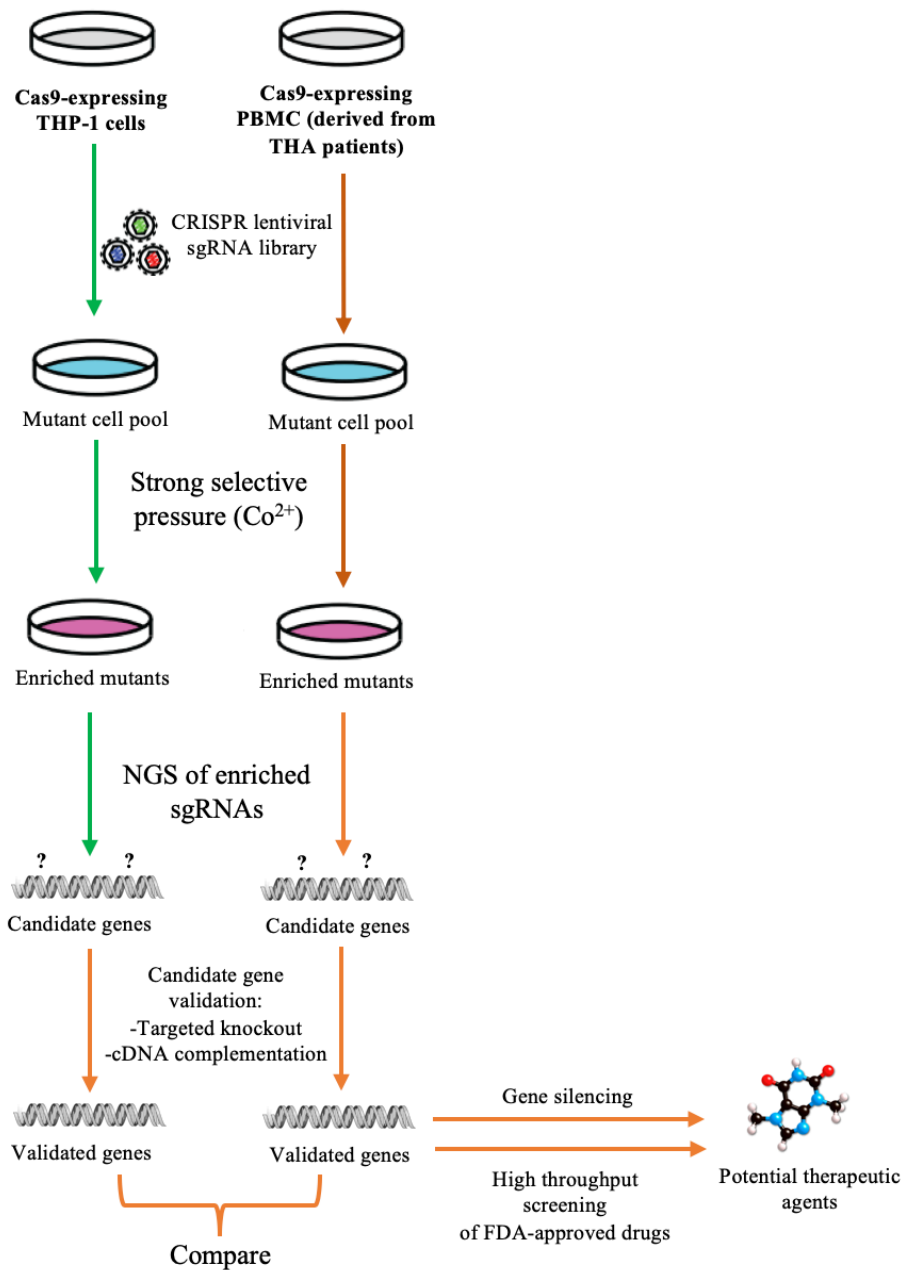
Genetic differences might underlie the greater susceptibility of some patients to cobalt-induced toxicity. For the first time, CRISPR/Cas9 gene editing technology was employed to identify cobalt susceptible genes, using THP-1 cell line as a model of human monocytes. Several “genes of interest” were pinpointed, which now require validation.

Koike-Yusa *et al.* [428] validated their candidate genes by constructing 4-5 sgRNA expression vectors for each gene, and testing them individually to see whether they could give rise to resistant cells. If cells transfected with a given sgRNA displayed sensitivity to the toxin similar to that of the wild-type cells, they were considered to be false positives. The resistant cells could then be transfected with cDNA expression vectors for the chosen candidate genes to see if their overexpression changes cell sensitivity to the toxin. If the transfected cells revert to wild-type sensitivity levels, it is likely that inactivation of the relevant genes occurred as a result of on-target cleavage.

Previous studies comparing the activity of THP-1 cells with that of their physiological counterparts (peripheral blood monocytes derived from blood of healthy volunteers) noted a number of differences between the two. For example, the human cells expressed more CD14 (a type of monocyte differentiation antigen), and were much more sensitive to lipopolysaccharide (a component of bacterial cell wall) [454]. Differential gene expression patterns might influence cell sensitivity to cobalt and the observed effects. It follows the assay should be repeated on peripheral blood monocytes harvested from THA patients with and without cobalt toxicity symptoms. This will help to check how comparable results obtained in THP-1 cells are to those in their physiological counterparts, and verify their clinical relevance.

The ultimate goal of this *in vitro* project is to develop protective therapies for cobalt-sensitive THA patients. The validated gene targets could be used to develop gene silencing strategies. Alternatively, chemical compounds capable of exerting protective effects on cobalt-susceptible cells could be identified through screening commercially-available drugs libraries (Figure 7.1).

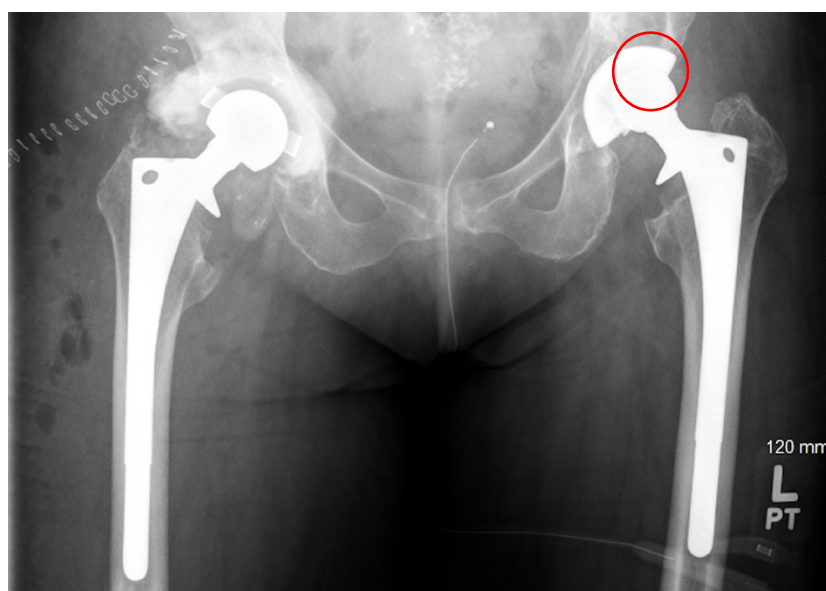




**Figure 7.1. Summary of completed steps (green arrows) and suggested future work (orange arrows).**

Rising popularity of uncemented prostheses is associated with an increased use of titanium in hip implant manufacture. It has been repeatedly suggested in the literature that measurement of blood titanium could be used to assess implant function. Despite an increasing interest in this biomarker, it is unclear what blood concentrations should raise concerns and warrant further investigation. Current recommendations are derived from small-scale studies that used analytical instruments with relatively high LoD, and are therefore unreliable. In the present work, a high resolution instrument was used to

define the upper normal threshold level for blood and plasma titanium associated with well-functioning implants. The next step would be to apply these guidelines to other patients with titanium-based implants, and look for radiographic signs of ARMD, implant loosening and wear. This approach could be a means of monitoring the tens of thousands of patients with titanium-based hips and, when combined with clinical examination and relevant imaging, could help predict which might develop clinical problems. For example, wearing polyethylene liners have been shown to promote increasing contact between the titanium acetabular shell and the femoral head, leading to accelerated wear of the former. A rising blood titanium level could be used to monitor this process, and allow for a timely revision operation before the liner wears through completely (Figure 7.2).



**Figure 7.2. Plain radiograph showing a worn polyethylene liner (red circle). The associated blood titanium level ( $6 \mu\text{g L}^{-1}$ ) was elevated with respect to the threshold value derived in this thesis ( $2.2 \mu\text{g L}^{-1}$ ).**

This thesis has demonstrated the potential of blood metal monitoring to assess implant function and risk of toxicity in THA patients, as well as highlighting a number of areas for further research. Future work in this field could lead to earlier diagnoses of patients in need of revision, as well as identification of patients who may be more susceptible to implant-related toxicity, to allow matching of metal implants to the most suitable people.


# **Appendix A**

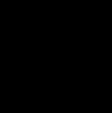
## **Ethical approvals and study documentation**



## A.1. Study described in Chapter 3.

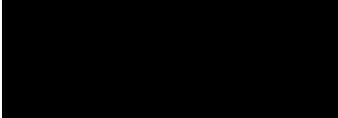
### A.1.1. Ethical approval

  
**Health Research Authority**  
Yorkshire & The Humber - Leeds East Research Ethics Committee

Telephone: 

**Please note:** This is an acknowledgement letter from the REC only and does not allow you to start your study at NHS sites in England until you receive HRA Approval

16 July 2018

Miss Ilona Swiatkowska  
Doctoral researcher  


Dear Miss Swiatkowska

<b>Study title:</b>	<b>Can orthopaedic implants cause systemic adverse effects?</b>
<b>REC reference:</b>	<b>18/YH/0245</b>
<b>Protocol number:</b>	<b>18/0136</b>
<b>IRAS project ID:</b>	<b>236498</b>

Thank you for your letter of 16th July. I can confirm the REC has received the documents listed below and that these comply with the approval conditions detailed in our letter dated 05 July 2018

**Documents received**

The documents received were as follows:

<i>Document</i>	<i>Version</i>	<i>Date</i>
IRAS Application Form [IRAS_Form_05072018]		05 July 2018

A Research Ethics Committee established by the Health Research Authority

Letters of invitation to participant [Invitation letter]	3	12 July 2018
Non-validated questionnaire [SSC]	3	12 July 2018
Participant consent form [CF]	3	12 July 2018
Validated questionnaire [NSC]		
Validated questionnaire [DN-4]		
Validated questionnaire [DNS]		
Validated questionnaire [MMSE]		

#### Approved documents

The final list of approved documentation for the study is therefore as follows:

<i>Document</i>	<i>Version</i>	<i>Date</i>
Evidence of Sponsor insurance or indemnity (non NHS Sponsors only) [Insurance confirmation]		29 May 2018
GP/consultant information sheets or letters [GP info sheet]	3	12 July 2018
IRAS Application Form [IRAS_Form_05072018]		05 July 2018
Letter from funder [Letter from funder]		27 April 2018
Letter from sponsor [Letter from UCL]		29 May 2018
Letters of invitation to participant [Invitation letter]	3	12 July 2018
Non-validated questionnaire [SSC]	3	12 July 2018
Participant consent form [CF]	2	28 June 2018
Participant consent form [CF]	3	12 July 2018
Participant information sheet (PIS) [PIS]	2	28 June 2018
Referee's report or other scientific critique report [Study design scientific review]		09 April 2018
Research protocol or project proposal [Study protocol]	2	28 June 2017
Summary CV for Chief Investigator (CI) [CI CV]		10 December 2017
Summary CV for student [Student CV]		12 June 2018
Summary CV for supervisor (student research) [Supervisor CV]		10 December 2017
Validated questionnaire [NSC]		
Validated questionnaire [DN-4]		
Validated questionnaire [DNS]		
Validated questionnaire [MMSE]		

You should ensure that the sponsor has a copy of the final documentation for the study. It is the sponsor's responsibility to ensure that the documentation is made available to R&D offices at all participating sites.

**18/YH/0245**

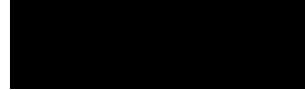
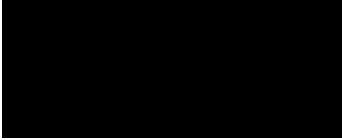
**Please quote this number on all correspondence**

Yours sincerely





Professor Alister Hart



13 August 2018

Dear Professor Hart

**HRA and Health and Care  
Research Wales (HCRW)  
Approval Letter**

<b>Study title:</b>	<b>Can orthopaedic implants cause systemic adverse effects?</b>
<b>IRAS project ID:</b>	<b>236498</b>
<b>Protocol number:</b>	<b>18/0136</b>
<b>REC reference:</b>	<b>18/YH/0245</b>
<b>Sponsor</b>	<b>University College London</b>

I am pleased to confirm that [HRA and Health and Care Research Wales \(HCRW\) Approval](#) has been given for the above referenced study, on the basis described in the application form, protocol, supporting documentation and any clarifications received. You should not expect to receive anything further relating to this application.

**How should I continue to work with participating NHS organisations in England and Wales?**

You should now provide a copy of this letter to all participating NHS organisations in England and Wales, as well as any documentation that has been updated as a result of the assessment.

Following the arranging of capacity and capability, participating NHS organisations should **formally confirm** their capacity and capability to undertake the study. How this will be confirmed is detailed in the "*summary of assessment*" section towards the end of this letter.

You should provide, if you have not already done so, detailed instructions to each organisation as to how you will notify them that research activities may commence at site following their confirmation of capacity and capability (e.g. provision by you of a 'green light' email, formal notification following a site initiation visit, activities may commence immediately following confirmation by participating organisation, etc.).

It is important that you involve both the research management function (e.g. R&D office) supporting each organisation and the local research team (where there is one) in setting up your study. Contact details of the research management function for each organisation can be accessed [here](#).

## B.1.2. Study documentation



### Patient Information Sheet

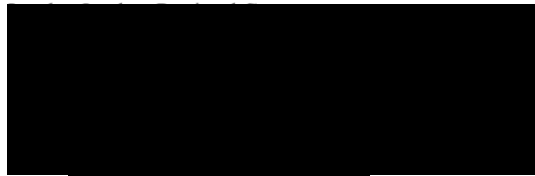
#### Can orthopaedic implants cause effects around the body?

23/07/2018

**Chief Investigator:** Prof. Alister Hart

**Research Coordinator:** Miss Ilona Swiatkowska (PhD student researcher)

**Sponsor:** University College London (UCL)



Email:

We would like to invite you to join our study, which is looking at patients' views on whether other organs and systems in the body are affected by hip replacements. Before you decide whether to take part it is important that you understand why the research is being done and what this study will involve. Please take time to read the following information carefully and discuss it with relatives, friends, and your GP if you wish. Ask us if anything is not clear or you would like more information. This leaflet will tell you why the research is being done and what it will involve for you. Please feel free to talk to others about the study if you wish.

#### **Why are you doing the study?**

We want to look at patients' views on whether orthopaedics implants can affect other organs and systems in the body. A few small studies suggest that metal ions, at very high levels, can affect the heart, nervous system, the thyroid and other organs. However, bigger studies indicate no such impact.

#### **Why have I been invited?**

You have been invited because you have an orthopaedic implant. This invitation is not because we are worried about how your implant is doing or your general health.

#### **What do I need to do?**

If you would like to take part, then please sign the participant slip enclosed and return it in the pre-paid envelope provided. You have two weeks to send the slip back to us. If you express interest in taking part in our study, you will be invited to an Outpatients Clinic at the Royal National Orthopaedic Hospital in Stanmore. Two patient groups will be recruited: one with high blood metal ions and one with low levels. In the Clinic, you will be allocated to either group, depending on your blood metal level results. Travel will be reimbursed for patients attending hospital appointments (capped at £20) upon submission of valid receipts. Once in the Clinic, you will have a chance to ask any questions you might have, before signing a consent form. Once the consent form is signed, clinical assessment will commence.

#### **What will the clinical assessment involve?**

Patient Information Sheet, IRAS: 236498, version 3.0 23/07/18



You will be given 5 questionnaires to complete. Three of these are self-assessment, meaning you will complete them on your own. The fourth questionnaire, which will be given by a clinical fellow, will involve a very simple physical examination. The remaining questionnaires will be administered by a PhD student researcher. It is estimated that the clinical assessment will take 1 hour in total.

**What will happen if I don't want to carry on with the study?**

You can withdraw from the study at any point, but information collected may still be used.

**What are the potential risks and benefits of taking part?**

You may not benefit from taking part, but you will have an assessment of your hip and some aspects of your general health. This is not a substitute for your normal health check with your GP. If we do incidentally find any systemic health concerns, then you may benefit from early diagnosis. We have a multidisciplinary research team encompassing orthopaedic surgeons, neurologists and cardiologists. Patients exhibiting signs of systemic disease will be referred either to an appropriate team member, or to an external specialty clinic for assessment. If we refer you to a different team we will ask your consent first.

**What will happen to the results of the research study?**

We will publish results on the London Implant Retrieval Centre (LIRC) website and in our newsletter. You can also contact us at the above address or attend one of the LIRC Open Days. Printed copy of the results will be sent to patients without internet access.

**Will my GP be told about my participation in this study?**

We will only inform your GP if you ask us to.

**Do I have to take part?**

No, you do not have to take part in the study if you don't want to. We understand if you cannot take part. It will not affect the rest of your care.

**What if there is a problem?**

If you have a concern about any aspect of this study, you should ask to speak to the researchers who will do their best to answer your questions. If you remain unhappy and wish to complain formally, you can do this. Please see NHS website for details on how to do this.

In the event that something does go wrong and you are harmed during the research and this is due to someone's negligence then you may have grounds for a legal action for compensation against UCL, but you may have to pay your legal costs. The normal National Health Service complaints mechanisms will still be available to you (if appropriate).

**Will my records be kept confidential?**

If you join the study, some parts of your medical records and the data collected for the study will be looked at by authorised persons from the company sponsoring and/or the company organising the research. They may also be looked at by authorised people to check that the study is being carried out correctly. Authorised non-clinical staff acting under arrangements with the RNOH may have access to patient identifiable information. All will have a duty of confidentiality to you as a research participant, and will do their best to meet this duty. UCL will collect information about you for this research study from the RNOH. The RNOH will not provide any identifying information about you to UCL. We will use this information to check if you are suitable for this research study.

UCL is the sponsor for this study based in the United Kingdom. We will be using information from you and your medical records in order to undertake this study and will act as the data controller for



this study. This means that we are responsible for looking after your information and using it properly. UCL will keep identifiable information about you for 3 years after the study has finished.

Your rights to access, change or move your information are limited, as we need to manage your information in specific ways in order for the research to be reliable and accurate. If you withdraw from the study, we will keep the information about you that we have already obtained. To safeguard your rights, we will use the minimum personally-identifiable information possible. You can find out more about how we use your information at <https://www.ucl.ac.uk/legal-services/privacy/ucl-staff-privacy-notice>

The RNOH will use your name, NHS number and contact details to contact you about the research study, and make sure that relevant information about the study is recorded for your care, and to oversee the quality of the study. Individuals from UCL and regulatory organisations may look at your medical and research records to check the accuracy of the research study. The RNOH will pass these details to UCL along with the information collected from you and your medical records. The only people in UCL who will have access to information that identifies you will be people who need to contact you about the research study, or audit the data collection process. The people who analyse the information will not be able to identify you and will not be able to find out your name, NHS number or contact details.

The RNOH will keep identifiable information about you from this study for 3 years after the study has finished.

**Who is organising and funding the research?**

The study is organised by Prof. Alister Hart, and it is in fulfilment of a PhD project. The study is sponsored by University College London and funded by Gwen Fish Orthopaedics Trust.

**Who has reviewed the study?**

All research in the NHS is looked at by independent group of people, called a Research Ethics Committee, to protect your interests. This study has been reviewed and given favourable opinion by Leeds East Research Ethics Committee. The Health Research Authority have also reviewed the study.

**Who do I contact for general information about research?**

You can contact the R&D office via [REDACTED]

**Who do I contact for specific information about this research project?**

You can contact Miss Ilona Swiatkowska at [REDACTED]

**Who do I contact if I'm unhappy with the study?**

Patient Advice and Liaison Service via [REDACTED]

Study Investigator: Professor Alister Hart via [REDACTED]

Study Coordinator: Miss Ilona Swiatkowska via [REDACTED]

Please do not hesitate to contact us if you have any further questions. If you are happy about the information provided and wish to participate in this study, please sign the attached participant slip and return it to us in the pre-paid envelope provided.

CONSENT FORM - Adult

Project title: Can orthopaedic implants cause effects around the body?

Patient Identification Number for this trial:

Name of Chief Investigator: Professor Alister Hart

Contact Number: XXXXXXXXXX

Please tick to confirm

1. I confirm that I have read and understood the information sheet version 3 for the above study. I have had the opportunity to consider the information, ask questions and have had these answered satisfactorily.
2. I understand that my participation is voluntary and that I am free to withdraw at any time, without giving any reason, without my medical care or legal rights being affected.
3. I understand that relevant sections of my medical notes and data collected during the study, may be looked at by individuals from the London Implant Retrieval centre, from regulatory authorities or from the NHS Trust, where it is relevant to my taking part in this research. I give permission for these individuals to have access to my records.
4. I agree to take part in the above study.
5. I would like the researchers to inform my GP of my participation in the study.

\_\_\_\_\_  
Name of Study participant

\_\_\_\_\_  
Date

\_\_\_\_\_  
Signature


\_\_\_\_\_  
Name of person taking consent

\_\_\_\_\_  
Date

\_\_\_\_\_  
Signature

## A.2. Study described in Chapter 6.

### A.2.1. Ethical approval

  
Health Research  
Authority

London - Riverside Research Ethics Committee

Tel: [REDACTED]

**Please note: This is the favourable opinion of the REC only and does not allow the amendment to be implemented at NHS sites in England until the outcome of the HRA assessment has been confirmed.**

30 July 2018

Mr Alister/J Hart  
Professor of Orthopaedic Surgery

[REDACTED]

Dear Mr Hart

**Study title:** Analysis of specimens from patients with painful metal on metal hip replacements.

**REC reference:** 07/Q0401/25

**Amendment number:** AM08 04/06/18

**Amendment date:** 04 June 2018

**IRAS project ID:**

Approval was sought for the following;

1. Patients with well-functioning orthopaedic implants have been included in the study design (referred to as the control group). The patients will undergo a blood and/or urine test to determine metal ion levels. The control group is needed in order to establish a "normal" reference range for metal levels that could then be used to assess patients with painful implants.
2. In the "Physical examination" and "Recruitment at research sites" sections, the wording was changed in order to highlight that patients with implants that are not of concern to the surgeon will also be asked for a blood/urine sample.

3. The "Study design flowchart" was updated to highlight that patients with well-functioning implants will be included in the study, and that they will undergo a blood/urine test. It was also restated that patients with failing implants will be additionally asked for a joint fluid sample. The minimal patient age was corrected from 11 to 6, in agreement with the current version of the consent form.
4. Patient Information Sheet (6-10 years old, 11-15 years old, 16-17 years old, adult, parent/guardian)- Revised 05/06/2018
5. It was restated that patients with failing implants will be additionally asked for a sample of urine/joint fluid, in agreement with the current version of the protocol.
6. Patient Information Sheet (control cohort)- Version 1.0 05/06/2018
7. A separate PIS was created for patients with well-functioning implants, who will undergo a blood and/or urine test to evaluate metal ion levels.
8. Consent Form (16-17 years old, adult, parent/guardian)- Revised 05/06/2018
9. Urine and joint fluid test was added to reflect the information contained in the PIS.

The above amendment was reviewed at the meeting of the Sub-Committee held on 30 July 2018 by the Sub-Committee in correspondence.

#### **Ethical opinion**

The members of the Committee taking part in the review gave a favourable ethical opinion of the amendment on the basis described in the notice of amendment form and supporting documentation.

#### **Approved documents**

The documents reviewed and approved at the meeting were:

<i>Document</i>	<i>Version</i>	<i>Date</i>
Covering letter on headed paper [Covering letter 180889 AM08 04.06.2018]		13 July 2018
Notice of Substantial Amendment (non-CTIMP) [1 - Notice of Amendment_page 1]	AM08 04/06/18	04 June 2018
Notice of Substantial Amendment (non-CTIMP) [2_Notic of Amendment_page2]	AM08 04/06/18	04 June 2018
Notice of Substantial Amendment (non-CTIMP) [3_Notic of Amendment_page3]	AM08 04/06/18	04 June 2018
Notice of Substantial Amendment (non-CTIMP) [4__Notic of Amendment_page4]	AM08 04/06/18	04 June 2018
Notice of Substantial Amendment (non-CTIMP) [5-_Notic of Amendment_page5]	AM08 04/06/18	04 June 2018
Notice of Substantial Amendment (non-CTIMP) [6__Notic of Amendment_page6]	AM08 04/06/18	04 June 2018
Notice of Substantial Amendment (non-CTIMP) [7__Notic of Amendment_page7]	AM08 04/06/18	04 June 2018
Other [Re 07Q040125 Substantial amendment to Implant Study - valid under consideration]		13 July 2018
Participant consent form [CF 16-17 clean]	2	05 June 2018
Participant consent form [CF 16-17 tracked]	2	05 June 2018
Participant consent form [CF clean]	5	04 June 2018

Participant consent form [CF parent or guardian clean]	2	05 June 2018
Participant consent form [CF parent or guardian tracked]	2	05 June 2018
Participant consent form [CF 16-17 tracked]	2	05 June 2018
Participant information sheet (PIS) [PIS control clean]	1	05 June 2018
Participant information sheet (PIS) [PIS parent guardian clean]	3	05 June 2018
Participant information sheet (PIS) [LIRC PIS parent guardian tracked]	3	30 July 2018
Participant information sheet (PIS) [PIS 6-10 tracked]	3	30 July 2018
Participant information sheet (PIS) [PIS 11-15 tracked]	3	30 July 2018
Participant information sheet (PIS) [PIS 16-17 tracked]	3	30 July 2018
Participant information sheet (PIS) [PIS case tracked]	3	30 July 2018
Participant information sheet (PIS) [PIS parent guardian tracked]	3	30 July 2018
Research protocol or project proposal [Protocol clean]	7	04 June 2018
Research protocol or project proposal [Protocol tracked]	7	04 June 2018

#### **Membership of the Committee**

The members of the Committee who took part in the review are listed on the attached sheet.

#### **Working with NHS Care Organisations**

Sponsors should ensure that they notify the R&D office for the relevant NHS care organisation of this amendment in line with the terms detailed in the categorisation email issued by the lead nation for the study.

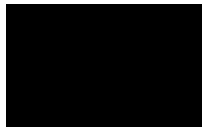
#### **Statement of compliance**

The Committee is constituted in accordance with the Governance Arrangements for Research Ethics Committees and complies fully with the Standard Operating Procedures for Research Ethics Committees in the UK.




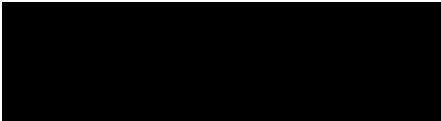
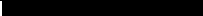
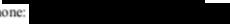
We are pleased to welcome researchers and R & D staff at our Research Ethics Committee members' training days – see details at <http://www.hra.nhs.uk/hra-training/>

<b>07/Q0401/25:</b>	<b>Please quote this number on all correspondence</b>
---------------------	---

Yours sincerely



## A.2.2. Study documentation

		
<b>Patient Information Sheet- control group</b> <b><u>Implant Study</u></b>		
Version 1, 05/06/2018		
		
Email: 		
Telephone: 		
<p>We would like to invite you to participate in a study looking into why some people's orthopaedic implants develop problems. Before deciding if you will give permission to take part in this study, you need to understand why the research is being done and what it will involve for you. Please take time to read the following information carefully. Talk to others about the study if you wish.</p>		
<b>Why Me?</b> Your implant is doing well and you don't need a revision. We would like to take a blood/urine sample from you to check your metal levels.		
<b>What do I need to do?</b> Before we can take a sample from you, we need your consent. We also need your consent to gain access to your relevant medical history including your clinical examination and X-ray.		
<b>How can I help the research?</b> The results of your tests will be used to define "normal" and "abnormal" metal levels when analysing patients with painful implants.		
<b>What tests will we conduct?</b> We will take a sample of your blood and/or urine to measure its metal content.		
<b>Where will the blood be taken from?</b> The blood will be taken from the arm in the usual way. It will take 30 seconds to collect and is similar to previous blood tests you will have had before your operation.		
<b>What are the Risks and Benefits of Taking Part?</b> The benefit of this research is that the samples you provide will further the understanding of failure of orthopaedic implants. There only risk is that of having a small blood sample being taken if you are one of the patients requiring this. The bleeding will be done by a qualified person in a clinical setting.		
<b>Will my records be kept confidential?</b> We adhere to the rules of the ethics committee which insists on national guidelines for "Good Clinical Practice" and includes confidential storage of records under the data protection act.		
<b>Will I be told the results of my tests?</b>		

Yes. We will send your surgeon on request a report once all of the data has been analysed. This report will also contain advice regarding your medical management.

**Will I be told the results of the research?**

Yes, after all results have been analysed you can contact us at the above address.

**Will my GP be told about my participation in this study?**

We will send the results of your analysis to you (if requested) and you are welcome to discuss these with your GP. We will not directly notify your GP about this study.

**What will happen if I do not take part in this study?**

Participation in this study is your choice.

Please do not hesitate to contact us if you have any further questions. If you are happy about the information provided and to participate in this study, please sign the consent form and return it to your surgeon.



Version 5 04/06/2018

Study Number:

Patient Identification Number for this trial:

## CONSENT FORM

**Title of Project:** Implant Study Ethics ref: Riverside Ethics 07/Q0401/25.

Please initial box

1. I confirm that I have read and understand the information sheet dated 05/06/2018, version 1 of the above study and have had the opportunity to ask questions.

2. I understand that my participation is voluntary and that I am free to withdraw at any time, without giving any reason, without my medical care or legal rights being affected.

3. I understand that sections of any of my medical notes may be looked at by responsible individuals working in the medical field or from regulatory authorities where it is relevant to my taking part in research. I give permission for these individuals to have access to my records.

4. I consent for my blood/urine sample to be taken and analysed by your laboratory.

5. I consent for my joint fluid sample to be taken and analysed by your laboratory.

6. I agree to take part in the above study.

7. I would like to be sent the results of this study.

Name of Patient

Date

Signature

\_\_\_\_\_

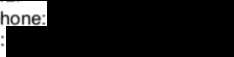
Contact Information

Prof. A Hart  
Consultant Orthopaedic Surgeon



Telephone:

Email:





# **Appendix B**

## **Publications, conferences and awards**



## **B.1. Full list of publications (current and intended)**

**Swiatkowska I**, Mosselmans J. F.W, Geraki T, Wyles C.C, Maleszewski J.J, Henckel J, Sampson B, Potter D.B, Osman I, Trousdale R.T, Hart A.J. Synchrotron analysis of human organ tissue exposed to implant material. *Journal of Trace Metals in Medicine and Biology* 46 (2018) 128–137.

**Swiatkowska I**, Martin N, Hart A.J. Blood titanium level as a biomarker of orthopaedic implant wear. *Journal of Trace Metals in Medicine and Biology* 53 (2019) 120–128.

**Swiatkowska I**, Martin N, Henckel J, Apthorp H, Hart A.J. Blood and plasma titanium levels associated with well-functioning hip implants. *Journal of Trace Metals in Medicine and Biology* 57 (2020) 9-17.

**Swiatkowska I**, Henckel J, Sabah, S, Hart A.J. Self-reported neurotoxic symptoms in hip arthroplasty patients with highly elevated blood cobalt: a case-control study (submitted).

Di Laura A, Hothi H, Henckel J, **Swiatkowska I**, Liow M.H.L, Kwon Y-M, Skinner J.A, Hart A.J. Retrieval analysis of metal and ceramic femoral heads on a single CoCr stem design. *Bone and Joint Research* 6 (2017) 345-350.

## **B.2. Conferences**

**Swiatkowska I**, Mosselmans J. F.W, Geraki T, Wyles C.C, Maleszewski J.J, Henckel J, Sampson B, Potter D.B, Osman I, Trousdale R.T, Hart A.J. Is Carcinogenic Chromium Found In Organs Of Total Joint Arthroplasty Patients? Podium presentation given at the Orthopaedic Research Society (ORS), New Orleans, LA, 2018

**Swiatkowska I**, Mosselmans J. F.W, Trousdale R.T, Wyles C.C, Maleszewski J.J, Sabah S, Henckel J, Sampson B, Hart A.J. Is Carcinogenic Chromium Found In Organs Of Total Joint Arthroplasty Patients? Poster presented at the American Academy of Orthopaedic Surgeons (AAOS), New Orleans, LA, 2018

### **B.3. Awards**

**Runner-up prize, UCL Research Poster Competition, 2018.** Swiatkowska I, Mosselmans J. F.W, Trousdale R.T, Wyles C.C, Maleszewski J.J, Sabah S, Henckel J, Sampson B, Hart A.J. Is Carcinogenic Chromium Found In Organs Of Total Joint Arthroplasty Patients?

**Robert Brown Travel Award, 2018**

## Bibliography

- [1] S. Lam, V. Amies, Hip arthritis presenting as knee pain, *BMJ Case Rep.* 2015 (2015) 2014–2016.
- [2] R. Karim, K.D. Goel, Avascular necrosis of the hip in a 41-year-old male: a case study, *J. Can. Chiropr. Assoc.* 48 (2004) 137–41.
- [3] M. Spalević, S. Milenković, M. Kocić, I. Stanković, L. Dimitrijević, V. Živković, H. Čolović, M. Spalević, Total hip replacement rehabilitation: results and dilemmas, *Acta Medica Median.* 57 (2018) 48–53.
- [4] S.R. Knight, R. Aujla, S.P. Biswas, 100 years of operative history, *Orthop. Rev. (Pavia)*. 3 (2011) 72–74.
- [5] F.S. Haddad, S. Konan, J. Tahmassebi, A prospective comparative study of cementless total hip arthroplasty and hip resurfacing in patients under the age of 55 years: a ten-year follow-up, *Bone Jt. J.* 97-B (2015) 617–622.
- [6] R. Sershon, R. Balkissoon, C.J.D. Valle, Current indications for hip resurfacing arthroplasty in 2016, *Curr. Rev. Musculoskelet. Med.* 9 (2016) 84–92.
- [7] A.J. Shimmin, D. Back, Femoral neck fractures following Birmingham hip resurfacing, *J. Bone Joint Surg. Br.* 87-B (2005) 463–464.
- [8] H. Pandit, S. Glyn-Jones, P. McLardy-Smith, R. Gundle, D. Whitwell, L.C.M. Gibbons, S. Ostlere, N. Athanasou, H.S. Gill, D. Murray, Pseudotumours associated with metal-on-metal hip resurfacings, *J Bone Jt. Surg [Br]*. 90 (2008) 920–3.
- [9] National Joint Registry for England, Wales, Northern Ireland and Isle of Man: 15th Annual Report 2018, 15th Annu. Rep. 1821 (2018) 218.
- [10] N.J. Eynon-Lewis, D. Ferry, M.F. Pearse, Themistocles Gluck: an unrecognised genius., *BMJ.* 305 (2014) 1534–6.
- [11] J. Charnley, Arthroplasty of the hip: A new operation, *Lancet.* 1 (1961) 1129–1132.
- [12] J. Caton, J.L. Prudhon, Over 25 years survival after Charnley’s total hip arthroplasty, *Int. Orthop.* 35 (2011) 185–188.
- [13] P. Massin, R. Lopes, B. Masson, D. Mainard, Does BioloX Delta ceramic reduce the rate of component fractures in total hip replacement?, *Orthop. Traumatol. Surg. Res.* 100 (2014) S317–S321.
- [14] H. Krishnan, S.P. Krishnan, G. Blunn, J.A. Skinner, A.J. Hart, Modular neck femoral stems, *Bone Jt. J.* 95 B (2013) 1011–1021.
- [15] J.J. Jacobs, H.J. Cooper, R.M. Urban, R.L. Wixson, C.J. Della Valle, What do we know about taper corrosion in total hip arthroplasty?, *J. Arthroplasty.* 29 (2014) 668–669.
- [16] H.J. Cooper, C.J. Della Valle, R.A. Berger, M. Tetreault, W.G. Paprosky, S.M. Sporer, J.J. Jacobs, Corrosion at the head-neck taper as a cause for adverse local tissue reactions after total hip arthroplasty, *J. Bone Jt. Surg. - Ser. A.* 94 (2012) 1655–1661.
- [17] I. De Martino, J.B. Assini, M.E. Elpers, T.M. Wright, G.H. Westrich, Corrosion and fretting of a modular hip system: a retrieval analysis of 60 Rejuvenate stems, *J. Arthroplasty.* 30 (2015) 1470–1475.
- [18] S. Banerjee, J.J. Cherian, J. V. Bono, S.M. Kurtz, R. Geesink, R.M. Meneghini, R.E. Delanois, M.A. Mont, Gross trunnion failure after primary total hip arthroplasty, *J. Arthroplasty.* 30 (2015) 641–648.
- [19] L.M. Ko, A.F. Chen, G.K. Deirmengian, W.J. Hozack, P.F. Sharkey, Catastrophic femoral head-stem trunnion dissociation secondary to corrosion, *J. Bone Jt. Surg. - Am. Vol.* 98 (2016) 1400–1404.
- [20] R. Pivec, R.M. Meneghini, W.J. Hozack, G.H. Westrich, M.A. Mont, Modular taper junction corrosion and failure: How to approach a recalled total hip arthroplasty implant, *J. Arthroplasty.* 29 (2014) 1–6.
- [21] I.P.S. Gill, J. Webb, K. Sloan, R.J. Beaver, Corrosion at the neck-stem junction as a cause of metal ion release and pseudotumour formation, *J. Bone Jt. Surg. - Br. Vol.* 94-B (2012) 895–900.
- [22] T. Hanawa, Research and development of metals for medical devices based on clinical

- needs, *Sci. Technol. Adv. Mater.* 13 (2012) 1–15.
- [23] H. Matusiewicz, Potential release of in vivo trace metals from metallic medical implants in the human body: from ions to nanoparticles - a systematic analytical review, *Acta Biomater.* 10 (2014) 2379–2403.
- [24] A.M. Khorasani, M. Goldberg, E.H. Doeven, G. Littlefair, Titanium in biomedical applications- properties and fabrication: a review, *J. Biomater. Tissue Eng.* 5 (2015) 593–619.
- [25] M.M. Morlock, E.C. Dickinson, K.-P. Günther, D. Bunte, V. Polster, Head taper corrosion causing head bottoming out and consecutive gross stem taper failure in total hip arthroplasty, *J. Arthroplasty.* 33 (2018) 3581-3590.
- [26] E.J. Mcpherson, M. V Dipane, S.M. Sherif, Massive pseudotumor in a 28mm ceramic-polyethylene revision THA: a case report, *JISRF Reconstr. Rev.* 4 (2014) 11–17.
- [27] E. Oral, K.K. Wannomae, N. Hawkins, W.H. Harris, O.K. Muratoglu,  $\alpha$ -Tocopherol-doped irradiated UHMWPE for high fatigue resistance and low wear, *Biomaterials.* 25 (2004) 5515–5522.
- [28] A.W.E. Hodgson, S. Kurz, S. Virtanen, V. Fervel, C.O.A. Olsson, S. Mischler, Passive and transpassive behaviour of CoCrMo in simulated biological solutions, *Electrochim. Acta.* 49 (2004) 2167–2178.
- [29] B. Scharf, C.C. Clement, V. Zolla, G. Perino, B. Yan, S.G. Elci, E. Purdue, S. Goldring, F. Macaluso, N. Cobelli, R.W. Vachet, L. Santambrogio, Molecular analysis of chromium and cobalt-related toxicity, *Sci. Rep.* 4 (2014) 1–12.
- [30] F. Pisanu, C. Doria, M. Androzzzi, M. Bartoli, L. Saderi, G. Sotgiu, P.T. Leali, Pleomorphic clinical spectrum of metallosis in total hip arthroplasty, *Int. Orthop.* 43 (2018) 85–96.
- [31] H.-I. Choi, J.A. Hong, M.-S. Kim, S.E. Lee, S.-H. Jung, P.W. Yoon, J.S. Song, J.-J. Kim, Severe cardiomyopathy due to arthroprosthetic cobaltism: report of two cases with different outcomes, *Cardiovasc. Toxicol.* 19 (2018) 82–89.
- [32] N. Cobelli, B. Scharf, G.M. Crisi, J. Hardin, L. Santambrogio, Mediators of the inflammatory response to joint replacement devices, *Nat. Rev. Rheumatol.* 7 (2011) 600–608.
- [33] D.R. Bijukumar, A. Segu, J.C.M. Souza, X.J. Li, M. Barba, L.G. Mercuri, J. J. Jacobs, M.T. Mathew, Systemic and local toxicity of metal debris released from hip prostheses: a review of experimental approaches, *Nanomedicine Nanotechnology, Biol. Med.* 14 (2018) 951–963.
- [34] A. Di Laura, P.D. Quinn, V.C. Panagiotopoulou, H.S. Hothi, J.J. Powell, F. Berisha, F. Amary, J.F.W. Mosselmans, J.A. Skinner, A.J. Hart, The chemical form of metal species released from corroded taper junctions of hip implants : synchrotron analysis of patient tissue, *Sci. Rep.* 7 (2017) 1–13.
- [35] S.D. Rogers, D.W. Howie, S.E. Graves, M.J. Percy, D.R. Haynes, In vitro human monocyte response to wear particles of titanium alloy containing vanadium or niobium, *J. Bone Jt. Surg.* 79 (1997) 311–315.
- [36] C.M. Sayes, R. Wahi, P.A. Kurian, Y. Liu, J.L. West, K.D. Ausman, D.B. Warheit, V.L. Colvin, Correlating nanoscale titania structure with toxicity: a cytotoxicity and inflammatory response study with human dermal fibroblasts and human lung epithelial cells, *Toxicol. Sci.* 92 (2006) 174–185.
- [37] L.K. Braydich-Stolle, N.M. Schaeublin, R.C. Murdock, J. Jiang, P. Biswas, J.J. Schlager, S.M. Hussain, Crystal structure mediates mode of cell death in TiO<sub>2</sub> nanotoxicity, *J. Nanoparticle Res.* 11 (2009) 1361–1374.
- [38] J. Zhang, W. Song, J. Guo, J. Zhang, Z. Sun, L. Li, F. Ding, M. Gao, Cytotoxicity of different sized TiO<sub>2</sub> nanoparticles in mouse macrophages, *Toxicol. Ind. Health.* 29 (2012) 523–533.
- [39] M.G. Choi, H.S. Koh, D. Klues, D. O'Connor, A. Mathur, G.A. Truskey, J. Rubin, D.X.F. Zhou, K.-L.P. Sung, Effects of titanium particle size on osteoblast functions in vitro and in vivo, *Proc. Natl. Acad. Sci.* 102 (2005) 4578–4583.
- [40] Z. Xia, B.F. Ricciardi, Z. Liu, C. von Ruhland, M. Ward, A. Lord, L. Hughes, S.R. Goldring, E. Purdue, D. Murray, G. Perino, Nano-analyses of wear particles from



- metal-on-metal and non-metal-on-metal dual modular neck hip arthroplasty, *Nanomedicine Nanotechnology, Biol. Med.* 13 (2017) 1205–1217.
- [41] I. Catelas, M.A. Wimmer, New insights into wear and biological effects of metal-on-metal bearings, *J. Bone Jt. Surg. - Ser. A.* 93 (2011) 76–83.
- [42] H. Shi, R. Magaye, V. Castranova, J. Zhao, Titanium dioxide nanoparticles: a review of current toxicological data, *Cosm. Res.* 10 (2013) 1–33.
- [43] A.J. Hart, P.D. Quinn, F. Lali, B. Sampson, J.A. Skinner, J.J. Powell, J. Nolan, K. Tucker, S. Donell, A. Flanagan, J.F.W. Mosselmans, Cobalt from metal-on-metal hip replacements may be the clinically relevant active agent responsible for periprosthetic tissue reactions, *Acta Biomater.* 8 (2012) 3865–3873.
- [44] T. Hanawa, Metal ion release from metal implants, *Mater. Sci. Eng. C.* 24 (2004) 745–752.
- [45] Y. Okazaki, E. Gotoh, Comparison of metal release from various metallic biomaterials in vitro, *Biomaterials.* 26 (2005) 11–21.
- [46] K. Magone, D. Luckenbill, T. Goswami, Metal ions as inflammatory initiators of osteolysis, *Arch. Orthop. Trauma Surg.* 135 (2015) 683–695.
- [47] B.F. Shahgaldi, F.W. Heatley, A. Dewar, B. Corrin, In vivo corrosion of cobalt-chromium and titanium wear particles., *J. Bone Jt. Surgery, Br. Vol.* 77 (1995) 962–6.
- [48] D. Granchi, E. Cenni, G. Trisolino, A. Giunti, N. Baldini, Sensitivity to implant materials in patients undergoing total hip replacement, *J. Biomed. Mater. Res. - Part B Appl. Biomater.* 77 (2005) 257–264.
- [49] H.J. Münch, S.S. Jacobsen, J.T. Olesen, T. Menné, K. Soballe, J.D. Johansen, J.P. Thyssen, The association between metal allergy, total knee arthroplasty, and revision, *Acta Orthop.* 86 (2015) 378–383.
- [50] T. Schafer, E. Bohler, S. Ruhdorfer, L. Weigl, D. Wessner, B. Filipiak, H. Wichmann, Epidemiology of contact allergy in adults, *Allergy Eur. J. Allergy Clin. Immunol.* 56 (2001) 1192–1196.
- [51] W. Steens, G. von Foerster, A. Katzer, Severe cobalt poisoning with loss of sight after ceramic-metal pairing in a hip- a case report, *Acta Orthop.* 77 (2006) 830–832.
- [52] S.S. Tower, Arthroprosthetic cobaltism: neurological and cardiac manifestations in two patients with metal-on-metal arthroplasty: a case report, *J. Bone Jt. Surg.* 92 (2010) 2847–51.
- [53] N. Hallab, J. J. Jacobs, J. Black, Hypersensitivity to metallic biomaterials: a review of leukocyte migration inhibition assays, *Biomaterials.* 21 (2000) 1301–1314.
- [54] Y. Niki, H. Matsumoto, T. Otani, T. Yatabe, M. Kondo, F. Yoshimine, Y. Toyama, Screening for symptomatic metal sensitivity: A prospective study of 92 patients undergoing total knee arthroplasty, *Biomaterials.* 26 (2005) 1019–1026.
- [55] N. Hallab, K. Merritt, J.J. Jacobs, Metal sensitivity in patients with orthopaedic implants., *J. Bone Joint Surg. Am.* 83-A (2001) 428–36.
- [56] J. Wawrzynski, J.A. Gil, A.D. Goodman, G.R. Waryasz, Hypersensitivity to orthopedic implants: a review of the literature, *Rheumatol. Ther.* 4 (2017) 45–56. doi:6.
- [57] D. Barceloux, Cobalt, *J. Toxicol. Clin. Toxicol.* 37 (1999) 201–216.
- [58] R. Banerjee, S.W. Ragsdale, The many faces of vitamin B12: catalysis by cobalamin-dependent enzymes, *Annu. Rev. Biochem.* 72 (2003) 209–247.
- [59] N. GF, N. K, N. M, F. LT, Handbook on the toxicology of metals (third edition), *Handb. Toxicol. Met.* (2007) 445–486.
- [60] S.P. Stabler, Vitamin B12 deficiency, *N. Engl. J. Med.* 368 (2013) 149–160.
- [61] C.J. Ekabe, J. Kehbila, M.H. Abanda, B.M. Kadia, C.B. Sama, G.L. Monekosso, Vitamin B12 deficiency neuropathy: a rare diagnosis in young adults- a case report, *BMC Res. Notes.* 10 (2017) 10–13.
- [62] M.J. Glade, M.M. Meguid, A glance at antioxidant and antiinflammatory properties of dietary cobalt, *Nutrition.* 46 (2018) 62–66.
- [63] G. Lippi, M. Franchini, G.C. Guidi, Blood doping by cobalt. Should we measure cobalt in athletes?, *J. Occup. Med. Toxicol.* 1 (2006) 18.
- [64] H.M.L. Jansen, S. Knollema, L.V. Van Der Duin, A.T.M. Willemsen, A. Wiersma, J. Korfand, A.M.J. Paans, Pharmacokinetics and dosimetry of cobalt-55 and cobalt-57, J.

- Nucl. Med. 37 (1996) 2082–2086.
- [65] L.O. Simonsen, H. Harbak, P. Bennekou, Cobalt metabolism and toxicology- a brief update, *Sci. Total Environ.* 432 (2012) 210–215.
- [66] T. Skorringe, A. Burkhart, K.B. Johnsen, T. Moos, Divalent metal transporter 1 (DMT1) in the brain: implications for a role in iron transport at the blood-brain barrier, and neuronal and glial pathology, *Front. Mol. Neurosci.* 8 (2015) 1–13.
- [67] J. Howitt, U. Putz, J. Lackovic, A. Doan, L. Dorstyn, H. Cheng, B. Yang, T. Chan-Ling, J. Silke, S. Kumar, S.-S. Tan, Divalent metal transporter 1 (DMT1) regulation by *Ndfip1* prevents metal toxicity in human neurons, *Proc. Natl. Acad. Sci.* 106 (2009) 15489–15494.
- [68] L.R. Walter, E. Marel, R. Harbury, J. Wearne, Distribution of chromium and cobalt ions in various blood fractions after resurfacing hip arthroplasty, *J. Arthroplasty.* 23 (2008) 814–821.
- [69] L.O. Simonsen, A.M. Brown, H. Harbak, B.I. Kristensen, P. Bennekou, Cobalt uptake and binding in human red blood cells, *Blood Cells, Mol. Dis.* 46 (2011) 266–276.
- [70] S. Catalani, R. Leone, M.C. Rizzetti, A. Padovani, P. Apostoli, The role of albumin in human toxicology of cobalt: contribution from a clinical case, *ISRN Hematol.* 2011 (2011) 1–6.
- [71] M.G. Zywieli, J.J. Cherian, S. Banerjee, A.C. Cheung, F. Wong, J. Butany, C. Gilbert, C. Overgaard, K. Syed, J.J. Jacobs, M.A. Mont, Systemic cobalt toxicity from total hip arthroplasties, *Bone Jt. J.* 98B (2016) 14–20.
- [72] M.C. Rizzetti, P. Liberini, G. Zarattini, S. Catalani, U. Pazzaglia, P. Apostoli, A. Padovani, Loss of sight and sound. Could it be the hip?, *Lancet.* 373 (2009) 1052.
- [73] S. Catalani, R. Leone, M.C. Rizzetti, A. Padovani, P. Apostoli, The role of albumin in human toxicology of cobalt: contribution from a clinical case., *ISRN Hematol.* 2011 (2011) 690620.
- [74] O. Posada, R. Tate, R.M. Meek, M. Grant, In vitro analyses of the toxicity, immunological, and gene expression effects of cobalt-chromium alloy wear debris and Co ions derived from metal-on-metal hip implants, *Lubricants.* 3 (2015) 539–568.
- [75] W.-C. Witzleb, J. Ziegler, F. Krummenauer, V. Neumeister, K.-P. Guenther, Exposure to chromium, cobalt and molybdenum from metal-on-metal total hip replacement and hip resurfacing arthroplasty, *Acta Orthop.* 77 (2006) 697–705.
- [76] P.A. Potnis, D.K. Dutta, S.C. Wood, Toll-like receptor 4 signaling pathway mediates proinflammatory immune response to cobalt-alloy particles, *Cell. Immunol.* 282 (2013) 53–65. 003.
- [77] H. Lawrence, D. Deehan, J. Holland, J. Kirby, A. Tyson-Capper, The immunobiology of cobalt: demonstration of a potential aetiology for inflammatory pseudotumours after metal-on-metal replacement of the hip, *Bone Jt. J.* 96B (2014) 1172–1177.
- [78] Y.-M. Kwon, Z. Xia, S. Glyn-Jones, D. Beard, H.S. Gill, D.W. Murray, Dose-dependent cytotoxicity of clinically relevant cobalt nanoparticles and ions on macrophages in vitro, *Biomed. Mater.* 4 (2009) 1–8.
- [79] I. Catelas, A. Petit, D.J. Zukor, O.L. Huk, Cytotoxic and apoptotic effects of cobalt and chromium ions on J774 macrophages- implication of caspase-3 in the apoptotic pathway, *J. Mater. Sci. Mater. Med.* 12 (2001) 949–953.
- [80] O.L. Huk, I. Catelas, F. Mwale, J. Antoniou, D.J. Zukor, A. Petit, Induction of apoptosis and necrosis by metal ions in vitro, *J. Arthroplasty.* 19 (2004) 84–87.
- [81] A. Davies, H. Willert, P. Campbell, I. Learmonth, C. Case, An unusual lymphocytic perivascular infiltration in tissues around joint replacements, *J. Bone Jt. Surg.* 87-A (2005) 18–27.
- [82] E. Paukkeri, R. Korhonen, M. Hämäläinen, M. Pesu, A. Eskelinen, The inflammatory phenotype in failed metal-on-metal hip arthroplasty correlates with blood metal concentrations, *PLoS One.* 11 (2016) 1–13.
- [83] H. Willert, G. Buchhorn, A. Fayyazi, R. Flury, M. Windler, G. Koster, C. Lohmann, Metal-on-metal bearings and hypersensitivity in patients with artificial hip joints: a clinical and histomorphological study, *J. Bone Jt. Surg.* 87 (2005) 28–36.
- [84] Y.-M. Kwon, S. Glyn-Jones, D.J. Simpson, A. Kamali, P. McLardy-Smith, H.S. Gill,

- D.W. Murray, Analysis of wear of retrieved metal-on-metal hip resurfacing implants revised due to pseudotumours., *J Bone Jt. Surg Br.* 92 (2010) 356–361.
- [85] A. Hsu, C. Gross, B. Levine, Pseudotumor from modular neck corrosion after ceramic-on-polyethylene total hip arthroplasty, *Am. J. Orthop.* 41 (2012) 422–426.
- [86] X. Mao, G.H. Tay, D.B. Godbolt, R.W. Crawford, Pseudotumor in a well-fixed metal-on-polyethylene uncemented hip arthroplasty, *J. Arthroplasty.* 27 (2012) 493.e13-493.e17.
- [87] T. Clyburn, Pseudotumor in Metal-on-Polyethylene Total Hip Arthroplasty, *Jt. Implant Surg. Res. Found.* (2013) 18–21.
- [88] R. Sauni, A. Linna, P. Oksa, H. Nordman, M. Tuppurainen, J. Uitti, Cobalt asthma- a case series from a cobalt plant., *Occup. Med. (Chic. Ill).* 60 (2010) 301–6. doi:kqq023.
- [89] M.G. Zywiell, J.-M. Brandt, C.B. Overgaard, a C. Cheung, T.R. Turgeon, K. a Syed, Fatal cardiomyopathy after revision total hip replacement for fracture of a ceramic liner, *Bone Joint J.* 95-B (2013) 31–7.
- [90] D. Pelclova, M. Sklensky, P. Janicek, K. Lach, Severe cobalt intoxication following hip replacement revision: clinical features and outcome, *Clin. Toxicol.* 50 (2012) 262–265.
- [91] L. Leyssens, B. Vinck, C. Van Der Straeten, F. Wuyts, L. Maes, Cobalt toxicity in humans. A review of the potential sources and systemic health effects., *Toxicology.* 387 (2017) 43–56.
- [92] S. Megaterio, F. Galetto, E. Alossa, S. Capretto, Effetti a distanza del rilascio di ioni metallo in usura della testa protesica: presentazione di un caso, *Sci. Total Environ.* (2001) 173–175.
- [93] C. Kim, Y.H. Choi, M.Y. Jeong, Cobalt intoxication heart failure after revision total hip replacement for ceramic head fracture: a case report, *Hip Pelvis.* 28 (2016) 259–263.
- [94] J. Griffiths, A. Colvin, P. Yates, D. Meyerkort, A. Kop, G. Prosser, Extreme cobalt toxicity: bearing the brunt of a failed ceramic liner, *JBJS Case Connect.* 5 (2015) 1–7.
- [95] K.M. Stepien, Z. Abidin, G. Lee, R. Cullen, P. Logan, G.M. Pastores, Metallosis mimicking a metabolic disorder: a case report, *Mol. Genet. Metab. Reports.* 17 (2018) 38–41.
- [96] T. Ikeda, K. Takahashi, T. Kabata, D. Sakagoshi, K. Tomita, M. Yamada, Polyneuropathy caused by cobalt-chromium metallosis after total hip replacement, *Muscle and Nerve.* 42 (2010) 140–143.
- [97] K.P. Weber, C. Schweier, V. Kana, T. Guggi, K. Byber, K. Landau, Wear and tear vision, *J. Neuro-Ophthalmology.* 35 (2015) 82–85.
- [98] M.I. Sanz Pérez, A.M. Rico Villoras, A. Moreno Velasco, S. Bartolomé García, J. Campo Loarte, Heart transplant secondary to cobalt toxicity after hip arthroplasty revision, *HIP Int.* (2019) 1–5.
- [99] H.Y. Samar, M. Doyle, R.B. Williams, J.A. Yamrozik, M. Bunker, R.W.W. Biederman, M.B. Shah, Novel use of cardiac magnetic resonance imaging for the diagnosis of cobalt cardiomyopathy, *JACC Cardiovasc. Imaging.* 8 (2015) 1231–1232.
- [100] B.A. Mosier, L. Maynard, N.G. Sotereanos, J.J. Sewecke, Progressive cardiomyopathy in a patient with elevated cobalt ion levels and bilateral metal-on-metal hip arthroplasties, *Am. J. Orthop.* (2016) 132–135.
- [101] C.J. Gilbert, A. Cheung, J. Butany, M.G. Zywiell, K. Syed, M. McDonald, F. Wong, C. Overgaard, Hip pain and heart failure: the missing link, *Can. J. Cardiol.* 29 (2013) 639.e1-639.e2.
- [102] R. Yu, Cobalt toxicity- an overlooked cause of hypothyroidism, *J Endocrinol Thyroid Res.* 1 (2017) 1–4.
- [103] V. Ho, A. Arac, P. Shieh, Hearing and vision loss in an older man, *JAMA Neurol.* (2018) E1-2.
- [104] J. Martin, L. Spencer-Gardner, C. Camp, J. Stulak, R. Sierra, Cardiac cobaltism: a rare complication after bilateral metal-on-metal total hip arthroplasty, *Arthroplast. Today.* 1 (2015) 99–102.
- [105] K.A. Fox, T.M. Phillips, J.H. Yanta, M.G. Abesamis, Fatal cobalt toxicity after total

- hip arthroplasty revision for fractured ceramic components., *Clin. Toxicol.* 54 (2016) 874–877.
- [106] P.L. Day, S.J. Eckdahl, J.J. Maleszewski, T.C. Wright, D.L. Murray, Establishing human heart chromium, cobalt and vanadium concentrations by inductively coupled plasma mass spectrometry, *J. Trace Elem. Med. Biol.* 41 (2017) 60–65.
- [107] A.H. Khan, R. Verma, A. Bajpai, S. Mackey-Bojack, Unusual Case of Congestive Heart Failure: Cardiac Magnetic Resonance Imaging and Histopathologic Findings in Cobalt Cardiomyopathy, *Cardiovasc. Imaging.* 8 (2015) 1–3.
- [108] R. Peters, P. Willemse, P. Rijk, M. Hoogendoorn, Fatal cobalt toxicity after a non-metal-on-metal total hip arthroplasty, *Case Reports Orthop.* 2017 (2017) 1–5.
- [109] S.J. Lee, H.S. Kwak, J.J. Yoo, H.J. Kim, Bearing change to metal-on-polyethylene for ceramic bearing fracture in total hip arthroplasty- does it work?, *J. Arthroplasty.* 31 (2016) 204–208.
- [110] P. Lecoanet, M. Blangis, M. Garcia, Y. Legallois, T. Fabre, Chromium-cobalt intoxication with intense systemic complications following total hip revision after per-operative ceramic fracture, *Case Reports Orthop.* 2019 (2019) 1–4.
- [111] M.L. Grant, J.K. Karp, M. Palladino, N. Le, N. Hall, J.H. Herman, Does therapeutic plasma exchange have a role in the treatment of prosthetic hip-associated cobalt toxicity? A case report and literature review, *Hemapheresis.* 56 (2016) 2368–2373.
- [112] J.H. Ho, J.B. Leikin, P.I. Dargan, J.R.H. Archer, D.M. Wood, J. Brent, Metal-on-Metal Hip Joint Prostheses: a retrospective case series investigating the association of systemic toxicity with serum cobalt and chromium concentrations, *J. Med. Toxicol.* (2017) 13:321-328.
- [113] L. Grillo, H. Nguyen, S. Tsang, D. Hood, J. Odel, Cobalt-Chromium Metallosis with Normal ERG: A Case Report and Review, *J. Neuro-Ophthalmology.* 36 (2015) 383–388.
- [114] C. Esteban Sanchez, L. Pasto-Cardona, Cobalt intoxication in a patient with hip prosthesis, *Eur. J. Clin. Pharm.* 18 (2016) 189–190.
- [115] K. Dahms, Y. Sharkova, P. Heitland, S. Pankuweit, J.R. Schaefer, Cobalt intoxication diagnosed with the help of Dr House, *Lancet.* 383 (2014) 574.
- [116] A. Harris, J. Johnson, P.K. Mansuripur, R. Limbird, Cobalt toxicity after revision to a metal-on-polyethylene total hip arthroplasty for fracture of ceramic acetabular component, *Arthroplast. Today.* 1 (2015) 89–91.
- [117] M. Oldenburg, R. Wegner, X. Baur, Severe Cobalt Intoxication Due to Prosthesis Wear in Repeated Total Hip Arthroplasty, *J. Arthroplasty.* 24 (2009) 825.e15-825.e20.
- [118] W. Apel, D. Stark, A. Stark, S. O’Hagan, J. Ling, Cobalt-chromium toxic retinopathy case study, *Doc. Ophthalmol.* 126 (2013) 69–78.
- [119] A. Giampreti, D. Lonati, C.A. Locatelli, Chelation in Suspected Prosthetic Hip-Associated Cobalt Toxicity, *CJCA.* 30 (2014) 465.e13.
- [120] L.A. Allen, A. V. Ambardekar, K.M. Devaraj, J.J. Maleszewski, E.E. Wolfel, Missing Elements of the History, *N. Engl. J. Med.* 370 (2014) 559–566.
- [121] J.B. Leikin, H.C. Karydes, P.M. Whiteley, B.K. Wills, K.L. Cumpston, J.J. Jacobs, Outpatient toxicology clinic experience of patients with hip implants., *Clin. Toxicol. (Phila).* 51 (2013) 230–6.
- [122] R. Tilney, M.R. Burg, M.A. Sammut, Cobalt Cardiomyopathy Secondary to Hip Arthroplasty : An Increasingly Prevalent Problem, *Case Reports Cardiol.* 2017 (2017) 1–4.
- [123] S. Moniz, S. Hodgkinson, P. Yates, Cardiac transplant due to metal toxicity associated with hip arthroplasty, *Arthroplast. Today.* (2017) 4–6.
- [124] R.S. Charette, A.L. Neuwirth, C.L. Nelson, Arthroprosthetic cobaltism associated with cardiomyopathy, *Arthroplast. Today.* 3 (2017) 225–28.
- [125] E. O’Connell, N. Mead, H. Fesniak, Idiopathic Cardiomyopathy Following Metal-on-Metal Hip Arthroplasty: The New Face of “Beer Drinker’s Cardiomyopathy”, *Healthc. Bull.* 2 (2013).
- [126] J. McLaughlin, L. Castrodale, S.S. Tower, Cobalt Toxicity in Two Hip Replacement Patients, *Epi. Alaska. Gov.* (2010).

- [127] H.M.G. Bonilla, A. Bhimaraj, A case of cobalt cardiomyopathy, *J. Am. Coll. Cardiol.* 71 (2018) A2386.
- [128] S.S. Tower, Arthroprosthetic cobaltism associated with metal on metal hip implants, *J Bone Jt. Surg Am.* 344 (2012) e430–e430.
- [129] N.I. Olmedo-Garcia, L. Zagra, High risk of complications using metal heads after ceramic fracture in total hip arthroplasty, *HIP Int.* 29 (2018) 373–78.
- [130] N.L. Vasukutty, T.H.A. Minhas, Systemic effects of cobalt toxicity after revision hip replacement can manifest in intermediate to long term follow-up, *Hip Int.* 26 (2016) e31–e34.
- [131] S.K. Ng, A. Ebnetter, J.S. Gilhotra, Hip-implant related chorio-retinal cobalt toxicity., *Indian J. Ophthalmol.* 61 (2013) 35–37.
- [132] X. Mao, A. a Wong, R.W. Crawford, Cobalt toxicity-an emerging clinical problem in patients with metal-on-metal hip prostheses?, *Med. J. Aust.* 194 (2011) 649–651.
- [133] C. Machado, A. Appelbe, R. Wood, Arthroprosthetic Cobaltism and Cardiomyopathy, *Hear. Lung Circ.* 21 (2012) 759–760.
- [134] L. Berk, J. Burchenal, W. Castle, Erythropoietic effect of cobalt in patients with or without anemia, *N. Engl. J. Med.* 240 (1949) 754–761.
- [135] G. E, J. LO, F. W, P. LF, Studies on Erythropoiesis: The Effect of Cobalt on the Production of Erythropoietin, 7 (2015) 46–51.
- [136] J. Duckham, H. Lee, The treatment of refractory anaemia of chronic renal failure with cobalt chloride, *Q J Med.* 45 (1976) 277–294.
- [137] J. Little, R. Sunico, Cobalt-induced goiter with cardiomegaly and congestive failure, *J. Pediatr.* 52 (1958) 284–288.
- [138] J. Curtis, G. Goode, J. Herrington, L. Urdaneta, Possible cobalt toxicity in maintenance hemodialysis patients after treatment with cobaltous chloride: a study of blood and tissue cobalt concentrations in normal subjects and patients with terminal and renal failure, *Clin. Nephrol.* 5 (1976) 61–65.
- [139] A.C. Lantin, A. Mallants, J. Vermeulen, N. Speybroeck, P. Hoet, D. Lison, Absence of adverse effect on thyroid function and red blood cells in a population of workers exposed to cobalt compounds, *Toxicol. Lett.* 201 (2011) 42–46.
- [140] B. Swennen, J.P. Buchet, D. Stanescu, D. Lison, R. Lauwerys, Epidemiological survey of workers exposed to cobalt oxides, cobalt salts, and cobalt metal., *Occup. Environ. Med.* 50 (2008) 835–842.
- [141] C.S. Alexander, Cobalt-beer cardiomyopathy. A clinical and pathologic study of twenty-eight cases, *Am. J. Med.* 53 (1972) 395–417.
- [142] A.C. Cheung, S. Banerjee, J.J. Cherian, F. Wong, J. Butany, C. Gilbert, C. Overgaard, K. Syed, M.G. Zywiell, J.J. Jacobs, M.A. Mont, Systemic cobalt toxicity from total hip arthroplasties: review of a rare condition. Part 1- history, mechanism, measurements and pathophysiology, *Bone Joint J.* 98-B (2016) 6–13.
- [143] J.L. Chamberlain, Thyroid enlargement probably induced by cobalt, *J. Pediatr.* 59 (1961) 81–86.
- [144] R. Gross, J. Kriss, T. Spaet, The hematopoietic and goitrogenic effects of cobaltous chloride in patients with sickle cell anemia, *Pediatrics.* 15 (1955) 284-290.
- [145] U.O.E. Schirrmacher, Case of Cobalt Poisoning, *Analgesia.* 1 (1967) 544–545.
- [146] C. Esteban Sánchez, L. Pastó Cardona, Cobalt intoxication in a patient with hip prosthesis, *Eur. J. Clin. Pharm.* 18 (2016) 189–190.
- [147] O. Karovic, I. Tonazzini, N. Rebola, E. Edström, C. Lövdahl, B.B. Fredholm, E. Daré, Toxic effects of cobalt in primary cultures of mouse astrocytes. Similarities with hypoxia and role of HIF-1 $\alpha$ , *Biochem. Pharmacol.* 73 (2007) 694–708.
- [148] S. Kikuchi, T. Ninomiya, T. Kohno, Cobalt inhibits motility of axonal mitochondria and induces axonal degeneration in cultured dorsal root ganglion cells of rat, *Cell Biol Toxicol.* 34 (2017) 93–107.
- [149] L. Yuan, X. Yang, Selective suppression of rod signal transmission by cobalt ions of low levels in carp retina, *Sci. China, Ser. C Life Sci.* 40 (1997) 128–136.
- [150] P. Apostoli, S. Catalani, A. Zaghini, A. Mariotti, P.L. Poliani, V. Vielmi, F. Semeraro, S. Duse, A. Porzionato, V. Macchi, A. Padovani, M.C. Rizzetti, R. De Caro, High doses

- of cobalt induce optic and auditory neuropathy, *Exp. Toxicol. Pathol.* 65 (2013) 719–727.
- [151] A. Hara, M. Niwa, H. Aoki, M. Kumada, T. Kunisada, T. Oyama, T. Yamamoto, O. Kozawa, H. Mori, A new model of retinal photoreceptor cell degeneration induced by a chemical hypoxia-mimicking agent, cobalt chloride, *Brain Res.* 1109 (2006) 192–200.
- [152] A. Licht, M. Oliver, R. Rachmilewitz, Optic atrophy following treatment with cobalt chloride in a patient with pancytopenia and hypercellular marrow., *Isr. J. Med. Sci.* 8 (1972) 61–66.
- [153] F. Gardner, The use of Cobaltous Chloride in Anaemia associated with Chronic Renal Disease, *J. Lab. Clin. Med.* 41 (1953) 56–64.
- [154] H. Meecham, P. Humphrey, Industrial exposure to cobalt causing optic atrophy and nerve deafness: A case report, *J. Neurol Neurosurg Psychiatry.* 54 (1994) 374–375.
- [155] A. Bala, C.T. Penrose, T.M. Seyler, T.R. Randell, S.S. Wellman, M.P. Bolognesi, Is Metal-On-Metal Total Hip Arthroplasty Associated With Neurotoxicity?, *J. Arthroplasty.* 31 (2016) 233-236.e1.
- [156] J.R. Prentice, C.S. Blackwell, N. Raoof, P. Bacon, J. Ray, S.J. Hickman, J.M. Wilkinson, Auditory and visual health after ten years of exposure to metal-on-metal hip prostheses: A cross-sectional study follow up, *PLoS One.* 9 (2014).
- [157] L. Leysens, B. Vinck, C. Van Der Straeten, K. De Smet, I. Dhooge, F.L. Wuyts, H. Keppler, S. Degeest, R. Valette, R. Lim, L. Maes, The Ototoxic Potential of Cobalt From Metal-on-Metal Hip Implants, *Ear Hear.* XX (2019) 1–14.
- [158] T. Unsworth-smith, M. Hons, J.C. Khan, R.J.K. Khan, F. Eng, E. Chelva, C.A. Lim, S. Haebich, B. Phys, M.L. Trevenen, Impact of Raised Serum Cobalt Levels From Recalled Articular Surface Replacement Hip Prostheses on the Visual Pathway, *J. Arthroplasty.* (2017).
- [159] B. Moretti, V. Pesce, G. Maccagnano, G. Vicenti, P. Lovreglio, L. Soleo, P. Apostoli, Peripheral neuropathy after hip replacement failure: is vanadium the culprit?, *Lancet.* 379 (2012) 1676.
- [160] D.J. Paustenbach, D. a Galbraith, B.L. Finley, Interpreting cobalt blood concentrations in hip implant patients., *Clin. Toxicol. (Phila).* 52 (2014) 98–112.
- [161] A. La Grutta, G. Amato, S. Fedele, S. Vitaliti, Intossicazione cronica da cobalto. Presentazione di un caso clinico di cardiomiopatia, *Minerva Pediatr.* 36 (1984) 691–697.
- [162] I.H. Manifold, M.M. Platts, a Kennedy, Cobalt cardiomyopathy in a patient on maintenance haemodialysis., *Br. Med. J.* 2 (1978) 1609.
- [163] M. Barborik, J. Dusek, Cardiomyopathy accompanying industrial cobalt exposure., *Br. Heart J.* 34 (1972) 113–116.
- [164] A. Kennedy, J. Dornan, R. King, Fatal myocardial disease associated with industrial exposure to cobalt, 317 (1981) 412–414.
- [165] a Linna, P. Oksa, K. Groundstroem, M. Halkosaari, P. Palmroos, S. Huikko, J. Uitti, Exposure to cobalt in the production of cobalt and cobalt compounds and its effect on the heart., *Occup. Environ. Med.* 61 (2004) 877–885.
- [166] F. D’Adda, D. Borleri, M. Migliori, G. Mosconi, G. Medolago, G. Virota, F. Colombo, P. Seghizzi, Cardiac function study in hard metal workers, *Sci. Total Environ.* 150 (1994) 179–186.
- [167] Y. Morin, A. Foley, G. Martineau, J. Roussel, Quebec beer-drinkers’ cardiomyopathy: forty-eight cases, *Can. Med. Assoc. J.* 97 (1967) 881–883.
- [168] M. Sullivan, B. Carson, J. Parker, Tissue cobalt content in “beer drinkers” myocardopathy”, *J. Lab. Clin. Med.* 71 (1968) 893–911.
- [169] H. Kesteloot, J. Roelandt, J. Willems, An enquiry into the role of cobalt in the heart disease of chronic beer drinkers, *Circulation.* 37 (1968) 854–64.
- [170] M. Packer, Cobalt cardiomyopathy: a critical reappraisal in light of a recent resurgence, *Circ. Hear. Fail.* 9 (2016) 1–10.
- [171] P. Seghizzi, F. D’Adda, D. Borleri, F. Barbic, G. Mosconi, Cobalt myocardopathy. A critical review of literature, *Sci. Total Environ.* 150 (1994) 105–109.

- [172] G. Rona, Experimental aspects of cobalt cardiomyopathy, *Br. Heart J.* 33 (1971) 171–174.
- [173] C.S. Alexander, Cobalt and the heart, *Ann Intern Med.* 70 (1969) 411–314.
- [174] M.H. Gillam, N.L. Pratt, M.C.S. Inacio, E.E. Roughead, S. Shakib, S.J. Nicholls, S.E. Graves, Heart failure after conventional metal-on-metal hip replacements, *Acta Orthop.* 3674 (2016) 1–9.
- [175] S.A. Sabah, J.C. Moon, S. Jenkins-Jones, C.L. Morgan, C.J. Currie, J.M. Wilkinson, M. Porter, G. Captur, J. Henckel, N. Chaturvedi, P. Kay, J.A. Skinner, A.H. Hart, C. Manisty, The risk of cardiac failure following metal-on-metal hip arthroplasty, *Bone Joint J.* 100-B (2018) 20–27.
- [176] L.H. Goodnough, A. Bala, J.I. Huddleston III, S.B. Goodman, W.J. Maloney, D.F. Amanatullah, Metal-on-metal total hip arthroplasty is not associated with cardiac disease, *Bone Joint J.* 100-B (2018) 28–32.
- [177] F. Lodge, R. Khatun, A. Fraser, Z. Yousef, Metal-on-metal hip replacements and subclinical evidence of myocardial dysfunction, *Heart.* 103 (2017) A1–A162.
- [178] J.R. Prentice, M.J. Clark, N. Hoggard, A.C. Morton, C. Tooth, M.N. Paley, I. Stockley, M. Hadjivassiliou, J.M. Wilkinson, Metal-on-metal hip prostheses and systemic health: A cross-sectional association study 8 years after implantation, *PLoS One.* 8 (2013) 1–9.
- [179] R. Berber, A. Abdel-Gadir, S. Rosmini, G. Captur, S. Nordin, V. Culotta, L. Palla, P. Kellman, G.W. Lloyd, J.A. Skinner, F. Orth, J.C. Moon, C. Manisty, A.J. Hart, F. Orth, Assessing for cardiotoxicity from metal-on-metal hip implants with advanced multimodality imaging techniques, *J. Bone Jt. Surg. Am.* 99 (2017) 1827–1835.
- [180] D. Juneau, G. Grammatopoulos, A. Alzahrani, R. Thornhill, J.R. Inacio, A. Dick, K.I. Vogel, J. Dobransky, P.E. Beaulé, G. Dwivedi, Is end-organ surveillance necessary in patients with well-functioning metal-on-metal hip resurfacings?, *Bone Joint J.* 101-B (2019) 540–546.
- [181] P. Hantson, Mechanisms of toxic cardiomyopathy., *Clin. Toxicol.* 0 (2018) 1–9.
- [182] C. Manisty, J. Skinner, J.C. Moon, Metal-on-metal hips and heart failure – Can we relax?, *Int. J. Cardiol.* (2018) 9–10.
- [183] A. Petit, F. Mwale, C. Tkaczyk, J. Antoniou, D.J. Zukor, O.L. Huk, Induction of protein oxidation by cobalt and chromium ions in human U937 macrophages, *Biomaterials.* 26 (2005) 4416–4422.
- [184] A. Hartwig, D. Beyersmann, A. Hartwig, Carcinogenic metal compounds: Recent insight into molecular and cellular mechanisms and cellular mechanisms, *Arch. Toxicol.* (2008) 82:493.
- [185] E.L. Baldwin, J.A.W. Byl, N. Osheroff, Cobalt Enhances DNA Cleavage Mediated by Human Topoisomerase II $\alpha$  in Vitro and in Cultured Cells, *Biochemistry.* 43 (2004) 728–735.
- [186] J.M. Matés, J.A. Segura, F.J. Alonso, J. Márquez, Roles of dioxins and heavy metals in cancer and neurological diseases using ROS-mediated mechanisms, *Free Radic. Biol. Med.* 49 (2010) 1328–1341.
- [187] A.A. Shabaan, V. Marks, M.C. Lancaster, G.N. Dufeu, Fibrosarcomas induced by cobalt chloride (CoCl<sub>2</sub>) in rats, *Lab. Anim.* 11 (1977) 43–46.
- [188] D. Lison, M. De Boeck, V. Verougstraete, M. Kirsch-Volders, Update on the genotoxicity and carcinogenicity of cobalt compounds., *Occup. Environ. Med.* 58 (2001) 619–25.
- [189] E. Dunstan, D. Ladon, P. Whittingham-Jones, R. Carrington, T.W.R. Briggs, Chromosomal aberrations in the peripheral blood of patients with metal-on-metal hip bearings., *J. Bone Joint Surg. Am.* 90 (2008) 517–522.
- [190] A.T. Doherty, R.T. Howell, L.A. Ellis, I. Bisbinas, I.D. Learmonth, R. Newson, C.P. Case, Increased chromosome translocations and aneuploidy in peripheral blood lymphocytes of patients having revision arthroplasty of the hip, *J. Bone Jt. Surg.* 83 (2001) 1075–1081.
- [191] W. V. Christian, L.D. Oliver, D.J. Paustenbach, M.L. Kreider, B.L. Finley, Toxicology-based cancer causation analysis of CoCr-containing hip implants: A

- quantitative assessment of genotoxicity and tumorigenicity studies, *J. Appl. Toxicol.* 34 (2014) 939–967.
- [192] R. Tharani, F.J. Dorey, T.P. Schmalzried, The risk of cancer following total hip or knee arthroplasty, *J. Bone Joint Surg. Am.* 83-A (2001) 774–780.
- [193] T. Visuri, E. Pukkala, P. Paavolainen, P. Pulkkinen, E.B. Riska, Cancer risk after metal on metal and polyethylene on metal total hip arthroplasty, *Clin Orthop Relat Res.* 4000 (1996) S280-289.
- [194] T. Visuri, P. Pulkkinen, P. Paavolainen, E. Pukkala, Cancer risk is not increased after conventional hip arthroplasty: A nationwide study from the Finnish Arthroplasty Register with follow-up of 24,636 patients for a mean of 13 years, *Acta Orthop.* 81 (2010) 77–81.
- [195] K.T. Mäkelä, T. Visuri, P. Pulkkinen, A. Eskelinen, V. Remes, P. Virolainen, M. Junnila, E. Pukkala, Risk of cancer with metal-on-metal hip replacements: population based study., *BMJ.* 345 (2012) e4646.
- [196] T. Onega, J. Baron, T. MacKenzie, Cancer after total joint arthroplasty: A meta-analysis, *Cancer Epidemiol. Biomarkers Prev.* 15 (2006) 1532–1537.
- [197] E. Mathiesen, A. Ahlbom, G. Bermann, J. Lindgren, Total hip replacement and cancer. A cohort study, *J. Bone Joint Surg. Br.* 77-B (1995) 345–350.
- [198] A.J. Smith, P. Dieppe, M. Porter, A.W. Blom, Risk of cancer in first seven years after metal-on-metal hip replacement compared with other bearings and general population: linkage study between the National Joint Registry of England and Wales and hospital episode statistics., *BMJ.* 344 (2012) e2383.
- [199] V. Levašič, I. Milošev, V. Zadnik, Risk of cancer after primary total hip replacement : The influence of bearings , cementation and the material of the stem Risk of cancer after primary total hip replacement : The influence of bearings , cementation and the material of the stem A retros, *Acta Orthop.* 3674 (2018).
- [200] L. Signorello, W. Ye, J. Fryzek, L. Lipworth, J. Fraumeni Jr., W. Blot, J. McLaughlin, Nationwide study of cancer risk among hip replacement patients in Sweden, *J. Natl. Cancer Inst.* 93 (2001) 1405–1410.
- [201] T. Visuri, E. Pukkala, P. Pulkkinen, P. Paavolainen, Decreased cancer risk in patients who have been operated on with total hip and knee arthroplasty for primary osteoarthritis, *Acta Orthop. Scand.* 74 (2003) 351–360.
- [202] T.I. Visuri, E. Pukkala, P. Pulkkinen, P. Paavolainen, Cancer incidence and causes of death among total hip replacement patients: a review based on Nordic cohorts with a special emphasis on metal-on-metal bearings, *Nat. Nanotechnology.* 220 (2006) 399–407.
- [203] D.H. Brewster, D.L. Stockton, A. Reekie, G.P. Ashcroft, C.R. Howie, D.E. Porter, R.J. Black, Risk of cancer following primary total hip replacement or primary resurfacing arthroplasty of the hip: A retrospective cohort study in Scotland, *Br. J. Cancer.* 108 (2013) 1883–1890.
- [204] M. Yang, A current global view of environmental and occupational cancers, *J. Environ. Sci. Heal. - Part C Environ. Carcinog. Ecotoxicol. Rev.* 29 (2011) 223–249.
- [205] WHO, IARC Monographs on the evaluation of carcinogenic risks to humans. Cobalt in Hard Metals and Cobalt Sulfate , Gallium Arsenide , Indium Phosphide and Vanadium Pentoxide, *World Heal. Organ. Int. Agency Reserach Cancer, Lyon Fr.* 86 (2006) 3–5.
- [206] D.J. Paustenbach, B.E. Tvermoes, K.M. Unice, B.L. Finley, B.D. Kerger, A review of the health hazards posed by cobalt, *Crit. Rev. Toxicol.* 43 (2013) 316–62.
- [207] A. Nyga, A. Hart, T.D. Tetley, Importance of the HIF pathway in cobalt nanoparticle-induced cytotoxicity and inflammation in human macrophages Importance of the HIF pathway in cobalt nanoparticle-induced cytotoxicity and inflammation in human macrophages, *Nanotoxicology.* 5390 (2015) 905–917.
- [208] G. Semenza, HIF-1: mediator of physiological and pathophysiological responses to hypoxia, *J. Appl. Physiol.* 88 (2000) 1474–1480.
- [209] V. Waris, T. Sillat, E. Waris, L. Virkki, J. Mandelin, M. Takagi, Y.T. Konttinen, Role and regulation of VEGF and its receptors 1 and 2 in the aseptic loosening of total hip



- implants, *J. Orthop. Res.* 30 (2012) 1830–1836.
- [210] L. Samelko, M.S. Caicedo, S.J. Lim, C. Della-Valle, J. Jacobs, N.J. Hallab, Cobalt-Alloy Implant Debris Induce HIF-1 $\alpha$  Hypoxia Associated Responses: A Mechanism for Metal-Specific Orthopedic Implant Failure, *PLoS One.* 8 (2013) 1–7.
- [211] S.G. Lee, H. Lee, H.M. Rho, Transcriptional repression of the human p53 gene by cobalt chloride mimicking hypoxia, *FEBS Lett.* 507 (2001) 259–263.
- [212] C.J. Smith, T.A. Perfetti, In vitro cobalt-stimulated hypoxia-inducible factor-1 overexpression does not correlate with cancer risk from cobalt exposure in humans, *Toxicol. Res. Appl.* 3 (2019) 239784731985016.
- [213] D. Beyersmann, A. Hartwig, Carcinogenic metal compounds: Recent insight into molecular and cellular mechanisms, *Arch. Toxicol.* 82 (2008) 493–512.
- [214] S. Catalani, M. Rizzetti, A. Padovani, P. Apostoli, Neurotoxicity of cobalt, *Hum. Exp. Toxicol.* 31 (2012) 421–437.
- [215] E. Kopera, T. Schwerdtle, A. Hartwig, W. Bal, Co(II) and Cd(II) substitute for Zn(II) in the zinc finger derived from the DNA repair protein XPA, demonstrating a variety of potential mechanisms of toxicity, *Chem. Res. Toxicol.* 17 (2004) 1452–1458.
- [216] P.D. Darbre, Metalloestrogens: An emerging class of inorganic xenoestrogens with potential to add to the oestrogenic burden of the human breast, *J. Appl. Toxicol.* 26 (2006) 191–197.
- [217] C.S. Watson, Y.J. Jeng, M.Y. Kochukov, Nongenomic signaling pathways of estrogen toxicity, *Toxicol. Sci.* 115 (2010) 1–11.
- [218] U.E. Pazzaglia, P. Apostoli, T. Congiu, S. Catalani, M. Marchese, G. Zarattini, Cobalt, chromium and molybdenum ions kinetics in the human body : data gained from a total hip replacement with massive third body wear of the head and neuropathy by cobalt intoxication, *Arch. Orthop. Trauma Surg.* 131 (2011) 1299–1308.
- [219] R. Saha, R. Nandi, B. Saha, Sources and toxicity of hexavalent chromium, *J. Coord. Chem.* 64 (2011) 1782–1806.
- [220] R. Welling, J.J. Beaumont, S.J. Petersen, G. V Alexeeff, C. Steinmaus, Chromium(VI) and stomach cancer: a meta-analysis of the current epidemiological evidence., *Occup. Environ. Med.* 72 (2015) 151–9.
- [221] A. Levina, T.H.N. Pham, P.A. Lay, Binding of Chromium(III) to Transferrin Could Be Involved in Detoxification of Dietary Chromium(III) Rather than Transport of an Essential Trace Element, *Angew. Chemie - Int. Ed.* 55 (2016) 8104–8107.
- [222] L.E. Wu, A. Levina, H.H. Harris, Z. Cai, B. Lai, S. Vogt, D.E. James, P.A. Lay, Carcinogenic chromium(VI) compounds formed by intracellular oxidation of chromium(III) dietary supplements by adipocytes, *Angew. Chemie - Int. Ed.* 55 (2016) 1742–1745.
- [223] J.B. Vincent, The potential value and toxicity of chromium picolinate as a nutritional supplement, weight loss agent and muscle development agent, *Sport. Med.* 33 (2003) 213–230.
- [224] H.J. Cooper, R.M. Urban, R.L. Wixson, R.M. Meneghini, J.J. Jacobs, Adverse local tissue reaction arising from corrosion at the femoral neck-body junction in a dual-taper stem with a cobalt-chromium modular neck., *J. Bone Joint Surg. Am.* 95 (2013) 865–72.
- [225] A.J. Hart, P.D. Quinn, B. Sampson, A. Sandison, K.D. Atkinson, J.A. Skinner, J.J. Powell, J.F.W. Mosselmans, The chemical form of metallic debris in tissues surrounding metal-on-metal hips with unexplained failure, *Acta Biomater.* 6 (2010) 4439–4446.
- [226] M. Saxena, S.A. Loza-Rosas, K. Gaur, S. Sharma, S.C. Pérez Otero, A.D. Tinoco, Exploring titanium(IV) chemical proximity to iron(III) to elucidate a function for Ti(IV) in the human body, *Coord. Chem. Rev.* 363 (2018) 109–125.
- [227] C. Minoia, A. Cavalleri, Chromium in urine, serum and red blood cells in the biological monitoring of workers exposed to different chromium valency states, *Sci. Total Environ.* 71 (1988) 323–327.
- [228] K. Merritt, S.A. Brown, Release of hexavalent chromium from corrosion of stainless steel and cobalt—chromium alloys, *J. Biomed. Mater. Res.* 29 (1995) 627–633.

- [229] A. Bartolozzi, J. Black, Chromium concentrations in serum, blood clot and urine from patients following total hip arthroplasty, *Biomaterials*. 6 (1985) 2–8.
- [230] S.. MacDonald, R.. McCalden, D.. Chess, R.. Bourne, C.. Rorabeck, D. Cleland, F. Leung, Metal-on-metal versus polyethylene in hip arthroplasty: a randomized clinical trial., *Clin. Orthop. Relat. Res.* (2003) 282–96.
- [231] B. Finley, P.K. Scott, M.E. Glynn, D. Paustenbach, K.A. Thuett, B. Finley, P.K. Scott, M.E. Glynn, D. Paustenbach, E. Donovan, K.A. Thuett, Chromium speciation in the blood of metal-on- metal hip implant patients, *Toxicol. Environ. Chem.* 99 (2017) 48–64.
- [232] R.P. Wedeen, L. Qian, Chromium-induced kidney disease, *Environ. Health Perspect.* 92 (1991) 71–74.
- [233] G.M. Keegan, I.D. Learmonth, C.P. Case, A systematic comparison of the actual, potential, and theoretical health effects of cobalt and chromium exposures from industry and surgical implants., *Crit. Rev. Toxicol.* 38 (2008) 645–674.
- [234] P.J. Barnard, A. Levina, P.A. Lay, Chromium (V) peptide complexes: synthesis and spectroscopic characterization, *Inorg. Chem.* 44 (2005) 805–809.
- [235] K.P. Nickens, S.R. Patierno, S. Ceryak, Chromium genotoxicity: A double-edged sword, *Chem. Biol. Interact.* 188 (2010) 276–288.
- [236] J.J. Beaumont, R.M. Sedman, S.D. Reynolds, C.D. Sherman, L.H. Li, R.A. Howd, M.S. Sandy, L. Zeise, G. V. Alexeeff, Cancer mortality in a Chinese population exposed to hexavalent chromium in drinking water, *Epidemiology.* 19 (2008) 12–23.
- [237] A. Linos, A. Petralias, C.A. Christophi, E. Christoforidou, P. Kouroutou, M. Stolidis, A. Veloudaki, E. Tzala, K.C. Makris, M.R. Karagas, Oral ingestion of hexavalent chromium through drinking water and cancer mortality in an industrial area of Greece - An ecological study, *Environ. Heal. A Glob. Access Sci. Source.* 10 (2011) 50.
- [238] S.W. Fage, J. Muris, S.S. Jakobsen, J.P. Thyssen, Titanium: a review on exposure, release, penetration, allergy, epidemiology, and clinical reactivity, *Contact Dermatitis.* 74 (2016) 323–345.
- [239] A. Weir, P. Westerhoff, L. Fabricius, K. Hristovski, N. Von Goetz, Titanium dioxide nanoparticles in food and personal care products, *Environ. Sci. Technol.* 46 (2012) 2242–2250.
- [240] I.P. Parkin, R.G. Palgrave, Self-cleaning coatings, *J. Mater. Chem.* 15 (2005) 1689–1695.
- [241] M.C.E. Lomer, C. Hutchinson, S. Volkert, S.M. Greenfield, A. Catterall, R.P.H. Thompson, J.J. Powell, Dietary sources of inorganic microparticles and their intake in healthy subjects and patients with Crohn’s disease, *Br. J. Nutr.* 92 (2004) 947–955.
- [242] K.M. Buettner, A.M. Valentine, Bioinorganic Chemistry of Titanium, *Chem. Rev.* 112 (2012) 1863–1881.
- [243] A.D. Tinoco, E. V Eames, A.M. Valentine, Reconsideration of Serum Ti (IV) Transport : Albumin and Transferrin Trafficking of Ti(IV) and Its Complexes, *JACS.* 130 (2008) 2262–2270.
- [244] C.J.L. Silwood, M. Grootveld, Chemical nature of implant-derived titanium(IV) ions in synovial fluid, *Biochem. Biophys. Res. Commun.* 330 (2005) 784–790.
- [245] E. Fabian, R. Landsiedel, L. Ma-Hock, K. Wiench, W. Wohlleben, B. Van Ravenzwaay, Tissue distribution and toxicity of intravenously administered titanium dioxide nanoparticles in rats, *Arch. Toxicol.* 82 (2008) 151–157.
- [246] A. Sarmiento-González, J.M. Marchante-Gayón, J.M. Tejerina-Lobo, J. Paz-Jiménez, A. Sanz-Medel, High-resolution ICP-MS determination of Ti, V, Cr, Co, Ni, and Mo in human blood and urine of patients implanted with a hip or knee prosthesis, *Anal. Bioanal. Chem.* 391 (2008) 2583–2589.
- [247] B.R. Levine, A.R. Hsu, A.K. Skipor, N.J. Hallab, W.G. Paprosky, J.O. Galante, J.J. Jacobs, Ten-Year Outcome of Serum Metal Ion Levels After Primary Total Hip Arthroplasty, *J. Bone Jt. Surg.* 95 (2013) 512–518.
- [248] R.M. Urban, J.J. Jacobs, M.J. Tomlinson, J. Gavrilovic, J. Black, M. Peoc’h, Dissemination of wear particles to the liver, spleen, and abdominal lymph nodes of patients with hip or knee replacement, *J. Bone Joint Surg. Am.* 82-A (2000) 457–476.

- [249] J. Jacobs, R. Urban, J. Wall, J. Black, J. Reid, L. Veneman, Unusual Foreign-Body Reaction to a Failed Total Knee Replacement: Simulation of a Sarcoma Clinically and a Sarcoid Histologically, *J. Bone Jt. Surg.* 77-A (1995) 444–451.
- [250] P. Hallam, F. Haddad, J. Cobb, Pain in the well-fixed, aseptic titanium hip replacement, *J. Bone Jt. Surg.* 86-B (2004) 27–30.
- [251] J.C.K. Lai, M.B. Lai, S. Jandhyam, V. V. Dukhande, A. Bhushan, C.K. Daniels, S.W. Leung, Exposure to titanium dioxide and other metallic oxide nanoparticles induces cytotoxicity on human neural cells and fibroblasts, *Int. J. Nanomedicine.* 3 (2008) 533–545.
- [252] C. Jin, B. Zhu, X. Wang, Q. Lu, Cytotoxicity of Titanium Dioxide Nanoparticles in Mouse Fibroblast Cells Cytotoxicity of Titanium Dioxide Nanoparticles in Mouse Fibroblast, *Chem. Res. Toxicol.* 21 (2008) 1871–1877. doi:10.1021/tx800179f.
- [253] M. Goutam, C. Giriya-pura, S. Mishra, S. Gupta, Titanium allergy: A literature review, *Indian J. Dermatol.* 59 (2014) 630.
- [254] J.J. Wang, B.J.S. Sanderson, H. Wang, Cyto- and genotoxicity of ultrafine TiO<sub>2</sub> particles in cultured human lymphoblastoid cells, *Mutat. Res.* 628 (2007) 99–106.
- [255] J.J. Yao, E.A. Lewallen, W.H. Trousdale, W. Xu, R. Thaler, C.G. Salib, N. Reina, M.P. Abdel, D.G. Lewallen, A.J. Van Wijnen, Local Cellular Responses to Titanium Dioxide from Orthopedic Implants, *BioResearch.* 6 (2017) 94–103.
- [256] H. Zreiqat, T.N. Crotti, C.R. Howlett, M. Capone, B. Markovic, D.R. Haynes, Prosthetic particles modify the expression of bone-related proteins by human osteoblastic cells in vitro, *Biomaterials.* 24 (2003) 337–346.
- [257] D. Cadosch, E. Chan, O.P. Gautschi, L. Filgueira, Metal is not inert: Role of metal ions released by biocorrosion in aseptic loosening - Current concepts, *J. Biomed. Mater. Res. - Part A.* 91 (2009) 1252–1262.
- [258] M. Sakamoto, H. Watanabe, H. Higashi, H. Kubosawa, Pseudotumor caused by titanium particles from a total hip prosthesis, *Orthopedics.* 39 (2016) e162–e165.
- [259] L. Sheng, X. Wang, X. Sang, Y. Ze, X. Zhao, D. Liu, S. Gui, Q. Sun, J. Cheng, Z. Cheng, R. Hu, L. Wang, F. Hong, Cardiac oxidative damage in mice following exposure to nanoparticulate titanium dioxide, *J. Biomed. Mater. Res. - Part A.* 101 (2013) 3238–3246.
- [260] F. Hong, N. Wu, X. Zhao, Y. Tian, Y. Zhou, T. Chen, Y. Zhai, L. Ji, Titanium dioxide nanoparticle-induced dysfunction of cardiac hemodynamics is involved in cardiac inflammation in mice, *J. Biomed. Mater. Res. - Part A.* 104 (2016) 2917–2927.
- [261] H.R.H. Mohamed, N.A. Hussien, Genotoxicity Studies of Titanium Dioxide Nanoparticles (TiO<sub>2</sub>NPs) in the Brain of Mice, *Scientifica (Cairo).* 2016 (2016) 1–7.
- [262] R. Hu, X. Gong, Y. Duan, N. Li, Y. Che, Y. Cui, M. Zhou, C. Liu, H. Wang, F. Hong, Neurotoxicological effects and the impairment of spatial recognition memory in mice caused by exposure to TiO<sub>2</sub> nanoparticles, *Biomaterials.* 31 (2010) 8043–8050.
- [263] A. Mohammadipour, M. Hosseini, A. Fazel, H. Haghiri, H. Rafatpanah, M. Pourganji, A.E. Bideskan, The effects of exposure to titanium dioxide nanoparticles during lactation period on learning and memory of rat offspring, *Toxicol. Ind. Health.* 32 (2016) 221–228.
- [264] A. Sarmiento-González, J.R. Encinar, J.M. Marchante-Gayón, A. Sanz-Medel, Titanium levels in the organs and blood of rats with a titanium implant, in the absence of wear, as determined by double-focusing ICP-MS, *Anal. Bioanal. Chem.* 393 (2009) 335–343.
- [265] J.L. Woodman, J.J. Jacobs, J.O. Galante, R.M. Urban, Metal ion release from titanium-based prosthetic segmental replacements of long bones in baboons: A long term study, *J. Orthop. Res.* 1 (1983) 421–430.
- [266] C.A. Moran, F.G. Mullick, K.G. Ishak, F.B. Johnson, W.B. Hummer, Identification of titanium in human tissues: Probable role in pathologic processes, *Hum. Pathol.* 22 (1991) 450–454.
- [267] Z. Chen, Y. Wang, L. Zhuo, S. Chen, L. Zhao, X. Luan, H. Wang, G. Jia, Effect of titanium dioxide nanoparticles on the cardiovascular system after oral administration, *Toxicol. Lett.* 239 (2015) 123–130.

- [268] H. Liu, L. Ma, J. Zhao, J. Liu, J. Yan, J. Ruan, F. Hong, Biochemical toxicity of nano-anatase TiO<sub>2</sub> particles in mice, *Biol. Trace Elem. Res.* 129 (2009) 170–180.
- [269] P.P. Fu, Q. Xia, H.M. Hwang, P.C. Ray, H. Yu, Mechanisms of nanotoxicity: Generation of reactive oxygen species, *J. Food Drug Anal.* 22 (2014) 64–75.
- [270] K. Onuma, Y. Sato, S. Ogawara, N. Shirasawa, M. Kobayashi, J. Yoshitake, T. Yoshimura, M. Iigo, J. Fujii, F. Okada, Nano-scaled particles of titanium dioxide convert benign mouse fibrosarcoma cells into aggressive tumor cells, *Am. J. Pathol.* 175 (2009) 2171–2183.
- [271] N. Coen, M.A. Kadhim, E.G. Wright, C.P. Case, C.E. Mothersill, Particulate debris from a titanium metal prosthesis induces genomic instability in primary human fibroblast cells, *Br. J. Cancer.* 88 (2003) 548–552.
- [272] IARC. Carbon black, titanium dioxide, and talc. IARC monographs on the evaluation of carcinogenic risks to humans, vol. 93. International Agency for Research on Cancer: Lyon, France, 2006.
- [273] NIOSH. Occupational Exposure to Titanium Dioxide. Department Of Health And Human Services, Centers for Disease Control and Prevention, National Institute for Occupational Safety and Health (2011).
- [274] A.J. Hart, A. Sandison, P. Quinn, B. Sampson, K.D. Atkinson, J. a Skinner, A. Goode, J.J. Powell, J.F.W. Mosselmans, Microfocus study of metal distribution and speciation in tissue extracted from revised metal on metal hip implants, *J. Phys. Conf. Ser.* 190 (2009) 1–5.
- [275] M. Huber, G. Reinisch, G. Trettenhahn, K. Zweymüller, F. Lintner, Presence of corrosion products and hypersensitivity-associated reactions in periprosthetic tissue after aseptic loosening of total hip replacements with metal bearing surfaces, *Acta Biomater.* 5 (2009) 172–180.
- [276] I. Swiatkowska, J.F.W. Mosselmans, T. Geraki, C.C. Wyles, J.J. Maleszewski, J. Henckel, B. Sampson, D.B. Potter, I. Osman, R.T. Trousdale, A.J. Hart, Synchrotron analysis of human organ tissue exposed to implant material, *J. Trace Elem. Med. Biol.* 46 (2018) 128–137.
- [277] C.P. Case, V.G. Langkamer, C. James, M.R. Palmer, A.J. Kemp, P.F. Heap, L. Solomon, Widespread dissemination of metal debris from implants, *J. Bone Jt. Surgery.* 76 (1994) 701–12.
- [278] R.M. Urban, M.J. Tomlinson, D.J. Hall, J.J. Jacobs, Accumulation in liver and spleen of metal particles generated at nonbearing surfaces in hip arthroplasty, *J. Arthroplasty.* 19 (2004) 94–101.
- [279] A. Abdel-Gadir, R. Berber, J.B. Porter, P.D. Quinn, D. Suri, P. Kellman, A.J. Hart, J.C. Moon, C. Manisty, J.A. Skinner, Detection of metallic cobalt and chromium liver deposition following failed hip replacement using T2\* and R2 magnetic resonance, *J. Cardiovasc. Magn. Reson.* 18 (2016) 29.
- [280] O. Addison, A.J. Davenport, R.J. Newport, S. Kalra, M. Monir, F.W. Mosselmans, D. Proops, R.A. Martin, Do “passive” medical titanium surfaces deteriorate in service in the absence of wear?, *J. R. Soc. Interface.* 9 (2012) 3161–3164.
- [281] K. De Smet, R. De Haan, A. Calistri, P.A. Campbell, E. Ebramzadeh, C. Pattyn, H.S. Gill, Metal ion measurement as a diagnostic tool to identify problems with metal-on-metal hip resurfacing, *J. Bone Jt. Surg. - Ser. A.* 90 (2008) 202–208.
- [282] D. Koller, P. Bramhall, J. Devoy, H. Goenaga-Infante, C.F. Harrington, E. Leese, J. Morton, S. Nuñez, J. Rogers, B. Sampson, J.J. Powell, Analysis of soluble or titanium dioxide derived titanium levels in human whole blood: consensus from an inter-laboratory comparison, *Analyst.* 143 (2018) 5520–5529.
- [283] J.R. Campbell, M.P. Estey, Metal release from hip prostheses: cobalt and chromium toxicity and the role of the clinical laboratory, *Clin. Chem. Lab. Med.* 51 (2013) 213–220.
- [284] C.I. Hur, T.R. Yoon, S.G. Cho, E.K. Song, J.K. Seon, Serum ion level after metal-on-metal THA in patients with renal failure, *Clin. Orthop. Relat. Res.* 466 (2008) 696–699.
- [285] C. Delaunay, I. Petit, I.D. Learmonth, P. Oger, P.A. Vendittoli, Metal-on-metal

- bearings total hip arthroplasty: The cobalt and chromium ions release concern, *Orthop. Traumatol. Surg. Res.* 96 (2010) 894–904.
- [286] A. Sarmiento-Gonzalez, J.M. Marchante-Gayon, J. Tejerina-Lobo, J. Paz-Jimenez, A. Sanz-Medel, ICP-MS multielemental determination of metals potentially released from dental implants and articular prostheses in human biological fluids, *Anal. Bioanal. Chem.* 382 (2005) 1001–1009.
- [287] C.P. Case, L. Ellis, J.C. Turner, B. Fairman, Development of a routine method for the determination of trace metals in whole blood by magnetic sector inductively coupled plasma mass spectrometry with particular relevance to patients with total hip and knee arthroplasty, *Clin. Chem.* 47 (2001) 275–280.
- [288] S.J. MacDonald, W. Brodner, J.J. Jacobs, A consensus paper on metal ions in metal-on-metal hip arthroplasties, *J. Arthroplasty.* 19 (2004) 12–16.
- [289] B.D. Kerger, R. Gerads, H. Gurleyuk, K.A. Thuett, B.L. Finley, D.J. Paustenbach, Cobalt speciation assay for human serum, Part I. Method for measuring large and small molecular cobalt and protein-binding capacity using size exclusion chromatography with inductively coupled plasma-mass spectroscopy detection, *Toxicol. Environ. Chem.* 95 (2013) 687–708.
- [290] J. Jacobs, A. Skipor, J. Black, R. Urban, J. Galante, Release and excretion of metal in patients who have a total hip-replacement component made of titanium-base alloy, *J. Bone Jt. Surg.* 73-A (1991) 1475–1486.
- [291] J. Jacobs, A. Skipor, L. Patterson, N. Hallab, W. Paprosky, J. Black, J. Galante, Metal Release in Patients Who Have Had a Primary Total Hip Arthroplasty. A Prospective, Controlled, Longitudinal Study, *J. Bone Jt. Surg.* 80-A (1998) 1447–1458.
- [292] D. Granchi, L. Savarino, L. Savarino, G. Ciapetti, E. Cenni, R. Rotini, M. Mieti, N. Baldini, A. Giunti, Immunological changes in patients with primary osteoarthritis of the hip after total joint replacement, *Bone Joint J.* 85-B (2003) 758–64.
- [293] L. Savarino, G. Padovani, M. Ferretti, M. Greco, E. Cenni, G. Perrone, F. Greco, N. Baldini, A. Giunti, Serum ion levels after ceramic-on-ceramic and metal-on-metal total hip arthroplasty: 8-Year minimum follow-up, *J. Orthop. Res.* 26 (2008) 1569–1576.
- [294] L. Balcaen, E. Bolea-Fernandez, M. Resano, F. Vanhaecke, Accurate determination of ultra-trace levels of Ti in blood serum using ICP-MS/MS, *Anal. Chim. Acta.* 809 (2014) 1–8.
- [295] C.F. Harrington, C. Mckibbin, M. Rahanu, D. Langton, Titanium in hip replacement patients by Inductively Coupled Plasma Optical Emission Spectroscopy (ICP-OES), *Ann. Clin. Biochem.* 0 (2016) 1–8.
- [296] J.Y. Lazennec, P. Boyer, J. Poupon, M.A. Rousseau, C. Roy, P. Ravaud, Y. Catonné, Outcome and serum ion determination up to 11 years after implantation of a cemented metal-on-metal hip prosthesis, *Acta Orthop.* 80 (2009) 168–173.
- [297] B.L. Finley, K.M. Unice, B.D. Kerger, J.M. Otani, D.J. Paustenbach, D.A. Galbraith, B.E. Tvermoes, 31-day study of cobalt(II) chloride ingestion in humans: pharmacokinetics and clinical effects, *J. Toxicol. Environ. Heal. - Part A Curr. Issues.* 76 (2013) 1210–1224.
- [298] D. J, Z. H, P. PB, M. DJW, The validity of serum levels as a surrogate measure of systemic exposure to metal ions in hip replacement., *J. Bone Jt. Surg.* 89-B (2007) 736–41.
- [299] J. Daniel, H. Ziaee, C. Pradhan, P. Pynsent, D. McMinn, Blood and urine metal ion levels in young and active patients after Birmingham hip resurfacing arthroplasty, *J. Bone Joint Surg. Br.* 89-B (2007) 989–989.
- [300] G.A. Afolaranmi, J. Tetley, R.M.D. Meek, M.H. Grant, Release of chromium from orthopaedic arthroplasties., *Open Orthop. J.* 2 (2008) 10–18.
- [301] A.W. Newton, L. Ranganath, C. Armstrong, V. Peter, N.B. Roberts, Differential distribution of cobalt, chromium, and nickel between whole blood, plasma and urine in patients after metal-on-metal (MoM) hip arthroplasty, *J. Orthop. Res.* 30 (2012) 1640–1646.
- [302] I.A. Malek, J. Rogers, A.C. King, J. Clutton, D. Winson, A. John, H. Park, C. Cf, The Interchangeability of Plasma and Whole Blood Metal Ion Measurement in the

- Monitoring of Metal on Metal Hips, Arthritis. 2015 (2015) 1–7.
- [303] J.M. Smolders, A. Hol, C. Van Der Straeten, B.W. Schreurs, Metal ion interpretation in resurfacing versus conventional hip arthroplasty and in whole blood versus serum. How should we interpret metal ion data?, *Hip Int.* 21 (2011) 587–595.
- [304] Z. Yi, Z. Bo, S. Bin, Y. Jing, Z. Zongke, P. Fuxing, Clinical Results and Metal Ion Levels After Ceramic-on-Metal Total Hip Arthroplasty: A Mean 50-Month Prospective Single-Center Study, *J. Arthroplasty.* 31 (2016) 438–441.
- [305] M. Rahmé, M. Lavigne, J. Barry, C.M. Cirtiu, P. Bélanger, P.A. Vendittoli, Whole blood metal ion measurement reproducibility between different laboratories, *J. Arthroplasty.* 29 (2014) 2214–2218.
- [306] B.D. Kerger, R. Gerads, H. Gurleyuk, A. Urban, J. Dennis, B.D. Kerger, R. Gerads, H. Gurleyuk, A. Urban, J. Dennis, Total cobalt determination in human blood and synovial fluid using inductively coupled plasma- mass spectrometry: method validation and evaluation of performance variables affecting metal hip implant patient samples, *Toxicol. Environ. Chem.* 97 (2015) 1145–1163.
- [307] S. Grassin-Delyle, M. Martin, O. Hamzaoui, E. Lamy, C. Jayle, E. Sage, I. Etting, P. Devillier, J.C. Alvarez, A high-resolution ICP-MS method for the determination of 38 inorganic elements in human whole blood, urine, hair and tissues after microwave digestion, *Talanta.* 199 (2019) 228–237.
- [308] C.S. Muñiz, J.L. Fernández-Martin, J.M. Marchante-Gayón, J.I.G. Alonso, J.B. Cannata-Andía, A. Sanz-Medel, Reference values for trace and ultratrace elements in human serum determined by double-focusing ICP-MS, *Biol. Trace Elem. Res.* 82 (2001) 259–272.
- [309] C. Jantzen, H.L. Jørgensen, B.R. Duus, S.L. Spørring, J.B. Lauritzen, Chromium and cobalt ion concentrations in blood and serum following various types of metal-on-metal hip arthroplasties: a literature overview., *Acta Orthop.* 84 (2013) 229–36.
- [310] P. Wretenberg, Good function but very high concentrations of cobalt and chromium ions in blood 37 years after metal-on-metal total hip arthroplasty, *Med. Devices Evid. Res.* 1 (2008) 31–32.
- [311] A. Beraudix, S. Stea, D. De Pasquale, B. Bordini, S. Catalani, P. Apostoli, A. Toni, Metal ion release: Also a concern for ceramic-on-ceramic couplings?, *HIP Int.* 24 (2014) 321–326.
- [312] V.J. Rasquinha, C.S. Ranawat, J. Weiskopf, J.A. Rodriguez, A.K. Skipor, J.J. Jacobs, Serum Metal Levels and Bearing Surfaces in Total Hip Arthroplasty, *J. Arthroplasty.* 21 (2006) 47–52.
- [313] D. Nam, J.A. Keeney, R.M. Nunley, S.R. Johnson, J.C. Clohisy, R.L. Barrack, Metal ion concentrations in young, active patients following total hip arthroplasty with the use of modern bearing couples, *J. Arthroplasty.* 30 (2015) 2227–2232.
- [314] Medicines and Healthcare products Regulatory Agency (MHRA). Medical device alert: all metal-on-metal (MoM) hip replacements, 2010.
- [315] B. Sampson, A. Hart, Clinical usefulness of blood metal measurements to assess the failure of metal-on-metal hip implants., *Ann. Clin. Biochem.* 49 (2012) 118–31.
- [316] C. Van Der Straeten, G. Grammatopoulos, H.S. Gill, A. Calistri, P. Campbell, K.A. De Smet, The 2012 Otto Aufranc Award: The interpretation of metal ion levels in unilateral and bilateral hip resurfacing., *Clin. Orthop. Relat. Res.* 471 (2013) 377–385.
- [317] K.A. De Smet, C. Van Der Straeten, M. Van Orsouw, R. Doubi, K. Backers, G. Grammatopoulos, Revisions of metal-on-metal hip resurfacing: lessons learned and improved outcome, *Orthop. Clin. North Am.* 42 (2011) 259–269.
- [318] Y.A. Fillingham, C.J. Della Valle, D.D. Bohl, M.P. Kelly, D.J. Hall, R. Pourzal, J.J. Jacobs, Serum Metal Levels for Diagnosis of Adverse Local Tissue Reactions Secondary to Corrosion in Metal-on-Polyethylene Total Hip Arthroplasty, *J. Arthroplasty.* 32 (2017) S272–S277.
- [319] F. Hannemann, A. Hartmann, J. Schmitt, J. Lützner, A. Seidler, P. Campbell, C.P. Delaunay, H. Drexler, H.B. Ettema, E. García-Cimbrelo, H. Huberti, K. Knahr, J. Kunze, D.J. Langton, W. Lauer, I. Learmonth, C.H. Lohmann, M. Morlock, M.A. Wimmer, L. Zagra, K.P. Günther, European multidisciplinary consensus statement on

- the use and monitoring of metal-on-metal bearings for total hip replacement and hip resurfacing, *Orthop. Traumatol. Surg. Res.* 99 (2013) 263–271.
- [320] United States Food and Drug Administration. Information for Orthopaedic Surgeons about Metal-on-Metal Hip Implant Surgery. 8 July, 2012.
- [321] G. Grammatopoulos, M. Munemoto, A. Pollalis, N.A. Athanasou, Correlation of serum metal ion levels with pathological changes of ARMD in failed metal-on-metal-hip-resurfacing arthroplasties, *Arch. Orthop. Trauma Surg.* 137 (2017) 1129–1137.
- [322] L. Lehtovirta, A. Reito, J. Parkkinen, S. Pera, A. Eskelinen, Association between periprosthetic tissue metal content, whole blood and synovial fluid metal ion levels and histopathological findings in patients with failed metal-on-metal hip replacement, *PLoS One.* 13 (2018) 1–13.
- [323] I.A. Malek, A. King, H. Sharma, S. Malek, K. Lyons, S. Jones, A. John, The sensitivity, specificity and predictive values of raised plasma metal ion levels in the diagnosis of adverse reaction to metal debris in symptomatic patients with a metal-on-metal arthroplasty of the hip, *J. Bone Joint Surg. Br.* 94-B (2012) 1045–1050.
- [324] J. Antoniou, D.J. Zukor, F. Mwale, W. Minarik, A. Petit, O.L. Huk, Metal ion levels in the blood of patients after hip resurfacing: a comparison between twenty-eight and thirty-six-millimeter-head metal-on-metal prostheses., *J. Bone Joint Surg. Am.* 90 Suppl 3 (2008) 142–148.
- [325] A. Malviya, J.R. Ramaskandhan, R. Bowman, M. Hashmi, J.P. Holland, S. Kometa, E. Lingard, What advantage is there to be gained using large modular metal-on-metal bearings in routine primary hip replacement?, *J. Bone Joint Surg. Br.* 93-B (2011) 1602–1609.
- [326] P. Craig, G. Bancroft, A. Burton, S. Collier, P. Shaylor, A. Sinha, Raised levels of metal ions in the blood in patients who have undergone uncemented metal-on-polyethylene Trident-Accolade total hip replacement, *Bone Jt. J.* 96 B (2014) 43–47.
- [327] A.J. Hart, S. Sabah, J. Henckel, A. Lewis, J. Cobb, B. Sampson, A. Mitchell, J.A. Skinner, The painful metal-on-metal hip resurfacing, *J. Bone Jt. Surg. - Br. Vol.* 91-B (2009) 738–744.
- [328] A.J. Hart, S.A. Sabah, A.S. Bandi, P. Maggiore, P. Tarassoli, B. Sampson, J. A. Skinner, Sensitivity and specificity of blood cobalt and chromium metal ions for predicting failure of metal-on-metal hip replacement, *Bone Joint J.* 93-B (2011) 1308–1313.
- [329] A.K. Matthies, J.A. Skinner, H. Osmani, J. Henckel, A.J. Hart, Pseudotumors are common in well-positioned low-wearing metal-on-metal hips, *Clin. Orthop. Relat. Res.* 470 (2012) 1895–1906.
- [330] D.J. Langton, S.S. Jameson, T.J. Joyce, N.J. Hallab, S. Natsu, A.V.F. Nargol, Early failure of metal-on-metal bearings in hip resurfacing and large-diameter total hip replacement, *J. Bone Joint Surg. Br.* 92-B (2010) 38–46.
- [331] B.E. Tvermoes, B.L. Finley, K.M. Unice, J.M. Otani, D.J. Paustenbach, D.A. Galbraith, Cobalt whole blood concentrations in healthy adult male volunteers following two-weeks of ingesting a cobalt supplement, *Food Chem. Toxicol.* 53 (2013) 417–424.
- [332] B.E. Tvermoes, K.M. Unice, D.J. Paustenbach, B.L. Finley, J.M. Otani, D.A. Galbraith, Effects and blood concentrations of cobalt after ingestion of 1 mg/d by human volunteers for 90 d, *Am. J. Nutr.* 99 (2014) 632–646.
- [333] K.M. Unice, A.D. Monnot, S.H. Gaffney, B.E. Tvermoes, K.A. Thuett, D.J. Paustenbach, B.L. Finley, Inorganic cobalt supplementation: prediction of cobalt levels in whole blood and urine using a biokinetic model, *Food Chem. Toxicol.* 50 (2012) 2456–2461.
- [334] K.M. Unice, B.D. Kerger, D.J. Paustenbach, B.L. Finley, B.E. Tvermoes, Refined biokinetic model for humans exposed to cobalt dietary supplements and other sources of systemic cobalt exposure, *Chem. Biol. Interact.* 216 (2014) 53–74.
- [335] S. Tower, Arthroprosthetic cobaltism: identification of the at-risk patient., *Alaska Med.* 52 (2010) 28–32.
- [336] J.J. Jacobs, A.K. Skipor, P.A. Campbell, N.J. Hallab, R.M. Urban, H.C. Amstutz, Can

- metal levels be used to monitor metal-on-metal hip arthroplasties?, *J. Arthroplasty*. 19 (2004) 59–65.
- [337] T.D. Richardson, S.J. Pineda, K.B. Streng, T.A. Van Fleet, M. Macgregor, J.C. Milbrandt, J.A. Espinosa, P. Freitag, Serum titanium levels after instrumented spinal arthrodesis, *Spine (Phila. Pa. 1976)*. 33 (2008) 792–796.
- [338] C. Engh, S. MacDonald, S. Sritulanondha, A. Thompson, D. Naudie, C. Engh, Metal ion levels after metal-on-metal total hip arthroplasty: a randomized trial, *Clin Orthop Relat Res*. 467 (2009) 101–111.
- [339] Y. Nuevo Ordóñez, M. Montes-Bayón, E. Blanco-González, J. Paz-Jiménez, J.M. Tejerina-Lobo, J.M. Peña-López, A. Sanz-Medel, Metal release in patients with total hip arthroplasty by DF-ICP-MS and their association to serum proteins, *J. Anal. At. Spectrom*. 24 (2009) 1037–1043.
- [340] Y. Nuevo-Ordóñez, M. Montes-Bayón, E. Blanco-González, J. Paz-Aparicio, J.D. Raimundez, J.M. Tejerina, M.A. Peña, A. Sanz-Medel, Titanium release in serum of patients with different bone fixation implants and its interaction with serum biomolecules at physiological levels, *Anal. Bioanal. Chem*. 401 (2011) 2747–2754.
- [341] E. Dunstan, A.P. Sanghrajka, S. Tilley, P. Unwin, G. Blunn, S.R. Cannon, T.W.R. Briggs, Metal ion levels after metal-on-metal proximal femoral replacements: a 30-year follow-up., *J. Bone Joint Surg. Br*. 87 (2005) 628–631.
- [342] P.-A. Vendittoli, A. Roy, S. Mottard, J. Girard, D. Lusignan, M. Lavigne, Metal ion release from bearing wear and corrosion with 28 mm and large-diameter metal-on-metal bearing articulations: A follow-up study, *J. Bone Jt. Surg.* 92-B (2010) 12–19.
- [343] G.W. Omlor, J.P. Kretzer, J. Reinders, M.R. Streit, T. Bruckner, T. Gotterbarm, P.R. Aldinger, C. Merle, In vivo serum titanium ion levels following modular neck total hip arthroplasty-10 year results in 67 patients, *Acta Biomater*. 9 (2013) 6278–6282.
- [344] W. Gofton, P.E. Beaulé, Serum metal ions with a titanium modular neck total hip replacement system, *J. Arthroplasty*. 30 (2015) 1781–1786.
- [345] L. Dorr, R. Bloebaum, J. Emmanuel, R. Meldrum, Histologic, biochemical, and ion analysis of tissue and fluids retrieved during total hip arthroplasty, (1990) 82–95.
- [346] I.P. McAlister, M.P. Abdel, Elevated serum titanium level as a marker for failure in a titanium modular fluted tapered stem, *Orthopedics*. 39 (2016) e768–e770.
- [347] S. Grosse, H.K. Haugland, P. Lilleng, P. Ellison, G. Hallan, P. Johan, Wear particles and ions from cemented and uncemented titanium-based hip prostheses — A histological and chemical analysis of retrieval material, *J. Biomed. Mater. Res. Part B Appl. Biomater.* (2014) 709–717.
- [348] H. Quitmann, C. Wedemeyer, M. Von Knoch, K. Russe, G. Saxler, Titanium serum levels may remain elevated despite hip revision surgery for wear-through of an acetabular component, *Biomed. Tech*. 51 (2006) 27–29.
- [349] W. Brodner, P. Bitzan, V. Meisinger, A. Kaider, F. Gottsauner-Wolf, R. Kotz, Serum cobalt levels after metal-on-metal total hip arthroplasty, *J. Bone Jt. Surg. - Am. Vol*. 85 (2003) 2168–73.
- [350] S.E. Chandran, N.J. Giori, Nine-year incidence of kidney disease in patients who have had total hip arthroplasty., *J. Arthroplasty*. 26 (2011) 24–7.
- [351] D. Aslan, F. Apple, Clinical and analytical review of ischemia-modified albumin measured by the albumin cobalt binding test, *Adv. Clin. Chem*. 39 (2005) 1–10.
- [352] D. Bar-Or, E. Lau, J. V Winkler, A novel assay for cobalt-albumin binding and its potential as a marker for myocardial ischemia—a preliminary report, *J. Emerg. Med*. 19 (2000) 311–315.
- [353] A. Piwoski, M. Knapik-Kordecka, M. Warwas, Ischemia-modified albumin level in type 2 diabetes mellitus- preliminary report, *Dis. Markers*. 24 (2008) 311–7.
- [354] D. Bar-Or, L.T. Rael, E.P. Lau, N.K.R. Rao, G.W. Thomas, J. V. Winkler, R.L. Yukl, R.G. Kingston, C.G. Curtis, An analog of the human albumin N-terminus (Asp-Ala-His-Lys) prevents formation of copper-induced reactive oxygen species, *Biochem. Biophys. Res. Commun*. 284 (2001) 856–862.
- [355] R.C. Harris, N. Ismail, Extrarenal complications of the nephrotic syndrome, *Am. J. Kidney Dis*. 23 (1994) 477–497.



- [356] A. Phillips, A. Gerald Shaper, P. Whincup, Association between serum albumin and mortality from cardiovascular disease, cancer, and other causes, *Lancet*. 334 (1989) 1434–1436.
- [357] L. Minchiotti, M. Galliano, U. Kragh-Hansen, T. Peters, Mutations and polymorphisms of the gene of the major human blood protein, serum albumin, *Hum. Mutat.* 29 (2008) 1007–1016.
- [358] F. Facchin, S. Catalani, E. Bianconi, D. De Pasquale, S. Stea, A. Toni, S. Canaider, A. Beraudi, Albumin as marker for susceptibility to metal ions in metal-on-metal hip prosthesis patients, *Hum. Exp. Toxicol.* 36 (2017) 319–327.
- [359] S.C. Corr, L.A. O’Neill, Genetic variation in toll-like receptor signalling and the risk of inflammatory and immune diseases, *J. Innate Immun.* 1 (2009) 350–357.
- [360] A.J. Tyson-Capper, H. Lawrence, J.P. Holland, D.J. Deehan, J.A. Kirby, Metal-on-metal hips: cobalt can induce an endotoxin-like response, *Ann. Rheum. Dis.* 72 (2013) 460–461.
- [361] A. Del Buono, V. Denaro, N. Maffulli, Genetic susceptibility to aseptic loosening following total hip arthroplasty: A systematic review, *Br. Med. Bull.* 101 (2012) 39–55.
- [362] W.M. Mihalko, A. Kerkhof, Y. Jiao, J.D. Hallock, J. Yan, W. Gu, Genetic Predispositions in a Group of Failed Metal-on-Metal Total Hip Replacement Patients, *Orthop. Proc.* 99B (2018) 5.
- [363] H.S. Bachmann, S. Hanenkamp, B. Kornacki, U.H. Frey, M. Bau, W. Siffert, C. Wedemeyer, Gender-dependent association of the GNAS1 T393C polymorphism with early aseptic loosening after total hip arthroplasty, *J. Orthop. Res.* 26 (2008) 1562–1568.
- [364] D. Langton, R. Sidaginamale, S. Wells, B. Wainwright, J. Holland, D. Deehan, T. Joyce, A. Jafri, A. Nargol, S. Natu, Is there a genetic predisposition to ALVAL?, *Orthop. Proc.* 101B (2019) 25.
- [365] M.J. Clark, J.R. Prentice, N. Hoggard, M.N. Paley, M. Hadjivassiliou, J.M. Wilkinson, Brain structure and function in patients after metal-on-metal hip resurfacing, *Am. J. Neuroradiol.* 35 (2014) 1753–1758.
- [366] C. Van Der Straeten, D. Van Quickenborne, S. Pennynck, K. De Smet, J. Victor, Systemic toxicity of metal ions in a metal-on-metal hip arthroplasty population, *Orthop. Proc.* 95-B (2013) 187.
- [367] C.P. Van Lingen, H.B. Ettema, C. Van Der Straeten, B.J. Kollen, C.C.P.M. Verheyen, Self-reported neurological clinical manifestations of metal toxicity in metal-on-metal hip arthroplasty, *HIP Int.* 24 (2014) 568–574.
- [368] J. Jelsma, R. Senden, M. Schotanus, N. Kort, B. Grimm, I. Heyligers, Self-reported systemic complaints in patients with metal-on-metal hip arthroplasty, *Bone Jt. J.* 99-B (2017) 47.
- [369] K. Juster-Switlyk, A.G. Smith, Updates in diabetic peripheral neuropathy, *F1000Research.* 5 (2016) 738.
- [370] P. Romero-Aroca, Managing diabetic macular edema: The leading cause of diabetes blindness, *World J. Diabetes.* 2 (2011) 98.
- [371] M. Viaene, Overview of the neurotoxic effects in solvent-exposed workers, *Arch Public Heal.* (2002) 217–232.
- [372] J. Hooisma, H. Hanninen, H. Emmen, B. Kulig, Symptoms indicative of the effects of organic solvent exposure in Dutch painters, *Neurotoxicol. Teratol.* 16 (1994) 613–622.
- [373] J. Hooisma, H. Emmen, Onderzoek naar de grenswaarden voor de Neurotoxic Symptom Checklist 60 (NSC-60). Publicatie Stichting Arbouw, Amsterdam, (1992).
- [374] M.K. Viaene, R. Masschelein, J. Leenders, M. De Groof, L.J. Swerts, H.A. Roels, Neurobehavioural effects of occupational exposure to cadmium: a cross sectional epidemiological study, *Occup. Environ. Med.* 57 (2000) 19–27.
- [375] J.W.G. Meijer, A.J. Smit, E. V. Sonderen, J.W. Groothoff, W.H. Eisma, T.P. Links, Symptom scoring systems to diagnose distal polyneuropathy in diabetes: The diabetic neuropathy symptom score, 2002.
- [376] A. Ambreen, M. Hameed, U. Khan, N. Ahmed, M. Butt, Reliability of the neurological

- scores for assessment of sensorimotor neuropathy in type 2 diabetics Abstract, J Pak Med Assoc. (2000) 166.
- [377] D. Bouhassira, N. Attal, H. Alchaar, F. Boureau, B. Brochet, J. Bruxelles, G. Cunin, J. Fermanian, P. Ginies, A. Grun-Overdyking, H. Jafari-Schluep, M. Lantéri-Minet, B. Laurent, G. Mick, A. Serrie, D. Valade, E. Vicaut, Comparison of pain syndromes associated with nervous or somatic lesions and development of a new neuropathic pain diagnostic questionnaire (DN4), *Pain*. 114 (2005) 29–36.
- [378] B. Green, E. Griffiths, S. Almond, Neuropsychiatric symptoms following metal-on-metal implant failure with cobalt and chromium toxicity, *BMC Psychiatry*. 17 (2017) 33.
- [379] M. Folstein, S. Folstein, “Mini-mental state”: A practical method for grading the cognitive state of patients for the clinician, *J. Psychiatr. Res.* 12 (1975) 189–198.
- [380] T. Tombaugh, N. McIntyre, The Mini-Mental State Examination: A Comprehensive Review, *J. Am. Geriatr. Soc.* 40 (1992) 922–935.
- [381] C.P. Van Lingen, H.B. Ettema, J.R. Timmer, G. De Jong, C.C.P.M. Verheyen, Clinical manifestations in ten patients with asymptomatic metal-on-metal hip arthroplasty with very high cobalt levels, *HIP Int.* 23 (2013) 441–444.
- [382] M.R. Rahimzadeh, M.R. Rahimzadeh, S. Kazemi, A.A. Moghadamnia, Cadmium toxicity and treatment: An update, *Casp. J. Intern. Med.* 8 (2017) 135–145.
- [383] J.F.W. Mosselmans, P.D. Quinn, A.J. Dent, S.A. Cavill, S.D. Moreno, A. Peach, P.J. Leicester, S.J. Keylock, S.R. Gregory, K.D. Atkinson, J.R. Rosell, I18 - The microfocus spectroscopy beamline at the Diamond Light Source, *J. Synchrotron Radiat.* 16 (2009) 818–824.
- [384] K. Geraki, M.J. Farquharson, D. a Bradley, Concentrations of Fe, Cu and Zn in breast tissue: a synchrotron XRF study., *Phys. Med. Biol.* 47 (2002) 2327–2339.
- [385] S. Fitzgerald, Non-Destructive Micro-Analysis of Art and Archaeological Objects Using Micro-Xrf, *Archeometriai Műhely.* 3 (2008) 73–78.
- [386] S. Salem, S. Panossian, R. Krause, Experimental K and L relative x-ray emission rates, *At. Data Nucl. Data Tables.* 14 (1974) 91–109.
- [387] F. Porcaro, S. Roudeau, A. Carmona, R. Ortega, Advances in element speciation analysis of biomedical samples using synchrotron-based techniques, *Trends Anal. Chem.* 104 (2017) 22–41.
- [388] M. Costa, Toxicity and carcinogenicity of Cr(VI) in animal models and humans, *Crit. Rev. Toxicol.* 27 (1997) 431–442.
- [389] M.G. Shettlemore, K.J. Bundy, Examination of in vivo influences on bioluminescent microbial assessment of corrosion product toxicity, *Biomaterials.* 22 (2001) 2215–2228.
- [390] M. Haeri, W. Torsten, G.M. Langford, J.L. Gilbert, Biomaterials Electrochemical control of cell death by reduction-induced intrinsic apoptosis and oxidation-induced necrosis on CoCrMo alloy in vitro, *Biomaterials.* 33 (2012) 6295–6304.
- [391] Y. Hedberg, I.O. Wallinder, Metal release and speciation of released chromium from a biomedical CoCrMo alloy into simulated physiologically relevant solutions, *J. Biomed. Mater. Res. - Part B Appl. Biomater.* 102B (2014) 693–699.
- [392] P. Campbell, R. Urban, I. Catelas, A. Skipor, T. Schmalzried, Autopsy analysis thirty years after metal-on-metal total hip replacement, *J. Bone Jt. Surg.* 85 (2003) 2218–2222.
- [393] V.A. Solé, E. Papillon, M. Cotte, P. Walter, J. Susini, A multiplatform code for the analysis of energy-dispersive X-ray fluorescence spectra, *Spectrochim. Acta - Part B At. Spectrosc.* 62 (2007) 63–68.
- [394] B. Ravel, M. Newville, ATHENA, ARTEMIS, HEPHAESTUS: Data analysis for X-ray absorption spectroscopy using IFEFFIT, *J. Synchrotron Radiat.* 12 (2005) 537–541.
- [395] M.F. Ruiz-Lopez, A. Munoz-Paez, A theoretical study of the XANES spectra of rutile and anatase, *J. Phys. Condens. Matter.* 3 (1991) 8981–8990.
- [396] R. Michel, M. Noite, M. Reich, Systemic effects of implanted prostheses made of cobalt-chromium alloys, *Arch. Orthop. Trauma Surg.* 110 (1991) 61–74.

- [397] M.A. Koronfel, A.E. Goode, J.N. Weker, S.E.R. Tay, C.A. Stitt, T.A. Simoes, J.F.W. Mosselmans, P. Quinn, R. Brydson, A. Hart, M.F. Toney, A.E. Porter, M.P. Ryan, Understanding the reactivity of CoCrMo-implant wear particles, *Npj Mater. Degrad.* 2 (2018) 1–5.
- [398] B.F. Shahgaldi, F.W. Heatley, A. Dewar, B. Corrin, In vivo corrosion of cobalt-chromium and titanium wear particles, *J. Bone Joint Surg. Br.* 77 (1995) 962–6.
- [399] S. Bajt, S.B. Clark, S.R. Sutton, M.L. Rivers, J. V Smith, Synchrotron X-ray microprobe determination of chromate content using X-ray absorption near-edge Structure, *Anal. Chem.* 65 (1993) 1800–1804.
- [400] A. Levina, P.A. Lay, Solution structures of chromium(VI) complexes with glutathione and model thiols, *Inorg. Chem.* 43 (2004) 324–335.
- [401] E. Strub, R. Plarre, M. Radtke, U. Reinholz, H. Riesemeier, U. Schoknecht, K. Urban, P. Jüngel, Determination of Cr(VI) in wood specimen: A XANES study at the Cr K edge, *Nucl. Instruments Methods Phys. Res. Sect. B.* 266 (2008) 2405–2407.
- [402] M.W. Kendig, A.J. Davenport, H.S. Isaacs, The mechanism of corrosion inhibition by chromate conversion coatings from x-ray absorption near edge spectroscopy (Xanes), *Corros. Sci.* 34 (1993) 41–49.
- [403] M.L. Peterson, G.E. Brown, G.A. Parks, Quantitative determination of chromium valence in environmental samples using XAFS spectroscopy, 432 (1997) 75–80.
- [404] R. Bartholomäus, K. Harms, A. Levina, P.A. Lay, Synthesis and characterization of a chromium(V) cis-1,2-cyclohexanediolato complex: a model of reactive intermediates in chromium-induced cancers., *Inorg. Chem.* 51 (2012) 11238–11240.
- [405] R. Codd, J.A. Irwin, P.A. Lay, Sialoglycoprotein and carbohydrate complexes in chromium toxicity, *Curr. Opin. Chem. Biol.* 7 (2003) 213–219.
- [406] A. Levina, R. Codd, G.J. Foran, T.W. Hambley, T. Maschmeyer, A.F. Masters, P.A. Lay, X-ray absorption spectroscopic studies of chromium(V/IV/III)-2-Ethyl-2-hydroxybutanoato(2-/1-) complexes, *Inorg. Chem.* 43 (2004) 6208–6216.
- [407] S. De Flora, A. Camoirano, M. Bagnasco, C. Bennicelli, G.E. Corbett, B.D. Kerger, Estimates of the chromium(VI) reducing capacity in human body compartments as a mechanism for attenuating its potential toxicity and carcinogenicity, *Carcinogenesis.* 18 (1997) 531–537. doi:10.1093/carcin/18.3.531.
- [408] R. Codd, C.T. Dillon, A. Levina, P.A. Lay, Studies on the genotoxicity of chromium: from the test tube to the cell, *Coord. Chem. Rev.* 216–217 (2001) 537–582.
- [409] A. Levina, P.A. Lay, Mechanistic studies of relevance to the biological activities of chromium, *Coord. Chem. Rev.* 249 (2005) 281–298. doi:10.1016/j.ccr.2004.02.017.
- [410] G.T. Rogers, In vivo production of hexavalent chromium, *Biomaterials.* 5 (1984) 244–245.
- [411] H.H. Harris, A. Levina, C.T. Dillon, P.A. Lay, Time-dependent uptake, distribution and biotransformation of chromium(VI) in individual and bulk human lung cells: application of synchrotron radiation techniques, *J Biol Inorg Chem.* 10 (2005) 105–118.
- [412] K.M. Shah, P.D. Quinn, A. Gartland, J.M. Wilkinson, Understanding the tissue effects of tribo-corrosion: wptake, distribution, and speciation of cobalt and chromium in human bone cells, *J. Orthop. Res.* 33 (2015) 114–121.
- [413] C.T. Dillon, P.A. Lay, B.J. Kennedy, A.P.J. Stampfl, Z. Cai, P. Ilinski, W. Rodrigues, D.G. Legnini, Hard X-ray microprobe studies of chromium(VI)-treated V79 Chinese hamster lung cells: intracellular mapping of the biotransformation products of a chromium carcinogen, *J. Biol. Inorg. Chem.* 7 (2002) 640–645.
- [414] A. Levina, H.H. Harris, P.A. Lay, X-ray absorption and EPR spectroscopic studies of the biotransformations of chromium(VI) in mammalian cells. Is chromodulin an artifact of isolation methods?, *J. Am. Chem. Soc.* 129 (2007) 1065–1075.
- [415] B.J. Goldstein, K. Mahadev, X. Wu, L. Zhu, H. Motoshima, Role of insulin-induced reactive oxygen species in the insulin signaling pathway, *Antioxid. Redox Signal.* 7 (2005) 1021–31.
- [416] A. Levina, I. Mulyani, P.A. Lay, Redox chemistry and biological activities of chromium(III) complexes, *Nutr. Biochem. Chromium(III).* Chapter 11 (2007) 223–

255.

- [417] I. Mulyani, A. Levina, P.A. Lay, Biomimetic oxidation of chromium(III): does the antidiabetic activity of chromium(III) involve carcinogenic chromium(VI)?, *Angew. Chemie - Int. Ed.* 43 (2004) 4504–4507.
- [418] J. Wang, G. Zhou, C. Chen, H. Yu, T. Wang, Y. Ma, G. Jia, Y. Gao, B. Li, J. Sun, Y. Li, F. Jiao, Y. Zhao, Z. Chai, Acute toxicity and biodistribution of different sized titanium dioxide particles in mice after oral administration, *Toxicol. Lett.* 168 (2007) 176–185.
- [419] M. Jinek, K. Chylinski, I. Fonfara, M. Hauer, J. Doudna, E. Charpentier, A programmable dual-RNA-guided DNA endonuclease in adaptive bacterial immunity, *Science* 337 (2012) 816–821.
- [420] E. Pennisi, The CRISPR craze, *Science* 341 (2015) 833–836.
- [421] D. Rodríguez-Leal, Z.H. Lemmon, J. Man, M.E. Bartlett, Z.B. Lippman, Engineering quantitative trait variation for crop improvement by genome editing, *Cell.* 171 (2017) 470-480.e8.
- [422] Y. Dong, M.L. Simões, E. Marois, G. Dimopoulos, CRISPR/Cas9 -mediated gene knockout of *Anopheles gambiae* FREP1 suppresses malaria parasite infection, *PLoS Pathog.* 14 (2018) 1–16.
- [423] Q. Xiao, D. Guo, S. Chen, Application of CRISPR/Cas9-based gene editing in HIV-1/AIDS therapy, *Front. Cell. Infect. Microbiol.* 9 (2019) 1–15. full.
- [424] Y. Fu, High-frequency off-target mutagenesis induced by CRISPR-Cas nucleases in human cells, *Nat. Biotechnol.* 31 (2013) 822–826.
- [425] T. Hart, M. Chandrashekhar, M. Aregger, Z. Steinhart, K.R. Brown, G. MacLeod, M. Mis, M. Zimmermann, A. Fradet-Turcotte, S. Sun, P. Mero, P. Dirks, S. Sidhu, F.P. Roth, O.S. Rissland, D. Durocher, S. Angers, J. Moffat, High-resolution CRISPR screens reveal fitness genes and genotype-specific cancer liabilities, *Cell.* 163 (2015) 1515–1526.
- [426] O. Shalem, N. Sanjana, E. Hartenian, X. Shi, D. Scott, T. Mikkelsen, D. Heckl, B. Ebert, D. Root, J. Doench, F. Zhang, Genome-Scale CRISPR-Cas9 Knockout Screening in Human Cells, *Science* (80-. ). 343 (2014) 84–87.
- [427] M. Kurata, S.K. Rathe, N.J. Bailey, N.K. Aumann, J.M. Jones, G.W. Veldhuijzen, B.S. Moriarity, D.A. Largaespada, Using genome-wide CRISPR library screening with library resistant DCK to find new sources of Ara-C drug resistance in AML, *Sci. Rep.* 6 (2016) 4–13.
- [428] H. Koike-Yusa, Y. Li, E.P. Tan, M.D.C. Velasco-Herrera, K. Yusa, Genome-wide recessive genetic screening in mammalian cells with a lentiviral CRISPR-guide RNA library, *Nat. Biotechnol.* 32 (2014) 267–273.
- [429] F. Sanger, S. Nicklen, A. Coulson, DNA sequencing with chain-terminating inhibitors, *Proc. Natl. Acad. Sci.* 74 (1977) 5463–67.
- [430] V. Chaitankar, G. Karakulah, R. Ratnapriya, F.O. Giuste, M.J. Brooks, A. Swaroop, Next generation sequencing technology and genomewide data analysis: Perspectives for retinal research, *Prog. Retin. Eye Res.* 55 (2016) 1–31.
- [431] Z. Qin, The use of THP-1 cells as a model for mimicking the function and regulation of monocytes and macrophages in the vasculature, *Atherosclerosis.* 221 (2012) 2–11.
- [432] X.S. Liu, F. Zhang, R.A. Irizarry, T. Xiao, L. Cong, M.I. Love, W. Li, H. Xu, J.S. Liu, M. Brown, MAGeCK enables robust identification of essential genes from genome-scale CRISPR/Cas9 knockout screens, *Genome Biol.* 15 (2014) 1–12.
- [433] T. Hart, A. Tong, K. Chan, J. van Leeuwen, A. Seetharaman, M. Aregger, M. Chandrashekhar, N. Hustedt, S. Seth, A. Noonan, A. Habsid, O. Sizova, L. Nedyalkova, R. Climie, K. Lawson, M.A. Sartori, S. Alibai, D. Tieu, S. Masud, P. Mero, A. Weiss, K.R. Brown, M. Ušaj, M. Billmann, M. Rahman, M. Costanzo, C.L. Myers, B. Andrews, C. Boone, D. Durocher, J. Moffat, Evaluation and design of genome-wide CRISPR/Cas9 knockout screens, *BioRxiv.* (2017) 1–34.
- [434] I. Catelas, A. Petit, H. Vali, C. Fragiskatos, R. Meilleur, D.J. Zukor, J. Antoniou, O.L. Huk, Quantitative analysis of macrophage apoptosis vs. necrosis induced by cobalt and chromium ions in vitro, *Biomaterials.* 26 (2005) 2441–2453.

- [435] H. von Schroeder, D. Smith, A. Gross, R. Piliar, R. Kandel, R. Chernecky, S. Lugowski, Titanemia from total knee arthroplasty, *J. Arthroplasty*. 11 (1996) 620–625.
- [436] A. Bistolfi, A. Cimino, G.C. Lee, R. Ferracini, G. Maina, P. Berchiolla, G. Massazza, A. Massè, Does metal porosity affect metal ion release in blood and urine following total hip arthroplasty? A short term study, *HIP Int.* 28 (2018) 522–530.
- [437] I. Swiatkowska, N.G. Martin, J. Henckel, H. Apthorp, J. Hamshere, A.J. Hart, N. West, L. Pathology, C.C. Hospital, W. London, Blood and plasma titanium levels associated with well-functioning hip implants, *J. Trace Elem. Med. Biol.* 57 (2020) 9–17.
- [438] P.-A. Vendittoli, A. Roy, S. Mottard, J. Girard, D. Lusignan, M. Lavigne, Metal ion release from bearing wear and corrosion with 28 mm and large-diameter metal-on-metal bearing articulations: a follow-up study, *J. Bone Jt. Surg.* 92-B (2010) 12–19.
- [439] D.W. Murray, R. Fitzpatrick, K. Rogers, H. Pandit, D.J. Beard, A.J. Carr, J. Dawson, The use of the Oxford hip and knee scores, *J. Bone Jt. Surg.* 89-B (2007) 1010–1014.
- [440] G.S. Matharu, F. Berryman, L. Brash, P.B. Pynsent, R.B. Treacy, D.J. Dunlop, Influence of implant design on blood metal ion concentrations in metal-on-metal total hip replacement patients, *Int. Orthop.* 39 (2015) 1803–1811.
- [441] A. Borgwardt, L. Borgwardt, B. Zerahn, H. Daugaard, L. Borgwardt, S. Ribel-Madsen, A randomized seven-year study on performance of the stemmed metal M2a-Magnum and ceramic C2a-taper, and the resurfacing ReCap hip implants, *J. Arthroplasty*. 33 (2018) 1412–1420.
- [442] J. Dawson, R. Fitzpatrick, A. Carr, D. Murray, Questionnaire on the perceptions of patients about total hip replacement, *J. Bone Joint Surg.* 78-B (1996) 185–190.
- [443] Y. Kalairajah, K. Azurza, C. Hulme, S. Molloy, K.J. Drabu, Health outcome measures in the evaluation of total hip arthroplasties- a comparison between the harris hip score and the Oxford hip score, *J. Arthroplasty*. 20 (2005) 1037–1041.
- [444] V. Wylde, I. Learmonth, V. Cavendish, The Oxford hip score: the patient's perspective, *Health Qual. Life Outcomes*. 3 (2005) 1–8.
- [445] J.R. Campbell, M.P. Estey, Metal release from hip prostheses: Cobalt and chromium toxicity and the role of the clinical laboratory, *Clin. Chem. Lab. Med.* 51 (2013) 213–220.
- [446] J. Barry, M. Lavigne, P.A. Vendittoli, Evaluation of the method for analyzing chromium, cobalt and titanium ion levels in the blood following hip replacement with a metal-on-metal prosthesis, *J. Anal. Toxicol.* 37 (2013) 90–96.
- [447] Eurachem Method Validation Working Group, The fitness for purpose of analytical methods a laboratory guide to method validation and related topics (2014).
- [448] T.-K. Liu, S.-H. Liu, C.-H. Chang, R.-S. Yang, Concentration of metal elements in the blood and urine in the patients with cementless total knee arthroplasty, *J. Exp. Med.* 185 (1998) 253–262.
- [449] L. Savarino, M. Greco, E. Cenni, L. Cavasinni, R. Rotini, N. Baldini, A. Giunti, Differences in ion release after ceramic-on-ceramic and metal-on-metal total hip replacement, *J. Bone Joint Surg.* 88-B (2006) 472–476.
- [450] Y. Nuevo-Ordonez, M. Montes-Bayon, E. Blanco Gonzalez, A. Sanz-Medel, Y. Nuevo-Ordoñez, M. Montes-Bayón, E. Blanco González, A. Sanz-Medel, Titanium preferential binding sites in human serum transferrin at physiological concentrations., *Met. Integr. Biometal Sci.* 3 (2011) 1297–303.
- [451] M. Esposito, *Titanium in Medicine: Material Science, Surface Science, Engineering, Biological Responses and Medical Applications*. Springer, Germany (2001).
- [452] K. Merritt, S.A. Brown, Storage and elimination of titanium, aluminum, and vanadium salts in vivo, *J. Biomed. Mater. Res.* 26 (1992) 1503–1515.
- [453] S. Takai, N. Yoshino, Y. Kusaka, Y. Watanabe, Y. Hirasawa, Dissemination of metals from a failed patellar component made of titanium-base alloy, *J. Arthroplasty*. 18 (2003) 931–935.
- [454] H. Bosshart, M. Heinzlmann, THP-1 cells as a model for human monocytes, *Ann. Transl. Med.* 4 (2016) 438–438.